INVESTIGATION OF GAS SPECIES AND THERMAL SEPARATION IN RANQUE-HILSCH VORTEX TUBE

By
MIHIR CHATTERJEE

Enrolment No. ENGG01201304034

Bhabha Atomic Research Centre, Mumbai

A thesis submitted to the

Board of Studies in Engineering Sciences

In partial fulfilment of requirements
For the Degree of

DOCTOR OF PHILOSOPHY

Of

HOMI BHABHA NATIONAL INSTITUTE

September, 2020

HomiBhabha National Institute[1]

Recommendations of the Viva Voce Committee

As members of the Viva Voce Committee, we certify that we have read the dissertation prepared by Mihir Chatterjee entitled "Investigation of gas Species and Thermal Separation in Ranque-Hilsch Vortex Tube" and recommend that it may be accepted as fulfilling the thesis requirement for the award of Degree of Doctor of Philosophy.

Chairman - Prof. G. Sugilal Date:	14.9.20
Guide / Convener - Prof. S. Mukhopadhyay Date: 14-09-2020	
Co-guide - Prof. P. K. Vijayan Date: 14-09-2020	
Examiner - Prof. KannanIyer Date:14-09-2020	
Member 1- Prof. S. Mukhopadhyay Date: 14-09-2020	
Member 2- Prof. R. N. Singh Date:	
Member 3- Prof. Deep Prakash Date: 14-09-2020	

Final approval and acceptance of this thesis is contingent upon the candidate's submission of the final copies of the thesis to HBNI.

We hereby certify that we have read this thesis prepared under our direction and recommend that it may be accepted as fulfilling the thesis requirement.

Date: 14-09-2020

Place: BARC,Trombay **Signature** **Signature**

Co-guide:Prof P. K. Vijayan **Guide: Prof S. Mukhopadhyay**

[1] This page is to be included only for final submission after successful completion of viva voce.

STATEMENT BY AUTHOR

This dissertation has been submitted in partial fulfilment of requirements for an advanced degree at Homi Bhabha National Institute (HBNI) and is deposited in the Library to be made available to borrowers under rules of the HBNI.

Brief quotations from this dissertation are allowable without special permission, provided that accurate acknowledgement of source is made. Requests for permission for extended quotation from or reproduction of this manuscript in whole or in part may be granted by the Competent Authority of HBNI when in his or her judgment the proposed use of the material is in the interests of scholarship. In all other instances, however, permission must be obtained from the author.

Mihir Chatterjee

(Mihir Chatterjee)

DECLARATION

I, hereby declare that the investigation presented in the thesis has been carried out by me. The work is original and has not been submitted earlier as a whole or in part for a degree / diploma at this or any other Institution / University.

Mihir Chatterjee

(Mihir Chatterjee)

Enrolment No. ENGG01201304034)

List of Publications arising from the thesis

Journal papers

[1] "Experimental study of heat and mass transfer in Ranque Hilsch Vortex tube", Chatterjee, M., Mukhopadhyay, S., Vijayan, P. K., International Journal of Advance Research (2016), 4 (7): pp. 666-674. (ISSN 2320-5407).

[2] "1-D model for mass transfer calculation in vortex tube using heat and mass transfer analogy", Chatterjee, M., Mukhopadhyay, S., Vijayan, P. K., American Journal of Heat and Mass Transfer, (2017). Vol. 4 No. 1:1-24. https://doi.org/ 10.7726/ajhmt.2017.1001.

[3] "Species separation in Ranque-Hilsch vortex tube using air as working fluid", Chatterjee, M., Mukhopadhyay, S., Vijayan, P. K., Heat and Mass Transfer, (2018). Vol. May 2018 No. 1: pp. 1-14. https://doi.org/10.1007/s00231-018-2386-3.

[4] "Estimation of swirl velocity of gas in Ranque-Hilsch vortex tube using a combined thermal and species separation model", Chatterjee, M., Mukhopadhyay, S., Vijayan, P. K., (2020), Energy Sources Part A: Recovery, Utilization and Environmental effects https://doi.org/10.1080/15567036.2020.1795312

Conference papers

[1] "Thermal and species separation in Ranque Hilsch Vortex Tube", Chatterjee, M., Mukhopadhyay, S., Vijayan, P. K., (2014), CHEMCON-2014, Chandigarh, IICHE.

[2] "Analysis of Heat and mass transfer in counter-current Ranque Hilsch Vortex Tube", Chatterjee, M., Mukhopadhyay, S., Vijayan, P. K., (2015), IHMTC-2015, December, 2015,Thiruvanantapuram, ISHMT.

[3] "A combined heat and mass transfer model for the Ranque-Hilsch Vortex tube", Chatterjee, M., Mukhopadhyay, S., Vijayan, P. K., (2017), IHMTC-2017, December, 2017, BITS Pilani, Hyderabad.

Mihir Chatterjee
7/09/20

Mihir Chatterjee

DEDICATIONS

To my parents

ACKNOWLEDGEMENTS

Firstly, I would like to express my sincere gratitude to my advisors Prof. S. Mukhopadhyay and Prof. P. K. Vijayan for their continuous support towards my Ph.D study and related research. I am indebted to them for their patience, motivation, and immense knowledge. Their guidance helped me throughout all the time of research and writing of this thesis. I could not have imagined having a better advisor and mentor for my Ph.D study.

Besides my advisors, I would like to thank the rest of my thesis committee: Prof. G. Sugilal, Prof Smt S. B. Roy, Prof. R. N. Singh and Prof. Deep Prakash for their insightful comments which helped me to widen my research from various perspectives. I am thankful to my examiners Prof. Kannan Iyer and Prof. Mihir Sen for their thoughtful comments on my thesis which helped me to improve its quality to a great extent. My sincere thanks also goes to Dr. Kausik Nandy, who has provided me an opportunity to explore and add few crucial aspects to my doctoral thesis.

I am thankful to my senior researchers in my parent organization BARC specifically Dr. T. K. Bera, Sri S. Sarkar, Sri S. Sanyal and Sri Puneet Tulsyan who gave access to the laboratory and research facilities. Without their precious support it would not be possible to conduct this research.

I thank my fellow PhD researchers Sri Vinay Kumar, Sri Abhay Chaturvedi, Sri Tarun Devangan, Sri Nafees Ahmed and Sri Karimulla Seikh for the stimulating discussions and for all the fun we have had. Also I thank my friends and co-workers in my department and other organizations. In particular, I am grateful to Sri Mahesh Gupta, Sri Vinod Karbale, Sri Dinesh Sawant, Sri Sandesh Name and Sri Basanta Patra for their active support in experimental work.

Last but not the least; I would like to thank my family: my parents, my wife and son for supporting me physically, mentally and spiritually throughout the course work, research and publication, preparation of thesis and my life in general.

CONTENTS

LIST OF FIGURES

LIST OF TABLES

Summary on conclusions

Objective of the present research work is to investigate experimentally and numerically separation of gas species and energy under different operating conditions in a RHVT. The work was initiated by a simple set of experiments with a commercially available RHVT in which inter-dependence of mass and thermal separation in RHVT was studied. It was concluded from the experiment that mass and heat transfer are dependent on each other. Based on this finding a coupled thermal and mass separation model was built that uses the Chilton-Colburn analogy of simultaneous heat and mass transfer. A computer code based on this model can calculate the thermal and concentration profile along the axial length of the RHVT. Results from the computer code have been verified with data available in literature. Further a laboratory scale experimental setup was built in which both thermal and species separation could be studied using air as a binary mixture of oxygen and nitrogen. Experimental data obtained from this setup has been used to validate the code extensively. Next, a number of important geometric and operating parameters were identified. The computer code developed and the experimental setup were used to carry out parametric studies of the RHVT performance with respect to species separation. Also supporting data available in the literature has been used for parametric study.

SUMMARY

The Ranque Hilsch Vortex Tube (RHVT) is a device that generates cold and hot gas at two outlets from compressed gas at the inlet. Apart from a thermal separator RHVT is also mentioned in literature as a gas species separation device (*Helikon vortex separation process)*, but not many studies on gas species separation with the RHVT has been reported in the literature. This separation device has several advantages like simple construction, ready availability, absence of rotating parts and therefore zero maintenance. The quoted separation factor for this device is high but this large separation factor can be obtained at a very small value of cut (ratio of product to inlet flow rate). Improvements in these aspects are required. Also the underlying physical process of heat and mass transfer inside the device is not completely resolved in the past. The phenomenon in RHVT involves compressible fluid dynamics of turbulent and unsteady flow; thermodynamics, heat transfer and species separation. These aspects make the research complicated and challenging. Hence problem statement of the current research work is, "The reason behind gas species and thermal separation phenomena inside a Ranque-Hilsch vortex tube is not fully understood and we need to establish a model that can adequately explain the heat and mass transfer phenomena inside the tube." Objectives of the research conceived in the present work have been listed as follows:

- Development of a combined heat and mass transfer model
- Validation of the combined heat and mass transfer model
- Parametric studies

Hence essence of the current research work is **"To investigate experimentally and numerically separation of gas species and energy under different operating conditions in a Ranque Hilsch Vortex Tube (RHVT)."**

It is well known that the mechanisms of heat and mass transfer are similar and analogical. Now the RHVT is divided into two flow regions i.e. wall flow region (peripheral stream) and core flow region (axial stream and axial return flow stream). Now applying Chilton Colburn analogy, the mass transfer coefficient between these two regions is calculated using the heat transfer coefficient value. The heat transfer coefficient can be calculated using Seider-Tate correlation that is applicable for forced convection for turbulent pipe flow. A component balance along a control volume of the RHVT gives rise to an Ordinary Differential Equation (ODE) which is solved for getting the concentration profile along the

length of the vortex tube. Further, an extension of this modelling work on mass transfer is done by combining an analytical model for heat transfer available in literature. Together with these set of numerically calculated thermal data the previously developed mass transfer model can calculate the concentration gradient along the axial direction of the RHVT, and thus becomes fully theoretical.

A laboratory scale experimental unit has been commissioned to study the thermal and species separation of air as a binary mixture of oxygen and nitrogen. The setup has been designed to experiment with different sizes of vortex tubes and sample of the separated gas streams can be collected from the hot and cold ends of the RHVT and analyzed by a Residual Gas Analyzer (RGA). Thus the species as well as thermal separation can be calculated in terms of the measured temperature and concentration of the hot and cold end gas stream respectively. A comparison of experimental values of thermal and species separation with those computed from the model has been carried out. Further a set of verification study of the computer code based on the simultaneous heat and mass transfer model has been carried out with data available in literature. It was observed that the percentage error in component and overall mass balance are within acceptable limit.

In the next phase of the research work a parametric study has been carried out in order to understand the effect of different parameters of a RHVT on the separation characteristics of the device, particularly on species separation. For each parameter, the thermal and species separation mechanism and the flow-fields inside the vortex tube are explored by investigating the pressure, velocity, and temperature fields. For carrying out the parametric studies data obtained from literature, in house experimental setup and the code developed in the present work have been extensively used. Air is used as the working fluid in all the experiments.

Chapter 1
Introduction

"*The greatest challenge to any thinker is stating the problem in a way that will allow a solution*".

-Bertrand Russell

1.1 Introduction

The Ranque Hilsch Vortex Tube (RHVT) is a device that generates cold and hot gas streams at two outlets from compressed gas at the inlet. Hence it can act as a thermal device operating as a cooling and heating machine simultaneously. RHVT is a simple and compact low-cost device. This device is maintenance-free as it has no moving part. The device does not require any power supply and the temperature of hot and cold end fluid can be easily adjusted by changing the opening of a flow control valve at the hot gas outlet. Due to simple construction and maintenance-free operation without any electricity, commercially available RHVT is widely used in industry for spot heating and cooling operation. Apart from a thermal separator RHVT is also mentioned in literature as a gas species separation device, but not many studies on gas species separation with the RHVT has been reported in the literature. The species separation process using RHVT is known as *Helikon vortex separation process.* This method is classified as an aerodynamic Uranium enrichment process. British Physicist and Nobel laureate Paul Dirac thought of the idea for isotope separation using vortex tube. In 1934 Dirac devised this method of isotopic separation in the laboratory of Soviet Physicist and Nobel Laureate Peter Kapitza at Cambridge. Later this method was designed for a production plant for isotopic separation and used in South Africa for production of reactor-grade fuel with 3-5% enriched Uranium-235 content. Hence we can see that RHVT is an important device that can be used for both thermal as well as species separation. But till this date, the mechanism of thermal as well as species separation inside a RHVT is never been fully understood. Hence a requirement exists for a better understanding of the thermal and species separation and the Ranque-Hilsch effect. In the following chapters, a number of theoretical and experimental studies carried out to explain the Ranque-Hilsch effect will be described, followed by a new mathematical model that predicts the mass transfer in a counter-current RHVT. The aim of the present work is to present and establish this new mathematical model by validation with data obtained from in house experimental setup and literature.

1.2 Principle of working

The Ranque Hilsch Vortex Tube (RHVT) is a device that generates cold and hot gas streams at two outlets from compressed gas at the inlet, as shown in figure 1.1a. When a gaseous mixture of two species enters tangentially into the vortex chamber via the inlet nozzle at high pressure, a swirling flow is generated inside the vortex chamber by a vortex generator. When the gas swirls at the centre of the chamber, it expands and thus cools down by losing heat. In the vortex chamber, one part of the rotating gas moves towards the hot end, and another part exits via the cold exhaust. The fraction of the gas moving toward the hot end of the RHVT reverses its flow direction after colliding with the hot end control valve and moves axially from the hot end to the cold end. At the hot outlet, the gas releases with a higher temperature, while at the cold outlet, the gas released has a lower temperature compared to the inlet temperature. Also due to the high-speed swirling motion, the gas mixture is subjected to a centrifugal force. The RHVT species separation process uses this centrifugal force to create a density gradient in a gas mixture containing components of different molecular weights. Centrifugal force causes the heavier molecules to move closer to the outer wall of the RHVT than the lighter molecules. This heavier fraction is collected from the peripheral stream coming out from the hot end of the RHVT as shown in figure 1.1a. The lighter fraction is collected from the axial stream coming out from the cold end of the RHVT. Figure 1.1b is a photograph of a RHVT with its components.

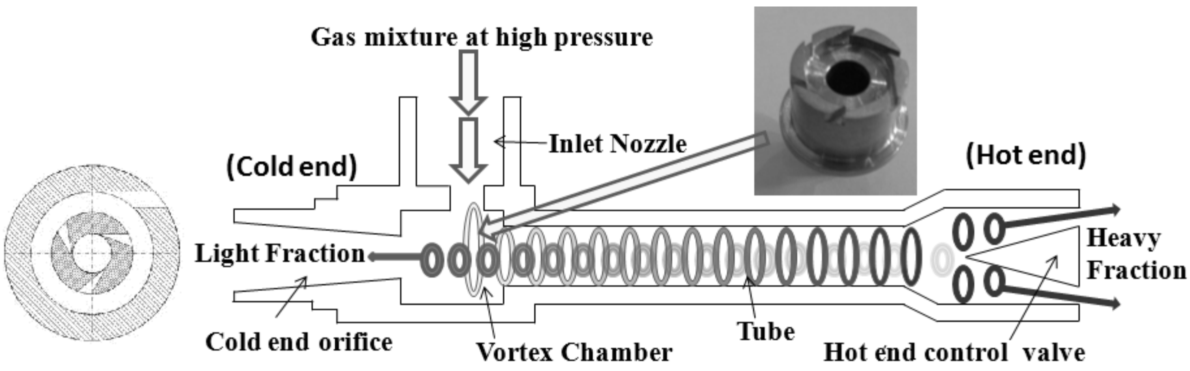

a.

b.

Fig. 1.1 a. Components of a RHVT and its inlet and outlet streams and side view; (Inset: a vortex generator) b. Photograph of a RHVT and its components

1.3 Types of RHVT

As per the direction of flow inside the tube, an RHVT can be of two types. The first is the counter-current type where the cold and hot stream comes out from two different sides of the RHVT and these outlets are called cold and hot end respectively. A schematic diagram of this type of RHVT is shown in figure 1.2a. On the other hand in a co-current type of RHVT. both the cold and hot streams are drawn out from a single side of the device. This side is located at the end of the tube away from the inlet. Hot gas is drawn out from the periphery of the outlet while the cold gas is drawn out of the system from the central region of the same side. A schematic of this type of RHVT is shown in figure 1.2b. The counter-current type of RHVT is the commonly available RHVT in the market and for all further study, this type of RHVT will be used.

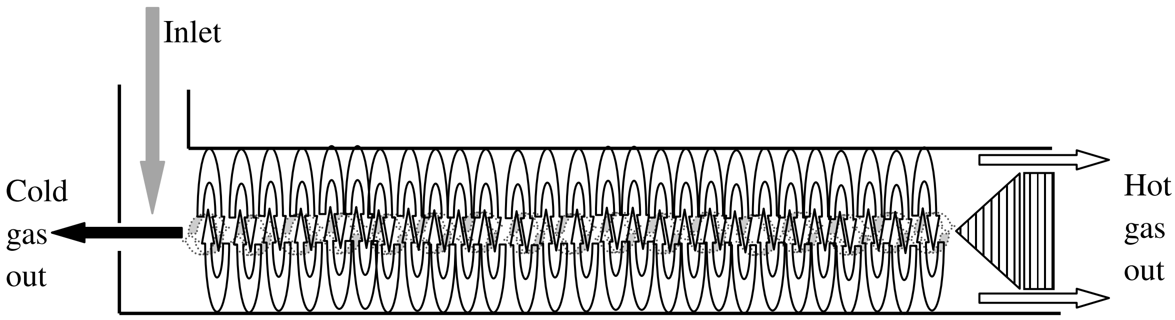

a.

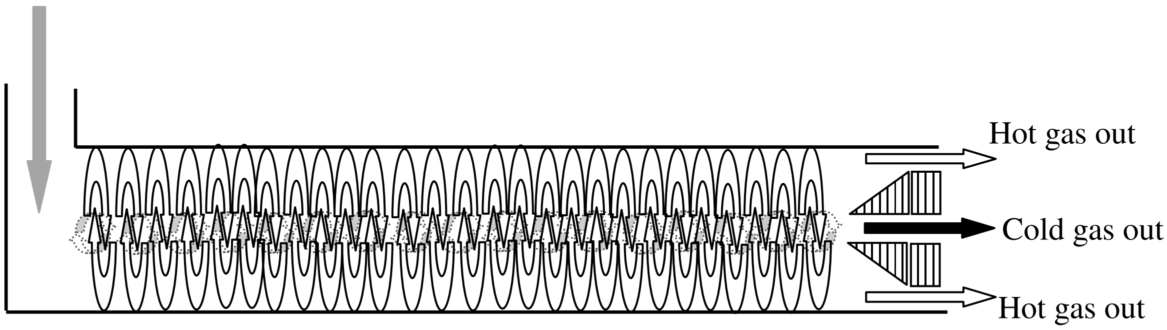

b.

Fig. 1.2 Two types of RHVTs a. Counter-current RHVT b. Co current RHVT

1.4 Application of RHVT in industry

Commercially available RHVTs are almost exclusively used for spot cooling or heating in industrial applications and use compressed air as the working fluid. In addition, RHVTs have been gaining lots of attention in air-conditioning and refrigeration research, because of the possibility to replace the expansion valve of vapor compression systems with this low-cost device. This device can recover expansion work that would otherwise be lost in the isenthalpic throttling process. With no moving parts, no electricity and no Freon required, RHVTs are regularly used for refrigeration. A flow control valve in the hot air outlet is used to adjust temperatures and flows and in turn refrigeration capacity of the RHVT over a wide range. The operation is intrinsically safe as no refrigerant is involved. The device is compact, lightweight and easy to install. RHVTs are also used for cooling of cutting tools i.e. in lathes and mills. A fast jet of cold air from RHVT provides both cooling and removal of the metallic chips produced by the tool. This eliminates the requirement of liquid coolant, which is messy, expensive and environmentally hazardous. RHVTs can be used in remote areas for producing ice using compressed air generated by fuel or coal combustion. Other applications of RHVT are low-temperature cooling of electronic devices, testing of thermal sensors, local cooling/heating of enclosures, cooling of instrumentation panels, thermal testing, dehumidification of gases, separation of gas-gas mixtures, liquefying natural gas and in nuclear reactors (Shamsoddini *et. al.* [163]). Some of the important applications of RHVT are discussed in the following sections.

1.4.1. Isotopic separation

When high-pressure gas mixture enters tangentially into the vortex chamber via the inlet nozzle, one part of the gas swirls to the far end of the tube and escapes with a higher temperature than the inlet. The remaining part comes out from the other end with a lower temperature than the inlet. Also due to the high-speed swirling motion, the gas mixture is subjected to a centrifugal force. The RHVT species (isotopic mixture) separation process uses this centrifugal force to create a density gradient in a gas mixture containing components of different molecular weights. Centrifugal force causes the heavier molecules to move closer to the outer wall of the RHVT than the lighter molecules as shown in figure 1.3. An isotopic separation process called Helikon process developed in South Africa uses the principle of species separation in RHVT described above (Whitaker [197], Alant and Schumann [9]).

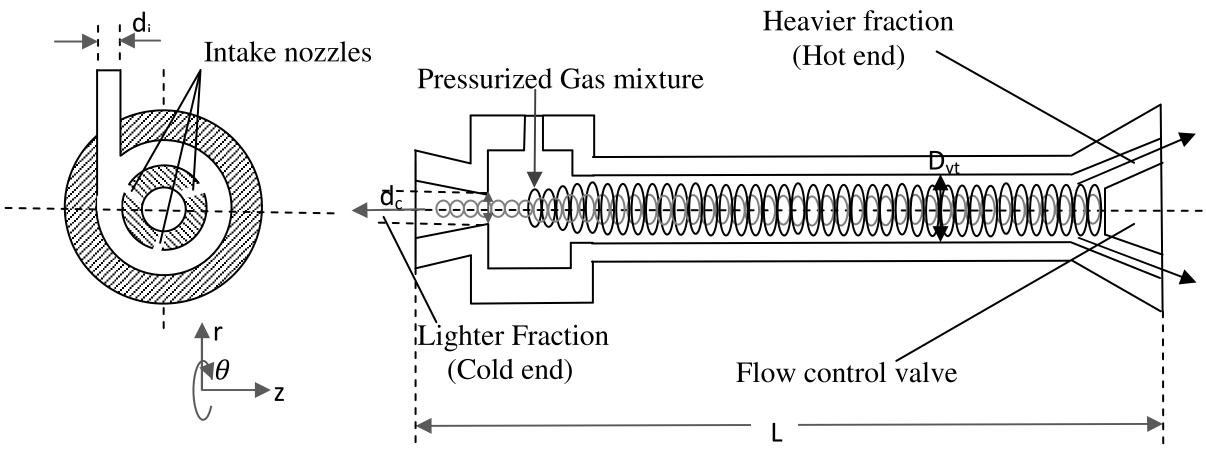

Fig. 1.3 Schematic diagram (with side view) of species separation in a countercurrent RHVT

This technique is classified as aerodynamic separation process for isotopic separation (Krass *et al.* [98]). As diluted Uranium Hexafluoride gas mixture spirals around the tube, the concentration of lighter component increases near the axis while the concentration of heavier component increases at the outer periphery. When the gas reaches the far end of the tube the heavier component rich outer stream is withdrawn from the outer periphery.

The lighter component rich inner stream reverses its direction after bouncing over a control valve that acts as a flow obstruction. This reversed stream is withdrawn separately from the other side of the RHVT. The kinetic energy of the swirling flow decays at downstream of the feed inlet due to friction of the wall. Figure 1.3 shows a schematic diagram of a RHVT. The working material for this process is a mixture of 1-2 percent uranium hexafluoride (UF_6) and 98-99 per cent hydrogen (H_2). UF_6 is diluted to attain very high rotational velocity inside the RHVT. The gas mixture is injected at high pressure and velocity through the inlet. This inlet mixture gains both tangential (v_θ) and axial (v_z) component of velocity as it passes through the nozzles of a vortex generator shown in figure 1.3. As the gas spirals around the tube, the concentration of lighter component increases near the axis while the concentration of heavier component increases at the outer periphery. A similar phenomenon is observed in the rotating centrifuge or jet nozzle. When the gas reaches the far end of the tube the heavier component rich outer stream is withdrawn from the outer periphery.

1.4.2 Waste heat recovery

RHVT is used in several industries for waste heat and pressure energy recovery to enhance economic feasibility and increase recovery efficiency of waste heat and pressure energy. Most of the major heat and pressure energy sources provide energy in ranges that can be easily harnessed using vortex tube. Some of these which can act as major waste heat and pressure energy sources are tabulated in table 1.1 below.

Table 1.1: Major waste heat and pressure energy sources (Gupta *et al*. [77])

Source	Temperature (K)	Pressure (bar)	Application
Exhaust steam from boiler	500-750	3-5	Combustion air preheating
Exhaust gas from gas turbine	640-810	6-100	Electricity production
Thermal power plant	560-760	5-30	Furnace load preheating,

gas exhaust			feed-water preheating
Exhaust gas from blast furnace	1170-1920	6-10	Steam generation for mechanical process
Cooling water from engines, compressors, furnace doors	300-500	-	Space heating, domestic water heating

Methods using RHVT for waste heat and pressure recovery include transferring heat energy between gases and liquids, generating mechanical and/or electrical power and using waste heat with a heat pump for heating or cooling facilities. Since pressures of many waste energy sources fall in the range of 0 bars to 10 bars as shown in table 1.1 above, RHVT is suitable for energy recovery from these sources. Robustness of this method, simple design and small size as compared to other methods proves it as a better alternative for isotopic separation.

1.4.3. Refrigeration

Industries that generate or have access to compressed air or waste gases utilise RHVT for cooling or heating applications. RHVT based refrigeration can be used in industries like agriculture, transportation, food, medicine, dairy etc.

1.4.4 Cooling suits and masks

There are several industries where personnel need to enter and work in the hazardous zone of high temperature or zones containing dust, fumes, toxic and/or radioactive environment. These include locations like coal mines, foundries, sandblasting, welding, furnaces, etc. Cooling suits and masks using RHVT protect the workers as well as increased working hours due to the conditioned environment inside the suits and masks.

1.4.5 Micro-power system

Arslan *et. al.* [15] have shown RHVT can be used to increase the total efficiency of power systems, especially micro power systems like micro-turbines. The RHVT is considered in conjunction with a Heat Recovery Steam Generator (HRSG) in micro-turbine. RHVT splits the turbine exhaust flow into hotter and cooler streams. The cooler stream is still hot enough to supply the heat required in the economizer section, leaving the hotter stream to increase the exit temperature from the super-heater. In this way both the air leaving the HRSG and going to the steam turbine will have an increased enthalpy and cycle efficiencies are improved. In addition, the steam turbine exit quality is increased.

1.4.6 Cooling in high-speed machining and laser cutting

Heat generated during metal cutting affects the quality of a work-piece and limits the life of the cutting tool. Researchers have used RHVT for cooling purpose in metal cutting. Cooling approaches using RHVT include pre-cooling of the work piece, indirect cooling of cutting tools and direct cooling of the cutting tools (Nexflow brochure [132]). Chen *et al.* [37] have shown that RHVT can also be used to diminish Heat Affected Zone (HAZ) in laser cutting of Glass Fibre Reinforced Plastic (GFRP).

1.5 Some important terms relevant to isotope separation and their definitions

In this section, some important terms relevant to isotopic separation have been discussed. These terms would be required for further discussions.

1.5.1 Abundance and separation factor

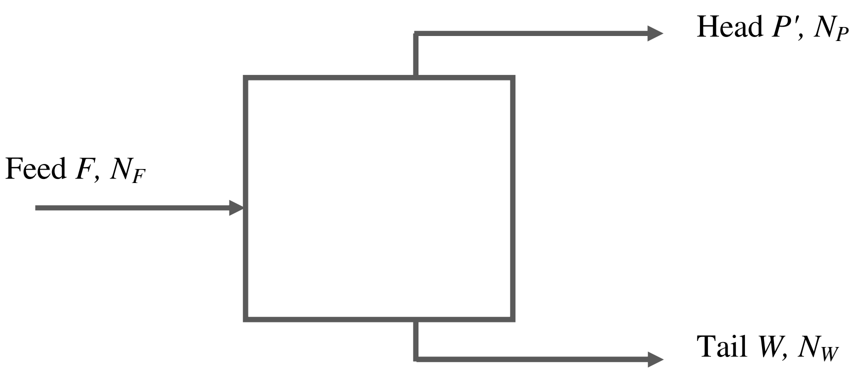

Fig 1.4 Separation in a three-stream separating element

For a three-stream species separating element, like the RHVT unit, we have the feed, product and waste flows. The magnitudes of these flows (in moles per unit time) are designated by F, P', and W respectively; the mole fraction of the desired isotope in any stream is designated as N with the appropriate subscript. In figure 1.4 F, P' and W are flow rate of feed, head fraction (product) and tail fraction (waste) respectively while N_F, N_P and N_W are the fraction of one of the isotopes in the mixture. If n is the total number of moles while n_a is the mole of component a present in the mixture, then

$$N = \frac{n_a}{n} = \frac{\rho_a}{\rho} = \frac{P_a}{P} \tag{1.1}$$

Now the abundance is defined as

$$R_{ab} = \frac{N}{1-N} \tag{1.2}$$

A measure of the separation between any two streams is the ratio of their respective abundances. Thus, we have individual separation factors for the feed-to-product stream and the waste-to-feed stream

Head separation factor: $\alpha = \frac{R_{ab,P}}{R_{ab,F}}$ (1.3)

Tail separation factor: $\beta = \frac{R_{ab,F}}{R_{ab,W}}$ (1.4)

1.5.2 Separative power and value function

The performance metric of a separating element must be a function of both the total separation it can produce ($\alpha\beta$) and the amount of material that the separating element can process per unit time. Thus, separative power or separative capacity is defined as:

$$\delta U = P'V(N_P) + WV(N_W) - FV(N_F) \tag{1.5}$$

where, V is a value function for a binary mixture defined in a way such that

- the lowest value is (arbitrarily) set to be for a 50:50 mixture of two components,
- the value increases as the mixture becomes purified in either component, and
- V scales in such a way that the work of n elements (arranged in a non-mixing cascade) will produce n times the work of a single element.

Unit of separative capacity is called Separative Work Unit or SWU. It can be shown that the value function is

$$V(N) \equiv (2N-1)ln\frac{N}{(1-N)} \qquad (1.6)$$

The importance of the separative capacity in isotope separation lies in the fact that it can be used as a measure of the quality of an isotope separation work. Many of the characteristics of the plant that make important contributions to its cost are proportional to the separative capacity. For example, the total power requirement, pump capacity, flow rate and area of barrier required for an isotopic separation plant based on gaseous diffusion method operating as an ideal cascade are all proportional to the separative capacity.

1.5.3 Cut

The ratio of head flow rate to feed rate is known as the *cut,*

$$\theta = \frac{P'}{F} = \frac{(N_F-N_W)}{(N_P-N_W)} \qquad (1.7)$$

Hence we can write

$$(1-\theta) = \frac{W}{F} = \frac{(N_P-N_F)}{(N_P-N_W)} \qquad (1.8)$$

Now the variation in the "value" of F moles of a mixture with composition N_F across a separating element is given in terms of cut values as

$$\delta U = \theta FV(N_P) + (1-\theta)FV(N_W) - FV(N_F) \qquad (1.9)$$

In the infinitesimal case, the separative potentials $V(N_W)\ and\ V(N_P)$ can be expanded in a Taylor series around N_F. Now neglecting all terms after the third and taking into account the material and component balances

$$\delta U = F\left[\theta\frac{(N_P-N_F)^2}{2} + (1-\theta)\frac{(N_W-N_F)^2}{2}\right]\frac{d^2V(N)}{dN^2} \qquad (1.10)$$

Equation 1.10 gives a relation among separative capacity, cut and value function.

1.5.4 Cascade

No single separating element like centrifuge or RHVT can enrich isotopes like Uranium from its natural concentration of about 0.7 percent Uranium-235 to the 3 to 5 percent required to fuel a nuclear reactor. In addition, the throughput of these separating elements is very small compared to the consumption of a reactor. To multiply the effects of the enrichment of one element and to achieve adequate throughput, large numbers of separating elements are interconnected to form cascades. The pattern of that connection is determined by the properties of the individual element and the required quantity and concentration of the final product. An enrichment plant usually holds thousands of such separating elements in parallel and series called a cascade.

A cascade consists of separation units, arranged in parallel that make up a single stage. The width of the cascade is an indicator of the number of elements in a stage. These elements receive feed with identical concentration and generate the same product and waste. The total flow rate through a stage is proportional to the width of the stage as each individual element is optimized for a given throughput. Hence in order to increase the output of a cascade, the number of machines per stage needs to be increased. Stages are connected in series. The number of stages in the cascade is determined by the concentration required in the product. In the isotope separation process, a counter-current scheme of a cascade is used where the enriched fraction or head feeds the higher stages and the depleted fraction or tail is sent for further striping in the lower stages. Enrichment in cascades is considered a continuous process, which means that the flow rates of the input and output of the stages are kept constant for most part of the operation. The external variables of a cascade are independent of internal mechanism and can be obtained considering the cascade as a black box. The same basic separation theory of individual separating elements applies to the overall cascade. The external variables of the cascade are the feed flowing at a rate of F and a concentration N_F of the desired isotope, the product (heads) flowing at a flow rate of P and a concentration N_P of the desired isotope and the waste (tails) flowing at a rate of W and having a composition of N_W. The internal variables of the cascade include the inter-stage flow rates and compositions.

In a counter-current cascade when the head and the tail inter-stage flow merge at each confluent point possessing the same concentration then the cascade is ideal. If the separating element is symmetric the head and the tail separation factors (given in equation 1.3 and 1.4 respectively) are equal, leading to a symmetric cascade. When the separating element is asymmetric then it leads to an asymmetric cascade. Consider an asymmetric element for which head separation factor, $\alpha = \beta^{p/q}$ (where β is the tail separation factor) then an ideal *p-stage up* and *q-stage down* cascade will avoid inter-stage mixing loss. In this *p-up* and *q-down* cascade, the enriched stream from $(i\text{-}p)^{th}$ stage and depleted stream from $(i+q)^{th}$ stage will mix to form the feed for i^{th} stage. In an ideal cascade, the flow and size of stage vary from stage to stage with continuity. In real life, the ideal cascade gets approximated by a series of square cascade forming a squared-off cascade. The conventional cascade design procedure does not give an optimum design because of squaring-off, the variation of flow rates and separation factor of the element with respect to stage location.

1.6 Brief description of different isotope separation techniques

The separation techniques for heavier isotopes (i.e. having higher molecular weight) are classified as follows

- Those based directly on the atomic weight of the isotope.
- Those based on the small differences in chemical reaction rates due to different atomic weights of the isotopes.
- Those based on properties not directly related to the atomic weight of isotopes, i.e. nuclear resonances.

Based on these principles following isotope separation processes have been developed.

1.6.1 Diffusion process

Commercial Uranium enrichment was first carried out by the diffusion process in the USA. It has since been used in other countries like UK, Russia, China, France and Argentina. It is a very energy-intensive process, requiring about 2400 kWh per SWU (Separative Work Unit - as discussed in section 1.3). The basic principle of this method is the equipartition principle of statistical mechanics (Krass *et al.* [98]).

1.6.2 Gas centrifugation

The gas centrifugation process utilizes a unique design that allows gas to constantly flow in and out of the centrifuge. Unlike most centrifuges the gas centrifuge utilizes continuous processing, allowing cascading, in which multiple identical processes occur in succession. In a gas centrifuge, the gas molecules are subjected to a strongly rotating centrifugal field (Benedict and Pigford, [27]). The heavier $U^{238}F_6$ molecules are thrown to the peripheral region while the lighter $U^{235}F_6$ molecules are concentrated near the centre.

1.6.3 Laser isotopic separation

Laser enrichment processes have been the focus of interest for some time. They are a possible third-generation technology that promises minimization of capital costs, energy inputs and lower tails assays. Together these result in significant cost-cutting advantages. Laser processes can be classified into two sub-processes: atomic and molecular.

1.6.4 Electromagnetic process

A very early endeavour for isotopic separation was the electromagnetic isotope separation (EMIS) process using Calutrons. A Calutron is a mass spectrometer used for separating the isotopes of Uranium (Krass, *et al.* [98]). Ions of heavier and lighter isotopes are separated because they describe arcs of different radii when they move through a magnetic field. The energy requirement of this process is very high, almost ten times that of diffusion. It was developed by Ernest O. Lawrence [1901-1958] during the Manhattan Project.

Details of the above isotopic separation processes are given in appendix A.

1.6.5 Aerodynamic process

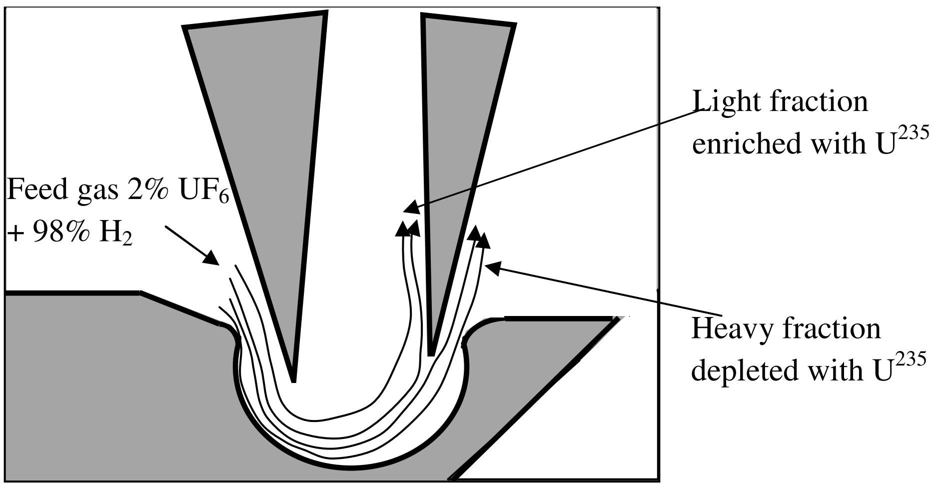

Fig 1.5 Jet nozzle process

Two aerodynamic processes were brought to the demonstration stage around the 1970s. One is the jet nozzle process, with demonstration plant built in Brazil, and the other is the Helikon vortex tube process developed in South Africa. In the jet nozzle process, a partial separation of isotopes is obtained in flowing gas stream that is subjected to a very high centrifugal acceleration through a curved semicircular path. The isotopic molecules, depending on their mass shall experience different centrifugal forces that effect separation. In this process, as shown in figure 1.5, feed gas consisting of a mixture of about 2% UF_6 and 98% H_2 is made to flow in a convergent-divergent curved nozzle. The nozzle accelerates the gas mixture to supersonic speed. The accelerated gas mixture moves in a curved path with a radius of curvature of the order of a fraction of a millimetre.

The centrifugal force is proportional to v^2/r, where v is the linear speed of the gas and r is the radius of curvature of the flow path, a high degree of centrifugal force is imparted on the gas molecules. The lighter $U^{235}F_6$ molecules experiencing lower centrifugal force tend to remain in the center while heavier $U^{238}F_6$ molecules tend to remain at the periphery. In a typical separation nozzle, the diameter of the deflecting groove is about 0.2 mm and the width of the nozzle at the throat is about 0.03 mm. The feed gas at a pressure of about 200-300 mbar and a temperature of around 40 °C, is expanded to obtain an optimum expansion ratio of about 4:1. The dilution of UF_6 with H_2 has a beneficial effect as the sonic speed for UF_6 is about 90 m/sec, whereas that for the mixture is about 400 m/sec. Thus it is possible to attain very high speed and thereby a higher separation factor.

In the RHVT based Helikon process, high-speed gas stream bearing the isotopic mixture being made to rotate through a very small radius, causing a pressure gradient similar to that in a gas centrifuge. The light fraction can be extracted towards the centre and the heavy fraction towards the outside. This method was designed and used in South Africa. The Uranium Enrichment Corporation of South Africa, Ltd. (UCOR) developed the process, operating a facility at Valindaba to produce enriched Uranium. Aerodynamic enrichment processes require a large amount of electricity and are not generally considered economically competitive because of high energy consumption and substantial requirements for removal of waste heat. There are two major advantages of this process. First, as the feed used in this process is highly diluted there is no concern of criticality involved in this process. The second advantage is this method is suitable for batch processing. This means Helikon-type plants are relatively compact.

Table 1.2 Comparison of different aspects of heavy isotope separation methods (source Krass et. al. [98])

	Diffusion	Centrifugation	Laser	Electromagnetic	Aerodynamic
Working material	UF_6	UF_6	UF_6 +N_2 or U vapour	UCl_4	UF_6(4%)+ H_2 (96%)
Single stage separation factor	1.004	1.3-1.6	5-15	20-40	1.025-1.030
Stage cut (θ)	0.5	0.5	NA	NA	0.25-0.05
Specific energy consumption (KWh/SWU)	2300-3000	100-300	10-50	3000-4000	3000-3500
Stage reflux mechanism	NA	Internal counter current	Recover and recycle U metal	Recover and recycle UCl_4	Recycle intermediate fraction
Status of the method	Plant level	Plant level	R& D	Uneconomical	Demonstration level

Different aspects of the five methods of heavy isotope separation discussed in this section are compared in table 1.2.

1.7 Problem statement

Isotope separation is the process of concentrating specific isotopes of a chemical element by removing other isotopes. Isotope separation capability of a nation is an extremely important process for many civilian and military nuclear technologies. Now separation of isotopes of lighter elements such as hydrogen is not a big problem as they can be removed by chemical means. The separation techniques for heavier isotopes are more challenging as chemical properties are very slightly affected by atomic mass. Several isotopic enrichment processes have been demonstrated historically by different researchers such as gaseous diffusion, gas centrifugation, laser isotopic separation, electromagnetic separation and aerodynamic separation as mentioned before. For any isotope separation technique to be industrially successful, following key performance objectives are to be met (Bera [28])

- Better separation factor for a single separating unit.
- Better Separative capacity for a single separating unit.
- Flexibility of single separating unit for cascade operation.
- Better energy efficiency of a single separating unit per unit separative capacity.

The Helikon vortex tube process of isotopic separation using a RHVT has several advantages like simple construction, ready availability, absence of rotating parts and therefore zero maintenance. The quoted separation factor for this process is reasonably high (1.025-1.030 as given by Krass *et. al.* [98]) but this high separation factor can be obtained at a small value of cut (θ). Improvements in these aspects are required. Also the underlying physical process of heat and mass transfer inside the device is not completely resolved in the past. The phenomenon in RHVT involves compressible fluid dynamics of turbulent and unsteady flow; thermodynamics, heat transfer and species separation. These aspects make the research complicated and challenging. Hence problem statement of the current research work is, **"The gas species and thermal separation phenomena inside a Ranque-Hilsch Vortex tube are not fully understood and we need to establish a model that can adequately explain the heat and mass transfer phenomena inside the tube."**

1.8 Objectives of the present work

In the preceding sections, the subject of present research work has been introduced along with some background. The problem statement related to its use as a species separation device has been discussed in the previous section. Objectives of the present research work have been listed as follows:

1.8.1 Development of a combined heat and mass transfer model

The heat and mass transfer phenomena happen simultaneously inside a RHVT and hence a combined heat and mass transfer model has been developed to explain the physical process inside the tube.

1.8.2 Validation of the combined heat and mass transfer model

To validate the results from above mentioned combined heat and mass transfer model a laboratory-scale experimental unit has been commissioned. This test setup has generated thermal as well as species separation data from a RHVT, which was used to validate results obtained from the combined model. Also, data available in literature has been used for validation.

1.8.3 Parametric studies

Parametric studies have been carried out with two important sets of parameters that influence the species separation performance of a RHVT. These are the design parameters and the operating parameters of the RHVT. For each parameter, the species separation mechanism and the flow-field inside the RHVT have been explored by investigating the pressure, flow rate, species concentration and temperature measured at the hot and cold end.

Hence the essence of the current research work is **"To investigate experimentally and numerically separation of gas species and energy under different operating conditions in a Ranque Hilsch Vortex Tube (RHVT)."**

1.9 Scope of present work

The problem statement and objective of the present research work have been defined in previous sections 1.5 and 1.6 respectively. Now in the present section, the extent of content that has been covered by means of the present research work is discussed. This helps to set the scopes of research and to arrive at logical conclusions from the research.

1.9.1 Selection of the RHVT

The necessary experiments have been carried out with commercially available RHVTs and vortex generators. These are counter flow, small and medium-sized RHVTs. The geometric dimensions of the different components of these tubes are known and have been used for parametric studies. The maximum value of pressure at the inlet of the RHVT is limited by the supply pressure from the compressor available in our setup.

1.9.2 Choice of working fluid

Air as a binary mixture of oxygen and nitrogen has been used as a working fluid in all our analysis and experiments. The difference in molecular weight between these two gases is

≡4.0 which is sufficient for the present research work. Since there is no chemical, radioactive or fire hazard involved in the handling of air, the laboratory-scale experimental setup is safe to operate for person conducting the experiment and no special clearance for operation is required. Moreover, most of the data available in literature obtained through experimental or theoretical means have used air as the working fluid. Hence these sets of data can be readily used for the present analysis.

1.9.3 Modelling of mass transfer

Initially, a one-dimensional mass transfer model of the RHVT has been planned to be developed. This model required some experimental data as well, to predict the performance of the RHVT. Hence the mathematical model was semi-empirical or hybrid in nature. Later a heat transfer model has been incorporated with the above model to make it fully theoretical.

1.9.4 Experimental studies

The main purpose of setting up the experimental facility is to generate experimental data for validating with the mathematical model developed. Further, this setup was used to generate experimental data required for the semi-empirical model of RHVT developed in this work. Also, parametric studies have been carried out to study the effect of different geometrical and operating parameters on the species separation performance of the RHVT.

1.10 Organization of the thesis

Chapter 2 of the thesis is dedicated to literature survey on the subject of research. A large volume of literature is available on the subject of RHVT. However, in this survey, the main aim is to restrict the discussion to relevant and more recent research work reported. The literature available on RHVT can be broadly subdivided into two categories. They are

1) Research work on thermal separation.
2) Research work on species separation.

Further, the studies in each category can be subdivided into two categories as shown below

1) Experimental work
2) Theoretical work

Hence the literature survey has been classified accordingly. Limitation of available models in the literature has been discussed in this chapter followed by a section describing gap areas found in the research till date.

The research methodology has been discussed in **chapter 3**. The methodologies adopted in the present research work are the following

- Modelling of heat and mass transfer inside a RHVT
- Validation of the model with experimental data
- Parametric studies

Brief overviews along with available resources for each of the above methods have been discussed in this chapter.

Chapter 4 gives a detailed description of the experimental setup commissioned with peripherals as well as of experimental procedure. The chapter begins with a description of various components of different types of RHVTs used for experimentation. Detailed specifications of the generators have been given. Specifications of the instruments to measure process parameters like flow rate, temperature and pressure have been given and associated error in the instruments have been analyzed. Also, the quadrupole mass spectrometer used for sample composition analysis has been briefly described. An experimental procedure adopted in the present research work has been outlined.

Chapter 5 describes in detail the mathematical model developed as part of the present research work to calculate simultaneous heat and mass transfer in the RHVT. Initially a semi-empirical model for mass transfer that makes use of the well known Chilton-Colburn analogy which requires experimental thermal data has been introduced. The Governing equations have been derived and inputs required have been discussed. The methods adopted to solve the governing equation have been described. Next, the chapter focuses on the validation of the semi-emperical heat and mass transfer model. Validation studies have been carried out and reported. The chapter has been concluded by describing the advantages and limitations of the present mathematical model.

In **chapter 6** a heat transfer model from literature has been introduced into the semi-empirical model developed in chapter 5. This makes the combined heat and mass transfer model fully theoretical. Hence the dependence of the semi-empirical model on experimental data has been removed. Output from this combined model has been verified with experimental data as well as with data available in the literature.

The output from the mathematical model described in chapter 6 as well as results from the experimental setup described in chapter 4 is presented in **chapter 7**. Experiments in the test setup were carried out to generate process data involving different operating parameters. The experimental set up has been extensively used to carry out validation studies of the result obtained from the mathematical model and validation test cases have been presented in chapter 7. Further experimental results from the test setup as well as results from the mathematical model have been used to understand the effect of various parameters on the separation characteristics of the RHVT as well the sensitivity of the principal operating parameters on thermal and species separation. The results are presented along with discussions in the following sections of this chapter.

Summary of the research work has been included in **chapter 8**. The key findings of the research work have been described in detail. The chapter is concluded with a future direction on the work.

1.11 Summary

This chapter serves as an introduction to the subject of research work. The chapter begins with a description of the RHVT device and its working principle. Next, an introduction to some important terms related to the field of species separation and their definitions are provided. Background information about the research topic is given in the subsequent section followed by two sections about the problem statement and objective of the present work. These two sections define the problem and introduce the aim of the research work respectively. The subsequent section defines the scope by which the present research work will remain bounded. Application of RHVT in the industry is described next. Chapter-wise organization of the thesis is given at the end of this chapter.

Chapter 2
Literature survey

"*Besides its possible importance as a practical device, the vortex tube presented a new and intriguing phenomenon in fluid dynamics*".

R. Westley

2.1 Introduction

In 1931, Georges Ranque, a French engineer, while working on the development of an industrial vacuum pump made a chance discovery, what is now called the Ranque effect, which led to the discovery of vortex tube. Ranque [150, 151] found that in this device a stream of air could be split into two streams, one of hot air and the other of cold air. In the year 1931, Ranque filed for a patent on the vortex tube and in 1933, he presented a research paper on it. The work of Ranque remained unnoticed until German physicist Rudolph Hilsch [88] improved the design and published a widely read paper on the device, which he called a Wirbelrohr (literally, whirl pipe). Since then, the Ranque-Hilsch tube or vortex tube has been the subject of numerous investigations carried out by researchers from the diverse field of Physics, Thermodynamics, Heat and Mass transfer and Computational Fluid Dynamics**.** Hence a large volume of literature is available on the subject of RHVT. However, in this survey, the main aim is to restrict the discussion to relevant and more recent research work reported with earlier works reported in a separate section. Also, an overview of early research work carried out mainly in the USA and Europe had been briefly discussed. The literature available on RHVT can be broadly subdivided into two categories. They are 1) Research work on thermal separation and 2) Research work on species separation. Further, the studies in each category can be subdivided into two categories. These are 1) Experimental work and 2) Theoretical work. Hence the literature survey has been classified accordingly. The following section gives an overview of early work carried out on RHVT during the years 1931-1979.

2.2 An overview of early global research (1931-1979)

The Ranque effect or Ranque-Hilsch effect or the vortex tube effect is a phenomenon which was known since 1930s. Though intensive experimentation and investigation (both experimental and theoretical) had been carried out by researchers all over the world, the mechanism that gives rise to thermal or species separation phenomena as a compressible fluid passes through the tube is not fully explained by the researchers till this date. Besides this lack of full understanding of the underlying mechanism in the RHVT, the coefficient of performance or COP (defined as the cooling power gained by the system divided by the work power input to the unit) is still quite low despite intensive research has been carried out over the years across the globe.

After World War II, considerable interest in the Hilsch's tubes was observed among the scientific community throughout Europe and America. An indicative of that early interest in the RHVT is the comprehensive survey carried out by Westley [125]. Widespread attention of American Scientists towards the RHVT device was attracted after an article on the device by Milton [125] was published. Many research works were carried out which were aimed at replacing complicated refrigeration system for cooling by this simple device. But it was found that thermal efficiency of this device was poor and in spite of its simplicity wide application of this device might not be possible. Henceforth, research efforts in the United States could be categorized into four main streams

- To find out an explanation of the RHVT phenomena
- To study the flow structure inside of RHVT
- To find out possible applications of RHVT

- To find out ways to increase the thermal efficiency of the device

Massachusetts Institute of Technology (MIT) took lead in American research work and a series of research work were published during 1947. The first experimental results on the internal flow inside RHVT were published by Reed [152]. Haddox *et al.* [80] have studied the performance of the RHVT. In the following years, two consecutive theoretical papers were published by Barnes [20] and Nickerson [135] from MIT. Meanwhile, in Canada, Johnson [92] had published a report on experimental investigation.

The first important theoretical work on RHVT was published by Kassner and Knoernschild [97] where it was assumed that a free vortex was initially formed inside the vortex chamber and later converted into a forced vortex as the gas spiralled along the tube portion of the RHVT. In Norway, Haar and Wergeland [79] have explained the process in RHVT by simple adiabatic cooling across the pressure gradient caused by the centrifugal field. A simultaneous theoretical paper to predict the performance of RHVT based on empirical correlation was published from Germany by Burkhadt [32]. In the same year, Fulton [69,70] had published two theoretical works from MIT. The first paper dealt with energy migration in RHVT while the second discussed the overall thermodynamics.

The first work solely on application of RHVT was published by Knoernschild and Morgenson [97]. The paper discussed the cooling of high-speed aircraft or missile system using RHVT. Experimental research was also carried out in General Electric Company with RHVT and an important summary of the experiments was published by Corr [48]. Corr [48] carried out experiments with a supersonic inlet nozzle but the results indicated a decrease in temperature drop. In a separate work on internal flow distribution, Dornbrand [53] of Republic Aviation Corporation had proposed a theory for flow in the laminar two-dimensional compressible vortex which was formed between two rotating cylinders.

Researchers in US universities other than MIT had also contributed to the investigation work about RHVT. Scheper [160] of Union College, Schenectody have studied the internal flow structure and temperature distribution inside the RHVT. He had proposed a heat transfer theory where radial outward heat transfer occurred from the vortex core due to a low static temperature (temperature without the effect of velocity) at the periphery. A thesis by Lustick [117] of Syracuse University had reviewed previous developments on the

RHVT and tried to find out ways to enhance RHVT thermal efficiency. MacGee [118] have worked on flow visualization on the wall of a glass RHVT at Boston University.

Meanwhile, two novel applications of RHVT could be seen. In General Electric Company's research laboratory Vonnegut [191] had used RHVT to eliminate the aerodynamic heating errors of free air temperature thermometers on aircraft. Also, Webster [192] from Du Pont had carried out an investigation of RHVTs for refrigeration application. A further application of RHVT was given by Applegate [13] for cooling of airborne electronic equipment. Westley [193] had worked on the application of RHVT to ventilated suit cooling in aircraft.

After the publication of Hilsch's paper, most of the RHVT investigations were carried out in the USA. Significant contributions from Europe started pouring in after 1950. William and Tompkins [199] had stated in their work that an inlet chamber with multi-inlet nozzles and with a diameter larger than the hot tube diameter would give improved performance. Sprenger [173] had suggested that the RHVT thermal separation phenomenon was due to the ultrasonic effect which was not solely restricted to the circular flow. A significant contribution to the theory of RHVT was given by Dutch scientist Van Deemter [188]. Similar to Fulton [68] Van Deemter [188] had suggested that temperature distribution in the vortex was determined by the ratio of work flux to heat flux but he added that heat flux in turbulent circular flow was not only proportional to the temperature gradient but also a term proportional to the radial acceleration.

Baker and Rathkamp [17] in a research report published from Oak Ridge National Laboratory (ORNL) had explained the phenomenon of thermal separation. According to them, thermal separation in a RHVT is due to combination of an adiabatic expansion of inlet gas and a "viscous-shear effect" which transfers heat energy from core region to peripheral region of the tube coupled with an energy release associated with the turnaround of the gas molecules at the stagnation point. They have also concluded that the device was not conducive to significant mass separation unless processes like gas diffusion and/or centrifugation might enhance the separation.

Krieth and Margolis [99] from Lehigh University, USA had suggested that the thermal separation phenomenon was primarily because of centrifugal force which induced a radial inward motion of warmer fluid and a radial outward motion of the cooler fluid. They have experimentally measured the heat transfer and friction coefficients for air and water flowing through a RHVT. Deissler & Perlmutter [52] had studied the causes of energy separation in RHVT and found that most important factor affecting the total (stagnation) temperature of a fluid element in a compressible vortex is the turbulent shear work done on or by the element. They have analyzed velocity, temperature and pressure distributions in a turbulent vortex with radial and axial flow and found turbulent mixing was the principal reason for energy separation.

Reynolds [153] used an order of magnitude analysis for dynamics of compressible turbulent fluid flow and extended the analysis to include energy fluxes in that flow to find an explanation for energy separation in the RHVT. He had proposed that the physical processes responsible for energy separation are heat flux due to turbulent mixing of the compressible fluid through radial pressure and temperature gradients, a flux of total energy produced by buoyancy forces and work done by two most important components of Reynolds' stresses. Parulekar [139], Otten [138], and Raiskii and Tunkel [149] employed divergent tubes for all or part of the vortex chamber in attempts to shorten the chamber and improve energy separation performance, but their emphasis was on the maximum and minimum temperatures in the outflowing streams.

Sibulkin [165] had done an equivalent unsteady-flow analysis for the development of flow inside a RHVT. Using this analysis he had calculated radial distributions of velocity and temperature at successive axial positions in the tube. A theory of vortex-tube performance based upon an idealized three-dimensional flow pattern for the RHVT was derived. Takahama [177] had investigated the relationship between velocity and temperature profile inside the vortex chamber and the dimensions of the main tube, nozzle and cold end orifice. He had proposed formulae for the profiles of velocity, temperature and energy of the air flowing. He had also obtained data for designing a RHVT with high efficiency of energy separation.

Linderstrom-Lang [113-116] published a series of research papers and reports on species separation in a RHVT. He presented theoretical and experimental studies on mass and energy transport and proposed a secondary flow model inside the RHVT. As per this model, there were re-circulation flows inside the RHVT. Linderstrom-Lang [113] had shown species separation in a RHVT took place mainly due to pressure diffusion (net movement of molecules or atoms down a pressure gradient) caused by centrifugal action. He had shown that a shorter length of RHVT produced a lower thermal separation and higher species separation.

Entov *et. al.* [63] had attempted to establish a relation between RHVT parameters and thermal separation effect based on damped vortical turbulent flow in the tube and a secondary flow structure. Martynov & Brodyanski [122] had presented experimental data on the parameters of a vortex flow measured along a RHVT under adiabatic and non-adiabatic conditions. They have shown a variation of the thickness of flow streams, temperature and heat transfer coefficient along the tube. Vennos [190] measured the velocity, total temperature, and total and static pressures inside a standard RHVT and reported the existence of considerable radial velocity inside the RHVT. Bruun [31] presented the experimental data of pressure, velocity and temperature profiles in a counter-flow RHVT with a cold mass fraction of 0.23. Using the equation of continuity, Bruun [31] showed an outward-directed radial velocity near the inlet nozzle and an inward radial velocity in the rest of the tube. He concluded that turbulent heat transport was responsible for most of the energy separation. Raiskii & Tunkel [149] had investigated the influence of various RHVT configurations (cylindrical, diffuser and step geometry) on the thermal separation performance. They have found that long cylindrical tubes are most effective for thermal separation. Nash [127] used vortex expansion cooling to cool infrared detector applications. A summary of the design parameters of the vortex cooler was reported by Nash [128]. Soni and Thomson [171] had used the method of Evolutionary Operation (EVOP) for experimental design of a RHVT as there was large number of variables and their interdependence was not known. Marshall [121] had confirmed the species separation reported by Linderstrom-Lang [113] and using several gas mixtures and sizes of tubes, demonstrated that there was a critical inlet Reynolds number for maximum separation. Hellyar [87] had reviewed the high-pressure natural gas liquefaction and separation processes using a RHVT.

Takahama *et al.* [178] investigated experimentally the energy separation performance of a steam-operated standard RHVT and reported that the performance worsened with the wetness of steam at the nozzle outlet because of the effect of evaporation. Energy separation was not observed for dryness fraction of the working fluid less than 0.98.

Collins and Lovelace [47] had shown that for a two-phase, liquid‑vapour mixture in a standard counter-flow RHVT and the inlet pressure of 0.791 MPa, significant separation was observed for a dryness fraction above 80% at the inlet. When the dryness fraction dips below 80%, the thermal separation became insignificant. But at this low value of dryness fraction, the discharge enthalpies still showed considerable differences indicating that the Ranque‑Hilsch process was still in effect.

2.3 Theories proposed by different researchers

Since the inception of RHVT, a number of researchers have suggested many theories to describe the working principle of a RHVT. A list of theories proposed by different researchers is compiled in table 2.1.

Table 2.1: Proposed theories about RHVT operation

No.	Theory	Researcher	Remarks
1.	Adiabatic expansion and compression of working fluid	Ranque [150,151]	Xue [201] have shown the difference between the theoretical calculation and the experimental results. This suggests the influence of factors in the thermal separation in a RHVT other than pure adiabatic expansion.
2.	Transfer of kinetic energy from the higher angular velocity axial region to the lower angular velocity peripheral	Corr[48], Fulton [69,70], Webster [192]	The explanation of radial pressure gradient of forced vortex remains debatable. Aljuwayhel *et. al.* [11] has shown temperature change based on the hypothesis of friction only, is 0.2 K.

	region with free and forced vortex flow inside the RHVT		
3.	Heat transfer between layers of fluid	Scheper [161]	Scheper [161] concluded that axial and radial velocity components were much smaller than the tangential velocity. He found that the static temperature decreased in a radially outward direction. This finding was contrary to most other observations that were made later.
4.	Internal friction and turbulent shear work	Van Deemter [188], Pengelly [140], Lay[107], Kreith and Margolis [99], Deissler and Perlmutter [51], Parulekar [139], Reynolds [153,154], Silbulkin [165], Alimov [10], Gutsol [78]	Theoretical and experimental investigations on strong rotating incompressible flow (Linderstorm-Lang [116]) showed the possibility of the thermal separation in the RHVT without the effect of pressure variation.
5.	Compressibility of the working fluid	Amitani *et al.* [12]	An experimental study conducted by Balmer [19] showed the thermal separation existed when high-pressure water was used as working media in the tube.
6.	Görtler vortex produced by the tangential velocity on the inside wall of the RHVT is a major driving force for the	Stephan *et al.* [174]	Görtler vortex is formed in a boundary layer flow near a concave wall when the centrifugal action creates a pressure variation (instability) across the boundary layer.

	energy separation		
7.	Acoustic streaming model	Kurosaka [104], Chu [42], Kuroda[103]	Kurosaka [104] experimented with a hollow cylinder instead of RHVT and only the temperature at the cold end of the tube was measured.
8.	Turbulent transfer of thermal energy in a compressible flow	Linderstrom-Lang [116]	Thermal separation was observed even at lower Reynolds number.
9.	Secondary flow model	Cockerill [44], Frohlingsdorf [67], Ahlborn and Groves [5], Ahlborn and Gorden [4], Gao [72]	The existence of the secondary flow in RHVTs has not been supported by all researchers like Behera [22].
10.	Heat transfer between supersonic and subsonic gas flows with the same stagnation parameters	Leont'ev [109]	The method is based on the difference between the equilibrium temperature of a thermally insulated wall in supersonic flow and the adiabatic stagnation temperature of the gas.
11.	Pressure gradient of forced vortex causing compression at high-pressure peripheral region and expansion in the lower pressure core region.	Eiamsa-ard [60], Farouk & Farouk [64]	As per experiments carried out by Gao [72] and simulations by Behara *et al.* [22], the pressure at any point in the tube is lower than the inlet pressure, which suggests that expansion happens everywhere in the tube, even at periphery.
12.	Thermal separation by turbulent eddies	Hartnett and Eckert [84]	Presented a model based on turbulent rotating flow with solid body rotation.

2.3.1 Limitations of existing models

It can be seen from the above table 2.1 that these theories are proposed to explain the thermal separation phenomenon in a RHVT. But these theories have their own limitations and some of them contradict each other. Hence it can be said that no universal theory that can explain the working principle of a RHVT is available till date. A detailed discussion on these theories and their limitations has been presented in this section.

Scheper [161], Aljuwayhel *et al.* [11] and Behera [22] have proposed a *static temperature gradient* along the radius as one of the reasons for thermal separation in a RHVT. Heat is transferred from core to peripheral region due to the negative static temperature gradient. But other researchers investigating the static temperature gradient have found different results. Gao [72] found static temperature increased towards the wall. Farouk [64] have reported similar results. This would lead to heat transfer from the outer layer to the inner layer and would destroy the Ranque effect. Hence these conflicting findings of static temperature gradient call for further investigation.

Researchers like Fulton [71], Gutsol [78], Gao [72], Frohlingsdorf *et al.* [67], Farouk *et al.* [64], Aljuwayhel *et al.* [11] have experimentally and theoretically investigated and found formation of a *secondary circulation loop* inside the RHVT and proposed this loop as the main cause of thermal separation. The secondary circulation can be described as an adiabatic expansion process and transfers thermal energy from the inner core to the outer flow region as shown by Ahlborn *et al.* [4-8]. Thermal energy is absorbed by the secondary circulation along the centreline on the way to the cold end and transferred to the peripheral flow when it flowed with the primary flow to the hot end. In this way, temperature of the outer layer increases and the temperature of the core region decreases. But researchers like Nimbalkar and Muller [135] and Behera [22] have found that the formation of the secondary circulation depends on the relative size of the cold nozzle. As the diameter of the cold nozzle increases, the intensity of secondary circulation decreases and completely disappears when the ratio of the cold end diameter to the tube diameter is 0.58. Hence it can be concluded that the theory of secondary circulation inside the RHVT needs further clarification.

Many researchers like Kurosaka [104], Gao [72], Chu [42], Kuroda [103], Zaslavskii [204] have measured acoustic signals produced by RHVT and found that there is a relationship between the *acoustic streaming* and the temperature distribution in the RHVT. Kurosaka [104] have shown that the directions of propagation of Rankine vortex formed at the inlet of RHVT and the acoustic streaming are always the same. According to him the tangential velocity of the swirl is accelerated by the acoustic streaming and the Rankine vortex gets converted to a forced vortex by the acoustic streaming. The temperature distribution is then determined by the pressure gradient of the forced vortex flow. But it is required to be noted that the geometry of RHVT used by Kurosaka [104] in his experiments was different from a regular RHVT and only the cold outlet temperature was reported and effect of acoustic streaming on parameters like velocity, temperature and pressure distribution were not reported. Also, many theoretical studies like Behera [22] have produced a comparable result to Kurosaka's [104] experiments without taking acoustic streaming into consideration. Hence due to insufficient evidence, acoustic streaming cannot be claimed as the main reason for thermal separation in a RHVT.

Fulton [71] had experimentally shown that the magnitude of tangential velocity of the peripheral layer in a RHVT was lower than that of the axial layer which implies existence of a free vortex. Now researchers like Kassner & Knoernschild [93], Hartnett & Eckert [85], Deissler & Perlmutter [51], Reynolds [153], Silbulkin [165], Alimov [10], Linderstrom-Lang [116], Yang [202], Zhang [206], Gutsol [78], Trofimov [185], Kazantseva [94] have shown by computation, theory and experiments that because of the *shear stress between different fluid layers*, the slow peripheral flow was accelerated by faster moving inner flow, while the inner flow was decelerated. Thus, kinetic energy was transferred from the faster rotating inner layer to the slower rotating outer layer of compressible fluid due to friction between consecutive layers. Additional energy transported by turbulence between the two layers helped the formation of temperature gradient in the RHVT. The heat generated by friction between wall of the tube and compressible fluid layer converts kinetic energy to thermal energy, which causes the rise in temperature. This can be approximately calculated by the shear stress equations. Calculations based on these equations with turbulent flow assumption show that temperature rise due to friction between air flow and wall is not sufficient to form the temperature gradient in a RHVT which typically has a temperature rise of around 30–80 K. Experimental results published by Aljuwayhel *et al.* [11] and Hamoudi *et al.* [82] have shown that for RHVT of varied lengths (from 20 mm to 2586 mm) friction between air and wall is not a significant contributor to the temperature rise.

Ranque [150, 151] had suggested that *pressure change* in the RHVT is an important reason for thermal separation inside RHVT. It was explained by other researchers like Behera *et al.* [22], Kassner *et al.* [93], Arbuzov *et al.* [14], Crocker *et al.* [49], Kazantseva *et al.* [94], Parulekar [139], Colgate *et al.* [46] and Benbella [26] that sudden expansion occurs when the compressed air enters into the tube and the temperature of the air in the core drops due to expansion cooling. But significant difference was observed between the results from theoretical calculation based on adiabatic expansion and experimental results. This indicates the influence of factors other than pressure change in thermal separation in a RHVT.

Crocker *et al.* [49] have suggested that the *generation of a forced vortex* is the main reason for the existence of a radial pressure gradient. Pressure gradient of forced vortex causes high temperature at periphery due to compression in the high pressure peripheral region and low temperature at core due to expansion in the low pressure core region. Behera *et al.* [22] have shown that a forced vortex occurs in most of the central region of the tube and a free vortex is found in periphery because of the presence of a viscous boundary layer near the wall. But the explanation of radial pressure gradient due to forced vortex remains debatable. As per experimental data provided by Gao [72] and numerical investigations carried out by Behera *et al.* [22], the pressure at any point in the tube is lower than the inlet pressure, which suggests that expansion happens everywhere in the tube, even at the periphery. These observations are contradictory to the theory of compression at the peripheral region. Further, an experimental study conducted by Balmer [19] showed the thermal separation existed even when high pressure water was used as working fluid in the RHVT. This result contradicts the assumption made by Amitani *et al.* [12] that the compressibility of working fluid is a necessary condition for thermal separation in a RHVT.

Hence it can be seen from the above discussion that many of the theories have limited range of applications where as some of them are contested by other researchers. Some of the theories can support a limited number of experimental data and can predict the hot and cold end temperature only partially correctly. Hence no universal theory that can explain entire range of RHVT operation is available till date.

2.3.2 Challenges in making improved models

A detailed literature review states that performance of RHVT varies considerably with changes in a large number of parameters like tube length, tube diameter, divergence angle of the RHVT, orifice diameter, number of intake nozzles, nozzle geometry, hot end control valve parameters like valve angle, shape and size, cold mass ratio, inlet pressure, inlet flow rate, moisture content of the inlet gas, molecular weight of the working gas. The range of variation in each of the parameters selected for experiments is also far wide. For example the length to diameter (L/D_{vt}) ratio is taken in the range from 0.6 to hundreds. Saidi and Valipour [158] conducted experiments with vortex tubes to find the effect of different L/D_{vt} ratios on the operational characteristics of RHVT and found the optimum value of L/D_{vt} ratio is in the range $20 \leq L/D_{vt} \leq 55.5$ whereas Gao [72] obtained maximum cold air temperature difference for a L/D_{vt} ratio of 64.7. Hence it can be observed that a large number of experiments need to be conducted for each combination of different parameters to arrive at a conclusion. Even there are differences in optimum values of a given parameter reported by different researchers. Some of the parameters like inlet flow rates, cold mass fraction etc. have greater influence on the RHVT performance compared to other parameters like hot end control valve angle. Also the interdependencies of many parameters are unknown and in most of the cases these dependencies are non linear. Therefore in order to identify and model the optimum value of each important parameter from the combinational value of different parameters, a large number of experiments need to be conducted. This increases the requirement of time and resources and in turn the challenges involved.

Theoretical models are based on certain assumptions and need to be validated with experimental data. While a large amount of data is available for thermal separation, species separation data is scarce. Also experimental conditions are not fully available in many published results. One way to eliminate this problem is to generate in house experimental data. This requires installation and commissioning of an experimental setup with efficient instrumentation and data acquisition system. Temperature, pressure, flow rate and concentration of different species in inlet as well as outlet stream need to be measured carefully and accurately.

2.4 Previous research on thermal separation

Takahama and Yokosawa [176] examined the possibility of shortening the chamber length of a standard RHVT by using divergent tubes for the vortex chamber. They compared their results with those from the straight vortex chambers. They found that the uses of a divergent tube with a small angle of divergence led to an improvement in thermal separation and enable the shortening of the chamber.

Kurosaka *et al.* [105] carried out an experiment to study the total thermal separation mechanism in a uni-flow RHVT to support their analysis and concluded that the mechanism of energy separation in the tube is due to acoustic streaming induced by the vortex whistle (a shrill sound generated by the RHVT).

Schlenz [162] investigated experimentally the flow field and the energy separation in a uni-flow RHVT with an orifice rather than a conical valve to control the flow. The velocity profiles were measured by using Laser-Doppler Velocimetry (LDV), supported by flow visualization.

Experimental studies of a counter-flow RHVT with short length by Amitani *et al.* [12] indicated that the shortened RHVT of L/D_{vt} ratio 6 had the same efficiency as a longer and smaller diameter RHVT when perforated plates are equipped to stop the rotation of the stream in the tube.

Stephan *et al.* [174] measured temperatures in the standard RHVT with air as a working medium in order to support a similarity relation of the cold gas exit temperature with the cold gas mass ratio, established using dimensional analysis.

Negm *et al.* [130,131] studied experimentally the process of energy separation in the standard RHVTs to support their correlation obtained using dimensional analysis. They have found that in a double stage RHVT the performance of the first stage is always higher than that of the second stage. Lin *et al.* [112] made an experimental investigation to study the heat transfer behaviour of a RHVT with air as working fluid.

Ahlborn *et al.* [8] carried out measurements in standard RHVTs to support their models for calculating limits of thermal separation. They also attributed the heating to the conversion of kinetic energy into heat and the cooling to the reverse process. Ahlborn *et al.* [8] studied the thermal separation in a low-pressure RHVT. Based on their model calculation, they concluded that the thermal separation effect depends on the normalized pressure ratio ($\mu = (P_1-P_c)/P_c$) rather than on the absolute values of the entrance pressure, P_1 and cold end exhaust pressure, P_c. Further, Ahlborn and Groves [5] measured axial and azimuthal velocities by using a small Pitot probe and found that the existence of secondary outward flow in the RHVT. Ahlborn *et al.* [6] identified the temperature splitting phenomenon of a RHVT in which a stream of gas divides itself into a hot and a cold flow as a natural heat pump mechanism, which is enabled by secondary circulation. Ahlborn and Gordon [4] considered the RHVT as a refrigeration device which could be analysed as a classical thermodynamic cycle.

Arbuzov *et al.* [14] concluded that the most likely physical mechanism (the Ranque effect) involved inside the RHVT was viscous heating of the gas in a thin boundary layer at the wall of the vortex chamber and the adiabatic cooling of the gas at the centre on account of the formation of an intense vortex braid near the axis. Gutsol [78] explained that the centrifugal separation of "stagnant" elements and their adiabatic expansion causes the energy separation in the RHVT system.

Piralishvili and Polyaev [141] made experimental investigations on so-called double-circuit RHVTs. The possibility of constructing a double-circuit RHVT refrigeration machine as efficient as a gas expansion system was demonstrated.

Lewins and Bejan [110] have proposed that angular velocity gradients in the radial direction give rise to frictional coupling between different layers of the rotating flow. This coupling results into energy transfer via shear work from the inner layers to the outer layers rotating of fluid flow. Trofimov [185] verified that the dynamics of internal angular momentum leads to the Ranque effect.

Guillaume and Jolly [75] demonstrated the functioning of two RHVTs placed in series by connecting the cold discharge of one stage into the inlet of the following stage. From their results, it was found that for a two-stage RHVT a higher temperature reduction could be produced than one of the RHVTs operating independently.

Saidi and Valipour [158] presented the classification of the parameters affecting RHVT operation. They have studied operating parameters such as type of gas, inlet pressure, cold mass fraction, dryness of inlet gas and geometric parameters like, outlet orifice diameter, length and diameter of RHVT and shape of entrance nozzle. Singh *et al.* [167] reported the effect of various parameters such as cold mass fraction, nozzle and cold orifice diameter, hot end area of the tube and L/D_{vt} ratio on the performance of the RHVT. They observed that the effect of nozzle design was more important than the cold orifice design in getting higher thermal separations and found that the length of the tube had no effect on the performance of the RHVT in the range L/D_{vt} ratio 45– 55.

Promvonge and Eiamsa-ard [146] experimentally studied the energy and thermal separations in the RHVT with a snail entrance. In their experimental results, the use of snail entrance could help to increase the cold air temperature drop and to improve the RHVT efficiency in comparison with those of original tangential inlet nozzles. In another study Promvonge and Eiamsa-ard [143] reported the effects of (1) the number of inlet tangential nozzles, (2) the cold orifice diameter, and (3) tube insulations on the temperature reduction and isentropic efficiency in the RHVT.

Gao *et al.* [73] used a special Pitot tube and thermocouple techniques to measure the pressure, velocity and temperature distribution inside the RHVT. The Pitot tube has a diameter of 1 mm with one hole (0.1 mm diameter). In their work, the influence of different inlet conditions was studied. They found that rounding off the entrance could enhance and extend the secondary circulation of gas flow and thus improved the systems performance.

Aydin and Baki [16] investigated experimentally the energy separation in a counter-flow RHVT with various geometrical and thermo-physical parameters. The geometry of the tube was optimised to maximise the temperature difference between the cold outlet and inlet temperatures by changing the various dimensions of the tube such as the length of the RHVT, the diameter of the inlet nozzle, and the angle of the control valve. Moreover, the effects of various inlet pressure and different working gases (air, oxygen, and nitrogen) on temperature difference in a RHVT were also studied.

Kurosaka [104] studied analytically the Ranque-Hilsch effect and demonstrated that the acoustic streaming induced by orderly disturbances with the swirling flow were an important cause of the Ranque-Hilsch effect. He showed analytically that the streaming induced by the pure tone, a spinning wave corresponding to the first tangential mode, deformed the base Rankine vortex into a forced vortex, resulting in thermal separation in the radial direction. This was confirmed by his measurements in the uni-flow RHVT.

Stephan *et al.* [174] formulated a general mathematical expression for the energy separation process but this could not be solved because of the complicated system of equations. The system of equations formulated led to a similarity relation for the prediction of the cold gas temperature that agreed with the similarity relation obtained through dimensional analysis by Stephan *et al.* [174] in their earlier work. Experiments with air, helium, and oxygen as working fluid confirmed that theoretical consideration and agreed well with the similarity relation.

Dimensional analysis was also used by Negm *et al.* [131] who found that for similarity of tube geometry, the inside tube diameter was the main parameter, and this was confirmed by their experimental measurements. The correlation obtained from the analytical and experimental results was used to predict the overall cooling performance of RHVTs.

Balmer [19] investigated theoretically the thermal separation phenomenon in a RHVT. He used the second law of thermodynamics to show that thermal separation effect with a net increase in entropy is possible when incompressible liquids are used in the tube. This was confirmed by experiments with liquid water which showed that thermal separation occurred when inlet pressure was sufficiently high.

Nash [129] analysed the thermodynamics of vortex expansion and evaluated the design limitations of RHVTs to enhance the tube design and carried out experiments with the enhanced designs, including applications in both high and low-temperature cryogenic refrigeration systems.

Borissov *et al.* [29] examined analytically the flow and temperature fields in a RHVT using a model based on the analytical solution of complex spatial vortex flow in bounded regions, and based on an incompressible flow approximation to yield the three components of velocity for the complex flow structure with a helical vortex. The velocity values were introduced into the energy equation in which only the convective heat transfer due to complex topology of hydrodynamic field was considered. The predicted temperature field was in qualitative agreement with the measured.

Ahlborn *et al.* [8] developed a two-component model to determine the limits for the increase and the decrease in temperature within the standard RHVT. They showed that experimental data with air as working fluid were within the calculated limits and that the flow inside the tube was always subsonic.

Gutsol [78] discussed the existing theories of the Ranque effect and a new approach to the vortex effect was formulated, which provided an explanation of experimental data. He studied the efficiency of thermal insulation of microwave-generated plasma using reverse vortex flow by the way of experimental and numerical simulations. They concluded that this effect would take place due to radial motion of turbulent micro-volumes with differing tangential velocities in the strong centrifugal field.

Cockerill [44] studied the RHVTs for use in gas liquefaction and mixture separation as applied to uranium enrichment in order to determine the basic performance characteristics, the relationship between cold air temperature and hot air temperature with cold mass fraction, and the variation of hot discharge tube wall temperature with hot end tube length. Cockerill [44] also reported a mathematical model for the simulation of a compressible turbulence flow in a RHVT.

Nimbalkar and Muller [135] had pointed that a swirling secondary loop was formed when the cold orifice diameter was smaller than the diameter of the axial backflow core, and a return flow was generated at the cold end, inside the RHVT.

Xue *et al.* [200] have experimentally visualized flow pattern inside a RHVT using water as a working fluid. They have revealed the existence of multiple circulation regions within the RHVT using visualization technique. A further experimental study by Xue *et al.* [201] with air as working fluid shows that the flow in the RHVT consists of a forced vortex formed near the inlet gradually transforming to a free vortex.

Subudhi & Sen [175] have reviewed the RHVT variables of interest and the important experimental results available in the literature. They have established curve-fitting equations using data from the literature which can provide a rough estimate of temperatures at the two outlets.

Ghezelbash *et al.* [74] have proposed a scheme that uses a RHVT instead of throttle valve to reduce natural gas pressure at pressure drop stations. Unlike the throttle valve, RHVT divides the incoming stream into two cold and hot streams. Cold stream enters the shell and tube heat exchanger and receives geothermal heat. Then the warmed cold stream mix with hot steam outgoing from the RHVT, and goes towards the heater at low pressure. The proposed system can reduce energy consumption up to 88%.

2.5 Computational and experimental flow structure studies of RHVT

Different researchers have used different *turbulence models* to simulate the complex flow inside the RHVT like standard k–ε model (Aljuwayhel *et al.*[11]), large eddy simulation (Farouk *et al.* [64]) and an algebraic Reynolds stress model (Eiamsa-ard *et al.*, [60]). These numerical studies based on different models showed reasonable agreement with the experimental results of some researchers but failed to match with others under similar geometric and flow conditions. The reason behind these differences observed are different turbulence parameters and often contradictory assumptions used in numerical investigation. Hence further research needs to be carried out to include the effect of different geometrical parameters in the turbulence models those have significant influence on RHVT performance. Dutta *et al.* [57] have compared the performance of standard k–ε, RNG (Re-Normalization Group) k– ε, standard k–ω and SST (Shear Stress Transport) k–ω turbulence in predicting the thermal separation in a RHVT and found thermal separation predicted by the standard k– ε turbulence model is closer to the experimental results. Rafiee and Sadeghiazad [148] carried out parametric optimization for separation performance using experimental methods and 3D-CFD simulation.

Frohlingsdorf and Unger [67] studied the phenomena of velocity and energy separation inside the RHVT through the code system CFX with the *k–ε* model. Promvonge [144, 145] introduced a mathematical model for the simulation of a strongly swirling compressible flow in a RHVT by using an algebraic Reynolds stress model (Algebraic Stress Model‒ASM) and the *k–ε* turbulence model to investigate flow characteristics and energy separation in a uni-flow RHVT. It was found that a thermal separation in the tube exists and predictions of the flow and temperature fields agree well with measurements reported by Hartnett and Eckert [84, 85]. The ASM yielded more accurate prediction than the *k–ε* model. Behera *et al.* [23] investigated the effect of the different types of nozzle profiles and number of nozzles on thermal separation in the counter-flow RHVT using the code system of Star-CD with Renormalization Group (RNG) version of the *k–ε* model.

Aljuwayhel *et al.* [11] reported the energy separation and flow phenomena in a counter-flow RHVT using the commercial CFD (Computational Fluid Dynamics) code FLUENT and found that the RNG *k–ε* model predicted the velocity and temperature variations better than the standard *k–ε* model. This is contrary to results of Skye *et al.* [168] who claimed that for RHVT's performance, the standard *k–ε* model performs better than the RNG *k–ε* model despite using the same commercial CFD code FLUENT. Some of these investigators tried to employ higher-order turbulence models but they could not get converged solutions due to numerical instability in solving the strongly swirling flows. The application of a mathematical model for the simulation of thermal separation in a RHVT was reported by Eiamsa-ard and Promvonge [59, 60]. The work had been carried out in order to provide an understanding of the physical behaviours of the flow, pressure, and temperature in a RHVT. A staggered finite volume approach with standard *k–ε* model and an ASM with Upwind, Hybrid, SOU, and QUICK schemes were used to carry out all the computations. The computations showed that results predicted by both turbulence models generally are in good agreement with measurements but better agreement between the numerical results and experimental data was obtained for ASM. Finally, the numerical computations with selective source terms of the energy equation suppressed (Eiamsa-ard & Promvonge [59]) showed that the diffusive transport of mean kinetic energy had a substantial influence on the maximum thermal separation occurring near the inlet region. In the downstream region far from the inlet, expansion effects and the stress generation with its gradient transport were also significant. Most of the computations found in the literature used simple or first-order turbulence models that are considered unsuitable for complex, compressible vortex-tube flows. Dutta *et al.* [56,57] have used a three dimensional CFD model to investigate energy and species separation in a RHVT with compressed air at normal room temperature and cryogenic temperature.

Schlenz [162] investigated numerically the flow field and the process of energy separation in a uni-flow RHVT. Calculations were carried out assuming a 2D axisymmetric compressible flow and using the Galerkin's approach with a zero-equation turbulence model to solve the mass, momentum, and energy conservation equations to calculate the flow and thermal fields. The calculations failed to predict the velocity and temperature profiles in the tube but agreed qualitatively with the measurements of Lay [107,108].

A numerical study of a large counter-flow RHVT with short length was conducted by Amitani *et al.* [12]. The mass, momentum and energy conservation equations in a 2D flow model with an assumption of a helical motion in the axial direction for an inviscid compressible perfect fluid was solved numerically. They reported a good agreement of predictions with their measurements and concluded that in radial flow in a RHVT compressibility is essential to thermal separation.

Thakre & Parekh [180] have carried out CFD study on counter flow RHVT using different gases at various values of cold mass fraction and using different turbulence models. Thakre *et al.* [181] have found the standard k-ε turbulence model is well capable to replicate the turbulence inside RHVT. The simulation had identified a re-circulating secondary flow near the inlet region of RHVT which is accompanied by backflow at cold end for smaller values of cold mass fraction. Thakre *et al.* [182] have also carried out a review of different experimental, computational and optimization studies of thermal separation and flow physics of RHVT.

Bej & Sinhamahapatra [24] have numerically shown that cascading of RHVTs is a possible strategy to extract significantly larger amount of useful work. Also they have studied the conversion of inlet pressure energy into thermal energy which is associated with the heat and work transfer due to shear along the radial, axial and tangential directions. They have concluded that the work transfer due to the action of tangential shear is always from the cold to hot fluid layers and is the most dominant factor in the thermal separation process.

Manimaran [120] described energy separation in a RHVT with the simulation of a three dimensional flow field with rectangular and trapezoidal shaped inlets and compared their performance by varying aspect ratio. From the results, it was observed that inlet with higher aspect ratio gives higher thermal separation. The trapezoidal inlet configuration is found to give higher thermal separation as compared to a rectangular shape.

Simo~es-Moreira [166] had considered the RHVT operations as a thermodynamic cycle and developed a control volume approach for conservation of mass and energy to develop a thermal model of the RHVT. He had shown that operations in a RHVT were highly irreversible. Subudhi and Sen [175] have developed relation among RHVT thermal performances and it's parameters by curve-fitting methods using data from the literature.

To explain the energy separation in a vortex tube, a description of the physical process of the air flow inside the tube and analysis of the velocity distribution are required. In early studies, flow visualization was employed to show the flow structure. In an early attempt MacGee [118] used a coloured dye in RHVT system to visualise the flow and later, water was used by Lay [107,108] in the RHVT system, but nothing could be observed in their experiments. A mixture of powdered carbon and oil by Sibulkin [165] and smoke by Smith [169,170] were used to visualise the flow in a vortex tube, but their results were not clear enough to draw a conclusion about the flow structure. The structure of the vortical double helix was visualized by Arbuzov *et al.* [14] by the method of Hilbert dichromatic filtering. He managed to observe the formation of an intense vortex flow near the axis for the first time.

Aydin and Baki [16] implemented flow visualization in their investigation, and presented the clear flow trace in a vortex tube. Flow visualizations were conducted in order to obtain a general impression of the flow within the tube. For the optimum geometry of the vortex tube explained above, a vortex tube made of perspex was constructed by Aydin and Baki [16] to visualize the flow inside.

Zepeda *et al.* [205] had built an acrylic vortex tube and flow inside the tube was visualized by introducing tracer particles (baby powder) at 5 atm. It was observed that air flows in a helical trajectory along the tube and a temperature difference of 11°C was achieved between the hot and cold ends of the Ranque-Hilsch tube. Abe *et al.* [2] visualized flow inside a counter flow type vortex tube. The flow visualization was performed by means of the tuft stick method. A tuft dyed with fluorescent dyes was used and the length of the tuft was changed. They have reported presence of a secondary flow. In a previous study Abe & Nakano [1] reported an experimental study and flow visualization in the counter-flow type vortex tube. The flow visualization was performed by means of liquid injection. The liquid used was water or ethyl alcohol dyed by fluorescence. They have found in case of water as working fluid, a helical line was observed on the inner wall of RHVT because of condensation of water. In the case of using ethyl alcohol the right helicoid and Gortler vortices are observed on the wall. They have also reported a rotating ring near the stagnation point and the inner flow except the axial flow was almost a spiral flow in the plane.

2.6 Previous research on species separation

A number of researchers have carried out species separation studies with RHVT aimed for different applications. Kevin *et al.* [95] have shown that a RHVT contactor can be used as an inexpensive mean to achieve carbon di-oxide separations by forcing an expanding gas and dispersed liquid absorbent into a turbulent rotational flow field where transfer of carbon di- oxide transfer to the absorbent phase is greatly enhanced.

Kulkarni and Sardesai [102] used a RHVT for separating methane and nitrogen from a mixture and found that there was partial species separation. This leads to an increased methane concentration of at one exit compared to the inlet and a lower concentration at the other exit. Hellyar [87] have reviewed the possibilities of using RHVT in liquefaction and separation of natural gas with emphasis on design and operating parameters.

Fekete [66] has measured the value of centrifugal acceleration in the RHVT to the order of 10^6 times of gravitational acceleration which was found stronger than centrifugal acceleration in other centrifugal separators. The tube has been extensively used in petroleum industry and many plant processes for mass separation of gases of different molecular weights. The separation of propane and other higher molecular weight hydrocarbons from natural gas was found feasible.

Cockerill [44] have reported use of RHVTs for gas liquefaction and mixture separation. Balepin *et al.* [18] and Crocker *et al.* [49] have shown that at very low temperature when compressed air enters the RHVT, along with energy transfer significant mass transfer is observed. The air is separated into one predominantly oxygen rich stream (upto 90% enriched) and another predominantly nitrogen rich stream. Hence RHVT can be used for in-flight air collection and enrichment system (ACES) of air breathing propulsion (Dutta *et al.*, [58]).

The conical RHVT was investigated theoretically by Khodorkov *et al.* [96]. Poshernev and Khodorkov [142] have suggested utilization of RHVT as a pre-cooling system for natural gas liquefaction.

Dust separation characteristics of a counter flow RHVT were investigated by Riu *et al.* [156]. They have shown that the RHVT can be used as an efficient pre-skimmer to separate dust particles from waste gas.

Yilmaz *et al.* [203] have observed that the RHVT used for gas liquefaction and separation can have much greater diameters than those available commercially. Liew *et al.* [111] have investigated the possibility to use the RHVT as a device for removing un-desired condensable components from gas mixtures. They have developed a model to simulate the droplet behaviour inside the RHVT. They observed that increasing the humidity at the inlet of the RHVT results in larger droplets and a higher liquid concentration. They have also reported that the separation process takes place near the inlet of the RHVT.

Kukis *et al.* [101] have shown that by using a RHVT in the recirculation loop of a diesel engine the nitrous oxide content of exhaust gas can be reduced significantly. Farouk *et al.* [65] used an axi-symmetric CFD model with Large Eddy Simulation (LES) technique to predict the thermal separation and the mass separation of nitrogen-helium mixture in a RHVT. The species separation was attributed to the Soret effect or thermal diffusion.

Presence of radial separation in a strong centrifugal field was also suggested by the authors.

Mohammadi & Farhadi [126] have investigated the separation performances of RHVT for a hydrocarbon mixture. The increase in concentration level achieved by a single RHVT is insufficient to obtain the desired concentration of hydrocarbon in a single step. Hence a number of RHVTs were connected in series. In order to obtain more throughput of material, the RHVTs were also connected in parallel in an industrial plant. The arrangement of species separating units connected in parallel and in series is called a 'cascade'. Mohammadi and Farhadi [126] have made a comparison between a distillation column and a cascade made of RHVTs providing similar separation and it was shown that a RHVT cascade performed better than the distillation column with respect to stage efficiency, capital and operating cost.

2.7 Previous research on Heat, Mass and Momentum transfer analogies

In the present research work a heat and mass transfer analogy has been introduced to calculate the value of mass transfer coefficient from the heat transfer coefficient. Hence a literature survey has been carried out to find out different available heat, mass and momentum transfer analogies and their applicability to rotating flow systems. Several research papers and book chapters had been published on the topic of heat, mass, and momentum transfer analogies for the fully developed turbulent as well as laminar flow of fluids in circular tubes. As the flow inside RHVT is rotational in nature, the literature survey carried out is limited to heat and mass transfer analogy applied to rotational flow.

For turbulent heat transfer from a rotating disk, semi-empirical calculations based on the friction analogy were first carried out by Cobb and Saunders [43] and later refined by Kreith *et al.* [99]. The analogy results of Kreith *et al.* [99] agree favourably with the experimental data. Tien and Campbell [183] experimentally investigated convective heat transfer from isothermal rotating cones by measuring sublimation rate from naphthalene-coated cones and using the analogy between heat and mass transfer. Dunthorn [55] had used the Chilton Colburn analogy to design a batch desublimer. Kyung *et al.* [106] determined the detailed heat transfer coefficients using a heat and mass transfer analogy in order to study, the effects of bleed flow on heat and/or mass transfer in a rotating square channel. Wilk [198] has applied the mass/heat transfer analogy to the investigation of convective laminar heat transfer in rotating and stationary short mini-channels. Wilk [198] has provided a general form of the mass/heat transfer analogy, assumptions and the dimensionless numbers and equations describing the analogy. He has described the application of the mass/heat transfer analogy by Chilton and Colburn [39] in the study of heat transfer in short rotating mini-channels. An important conclusion made by the author was that the uncertainty in mass/heat transfer analogy is of the same order of magnitude as the uncertainty of the heat transfer coefficient determined by means of a specific measuring technique or some suitable correlation. Harmand *et al.* [83] have reviewed methodologies which are used to study rotating and stationary surfaces with or without jet impingement and rotor-stator configurations with or without jet. The general experimental technique of naphthalene sublimation has been used by researchers like Chen *et al.* [38], Cho *et al.* [40,41], He *et al.* [86] and others to study the local convective heat transfer in rotating disk configurations. The Reynolds analogy is then used to link the mass transfer to the heat transfer using the local Nusselt, Sherwood, Schmidt and Prandtl numbers. Venkatesan and Fogler [189] have mentioned that in processes, such as wax deposition in petroleum pipelines and frost formation on heat exchanger surfaces, where the temperature gradient creates a concentration gradient, the usual heat-mass transfer analogy is not valid. In the present work the concentration gradient is a result of radial pressure gradient due to a strong centrifugal field.

2.8 Gap areas for research

A number of published literatures on RHVT have been surveyed. From the literature surveyed it became evident that research work carried out in the field of species separation using RHVT is far less than that carried out in the field of energy separation. It has also been found that data on RHVT as a species separation device are only a handful, although this area of research on species separation by RHVT is particularly of interest to the present research. At the same time, it has been strongly felt that in order to understand the species separation phenomenon it is of utmost importance that energy separation by a RHVT must be thoroughly studied. Further from the following observation of researchers like Eiamsa-ard & Promvonge [60] it can be attributed that results obtained in many previous studies related to energy separation are **inconclusive** or even **contradictory.**

"*Although many experimental and numerical studies on the vortex tubes have been made, the physical behaviour of the flow is not fully understood due to its complexity and the lack of consistency in the experimental findings. ... Most of the past work efforts based on theoretical and analytical studies have been unsuccessful to explain the energy separation phenomenon in the tube.*"

Hence the present research endeavour will focus on species separation in RHVT although this phenomenon will be studied in conjunction with energy separation phenomenon. Moreover the following research questions are generated during the literature survey:

- How the species separation depends on thermal separation and whether species separation is controlled by thermal separation?
- Can the thermal and species separation be explained and calculated using a single theory?
- What are the principal parameters that influence species separation using RHVT?
- What is the effect of different sizes of vortex generators on the thermal as well as species separation?
- Why a short RHVT produces lower thermal separation and higher species separation?
- What is the critical inlet Reynolds number at which the maximum species separation was observed?

A study to find out suitable answers of the above questions will form a part of the present research work.

2.9 Summary

This chapter is dedicated to literature survey on the subject of research and is opened with an overview of early global research conducted. This is followed by a detailed discussion of RHVT theories proposed by different researchers till date. Limitations of existing models and challenges involved in research extension to propose improvement over these models have been discussed. The literature survey work has been broadly classified into two categories of thermal and species separation and each category was further subdivided into experimental and theoretical work. The next section is dedicated to literature survey carried out on heat and mass transfer analogy applied to rotational flow. Applications of RHVT in different industries have been discussed in detail in the subsequent section.

Literature survey on flow visualization experiments inside vortex tube has been added followed by a section identifying gap areas for further research.

Chapter 3
Research methodology

"Highly organized research is guaranteed to produce nothing new."
Frank Herbert, Dune

3.1 Introduction

In the first chapter of this thesis we have introduced the topic of research. Also in this chapter the problem has been defined along with objectives of the present research work. In the second chapter the relevant literature study has been carried out and the limitations in the previous research work have been discussed. These led to identification of areas of further research. The research questions, for which appropriate answers need to be sought, have been posed. Hence the next logical step is to ascertain the research methodologies that can be adapted to find out answers to these research questions. In this chapter this issue of choosing the appropriate research methodology for the present research work have been discussed.

The use of the scientific method of research is intended to provide an objective, unbiased evaluation of data leading to useful theories or models that can be used in the relevant field of research. To investigate the research questions posed and evaluate the hypotheses assumed in a systematic way it is very important that a step by step approach of research work is adapted. The research methodologies adapted in the present research work are the following

- Modelling of heat and mass transfer inside a RHVT
- Experimental validation of the model
- Parametric studies

In the following sections of this chapter an outline of these methodologies has been given along with their suitability for the research. Requirement of these methodologies has been justified and connectivity among them has been established. Hence this chapter acts as a bridge between the previous two chapters where basics of the research have been covered and the next few chapters where the theoretical model have been developed, experimental results have been analyzed and parametric studies have been carried out.

3.2 Modelling of heat and mass transfer inside a RHVT

The first research question in section 2.8 of this thesis asks whether the thermal and species separation inside a RHVT are interrelated i.e. whether thermal separation depends on species separation or vice versa. An initial experiment has been planned to study this aspect of RHVT and it was found that heat and mass transfer phenomena inside a RHVT are dependent on each other. This leads to the question that whether a single theory can be used to explain or model the thermal and species separation phenomena inside a RHVT. This calls for the idea to apply the well known heat and mass transfer analogies described in heat and mass transfer literature to develop this model.

Review of previous studies characterising the heat and mass transfer in different heat and mass transfer devices has revealed that the mechanisms of heat and mass transfer are similar and analogous. Therefore, in cases where, either the heat or mass transfer data are not reliable or may not be available, the heat and mass transfer analogy can be used to determine the missing or unreliable set of data. In this regards, the Reynolds analogy is the simplest correlation and is applicable only for the special case where the Prandtl and Schmidt numbers are both equal to unity. Chilton and Colburn [39] introduced a correlation to predict the coefficient of mass transfer from the experimental data of heat transfer and fluid friction, which is applicable for fully developed flow inside the tubes or between parallel plates with; *0.6 <Pr <60* and *0.6 < Sc <3000.* This Chilton-Colburn analogy has the form

$$\frac{f}{2} = St\, Pr^{2/3} \equiv j_h, \qquad 0.6 < Pr < 60 \tag{3.1}$$

and,

$$\frac{f}{2} = St_m Sc^{2/3} \equiv j_m \qquad 0.6 < Sc < 3000 \tag{3.2}$$

where j_h and j_m are the Colburn *j* factors for heat and mass transfer, respectively. For laminar flow, equation 3.1 and 3.2 are only appropriate when p ressure gradient is negative, but in turbulent flow, conditions are less sensitive to the effect of pressure gradients and these equations remain approximately valid (Incropera *et. al.* [91]). If the analogy is valid at every point on a surface, it can be applied to the surface average coefficients.

The core idea of the present mass transfer modelling is to calculate species separation along the horizontal length of the RHVT. Air as a binary mixture of nitrogen and oxygen is considered as the working fluid. The RHVT is divided into two flow regions i.e. wall flow region and core flow region. Now at any point within the RHVT at a distance *z* from the inlet, the base rate of mass transfer to the wall flow region from the core flow region may be expressed as

$$\left(\frac{\partial m}{\partial t}\right)_z = M_1 K_1 (P - P_w) \tag{3.3}$$

The mass transfer coefficient K_1 is difficult to obtain for diverse system. Hence using Chilton Colburn analogy under acceptable domain we get the mass transfer coefficient, using the heat transfer coefficient value. The heat transfer coefficient h can be calculated using either experimental data or some empirical correlation. One such empirical correlation is Seider-Tate correlation that is applicable for forced convection for turbulent pipe flow under the condition that 0.7< Pr < 160, *Re* >10000 and $\frac{L}{D} \geq 10$. In the present calculation this correlation is used to determine the heat transfer coefficient and it is given by

$$Nu = 0.027 Re^{4/5}\, Pr^{1/3}\ \left(\frac{\mu}{\mu_s}\right)^{0.14} \tag{3.4}$$

The Sieder-Tate correlation takes into account the change in viscosity $\mu\ and\ \mu_s$, due to change in temperature between the gas average temperature at the core region and the heat transfer surface temperature, respectively.

In the above work the temperatures at the cold (T_2) and hot (T_3) outlet have been experimentally determined. A linear variation of temperature of the peripheral stream is assumed in the mathematical model from inlet temperature (ambient temperature) up to the hot outlet temperature (T_3). Thus this model requires experimental input and can simulate conditions for which experimental data is available. Hence this model can be regarded as a semi emperical model. Further, an extension of this modelling work on mass transfer is done by combining an analytical model for heat transfer in this model. This heat transfer model has been implemented to calculate the thermal gradient along the length of the RHVT. Together with these set of numerically calculated thermal data the previously developed mass transfer model can calculate the concentration gradient along the axial direction of the RHVT, and thus becomes fully theoretical.

Now in general, theoretical prediction of the RHVT performance requires the aid of a tool like Computational Fluid Dynamics (CFD) to resolve the flow distribution followed by solving diffusion equation to calculate species separation. CFD of the RHVT involves discretisation of flow domain and solution of high speed compressible flow field. Simulation of flow field and temperature distribution requires solution of three dimensional Navier Stokes equations along with the energy equation and ideal gas assumption. Generation of grid and running the solver requires large computation time. The computation time overhead increases considerably while employing advanced computational tools like Reynolds Average Navier Stokes (RANS), LES or Direct Numerical Simulation (DNS). In the present work a one dimensional mathematical model has been developed. This model can compute mass transfer in a counter current RHVT based on inlet pressure, temperature, species concentration, flow rate and outlet temperature and flow rate. This model can be used for rapid design and simulation of species separation in a RHVT.

3.3 Validation of the model with experimental data

As described in section 3.2 above a mathematical model has been developed for simulation and prediction of thermal as well as species separation in a RHVT. Now in order to validate the model, it becomes necessary to verify the outcome of the model with experimental data of thermal and species separation. It is found in the literature that a large number of experimental data are available on thermal separation but experimental data on species separation is scarce. Hence a laboratory scale experimental unit has been commissioned. In this setup the thermal and species separation of air as a binary mixture of oxygen and nitrogen can be studied. The setup has been designed to experiment with different sizes of vortex tubes and each RHVT can be fitted with different vortex generators inside it. This experimental setup has provision to control and measure the inlet flow rate and pressure of the air. Cut (defined by the product to feed ratio of a separating element) or cold mass fraction (defined by the ratio of cold outlet mass flow rate to inlet mass flow rate) of the RHVT unit can be varied by changing the opening of the hot end valve. Further the temperatures, flow rates and pressures at the two outlets (cold and hot) can be measured. Another important feature of the experimental setup is that sample of the separated gas streams can be collected from the hot and cold ends of the RHVT. These samples collected in gaseous form are analyzed by a Residual Gas Analyzer (RGA). Thus the species as well as thermal separation can be calculated in terms of temperature and concentration of the hot and cold end gas stream respectively.

The separation factor of the lighter species for a binary separation is defined by

$$\alpha = \left(\frac{1-N_3}{N_3}\right)\left(\frac{N_2}{1-N_2}\right) \tag{3.5}$$

and is a measure of the species separation inside the RHVT. Also in the present work the following expression is used as a measure for thermal separation

$$\textit{Thermal separation} = \frac{T_2/(T_1 - T_2)}{T_3/(T_3 - T_1)} \tag{3.6}$$

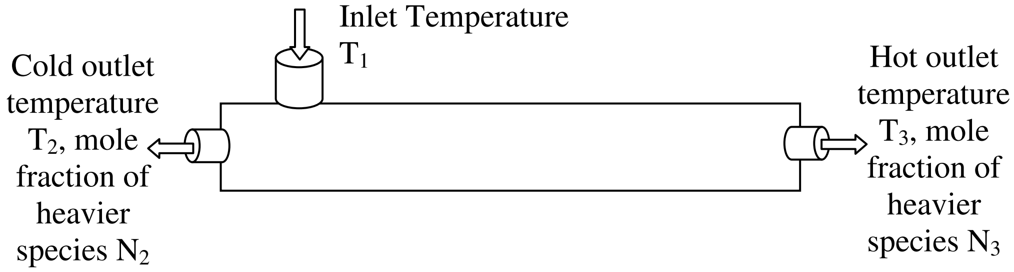

Fig.3.1 Temperature and concentration at the inlet and outlet of a RHVT

where the temperature and concentration are measured at the inlet and outlets of the RHVT as shown in the figure 3.1. The numerator of the expression denotes the ratio of cold outlet temperature and fall in cold outlet temperature with respect to the inlet gas temperature. The denominator of the expression denotes the ratio of hot outlet temperature and rise in hot outlet temperature with respect to the inlet gas temperature.

The aim of developing the one dimensional model for simultaneous heat and mass transfer inside a given RHVT is to predict the thermal and mass separation at the two ends (hot and cold) accurately for a set of inlet conditions. Hence the model is required to be validated for accuracy of its output and consequently it is needed to determine whether output from the model fulfils the above mentioned aim. Now, from the computer code the composition of two outlet streams of the RHVT can be computed. Using equation (3.5) the binary separation factors for a mixture of two gases (like air as a mixture of oxygen and nitrogen) can be computed. Initially when the thermal model is not used, the computer code requires experimentally measured thermal data at the inlet and two outlets. Hence separation factors were computed at experimental conditions where temperature and pressure data were available. The oxygen concentration values at the cold and hot outlets were computed using the computer code based on the model. Now a comparison of experimental and computed values of separation factors for a given vortex generator is plotted with inlet feed flow rate as the independent variable, for different values of hot end valve opening. Thus the values obtained from the model are validated with experimental data.

As an extension of the modelling work on mass transfer in a RHVT stated above, a mathematical model for heat transfer provided by Shannak [164] has been implemented to calculate the thermal gradient along the length of the RHVT. Together with these set of numerically calculated thermal data our previously developed mass transfer model can calculate the concentration gradient along the axial direction of the RHVT without any experimental input, and thus becomes fully theoretical. Now, Subudhi and Sen [175] had published a collection of experimentally obtained thermal separation data in RHVT for a range of lengths, diameters, inlet pressures and cold mass fractions with air as working fluid. Some of these data have been used to verify the result from the thermal model adapted in present work. It could be concluded from the comparison that the model could predict the thermal data published in the literature with acceptable accuracy for engineering purposes.

Further a set of verification study of the computer code based on the simultaneous heat and mass transfer model has been carried out. Values of the separation factors and percentage error in component balance of the heavier species as well as the overall mass balance are calculated for the set of data provided by Subudhi and Sen [175]. It was observed that the percentage error in component and overall mass balance are within acceptable limit. Hence the above work completes the validation and verification work of the proposed heat and mass transfer model and the code developed based on it, with respect to experimental data from the in house experimental setup as well as that from literature.

3.4 Parametric studies

In the next part of the research work a parametric study has been carried out in order to understand the effect of different parameters of a RHVT on the separation characteristics of the device, particularly on species separation. The RHVT parameters are broadly divided into two sets in order to carry out the parametric studies. The first set consists of the geometrical characteristics of the RHVT i.e.

- diameter of the hot and cold tubes
- length of the hot and cold tubes
- cold orifice diameter
- number of inlet nozzles

These are basically design parameters of the RHVTs and are fixed during their design. In the second set, effect of important operating parameters like

- inlet gas pressure
- inlet gas flow rate

- cold mass fraction

on the separation performance have been analyzed. For each parameter, the thermal and species separation mechanism and the flow-fields inside the RHVT are explored by investigating the pressure, velocity, and temperature fields. For carrying out the parametric studies data obtained from literature, in house experimental setup and the code developed in the present work have been extensively used.

These studies answer the research questions raised in chapter 2 like

- What are the principal parameters that influence species separation using RHVT?
- Why a short RHVT produces lower thermal separation and higher species separation?
- What is the critical inlet Reynolds number at which the maximum species separation was observed?

3.5 Summary

This chapter outlines the methods of research adapted in the present work. Each method is stated briefly along with the justification for adopting the method. The resources necessary for the method have been described. Also objective of each method has been discussed in brief. Further the connectivity among different methods adopted has been established. Hence this chapter serves as a brief overview of the research methodology proposed.

Chapter 4
Experimental setup

"We are at the very beginning of time for the human race. It is not unreasonable that we grapple with problems. But there are tens of thousands of years in the future. Our responsibility is to do what we can, learn what we can, improve the solutions, and pass them on".

- Richard Feynman

4.1 Introduction

In the present research work a mathematical model has been proposed for simulation and prediction of thermal as well as species separation in a RHVT. This model is described in details in the next chapter. Now in order to validate the model, it is necessary to verify the outcome of the model with experimental data of thermal and species separation. It is found in literature that a large number of experimental data are available on thermal separation but experimental data on species separation is scarce. Hence a laboratory scale experimental unit has been commissioned. In this setup the thermal and species separation of air as a binary mixture of oxygen and nitrogen can be studied. In this chapter a detailed description of this experimental setup with peripherals as well as the experimental procedure has been given.

4.2Experimental setup and methods

The schematic diagram of the RHVT test facility is shown in figure 4.1. A photograph of the setup has been given in figure 4.2. The RHVT is thermally insulated and tips of three Resistance Temperature Detectors (RTDs) T_1, T_2 and T_3 were connected to the inlet, cold outlet and hot outlet respectively for measuring the gas temperature. Three more RTDs are connected to the horizontal tube of the RHVT at equal intervals to measure the skin temperature of the RHVT. Out of these three RTDs the first one measuring temperature

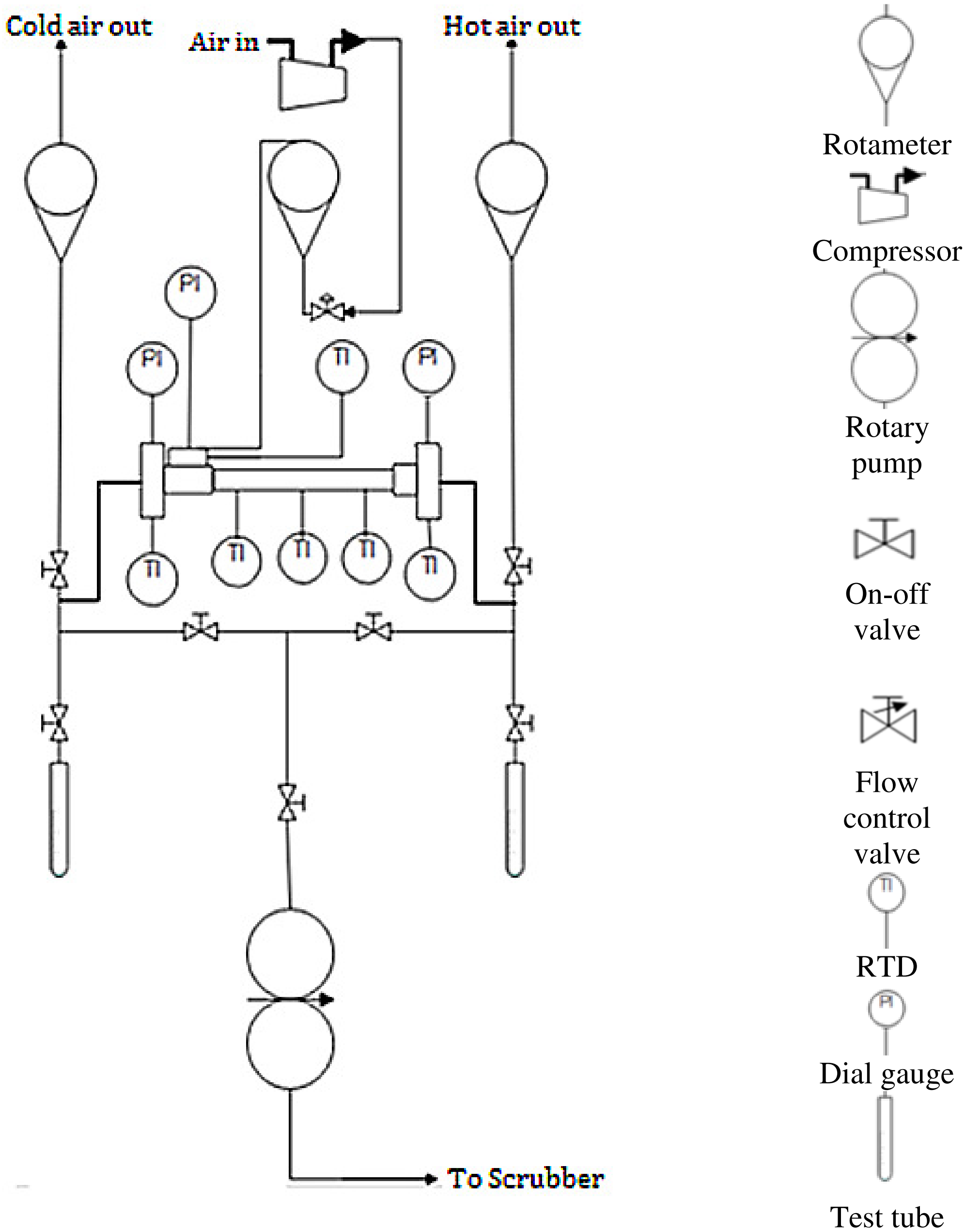

Fig. 4.1 Schematic diagram of experimental setup

T_{RTD1} is located near the hot end while the third RTD measuring temperature T_{RTD3} is located near the vortex chamber. The second RTD measuring temperatureT_{RTD2} is located halfway between these two RTDs. Both the cold and hot outlets of the RHVT are connected with two horizontal cylindrical chambers in order to obtain mixing cup temperatures at the outlets. Hence the temperature registered by RTDs at the cold and hot outlets (T_2 and T_3 respectively) are mixing cup temperature. All these six RTDs are connected to temperatures scanners which can show the temperature values during experimentation.

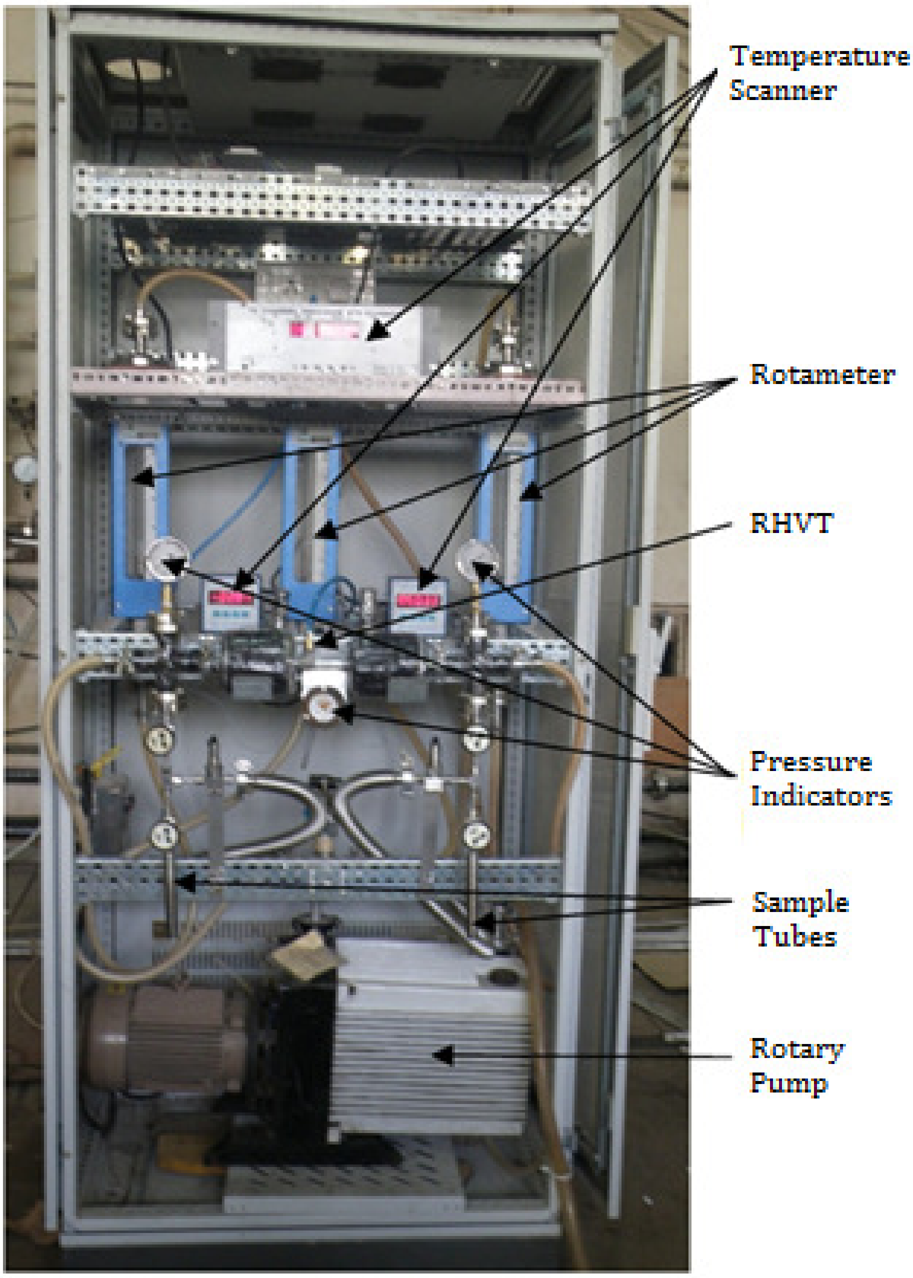

Fig. 4.2 Photograph of experimental setup

Three dial gauges were connected to the inlet, cold outlet and hot outlet respectively for measuring the gas pressure at these stations. Compressed air from an air compressor is passed through a dehumidifier and became moisture free. This high pressure air enters the RHVT inlet through a rotameter and the inlet volumetric flow rate was measured from the rotameter reading. Similarly the volumetric flow rates of air coming out from the cold and hot outlets of the RHVT were measured from the two rotameters attached to these outlets respectively. Temperature correction of flow at the hot and cold end of the RHVT is done using the mixing cup temperature readings T_3 and T_2 respectively. Inlet pressure and volumetric flow rate of air entering the RHVT were controlled by a flow control valve fitted in the inlet line.

Two sample collection lines were connected to the hot and cold ends of the RHVT in order to collect gaseous sample for mass spectrometric analysis. These two lines are connected with two sample tubes located at the end of the lines as shown in the schematic diagram. While sampling, both the sample tubes are isolated from the main system by closing the two isolation valves and then connected to a rotary pump. Thus the sample tubes are evacuated and the vacuum pumping lines are closed. Next the sample tubes are connected with the main system by opening the two control valves and gas samples flowing out of the hot and cold end of the RHVT enters the respective sample tubes connected to the lines due to pressure difference. Finally the valves situated upstream of the test tubes are closed and detached along with the tubes from the sample lines. Thus the samples become ready for composition analysis. Mass spectrometric analysis of the samples was carried out using a HIDEN™ make Residual Gas Analyzer (RGA) mass spectrometer.

4.3 Specification of the measuring instruments

All the measuring instruments are locally procured and conform to international standard. PT100 temperature sensors were used to measure the gas temperatures. Temperatures are logged in RTD scanners with accuracy of ±0.1°C. The maximum possible error in the case of temperature measurement was calculated from the minimum values of the temperatures measured and the accuracy of the instrument. The error in the temperature measurement is:

$$\frac{\partial T}{T} = \sqrt{\left(\frac{\partial T_{RTD}}{T_{min}}\right)^2 + \left(\frac{\partial T_{scanner}}{T_{min}}\right)^2} = \sqrt{\left(\frac{0.5}{10}\right)^2 + \left(\frac{0.1}{10}\right)^2} = 0.05 = 5\% \tag{4.1}$$

Bourdon-tube-type dial gauges were used to measure the gas pressure. These gauges conform to IS 3624:1987 (R2004) standards. The error in the transducer and reading error are of the order 0.01 kg/cm^2. Hence the error in the pressure measurement is:

$$\frac{\partial P}{P} = \sqrt{\left(\frac{\partial P_{tran}}{P_{min}}\right)^2 + \left(\frac{\partial P_{reading}}{P_{min}}\right)^2} = \sqrt{\left(\frac{0.01}{1.5}\right)^2 + \left(\frac{0.01}{1.5}\right)^2} = 0.01 = 1\% \tag{4.2}$$

Flow measurements were made using gas flow rotameter. Uncertainty analysis conducted according to the standard procedures has shown that the accuracy in the flow rate measurement is +/- 2% of full flow.

4.4 Details of the RHVTs and generators used

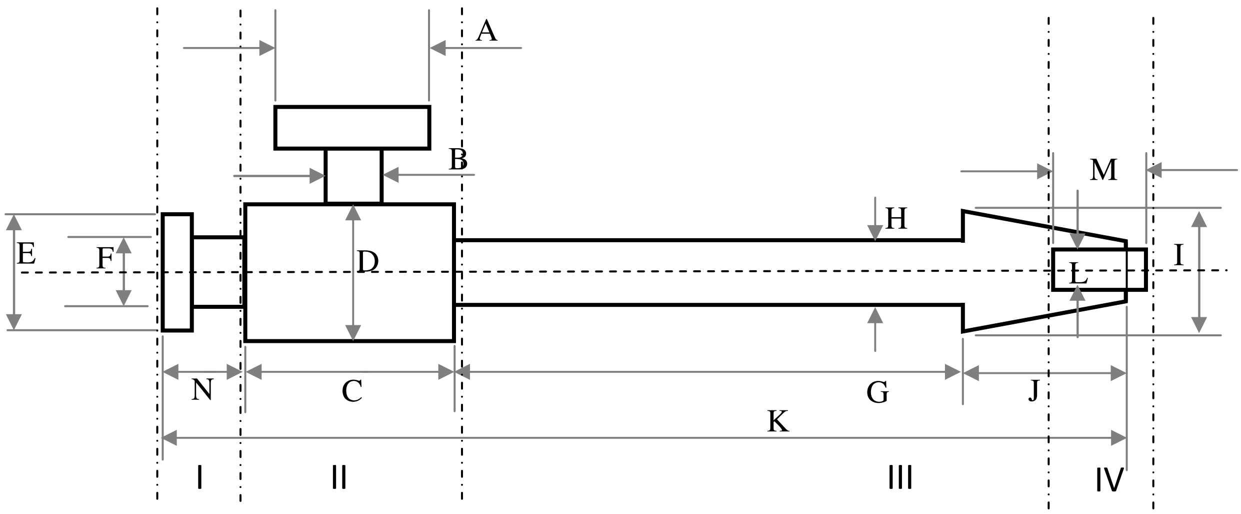

Fig. 4.3 Schematic diagram of RHVT (Parts of the figure are not to scale)

Two FRIGID-X^{TM} make RHVTs - one medium size and other small size (both stainless steel bodies) were used for experiments conducted in the present study. The RHVT body is made up of four different segments. Each of these segments is described in details below. A schematic diagram of the RHVT is given in figure 4.3. All the four segments of the RHVT are marked by Roman numerals in this figure. These segments are

I. Cold outlet section,
II. Vortex generation chamber section,
III. Vortex tube section and
IV. Hot outlet section

Lengths for different segments of a RHVT are shown by symbols in figure 4.3. Actual values against each symbol for both small and medium type RHVT are given in table 4.1.

Table 4.1 Dimensions of different parts of RHVT (All dimensions are in mm)

Serial no.	**RHVT parts**	**Symbols**	**Value for small RHVT**	**Value for medium RHVT**
1	Inlet outer diameter	A	10	14
2	Inlet inner diameter	B	06	10
3	Vortex generator chamber length	C	25	37
4	Vortex generator chamber outer diameter	D	21	29
5	Cold end outer diameter	E	19	25
6	Cold end inner diameter	F	11	17
7	RHVT length	G	45	65
8	RHVT outer diameter	H	10	12
9	Hot end outer diameter	I	14	16
10	Hot end length	J	27	32
11	RHVT total length	K	104	157.5
12	Hot end inner diameter	L	10	12
13	Hot end control valve length	M	21	24
14	Cold end length	N	20	23.5

4.4.1 Cold outlet section

The cold outlet section has three parts i.e. the cold exhaust tube, the cold outlet orifice and cold outlet plate. This section exhausts the cold gas stream from the center of the vortex chamber. The cold outlet plate is made of nylon in order to reduce heat transfer from the surrounding atmosphere. The cold outlet section is shown in more detail in figure 4.4. It has a straight nylon tube with inner diameter F and outer diameter of the exhaust is E.

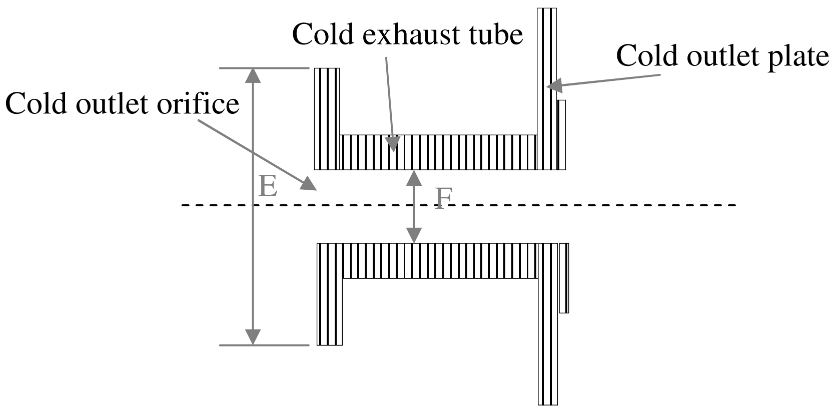

Fig. 4.4 Schematic diagram of cold section (Parts of the figure are not to scale)

4.4.2Vortex generator chamber section

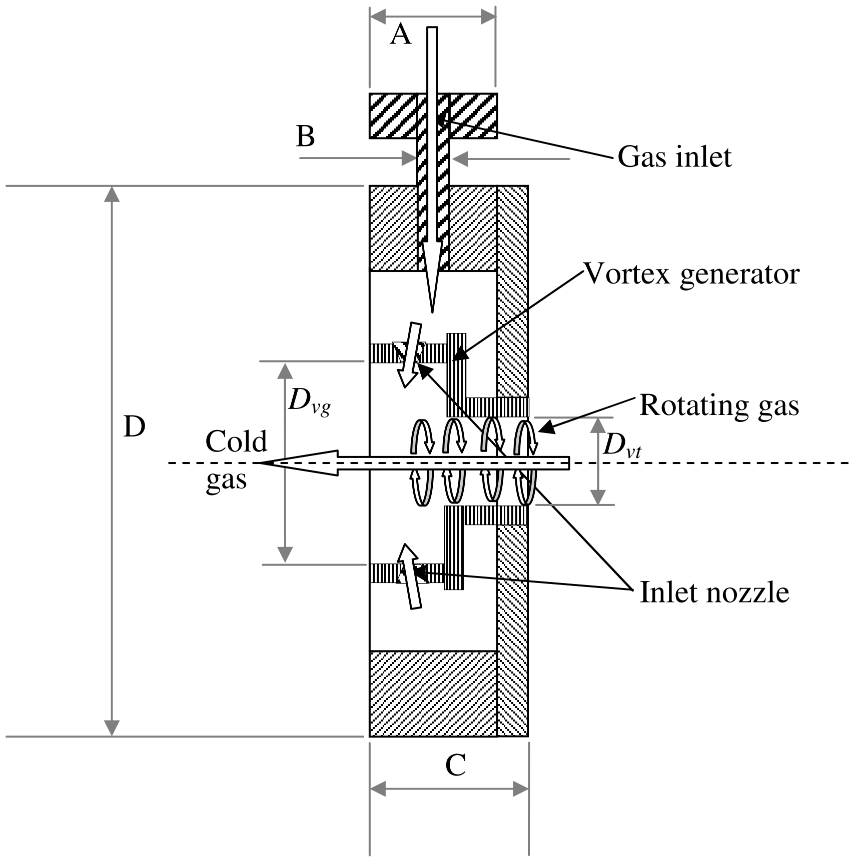

Fig. 4.5 Schematic diagram of vortex generator chamber section (Parts of the figure are not to scale)

Figure 4.5 shows a schematic of vortex generator chamber section or vortex chamber section of the RHVT. Diameter of this section is D and length of this section is C. This is the part of RHVT where the vortex is generated. In the present arrangement the two RHVTs used (medium and small size) for experimentation can accommodate detachable vortex generators. The vortex chamber section consists of two co-axial cylindrical parts, one outer and another central. The outer part is a ring that has the gas inlet nozzle. The detachable vortex generator forms the central part. High pressure gas enters the vortex generator chamber through the inlet and spread into the chamber uniformly. This high pressure gas enters the vortex generator tangentially through the symmetric and convergent inlet nozzles (generally six in numbers) of the vortex generator. Once the high pressure gas reaches the central part of the vortex generator (diameter of this part is denoted by D_{vg}), the pressure head gets converted into velocity head and the high speed rotational flow is generated. This rotating gas flow is shown in figure 4.5. Diameter of this part of the vortex generator section is denoted by D_{vt}. The rotating gas flow from the vortex generator section is directed towards the next section of the RHVT i.e. vortex tube section. On the other hand the axial cold gas stream enters the vortex chamber section from the RHVT section. After crossing the chamber section this cold gas stream enters the cold gas exhaust section. Thus the cold and hot gas streams cross the chamber section of the RHVT in opposite direction. During the experiments two different sizes of vortex chamber have been used. For the small RHVT the chamber length is 25 mm while the diameter is 21 mm. On the other hand for the medium RHVT the chamber length is 37 mm while the diameter is 29 mm.The detachable vortex generators placed at the centre of the vortex chamber perform the vital role of vortex generation by converting the pressure energy of incoming gas into kinetic energy. Also the spiralling motion of this high speed gas is generated in these generators.

Vortex generators of different sizes can be selected for required performance in cooling load or cooling temperature. The first series, designed for specific cooling load are called as *H* series vortex generators and are classified according to gas flow rate that can pass through them at a given inlet pressure and the corresponding cooling capacity they can deliver. The second series is called *C* series vortex generators and are classified according to the minimum cold temperature they can produce. The *H* series RHVTs are more commonly available in market and are used in the present studies. The designated flow rate at 100 psig (=790.8 X 10^3Pa) line pressure, cooling capacity and the type of RHVT in which these vortex generators can be used are shown in table 4.2. In the present research work thermal separation studies have been carried out with all the different types of vortex generators mentioned in table 4.2 while species separation studies have been carried out using 10H, 25H and 40H vortex generator.

Table 4.2 Flow rate, cooling capacity and RHVT size for H series vortex generators (Nex-flow™ product brochure [133])

Vortex generator	Gas flow rate (Scfm)	Gas flow rate (m^3/s) x 10^4	Cooling capacity (Watt)	Size of RHVT
2H	2	9.439	42	Small
4H	4	18.878	85	Small
8H	8	37.756	170	Small
10H	10	47.195	214	Medium
15H	15	70.792	322	Medium
25H	25	117.987	527	Medium
30H	30	141.584	615	Medium
40H	40	188.779	849	Medium

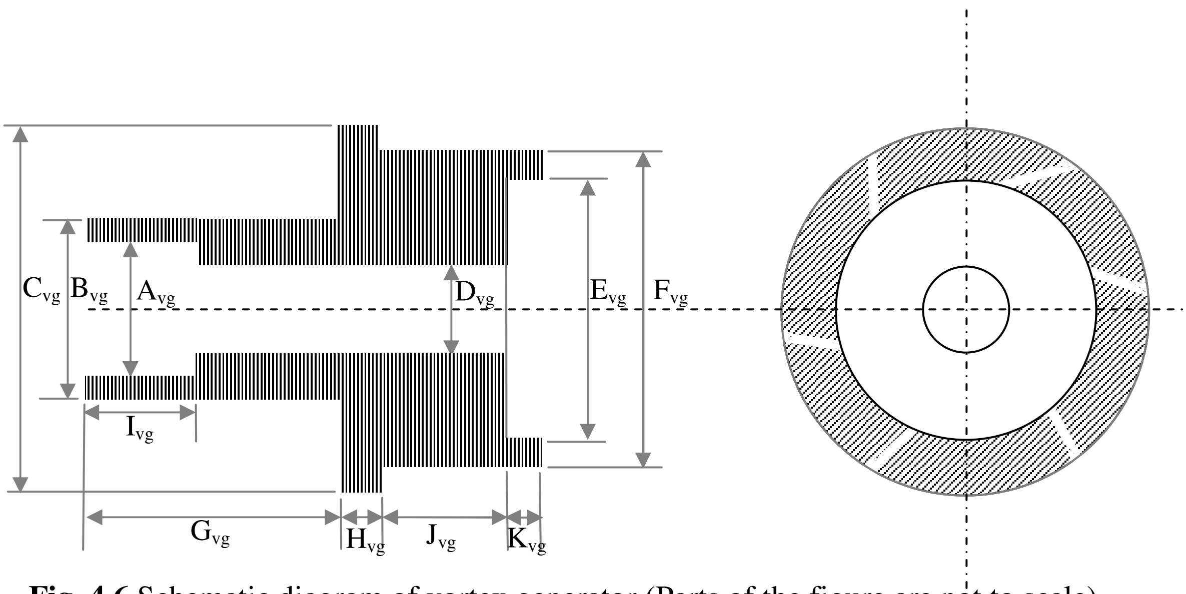

Fig. 4.6 Schematic diagram of vortex generator (Parts of the figure are not to scale)

A schematic diagram with side and top views of a vortex generator is given in figure 4.6. Dimensions of different parts of the vortex generator are indicated in the figure by alphabets (with subscript *vg*) and numerical values of the dimensions are given in table 4.3. The material of construction of the vortex generator used in this study is brass.

Table 4.3 Dimensions of different H series vortex generators (all dimensions are in mm)

Vortex generator	A_{vg}	B_{vg}	C_{vg}	D_{vg}	E_{vg}	F_{vg}	G_{vg}	H_{vg}	I_{vg}	J_{vg}	K_{vg}
2H	5.00	6.60	13.90	2.75	8.00	11.66	13.27	2.20	4.35	7.00	0.90
4H	5.05	6.60	13.90	2.80	8.10	11.66	13.77	2.40	4.66	7.25	1.00
8H	5.10	6.60	13.90	3.98	8.15	11.66	14.00	2.55	5.85	8.10	1.22
10H	8.05	9.80	23.50	4.80	14.20	18.90	13.04	1.88	15.45	12.60	1.25
15H	7.95	9.78	23.50	5.55	14.20	18.95	13.00	2.30	15.95	12.98	1.34
25H	7.95	9.75	23.50	6.40	14.00	19.00	13.10	2.20	11.55	13.66	1.94
30H	7.95	9.75	23.40	7.05	14.00	18.98	13.30	2.25	11.36	13.82	2.64
40H	8.30	9.75	23.40	8.30	14.00	18.98	13.20	2.20	11.36	14.92	3.14

Fig. 4.7a Brass generator (top view)

Fig. 4.7b Brass generator (side view)

Photographs of a vortex generator (size 40 H) are shown in figure 4.7a and 4.7b above. The material of construction of the vortex generator is brass. Figure 4.7a shows the top view of the vortex generator while figure 4.7b shows the side view of the generator. It can be seen from the above figures that there are 6 numbers of tangential inlets for this vortex generator model.

4.4.3 Vortex tube section

This is the tubular section where the rotating flow of compressible gas mixture subjected to a centrifugal force field takes place. The gas mixture shows thermal as well as species separation. Detail of the separation mechanism and their computation is given in chapter 5 and 6 of this thesis. It is observed that both thermal and species separation depends on length and diameter of the RHVT. The length and diameter of the vortex tube section for small and medium sized RHVT is given in table 4.1. Peripheral stream of the rotating flow enters the vortex tube section from the vortex generator section. On the other hand the axial stream enters the vortex tube section from the hot outlet section. Along with length and diameter of the vortex tube section two other parameters that influence thermal and species separation are material of construction and internal surface roughness. A schematic diagram of the tube section is given in figure 4.8.

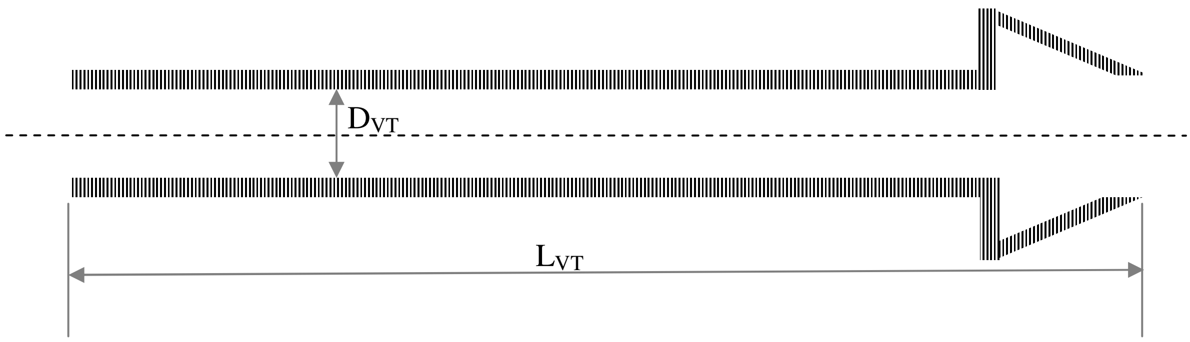

Fig. 4.8 Schematic diagram of RHVT section (dimensions are not to scale)

4.4.4 Hot outlet section

The fourth and final section of the RHVT is the hot outlet section. The peripheral stream enriched with higher concentration of heavier species and having higher temperature than the inlet gets exhausted from the RHVT through this section. A control valve called as hot end control valve is used to vary the flow rate of the hot and enriched stream at the outlet.

This hot end control valve also returns the axial flow as axial return flow after it bounces over the valve surface as shown in figure 4.9 below.

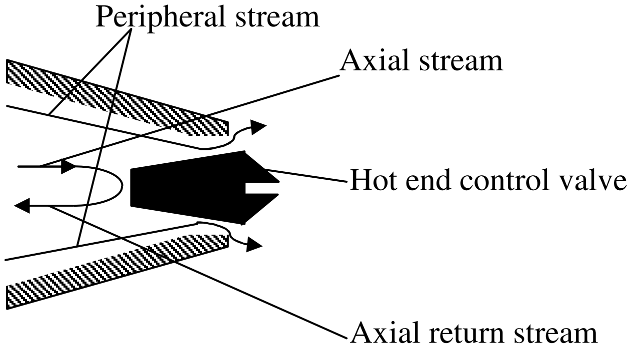

Fig. 4.9 Schematic diagram of hot outlet section; Arrows indicate flow direction

4.5 Quadrupole Mass Spectrometer used for composition analysis

A HIDEN™ make Quadrupole mass spectrometer (QMS) or gas analyser is used for composition analysis of the hot and cold stream collected from the hot and cold outlet section respectively. A brief description and operating principle of the mass spectrometer is given in appendix B.

4.6 Experimental procedure

In the present research work the thermal and species separation capacities of a RHVT have been studied with respect to the following three parameters

I. Vortex generator
II. Inlet pressure
III. Cold mass fraction

Now vortex generators come in different sizes and rated cooling capacities as described in section 4.4.2 of this chapter. The second parameter *i.e.* inlet pressure is a function of inlet flow rate and depends on supply line pressure. Hence we can write

$$\text{Inlet pressure} = f(\text{Inlet flow rate}) \tag{4.3}$$

Pressure and volumetric flow rate of air entering the RHVT were controlled by a control valve fitted in the inlet line. The maximum inlet pressure obtained in our setup is limited by the capacity of the air compressor connected to the inlet supply line.

The cold mass fraction is defined by

$$\theta_c = \frac{m_2}{m_2+m_3} \tag{4.4}$$

Now the values of the opening of hot end control valve is an indication of the cold mass fraction. Hence we can write

$$\text{Cold mass fraction} = g(\text{Hot end control valve opening}) \tag{4.5}$$

In the present work values of opening of hot end control valve were considered as a parameter as they are most frequently used for controlling the cold mass fraction by the operator. Hence in the experimental setup a given vortex generator is inserted in the RHVT and a cold mass fraction is set by fixing the hot end control valve opening. For this fixed value of control valve opening inlet flow rate or inlet pressure is varied. For each value of inlet pressure the flow rate and temperature at the inlet and two outlets are noted. Also the samples of exhaust gas from the hot and cold outlet are analysed for their composition using the quadrupole mass spectrometer.

4.7 Range of parameters for experimental studies

Experimental studies have been carried out in the experimental setup by varying the values of different control parameters of RHVT. These studies have been carried out to understand the effect of different parameters on the thermal as well as species separation performance of the RHVT. Also results of these experiments have been used to validate the theoretical model of thermal and species separation developed in the present work. The values of a parameter had been set at different range of values depending on several factors like

- aim of the experiment
- capacity of the equipment (e.g. supply line pressure of the compressor)
- values of other parameters

- vortex generators used

The important primary parameters whose values have been varied are inlet pressure, inlet volumetric flow rate and hot end control valve opening. A broad range of values of these parameters are given in table 4.4 below.

Table 4.4 Range of RHVT control parameter values used in experiment

Serial no.	Parameter name	Parameter values
1	Inlet pressure (kPa)	0 - 800
2	Inlet flow rate (m^3/s)	0 - 0.03
3	Hot end control valve opening (number of turns)	0.25 - 5.0

4.8 Summary

In this chapter, various components of different types of RHVTs used for experimentation have been described. Detailed specifications of the generators have been given. Also, a laboratory-scale experimental setup which can be used for experiments with these different types of RHVTs was built and commissioned. Different components of this setup have been described in this chapter. Specifications of the instruments to measure process parameters like flow rate, temperature and pressure have been given and error in their readouts have been analysed. Also, the quadrupole mass spectrometer used for sample composition analysis has been briefly described. Finally experimental procedure that has been adapted in the present research work has been outlined.

Chapter 5
Mathematical modelling of species separation in a RHVT and its validation

I am not young enough to know everything.
- Oscar Wilde

5.1 Introduction

This chapter introduces a new mathematical model that can predict mass transfer phenomenon in a counter current RHVT. The mass transfer model uses experimental temperature data. Results obtained from the semi-empirical mass transfer model developed and described in the present chapter have been validated with experimental data generated in-house as well as with data available in the literature.

5.2 Model and Solution methods

Researchers like Linderstrom-Lang [114] have shown that species separation phenomenon inside a RHVT can be explained by pressure diffusion (net movement of molecules or atoms down a pressure gradient) due to centrifugal field. The vortex tube acts like a centrifugal separator which depends on the principle of differential centripetal force experienced by molecules of different masses in a rotating mixture of gases. The molecules of different masses are physically separated in a gradient along the radius of a rotating gas field. The molecules with higher mass experience higher centripetal force along the radially outward direction and moves preferentially along the peripheral region. The molecules with lower molecular weight experience lower centripetal force along the radially outward direction and their concentration increases preferentially along the axial region. Thus a radial separation of the species of different molecular weight has been achieved.

One of the main merits of the centrifugal separation process is that in this process the separation factor depends on the difference of the molecular weight (*ΔM*) of the two species and not on the fraction *ΔM/M* or $\Delta M/M^2$. Therefore it is well suited for the separation of species of higher molecular weight. The rates of diffusional separation or separative exchange in radial direction per unit tube length is given by Linderstrom-Lang [113] as

$$\dot{r} = 2\pi.\rho Đ.\frac{\Delta M}{RT} v_\theta^2 N(1-N) \tag{5.1}$$

Hence apart from ΔM, separative exchange per unit length is dependent on angular velocity and average temperature for a given binary mixture. Now within the primary vortex motion inside the RHVT the flow splits into two zones. These are a hot outer stream and a cooler inner stream. The outer stream at higher temperature rotates around the periphery where fluid closer to the center rotates faster because of the presence of static peripheral wall. The inner stream at lower temperature rotates around the axis where fluid closer to the center rotates more slowly. As the swirling high speed gas mixture moves from the inlet towards the hot outlet of the RHVT the radial separation of gas species gets multiplied along the length of the vortex tube and the overall diffusional separation factor as given by equation 5.1 above is obtained. Thus the species separation in a RHVT can be explained on the basis that axial flows play an important role in establishing the net gas-separation effect.

5.2.1 Modelling of flow and mass transfer inside a RHVT

As discussed above the centrifugal species separation phenomena inside a RHVT can be postulated by two adjacent zones of axial flows in opposite direction. This postulate can be visually represented by figure 5.1 in 3 dimensions. As shown in the figure, the vortical flow inside the RHVT can be divided into two different flow regions based on their axial direction of flow. Flow occurs in the first of these two flow regions i.e. in the outer annular zone (between inner radius r_{in} and outer radius r_{out}) near the periphery of the vortex tube. In this region fluid closer to axis of rotation rotates faster and as we approach the stationary cylindrical wall, the rotational velocity decreases. This zone takes part in mass transfer while moving axially in a vortical flow from the RHVT inlet to the hot outlet i.e. positive *z* direction. Mass transfer takes place between two parallel fluid streams moving along the inner and outer boundary of this annular zone in the radial direction due to centripetal force.

The second region of fluid flow is the inner cylindrical zone (between axis of the cylinder and inner radius r_{in}) shown in figure 5.1. In this region fluid moves along the axis of the vortex tube in the opposite direction *i.e.* from hot end control valve to the cold outlet orifice *i.e.* negative *z* direction. As radius of this inner cylindrical flow zone is small (of the order of cold outlet orifice) the value of centripetal force acting on the fluid elements inside the cylinder is negligible. Hence mass transfer from the inner cylindrical region can be neglected.

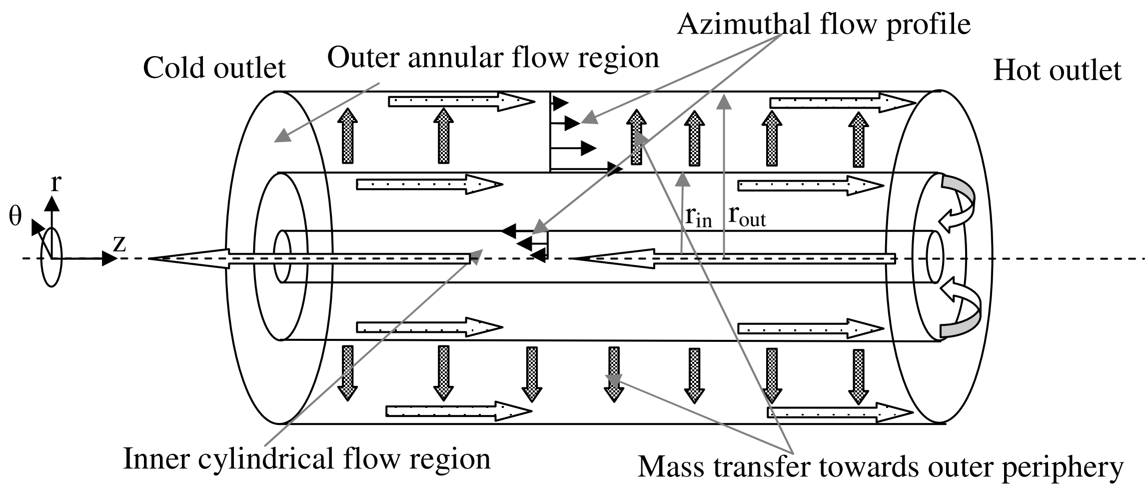

Fig. 5.1 Schematic view of species separation inside a RHVT

The current mathematical model calculates axial concentration gradient of the heavier species of a binary mixture as mass transfer takes place between two parallel streams (located at inner radius r_{in} and outer radius r_{out} respectively of the outer annular region) moving from inlet towards the hot outlet. The well established Chilton Colburn analogy is used to determine the mass transfer coefficient based on the heat transfer coefficient. The heat transfer coefficient is calculated using Seider-Tate correlation. The model can predict variation of concentration of the heavier species in both enriched and depleted stream along the length of the RHVT and mass separation factor. Details of the developed semi-empirical model, its solution methodology and validation studies have been described in details in the following sections of this chapter.

5.2.2 Semi-empirical model for mass transfer

When a binary gas mixture of a heavier species and a lighter species enters the vortex chamber of the RHVT a vortex flow is generated which advances towards the hot end of the tube. Mixture of the two different species in gas phase enters the RHVT at a very high pressure. This pressure head gets converted into kinetic energy head of the swirling flow. Hence the gas rotates at a very high speed and a centrifugal force field is created. Under the centrifugal field centripetal acceleration causes the molecules of two different species having different masses to experience different degrees of centripetal forces. Thus particles of different masses are physically separated from one another in a gradient along the radius of the vortex tube.

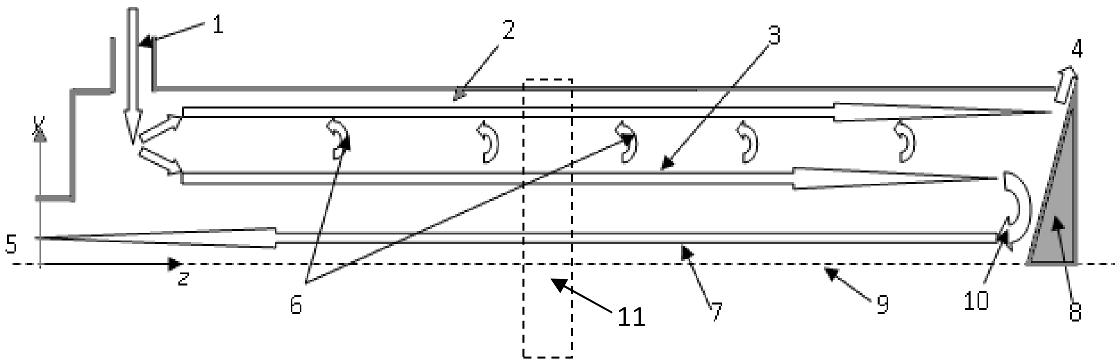

Fig. 5.2 The flow model for mass transfer in a RHVT with different components

In the present model the swirling flow path is divided into two distinct flow streams. The first is the peripheral stream (indicated by numeral 2 in figure 5.2) that moves towards the hot end along the *z* direction, located far from the centre line and adjacent to the cylindrical tube wall, while the second is the axial stream that moves in parallel to the peripheral stream (indicated by numeral 3 in figure 5.2) in the same direction but located near the centre line. A centrifugal separation field is created due to high speed rotation of the gas mixture which acts on the atoms/molecules of different masses in the gas mixture. Description of different parts of the present model as shown in figure 5.2 is given in table 5.1 below.

Table 5.1: Description of different components of the modelled RHVT in figure 5.2

Component No.	Description
1	Inlet
2	Peripheral stream, enriched in heavier species
3	Axial stream, depleted in heavier species
4	Peripheral outflow stream (hot end stream)
5	Axial outflow stream (cold end stream)
6	Transfer of heavier species from axial to peripheral stream
7	Axial return stream, depleted in heavier species
8	Hot end control valve
9	Centre line
10	Change in flow direction of axial stream
11	Control volume

As these two parallel streams (i.e. peripheral stream 2 and axial stream 3) move towards the hot end, atoms/molecules of the heavier species experience higher centripetal force towards the periphery as compared to the lighter species and preferentially get transferred to the peripheral stream. Fekete [66] has measured the value of centrifugal acceleration in the RHVT to the order of 10^6 times of gravitational acceleration which was found stronger than in other centrifugal separators. Thus along the length of the RHVT from the gas inlet to the hot outlet the peripheral stream gets enriched in heavier species while the axial stream gets depleted in heavier species. Consequently for a binary mixture the axial stream gets enriched in lighter species and the peripheral stream gets depleted in lighter species.

In the present model it has been assumed that the peripheral stream is withdrawn from the peripheral opening of the hot end of RHVT which is controlled by a hot end control valve. Hence the flow rate of the peripheral stream is experimentally measured by flow meter connected to the hot end of the RHVT. On the other hand the axial stream that moves in parallel to the peripheral stream up to the hot end control valve, collides with the stationary solid wall of the valve and turns back in the opposite direction and a new counter flow stream is generated which moves in the opposite direction of the axial stream, along the centre of the RHVT. This stream is indicated by numeral 7 in the figure 5.2 above and is designated as axial return stream. It is assumed in the present model that while mass transfer takes place only between peripheral and axial streams, the axial return stream does not take part in the process of mass transfer and hence it's concentration does not change from the hot end to the cold end. This assumption can be justified by the fact as the axial return stream rotates around the axis and in this region fluid closer to the center rotates more slowly. Hence azimuthal velocity v_θ in this stream is very small which results into a very feeble centrifugal field. Hence separation in this stream is negligible. The axial return stream comes out from the cold outlet and the flow rate is measured by flow meter connected to the cold end of the RHVT.

5.2.3 Assumptions made for the semi-empirical model of mass transfer

The assumptions made in the present mathematical model have been listed below:

1. Axial flow inside a RHVT is divided into three parts i.e. peripheral flow, axial flow and axial return flow. Mass transfer takes place between the axial flow and the peripheral flow. The axial return flow stream does not take part in mass transfer i.e. it's concentration does not change as it moves towards the cold outlet.
2. The peripheral stream is withdrawn from the peripheral opening of the hot end of RHVT.
3. The axial return stream is withdrawn through the cold end orifice of the RHVT.
4. Axial temperature variation is linear between two ports where temperature is known.
5. The gas concentration at a point along the axial direction inside the vortex tube does not change rapidly with time.
6. Axial mass diffusion is neglected.
7. Width of the control volume is small enough to neglect change in velocity across the width. This ensures that effect of peripheral mass flux on the axial velocity can be neglected.
8. The transient terms, viscous dissipation, axial conduction and pressure work terms in the energy equation are insignificant and hence neglected.

5.2.4 Governing equations

Figure 5.3 shows a control volume (as shown by component 11 in figure 5.2) of thickness Δz, cross section area A and perimeter P_e of the tube portion of the RHVT. The net gas mixture flow (peripheral stream + axial stream - axial return stream) enters the control volume from left side with a velocity v, and a concentration of heavier species x_z. Gas

Time rate of change of concentration of heavier species inside the control volume	=	Heavier species flow rate (in-out) of the control volume	-	Rate of molar flow of heavier species reaching the peripheral wall of the control volume	(5.2)

comes out from the right side of the control volume with a concentration of heavier species $x_{z+\Delta z}$. A net component balance inside the control volume can be given by the following conservation equation

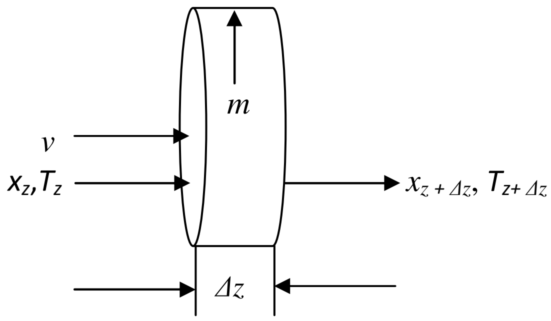

Fig. 5.3 A control volume to develop the mass transfer model

The first term of the above conservation equation *i.e.* the rate of change of concentration of heavier species stored inside the control volume per unit volume is

$$\frac{\partial}{\partial t}\left(\frac{x.A\Delta z}{A\Delta z}\right) = \frac{\partial x}{\partial t} \tag{5.3}$$

Now the molar flow rate (in - out) of heavier species can be expressed by,

$$Q = v(x_z - x_{z+\Delta z})A \tag{5.4}$$

Hence, differential representation of the change in concentration of heavier species in terms of spatial gradient of the heavier species flux is given by

$$\frac{Q}{A\Delta z} = -v\frac{\partial x}{\partial z} \tag{5.5}$$

Now, if m is the mass of heavier species reaching from the axial stream to a unit area of the peripheral wall then total moles of heavier species reaching the wall of the control volume

$$H_{wall} = P_e \Delta z \frac{m}{M_1} \tag{5.6}$$

Therefore, rate of molar flow of heavier species reaching the peripheral wall of the control volume, per unit volume is given by

$$\frac{\partial}{\partial t}\left(\frac{H_{wall}}{A\Delta Z}\right) = \frac{P_e}{M_1 A}\frac{\partial m}{\partial t} \tag{5.7}$$

Hence from equation (5.3) to (5.7), a component balance along the control volume (as given by the component balance in equation 5.2) gives

$$\frac{1}{v}\frac{\partial x}{\partial t} = -\frac{\partial x}{\partial z} - \frac{P_e}{M_1 v A}\left(\frac{\partial m}{\partial t}\right) \tag{5.8}$$

Now, the term vA in equation (5.8) is the total volumetric flow rate of the gas mixture. Hence if V is the molar flow rate of the lighter species then

$$V = vA(1-x) \tag{5.9}$$

Hence from equation (5.8) and (5.9) we get

$$\frac{1}{v}\frac{\partial x}{\partial t} + \frac{\partial x}{\partial z} + \frac{(1-x)}{V}\frac{P_e}{M_1}\left(\frac{\partial m}{\partial t}\right) = 0 \tag{5.10}$$

Now the gas concentration at a point does not change rapidly with time, hence neglecting the first term in equation (5.10) we can write the differential equation for mass transfer at location z

$$\frac{dx}{dz} = -\frac{(1-x)}{V}\frac{P_e}{M_1}\left(\frac{\partial m}{\partial t}\right)_z \tag{5.11}$$

Now, at any point within the RHVT at a distance z from the inlet, the rate of mass transfer to the peripheral region from the core region per unit area may be expressed as

$$\left(\frac{\partial m}{\partial t}\right)_z = M_1 K(P - P_w) = M_1 KP(1 - \kappa) \tag{5.12}$$

where, $\kappa = \frac{P_w}{P}$. The mass transfer coefficient K is difficult to obtain for different systems. Therefore we can apply Chilton Colburn analogy (Dunthorn [55]) within its applicable range (i.e. inside the flow domain Re > 10000 and 0.7< Pr < 160). Hence we can get the mass transfer coefficient from the following equation in terms of heat transfer coefficient.

$$j_m = \frac{KP_{gf}Sc^{\frac{2}{3}}}{(G/M_m)} = \frac{hPr^{\frac{2}{3}}}{C_m G} = j_h \tag{5.13}$$

It is assumed that the flow is fully developed at the downstream of the vortex generator which is also a necessary condition for application of Chilton Colburn analogy. Mass transfer coefficient K can be calculated from heat transfer coefficient using equation 5.13. The accuracy of the mass transfer coefficient thus estimated depends on the accuracy of the heat transfer coefficient data. The heat transfer coefficient data could be either experimental or the one obtained from a suitable correlation. Thus the mass transfer coefficient so obtained is as much accurate as the heat transfer coefficient, as stated by Wilk [198].

The term, P_{gf}, in the above relationship on expansion gives

$$P_{gf} = (P_i - P_{iw})/(\ln P_i - \ln P_{iw}) \tag{5.14}$$

where,
$$P_i = P_T - P = P_T - xP_T \tag{5.15}$$

and,
$$P_{iw} = P_T - P_w \tag{5.16}$$

Thus,
$$P_{gf} = P(1 - \kappa)/\ln\{(1 - P_w/P_T)/(1 - x)\} \tag{5.17}$$

Hence combining equations (5.12), (5.13) and (5.17) we get

$$\left(\frac{\partial m}{\partial t}\right)_z = \frac{M_1 h N' \ln\{(1-P_w/P_T)/(1-x)\}}{M_m C_m} \tag{5.18}$$

where, $$N' = (Pr/Sc)^{2/3} \tag{5.19}$$

Now from equation (5.11) and (5.18) we can get the ordinary differential equation for mass transfer as

$$\frac{dx}{dz} = -\frac{(1-x)}{V}\frac{hP_eN'}{M_mC_m}\ln\{(1-P_w/P_T)/(1-x)\} \tag{5.20}$$

The heat transfer coefficient h in equation (5.20) can be calculated using an empirical correlation like Seider-Tate correlation that is applicable for forced convection for turbulent pipe flow under the condition that 0.7< Pr < 160, Re >10000 and $\frac{L}{D_{vt}} \geq 10$. In the present calculation this correlation is used to determine the heat transfer coefficient and it is given by

$$Nu = 0.027\, Re^{4/5}\, Pr^{1/3} \left(\frac{\mu}{\mu_s}\right)^{0.14} \tag{5.21}$$

The Sieder-Tate correlation takes into account the change in viscosity μ *and* μ_s, due to change in temperature between the gas average temperature at the core region and the heat transfer surface temperature, respectively.

Now a heat transfer ODE for the system can be derived by an overall energy balance across the control volume shown in figure 5.3 as

Heat energy entering the control volume at axial location z by convection	-	Heat energy leaving the control volume at axial location $z+\Delta z$ by convection	=	Heat energy transferred to the wall of the control volume	(5.22)

Hence the rate of heat energy entering the control volume at location z along the axis per unit volume can be calculated by the following equation

$$E_{in} = \frac{\rho v A C_m T_z}{A\Delta z} \tag{5.23}$$

and rate of heat energy leaving the control volume at location $z + \Delta z$ along the axis per unit volume is given by

$$E_{out} = \frac{\rho v A C_m T_{z+\Delta z}}{A\Delta z} \tag{5.24}$$

Further the rate of heat energy transferred to the wall of the control volume per unit volume is given by

$$E_w = -\frac{hP_e\Delta z(T-T_w)}{A\Delta z} \tag{5.25}$$

Hence substituting the equations 5.23 to 5.25 into equations 5.22 we get

$$v\rho C_m \frac{(T_z-T_{z+\Delta z})}{\Delta z} = -\frac{hP_e(T-T_w)}{A} \tag{5.26}$$

which can be written after re-arrangement as

$$\frac{dT}{dz} = -\frac{hP_e(T-T_w)}{vA\rho C_m} \tag{5.27}$$

Now using equation 5.9 we can further modify the heat transfer equation to the form given below as

$$\frac{dT}{dz} = -\frac{h(1-x)P_e(T-T_w)}{V\rho C_m} \tag{5.28}$$

Hence equation 5.20 and 5.28 can be solved numerically along the length of the RHVT to get the concentration and temperature profile. It may be noted that equation 5.28 can also be solved analytically.

5.2.5 Input required and equations used for the semi-empirical model

The input required for the code based on the semi empirical model can be broadly divided into three parts. These are

- Physical properties
- Geometrical variables
- Process variables

Details of each type of properties and variable are given below.

The required **physical properties** of the working fluid are the mean molecular weight of the gas mixture, coefficient of diffusion, means specific heat of the gas mixture, ratio of specific heats, density of the gas mixture, viscosity of the gas mixture and thermal conductivity of the gas mixture. In the present work air is used as the working fluid and values for these physical properties for air are taken as following:

- Mean molecular weight of air (M_m): Air is a mixture of several gases, where the two most dominant components in dry air are 21 volume% oxygen and 78 volume% nitrogen. Oxygen has a molar mass of 15.9994 kg/mol and nitrogen has a molar mass of 14.0067 kg/mol. As both oxygen and nitrogen are di-atomic molecule the molar mass of these molecules are 32 kg/mol and 28 kg/mol respectively. Now the average molar mass of the gas mixture can be calculated by adding the product of mole fractions of each gas and the molar mass of that particular gas. Thus calculated, the mean molecular weight of air as a binary mixture of oxygen and nitrogen is 28.97 kg/mol.

- Coefficient of diffusion or diffusivity (Đ): A value of 1.76 X 10^{-5} m^2/s for the diffusivity of gaseous oxygen into air as a mixture of oxygen and nitrogen at STP is given by Cussler (50). This value is used in the present code.

- Ratio of specific heats (γ): This value is taken as 1.4.

- Mean specific heat of air (C_m): The mean specific heat of air varies with temperature and can be calculated using the following co-relation where C_m is in J/kg.K and temperature T is in K.

$$C_m = 7.875 \times 10^{-6}.T^2 + 0.1712.T + 949.72 \tag{5.29}$$

➢ Density of the gas mixture (ρ): Variation of air density with temperature can be calculated using the following co-relation where ρ is in kg/m^3 and temperature T is in K.

$$\rho = 358.517\, X\, T^{-1.00212} \tag{5.30}$$

➢ Viscosity of the gas mixture (μ): Viscosity of air varies with temperature of air and can be approximated with following equation where μ is in Pa-s and temperature T is in K.

$$\mu = -8.3123 \times 10^{-12}.T^2 + 4.4156 \times 10^{-8}.T + 6.2299 \times 10^{-8} \tag{5.31}$$

➢ Thermal conductivity of the gas mixture (k): Variation of thermal conductivity of air as a function of air temperature can be expressed by the following equation. In this equation unit of k is in W/m K and temperature T is in K.

$$k = -1.3707 \times 10^{-8}.T^2 + 7.616 \times 10^{-5}.T + 4.5968 \times 10^{-3} \tag{5.32}$$

The above expressions for different physical properties of air given in equations 5.29 to 5.32 are provided in the website https://neutrium.net/properties/properties-of-air/. At 1 atmospheric pressure these expressions are valid for a temperature range of 200 to 2000 K. These equations are useful for running a computer code as variation in the values of physical properties can be computed with temperature variation without using tables or requiring any input from the user during the execution of program. After calculating the physical properties the following two dimensionless numbers can be calculated.

Prandtl number: $$Pr = \frac{C_m \mu}{k} \tag{5.33}$$

Schmidt number: $$Sc = \frac{\mu}{\rho Ɖ} \tag{5.34}$$

Hence N' defined by equation 5.19 can be calculated.

The **geometrical variables** required by the code include vortex tube length L_{vt}, vortex tube diameter (D_{vt}) and inlet diameter (d_i). Hence the differential equation 5.20 is solved for a length of L_{vt}. The wetted perimeter (P_e), flow cross section area (A) and inlet cross section area (a_i) can be calculated respectively using the following equations

Wetted perimeter: $$P_e = \pi D_{vt} \tag{5.35}$$

Flow cross section area: $$A = \pi \frac{{D_{vt}}^2}{4} \tag{5.36}$$

Inlet cross section area: $$a_i = \pi \frac{{d_i}^2}{4} \tag{5.37}$$

The **process variables** required for the present model are inlet mass flow rate (m_1), concentration of heavier species in the inlet flow (x), inlet gas temperature (T_1), inlet pressure (P_1), cold mass fraction θ_c (ratio of cold outlet flow rate to inlet flow rate), cold outlet gas temperature (T_2) and hot outlet gas temperature (T_3).

In the present work the temperatures at the cold (T_2) and hot (T_3) outlets have been experimentally determined. It has been observed from experiments that the RHVT skin temperature roughly varies linearly from the inlet zone (minimum value) to the hot end control valve zone (maximum value). Hence a linear variation of temperature of the peripheral stream is assumed in the mathematical model from inlet temperature (ambient temperature) up to the hot outlet temperature (T_3). Similarly the temperature of the axial stream varies linearly from inlet ambient temperature to a temperature equal to the cold outlet temperature (T_2) near the hot end control valve. The axial return stream is maintained at this temperature (T_2) throughout the length of the RHVT i.e. the stream remains at isothermal condition.

The inlet volumetric flow rate (V_1) can be calculated from the inlet mass flow rate (m_1) from the following equation:

$$V_1 = \frac{m_1}{\rho} \tag{5.38}$$

Hence the inlet gas velocity (v_1) can be calculated from the values of inlet volumetric flow rate V_1 and flow inlet cross section area a_i as given in following equation

$$v_1 = \frac{V_1}{a_i} \tag{5.39}$$

Now during the experiment the cold mass fraction θ_c is controlled by opening or closing the hot end control valve. Hence they are interrelated. But during the experiment θ_c can be calculated directly from the inlet and cold outlet mass flow meter reading. Also values of the cold mass fraction are reported for almost all the literature. Hence these values can be directly used to calculate how inlet mass flow is divided into cold and hot outlet flows.

Cold outlet mass flow rate: $$m_2 = m_1\theta_c \tag{5.40}$$

Hot outlet mass flow rate: $$m_3 = m_1(1-\theta_c) \tag{5.41}$$

Now as per the model the inlet flow rate is divided into two streams. Mass flow rate of the peripheral stream is m_3 (in positive z direction) while the mass flow rate of the axial stream is m_2 (in positive z direction). As the axial stream bounces from the hot end control valve surface and its flow is reversed to form the axial return stream, the mass flow rate in the axial return stream is - m_2 (i.e. in negative z direction). Hence net mass flow rate in positive z direction at any cross section is $m_3 + m_2 - m_2 = m_3$. Also in the current model it is assumed that cross section area of the axial return flow region is very small compared to the cross section of the vortex tube. Hence net axial velocity of the gas stream is calculated by the following equation

$$v = \frac{m_3}{\rho A} \tag{5.42}$$

Hence it is possible to calculate the Reynolds number at the inlet of the RHVT as well as inside the tube portion of the RHVT where species separation takes place.

Reynolds number at inlet: $$Re = \frac{d_i v_1 \rho}{\mu} \tag{5.43}$$

Reynolds number inside tube: $$Re = \frac{D_{vt} v \rho}{\mu} \tag{5.44}$$

Hence local heat transfer coefficient h can be calculated using equations 5.21 as follows

$$h = 0.027\, Re^{4/5}\, Pr^{1/3} \left(\frac{\mu}{\mu_s}\right)^{0.14} \frac{k}{D_{vt}} \tag{5.45}$$

In this equation the Reynolds number can be replaced by inlet Reynolds number and vortex tube diameter D_{vt} can be replaced by inlet diameter d_i in order to calculate heat transfer coefficient at the inlet of the RHVT.

Next we need to calculate the pressure at a particular radius r in a rotational flow field. For this the method due to Gao [72] called Modified Ahlborn Model (MAM) has been used. Initially in this method the inlet Mach number can be calculated by the following equation using the inlet gas velocity v_1 and speed of sound in air (c).

Inlet Mach number: $$Ma_i = \frac{v_1}{c} \tag{5.46}$$

Now as an axi-symmetric rotational flow is generated inside the vortex generator (because of the axi-symmetric geometry) and the value of the azimuthal component of velocity v_θ is much bigger than the radial component v_r and axial component v_z of velocity. Hence the radial pressure distribution can be obtained from simplified momentum equation in cylindrical co-ordinate as given by Ahlborn *et. al.* [4]

$$\frac{\partial p}{\partial r} \cong \frac{\rho v_\theta^2}{r} \tag{5.47}$$

Thus the pressure distribution inside the vortex generator depends on the azimuthal velocity (v_θ) profile. The MAM model by Gao [72] assumes the azimuthal Rankine velocity (v_θ) profile as described by Ogawa [137].

$$v_\theta = \begin{cases} \omega_v r & 0 \le r \le r_{cr} \\ \frac{\Gamma}{r} & r_{cr} \le r \le r_{vg} \end{cases} \tag{5.48}$$

Here r_{cr} is the critical radius where rotational flow changes from forced vortex to free vortex type. In the present model r_{cr} is taken as the vortex tube radius i.e.

$$r_{cr} = r_{vt} = \frac{D_{vt}}{2} \tag{5.49}$$

and vortex generator radius: $$r_{vg} = \frac{D_{vg}}{2} \tag{5.50}$$

In equation 5.48 ω_v is the vorticity and Γ is the circulation of the vortex which can be calculated using the following relations

Vorticity: $$\omega_v = v_0 \frac{D_{vg}}{D_{vt}^2} \tag{5.51}$$

Circulation: $$\Gamma = v_0 \frac{D_{vg}}{2} \tag{5.52}$$

where v_0 is the nozzle exit velocity. Now the velocity distribution of equation 5.48 can be substituted in the momentum equation 5.47 and the following pressure distribution is obtained.

$$P_O - P_T = P_O \frac{\gamma}{2} Ma_i^2 \left(\frac{2r_{vg}^2 - r_{vt}^2}{r_{vt}^2} \right) \tag{5.53}$$

where P_O is the pressure at the outer radius of the vortex tube and P_T is the pressure at the central line i.e. axis of the vortex tube. Now equation 5.53 can be re-written to get the normalized pressure ratio as

$$\frac{P_O - P_T}{P_O} = \frac{\gamma}{2} Ma_i^2 \left(\frac{2}{\tau_r^2} - 1 \right) \tag{5.54}$$

where τ_r is a dimensionless ratio of two radius defined as

$$\tau_r = \frac{r_{vt}}{r_{vg}} = \frac{D_{vt}}{D_{vg}} \tag{5.55}$$

Now P_T can be calculated using the value of inlet pressure from the following expression based on compressible flow through a converging nozzle given by Gao [72] as

$$\frac{P_T}{P_1} = \frac{1-0.7Ma_i^2\left(\frac{2}{\tau_r^2}-1\right)}{\left(1+0.2Ma_i^2\right)^{3.5}} \tag{5.56}$$

In the present work partial pressure of heavier species in gas stream at wall is approximated by the following equation

$$P_W = xP_O \tag{5.57}$$

5.3 Numerical scheme for solving the governing equations

The numerical scheme used in a computer code to solve the governing equations (discussed in the previous section) to calculate the concentration profile along the length of the RHVT is discussed below.

Step 1: Specify the problem dependent input data as following

- Physical properties
  - Mean molecular weight of the binary mixture of two components (M_m)
  - Coefficient of diffusivity (Đ)
  - Mean specific heat (C_m)
  - Density of gas mixture (ρ)
  - Viscosity of gas mixture (μ)
  - Thermal conductivity of gas mixture (k)

- Geometrical variables
  - Vortex tube length (L)
  - Vortex tube diameter (D_{vt})
  - Vortex generator diameter (D_{vg})
  - RHVT inlet diameter (d_i)

- Process variables
  - Inlet mass flow rate (m_1)
  - Inlet temperature (T_1)
  - Inlet concentration of heavier species (x)
  - Cold mass fraction (θ_c)
  - Cold outlet temperature (T_2)

- Hot outlet temperature (T_3)
- Speed of sound in the working fluid at inlet condition (c)
- Ratio of specific heats (γ)

Step 2: Experimental temperature data at the inlet, cold outlet and hot outlet are obtained. Hence gas temperature values at all the points along the length of the wall of the RHVT are interpolated using the length of the tube. These values are used to initialize the axial temperature profile to start the calculation.

Step 3: The geometric parameters are used to calculate the wetted perimeter P_e (equation 5.35), flow cross section area A (equation 5.36) and inlet cross section area a_i (equation 5.37). Also calculate the ratio of vortex tube and vortex generator diameter τ_r (equation 5.55).

Step 4: The volumetric flow rate is calculated using the inlet mass flow rate (using equation 5.38), which is thereafter used to calculate the inlet velocity (using equation 5.39). This value of inlet velocity is now used to calculate the inlet Mach number (equation 5.46). Also the cold and hot outlet mass flow rate is calculated with the help of inlet mass flow rate and cold mass fraction value using equations 5.40 and 5.41 respectively.

Step 5: Choose time step Δt. Choose space step Δz and hence total number of discrete segments along the length of the RHVT.

Step 6: Start time looping. Here we may note both our PDEs are steady state equations and the time looping used here is pseudo time-stepping. In this method for the steady-state solution of time-evolving partial differential equations an initial guess is set and using time-marching scheme the solution is obtained.

Step 7: Start space looping. If space step is 1 initialize the temperature of the first point by the inlet temperature and concentration by inlet concentration else use the temperature and concentration calculated from the last time step.

Step 8: For present time step calculate physical properties like mean specific heat C_m (equation 5.29), gas density ρ (equation 5.30), viscosity of gas μ (equation 5.31) and thermal conductivity k (equation 5.32) using the local temperature value.

Step 9: Calculate axial velocity of gas stream inside the vortex tube v (by equation 5.42).

Step 10: Calculate the three dimensionless numbers *i.e.* Reynolds number *Re* (at inlet using equation 5.43 and local Reynolds number by equation 5.44), Prandtl number *Pr* (equation 5.33) and Schmidt number *Sc* (equation 5.34) respectively.

Step 11: Calculate viscosity of gas at wall surface (μ_s) using local wall temperature T_W (equation 5.31). Equation 5.45 can be used to calculate local heat transfer coefficient h.

Step 12: Using equation 5.56 the pressure at the central line (P_T) is calculated. In this equation the inlet pressure P_I , inlet Mach number Ma_i (see step 4) and ratio of vortex tube to vortex generator diameter τ_r (see step 3) were used.

Step 13: Next using equation 5.54 the pressure at the outer radius (P_O) is calculated as the values of P_T, γ, Ma_i and τ_r are known. Now the partial pressure of heavier species in gas stream P_w is calculated using equation 5.57.

Step 14: Now we can start solving the mass and heat transfer Ordinary Differential Equations (ODE) at the given space step. It can be seen that the mass and heat transfer ODEs are coupled (i.e. mass transfer ODE 5.20 has terms that vary with temperature T while heat transfer ODE 5.28 has concentration term x). Hence they are solved simultaneously using coupled fourth order Runge Kutta method to get the latest estimate of temperature and mole fraction at the next space step. The discretized equations for

Mass transfer:
$$x_{z+1}^{n} = x_{z}^{n-1} - \Delta z \frac{(1-x_z^n)}{V} \frac{hP_eN'}{M_mC_m} \, ln\left\{\frac{\left(1-\frac{P_W}{P_T}\right)}{1-x_z^{n-1}}\right\} \tag{5.58}$$

Heat transfer:
$$T_{z+1}^{n} = T_{z}^{n-1} - \Delta z \frac{(1-x_z^n)}{V} \frac{hP_e}{M_mC_m} \left(T_z^{n-1} - T_W\right) \tag{5.59}$$

Step 15: Equation 5.58 and 5.59 are solved for all points along the length of the RHVT to get the axial concentration and temperature profile for the present time step.

Step 16: Go to step 6 with most recent estimate of temperatures and mole fractions and repeat the calculation for the next time steps till a set of convergent values (that does not change with time) of quantities are arrived at. Once convergence is attained go to step 17.

Step 17: Print the output.

5.4 Results from the semi-empirical model

A set of results obtained by computation from the semi-empirical model described above are presented in this section. The results comprise of separation factor vs. inlet volumetric feed flow rate graphs for different values of hot end control valve (screw) opening. Separation factor of the lighter species for a binary separation is defined by

$$\alpha = \frac{1-N_3}{N_3} \frac{N_2}{1-N_2} \tag{5.60}$$

A computer code based on the semi-empirical model developed can predict the variation of compositions of the two parallel streams (axial and peripheral) along the length of the RHVT. Therefore we can obtain from the computer code the composition of two outlet streams (cold and hot) from the RHVT. Using equation (5.60) the binary separation factors for a mixture of two gases (like air as a mixture of oxygen and nitrogen) can be computed.

5.4.1 Feed flow rate vs. separation factor for different values of hot end valve opening

The computer code that solves the semi-empirical model for heat and mass transfer requires experimentally measured temperature data at the inlet (T_1) and two outlets (T_2 and T_3). Hence experiments were conducted in the experimental setup described in the previous chapter. Three different vortex generators were used for these experiments. These vortex generators are designated as 10H, 25H and 40H. Details of these generators are given in chapter 4. In these experiments for a given vortex generator and hot end control valve opening inlet pressure is varied from 1.5 kg/cm^2 to 5.0 kg/cm^2. For each value of inlet pressure the inlet volumetric flow rate and inlet air temperature is measured. For each of these inlet conditions the hot and cold outlet gas temperatures are measured. Also values of the cold mass fractions vary with the set values of hot end control valve opening. These values of cold mass fractions used in the code are measured from the ratio of cold outlet flow rate to inlet flow rate both obtained experimentally. In all these experiments carried out, only stable data values of flow rate and temperatures which do not change with time were considered. During experimental conditions, where flow rate or pressure values showed instability were not considered. Oxygen concentration values at the cold and hot outlets were computed using the computer code. Corresponding values of separation factors were obtained using equation 5.60. The inlet volumetric flow rate for each value of hot end control valve opening and inlet pressure for a 10H vortex generator is given in table 5.2 below.

Table 5.2: Inlet pressure vs. inlet flow rate for 10H vortex generator

Inlet pressure (kg/cm^2)	Inlet volumetric flow rate (m^3/s) x E+02 for different values of hot end control valve opening						
	2.0	2.5	3.0	3.5	4.0	4.5	5.0
3.5	1.061	0.991	0.991	1.085	1.085	1.085	1.109
4.0	1.203	1.109	1.085	1.203	1.213	1.227	1.203
4.5	1.274	1.203	1.156	1.297	1.307	1.321	1.297
5.0	1.345	1.321	1.392	1.439	1.439	1.439	1.415

It can be seen from table 5.2 that for a fixed value of hot end control valve opening inlet volumetric flow rate increases proportionately with inlet pressure. For 10H vortex generator instabilities in flow at the inlet and the two outlets were observed for inlet pressure values below 3.5 kg/cm^2. The upper limit of inlet pressure is restricted by the compressor capacity at the supply line of the vortex generator experimental setup. Similarly for hot end control valve opening values below 2.0, the flow rates are not stable. Hence separation factor values can be calculated for the 10H vortex generator for an inlet pressure range of 3.5 kg/cm^2 to 5.0 kg/cm^2 with the hot end control valve opening kept in the range 2.0 to 5.0. Variation in separation factor values with variable

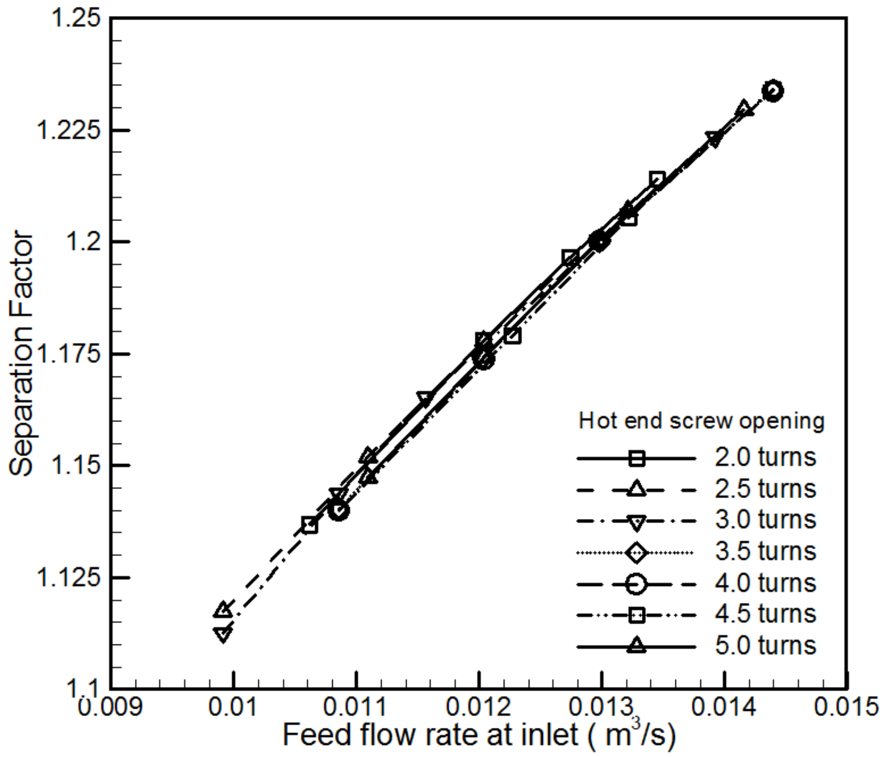

Fig. 5.4 a. Feed flow rate vs. separation factor (computed) at different values of hot end valve opening for a 10H vortex generator

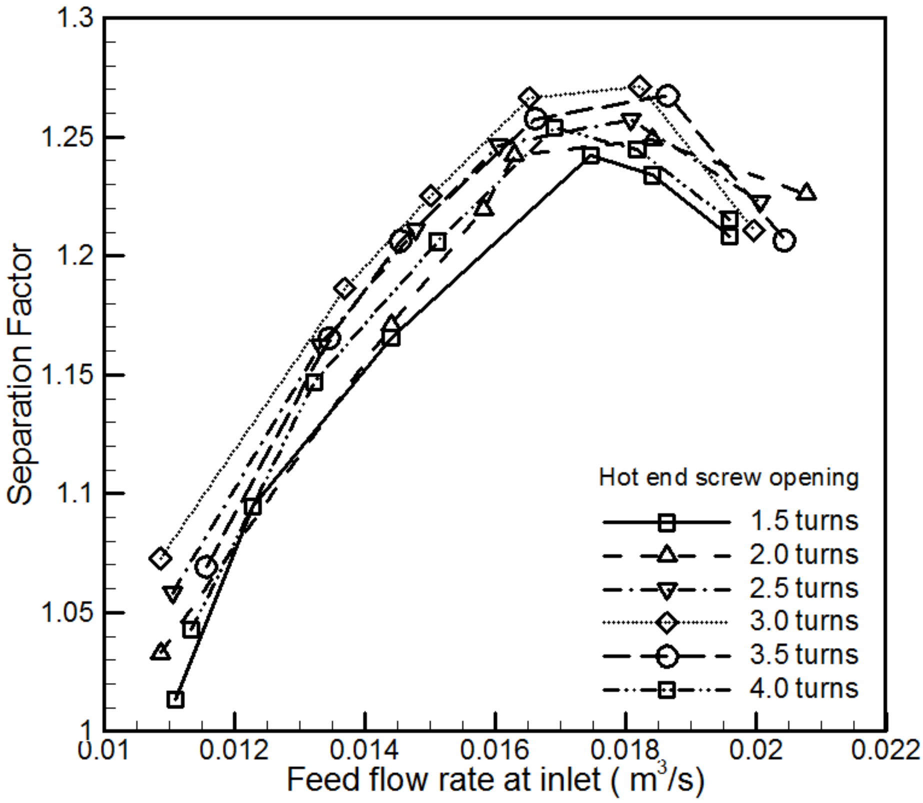

Fig. 5.4 b. Feed flow rate vs. separation factor (computed) at different values of hot end valve opening for a 25H vortex generator

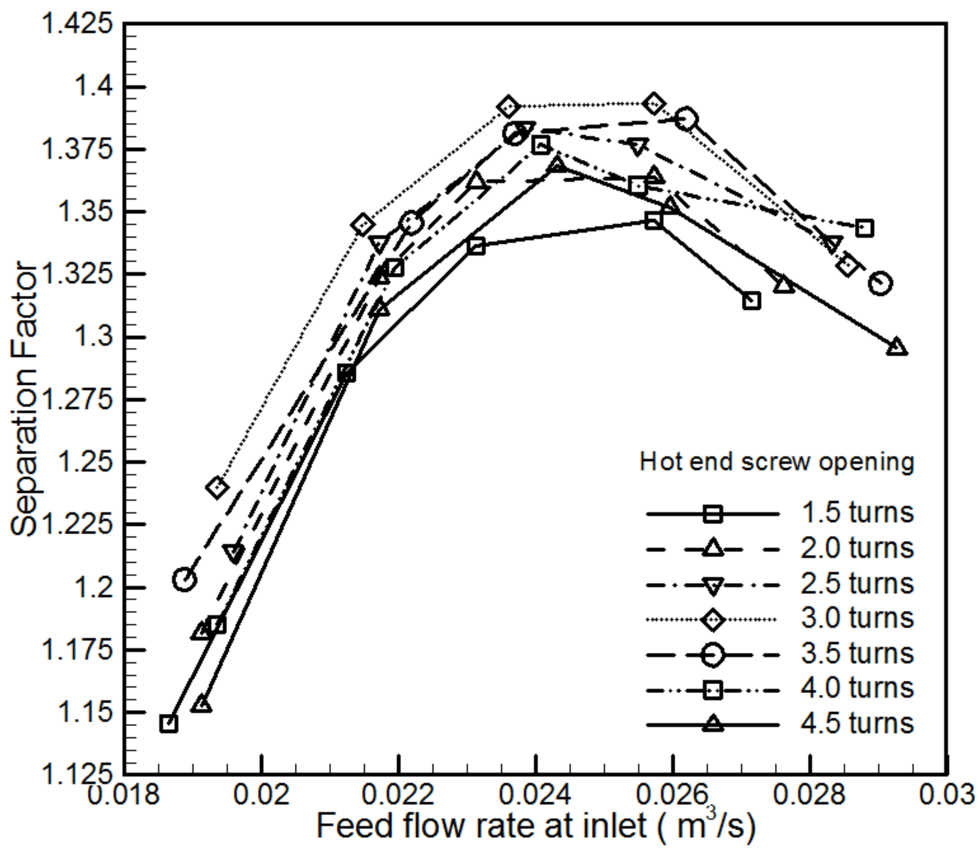

Fig. 5.4 c. Feed flow rate vs. separation factor (computed) at different values of hot end valve opening for a 40H vortex generator

feed flow rates and fixed value of hot end control valve opening for the 10H vortex generator is plotted in figure 5.4a.

The inlet volumetric flow rates for different values of hot end control valve opening and inlet pressure for a 25H vortex generator are given in table 5.3 below. For 25H vortex generator instabilities in flow at the inlet and the two outlets were observed for inlet pressure values below 1.5 kg/cm^2 and above 4.0 kg/cm^2. Similarly for hot end control valve opening values below 1.5 the flow rates are not stable. Hence separation factor values can be calculated for the 25H vortex generator for an inlet pressure range of 1.5 kg/cm^2 to 4.0 kg/cm^2 with hot end control valve opening kept in the range 1.5 to 4.0. No effects on separation factor values were observed beyond 4.0 opening. Variation in separation factor values with variable feed flow rates and fixed value of hot end control valve opening for the 25H vortex generator is plotted in figure 5.4b.

Table 5.3: Inlet pressure vs. inlet flow rate for 25H vortex generator

Inlet pressure (kg/cm^2)	Inlet volumetric flow rate (m^3/s) x E+02 for different values of hot end control valve opening					
	1.5	2.0	2.5	3.0	3.5	4.0
1.5	1.109	1.085	1.104	1.085	1.156	1.133
2.0	1.227	1.439	1.331	1.369	1.345	1.321
2.5	1.439	1.581	1.477	1.501	1.454	1.510
3.0	1.746	1.628	1.605	1.652	1.661	1.690
3.5	1.841	1.841	1.808	1.822	1.864	1.817
4.0	1.959	2.077	2.006	1.996	2.044	1.959

The inlet volumetric flow rates for different values of hot end control valve opening and inlet pressure for a 40H vortex generator are given in table 5.4 below.

Table 5.4: Inlet pressure vs. inlet flow rate for 40H vortex generator

Inlet pressure (kg/cm^2)	Inlet volumetric flow rate (m^3/s) x E+02 for different values of hot end control valve opening						
	1.5	2.0	2.5	3.0	3.5	4.0	4.5
2.0	1.864	1.911	1.959	1.935	1.888	1.935	1.911
2.5	2.124	2.171	2.171	2.147	2.218	2.195	2.171
3.0	2.313	2.313	2.383	2.360	2.369	2.407	2.431
3.5	2.572	2.572	2.549	2.572	2.619	2.549	2.596
4.0	2.714	2.761	2.832	2.855	2.902	2.879	2.926

For 40H vortex generator instabilities in flow at the inlet and the two outlets were observed for inlet pressure values below 2.0 kg/cm^2 and above 4.0 kg/cm^2. Similarly for hot end control valve opening values below 1.5 the flow rates are not stable. Hence separation factor values can be calculated for the 40H vortex generator for an inlet pressure range of 2.0 kg/cm^2 to 4.0 kg/cm^2 with hot end control valve opening kept in the range 1.5 to 4.5. No effects on separation factor values were observed beyond 4.5 opening. Variation in separation factor values with variable feed flow rates and fixed value of hot end control valve opening for the 40H vortex generator is plotted in figure 5.4c.

Species separation was observed in all the three cases shown in figure 5.4. Comparing the three graphs in figure 5.4 and tables 5.2, 5.3 and 5.4, it was observed that for a fixed value of inlet pressure, feed flow rate increases with increasing capacity of the vortex generators. This is due to increasing conductance across the vortex chamber. The range of values of the separation factors also increase from lower to higher capacity of vortex generators as the higher capacity generators can produce higher swirling motion in the gas mixture. It is observed that separation factor increases continuously with feed flow rate for 10H vortex generator. The maximum value of separation factor for 10H generator might be obtained at a higher value of inlet flow rate which is limited by the available inlet pressure from the compressor in our experimental setup. The separation factor goes through a maximum for 25H and 40H generators. This phenomenon can be explained in the following manner. We have seen in the three tables (table 5.2, 5.3 and 5.4) above that inlet flow rate increases with inlet pressure. This pressure head converts into velocity head and increases the rotational velocity. Now the species separation occurs due to differential diffusion of species of different masses in a centrifugal force field. Hence with increasing rotational velocity species separation increases. Therefore the values of separation factors increase with increasing inlet pressure. Now as species separation increases, more and more heavier component of the binary mixture gets deposited near the wall, increasing the partial pressure of the component. Hence from equation 5.12 as P_w increases, (P-P_w) the potential difference for mass transfer decreases. Hence at higher values of inlet pressure separation decreases and the values of separation factor start falling as seen in figure 5.4 b and c. The optimum value of feed flow rate is 0.0175 m^3/s for 25H vortex generator while it is 0.025 m^3/s for 40H vortex generator.

Further, the cold mass fraction is defined by

$$\theta_c = \frac{m_2}{m_2+m_3} \tag{5.61}$$

Thus if $m_1 = m_2 + m_3$ is the total inlet flow rate then according to the model the flow rate of the axial stream (as well as axial return stream) is given by $m_1\theta_c$ and the flow rate of the peripheral stream is given by $m_1(1-\theta_c)$. Now the values of the opening of hot end control valve is an indication of the cold mass fraction. In the present work values of opening of hot end control valve were considered as a parameter as they are most frequently used for controlling the cold mass fraction by the operator. It can be seen from the graphs in figure 5.4 b and c that for a fixed inlet feed flow rate with increasing values of hot end control valve opening, species separation initially increases, goes through a maximum and then comes down. This is similar to optimum value of product to feed ratio for species separation reported in gas centrifugal separation of binary mixture of gases. The optimum value of hot end control valve opening is found as 3.0 turns for both cases. Hence for this value of hot end control valve opening and for optimum values of feed flow rates, the maximum value of separation factor obtained were 1.27 and 1.39 for 25H and 40H vortex generator respectively.

5.4.2 Comparison of separation factors obtained experimentally and from the model

It was observed in the previous section that the semi-empirical mathematical model developed can predict the species separation performance for a wide range of values of hot end control valve opening and inlet flow rates. In this section a set of comparison studies have been carried out to validate the semi-empirical mathematical model. For the comparison purpose of computational and experimental results the values of hot end control valve opening selected are 2.5, 3.0, 3.5 and 4.0 turns. Experiments were conducted with these values of hot end valve openings and variable inlet flow rates. Hot and cold outlet temperature values are used as input to the computer code. The computed values of separation factors are shown with a solid line while the experimental values of separation factors are shown with solid squares. It may be noted here, since turns of valve may not be able to reproduce the same opening every time for a large number of experiments, we can replace the values of turns with reading of a micrometer attached with the valve of the hot end opening valve.

Figure 5.5 shows the comparison of experimental and computed values of separation factors for 10H vortex generator plotted with inlet feed flow rate, for four different values of hot end valve opening. It can be seen from the plots that the computed results have predicted the experimental values of separation factor with acceptable accuracy. The experimental values of separation factors are slightly over predicted for 2.5 opening while these values are slightly under predicted for 4.0 opening. These may be due to experimental error in temperature measurement.

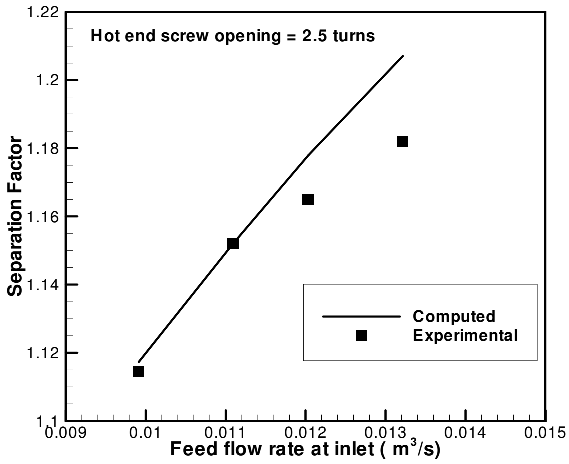

a. Hot end valve opening = 2.5 turns

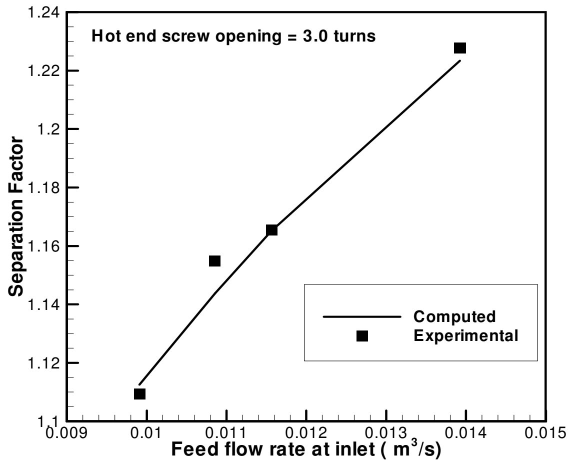

b. Hot end valve opening = 3.0 turns

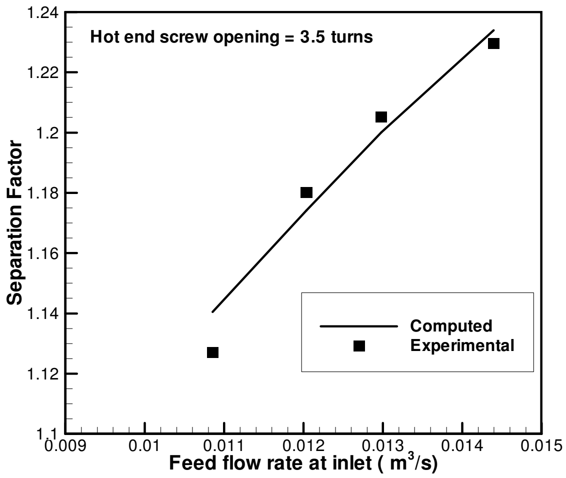

c. Hot end valve opening = 3.5 turns

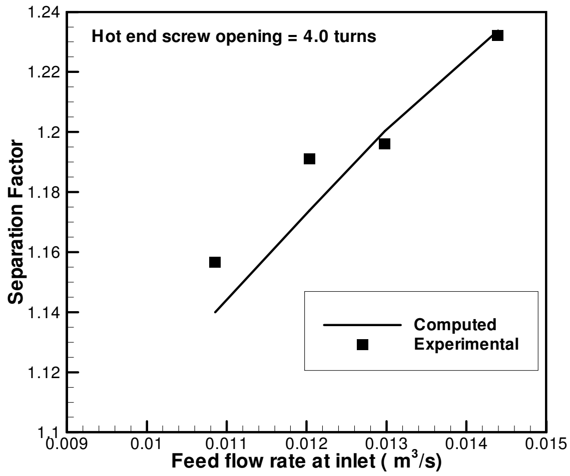

d. Hot end valve opening = 4.0 turns

Fig. 5.5 Feed flow rate vs. experimentally obtained and computed separation factors for different hot end valve opening for 10H vortex generator

Figure 5.6 shows the comparison of experimental and computed values of separation factors for the 25H vortex generator plotted with inlet feed flow rate. Here also it can be seen from the plots that the difference between computed values and experimentally obtained values of separation factors are slightly higher for lower values of hot end control valve opening like 2.5 to 3.5. It can be observed that for a higher value of hot end control valve opening like 4.0, the agreement between experimental and theoretical value improves.

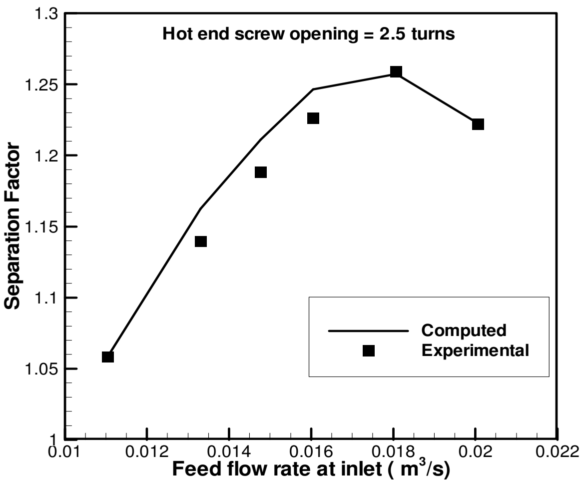

Hot end valve opening = 2.5 turns

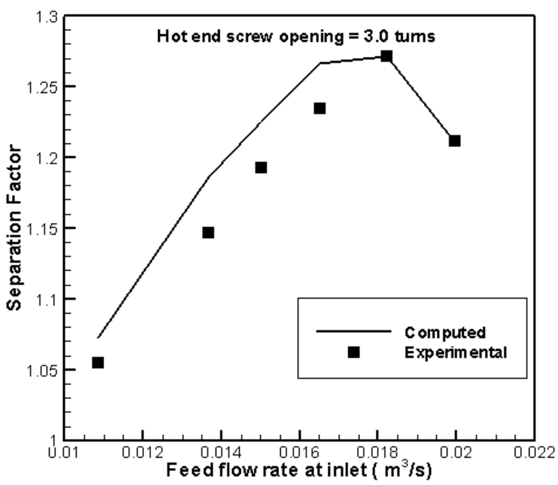

Hot end valve opening = 3.0 turns

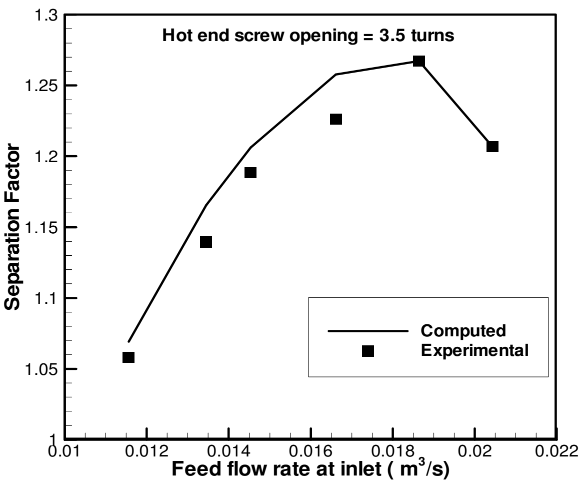

Hot end valve opening = 3.5 turns

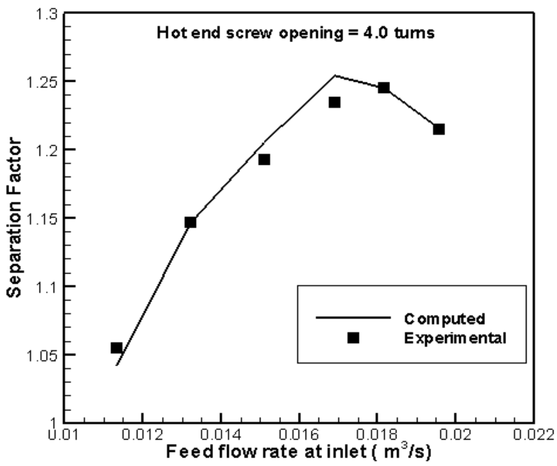

Hot end valve opening = 4.0 turns

Fig. 5.6 Feed flow rate vs. experimentally obtained and computed separation factors for different hot end valve opening for 25H vortex generator

Comparison of experimental and computed values of separation factors for the 40H vortex generator is plotted in figure 5.7. It can be seen from the graphs that for all the different values of hot end control valve opening the differences between experimental and computed values of separation factors are relatively small and the prediction by the model is acceptable.

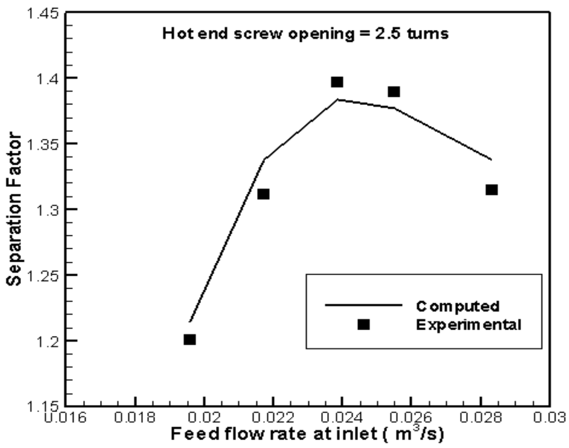

Hot end valve opening = 2.5 turns

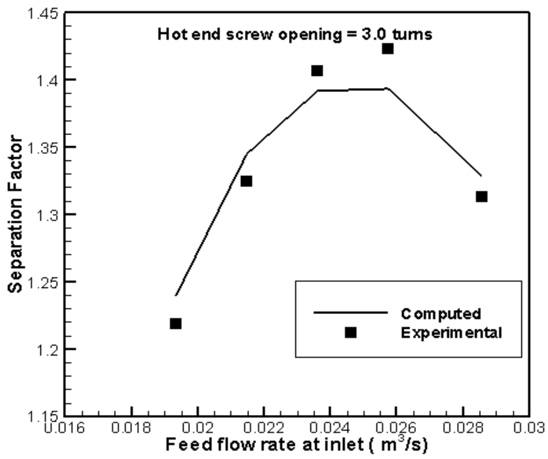

Hot end valve opening = 3.0 turns

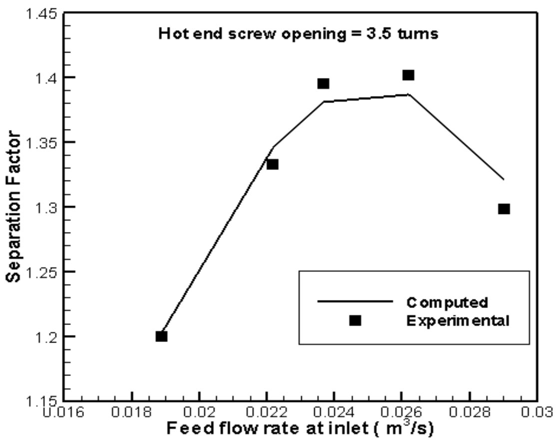

Hot end valve opening = 3.5 turns

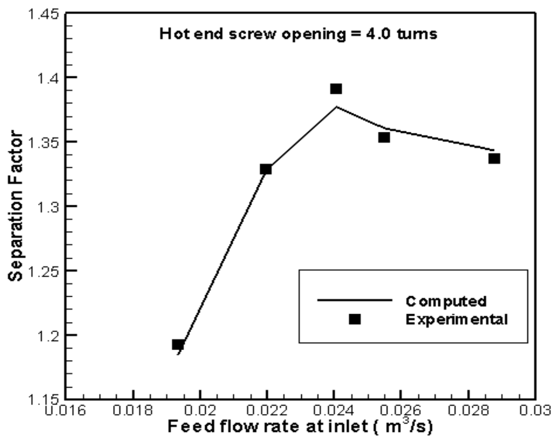

Hot end valve opening = 4.0 turns

Fig. 5.7. Feed flow rate vs. experimentally obtained and computed separation factors for different hot end valve opening for 40H vortex generator

5.5 Mechanistic model vs. present model

A mechanistic model assumes that a complex system can be understood by examining the workings of its individual parts and the manner in which they are coupled. Hence in a mechanistic model the basic elements of the model have a direct correspondence to the underlying mechanisms in the system being modelled. Now the present RHVT system is broadly subdivided into four parts and they are

- Cold outlet section,
- Vortex generation chamber section,
- Vortex tube section and
- Hot outlet section

It is understood from previous research work reported in the literature that the vortical flow is generated inside the vortex generation chamber section and it propagates insides the vortex tube section. The remaining two sections i.e. cold and hot outlet sections act as outlet of the cold and hot stream respectively. The centrifugal field acting on the rotating gas mixture is the driving force for species separation as indicated by Linderstrom-Lang [114,115]. Inside the vortex tube section, the gas molecules are subjected to a strongly rotating centrifugal field (Benedict and Pigford [27]). The heavier molecules of the gas mixture are thrown to the peripheral region of the tube while the lighter molecules of the gas mixture are concentrated near the centre. Now it is evident that the rotating gas mixture moves axially from the vortex generation chamber section towards the hot outlet section. Hence this axial flow can be divided into two parallel streams. The first is the peripheral stream that moves towards the hot end along the *z* direction, located far from the centre line and adjacent to the cylindrical tube wall, while the second is the axial stream that moves in parallel to the peripheral stream in the same direction but located near the centre line.

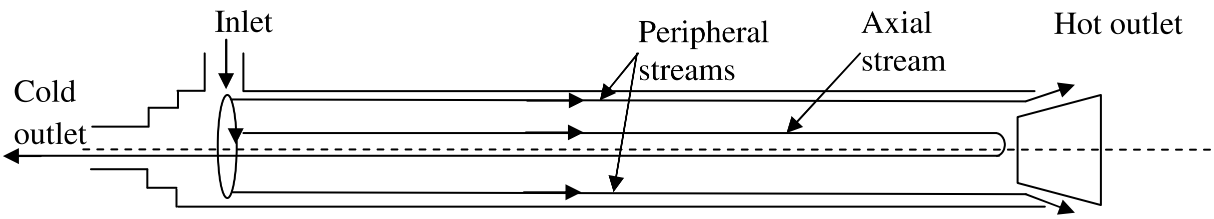

Fig. 5.8. Different flow streams in RHVT

As these two parallel streams move towards the hot end, atoms/molecules of the heavier species experience higher centrifugal force towards the periphery as compared to the lighter species and preferentially get transferred to the peripheral stream. The peripheral stream is collected from the outer periphery of the hot outlet while the axial stream bounces over the hot end control valve, takes a U turn and flows toward the cold exit and comes out of the cold exit.

Hence at any cross section of the tube there is a net inflow and a net outflow in the axial direction (both are convective in nature) and a diffusive net mass transfer in radial direction. The net mass transfer is expressed in terms of mass transfer coefficient and partial pressure difference of the heavier species in the radial direction. But many times data on mass transfer coefficient are not available for various systems. The best solution is to experimentally measure coefficients on a bench scale (using a wetted-wall column, etc.) and then use the results to design a full scale separation tube. When this isn't feasible, more approximate arrangements like use of heat mass and momentum transfer analogies are made. Using these analogies under applicable range we can calculate the mass transfer coefficient from the heat transfer coefficient for a device like RHVT where mass and heat transfer occurs simultaneously.

The Chilton–Colburn J-factor analogy is a successful and widely used analogy between heat, momentum, and mass transfer (McCabe *et. al.* [119]). The basic mechanisms and mathematics of heat, mass and momentum transport are essentially the same. The main assumption in this analogy is that heat flux q/A in a turbulent system is analogous to momentum flux τ. There are various mass, momentum and heat transfer analogies (like Reynolds analogy, Prandtl–Taylor analogy) available, which can directly relate heat transfer coefficients, mass transfer coefficients and friction factors. Out of these analogies Chilton and Colburn J-factor analogy proved to be the most accurate. Hence under the applicable range of the analogy the model is able to produce good and acceptable results, though it is not purely mechanistic in nature.

5.6 Summary

This chapter describes in detail the mathematical model developed as part of the present research work to calculate simultaneous heat and mass transfer in the RHVT. Initially a semi-empirical model for mass transfer has been introduced that makes use of the well known Chilton-Colburn analogy and requires experimental thermal data. The Governing equations have been derived and inputs required for the model have been discussed. A detailed description of the procedure adopted in the model to solve the heat and mass transfer ODEs have been provided. The model can calculate concentration of axial and peripheral gas stream along length of the RHVT. Hence separation factors which are the indicators of species separation can be calculated from the concentration of the outlet streams i.e. hot and cold outlets. Separation factors thus obtained from the mathematical model have been plotted with inlet feed flow rates for three different vortex generators and a range of hot end valve opening values. Further a set of comparison studies have been carried out to validate the semi-empirical mathematical model. In these studies separation factor values obtained from the semi-empirical model developed have been compared with the experimentally obtained values from the experimental setup and the match was found satisfactory.

The model requires experimental axial temperature profile of the RHVT, and hence is not purely theoretical. In order to eliminate the need of experimental thermal data a thermal model is introduced which makes the model fully theoretical. Introduction of this thermal model in the semi-empirical model developed is discussed in the next chapter. The following conclusions can be drawn from the discussions of this chapter:

- Using Chilton Colburn analogy we can calculate the mass transfer coefficient from the heat transfer coefficient for a device like RHVT where mass and heat transfer occurs simultaneously.
- In the range of inlet pressure considered while separation factor increases continuously with feed flow rate for 10H vortex generator, its value goes through a maxima for 25H and 40H vortex generators.
- The optimum value of inlet flow rate for which separation factor maximizes is found to be a function of hot end valve opening which is an indicator of cold mass fraction.
- The present mathematical model can compute mass transfer in a counter current RHVT based on inlet pressure, temperature, concentration, flow rate and outlet pressure, temperature and flow rate. This model can be used for rapid design and simulation of species separation in a RHVT

Chapter 6

Introduction of a heat transfer model in the semi empirical model

Not everything that can be counted counts and not everything that counts can be counted.
- Albert Einstein

6.1 Introduction

In the previous chapter the mathematical model developed as part of the present research work to calculate simultaneous heat and mass transfer in the RHVT has been described. This mass transfer model uses well known Chilton-Colburn analogy to calculate mass transfer coefficient and is semi-empirical in nature as it requires experimental thermal data. As an extension of the present modelling work on mass transfer in a RHVT, a mathematical model for heat transfer has been implemented to calculate the thermal gradient along the length of the RHVT. Together with these set of numerically calculated thermal data our previously developed mass transfer model can calculate the concentration gradient along the axial direction of the RHVT with-out any experimentally obtained temperature data, and thus becomes fully theoretical. Results from this combined numerical heat and mass transfer model has been presented in the following sections for wide range of inlet pressure and cold mass fraction values.

6.2 Heat transfer model adapted in the present work

In the present work the one dimensional analytical model for thermal separation given by Shannak [164] had been adapted to determine the temperature profile in the RHVT. In this model friction loss and heat loss inside the RHVT had been accounted for. The geometry of the RHVT was simplified to that of a tee junction system containing three tubes with an orifice plate at the cold outlet line (to mimic the vortex generator) as shown in figure 6.1. The model assumed a one dimensional flow and the RHVT was well insulated from its surroundings. The gas inside the RHVT was considered as an ideal gas and effect of gravity had been neglected.

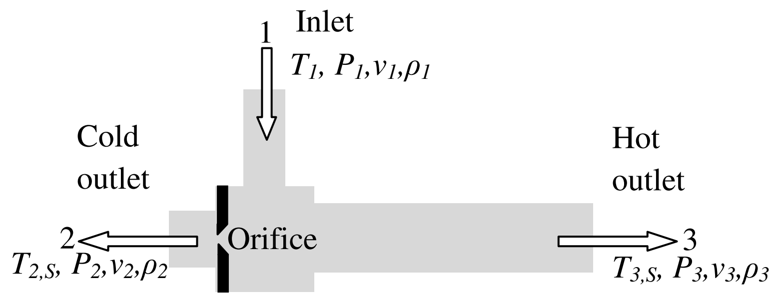

Fig. 6.1 Shannak [164] model for heat transfer calculation in a RHVT

The Bernoulli equation applied over a control volume for a fully developed flow between sections 1 and 2 and neglecting the difference in elevation between these two sections,

$$P_1 + \frac{\rho_1 v_1^2}{2} = P_2 + \frac{\rho_2 v_2^2}{2} + \Delta P_{f(1-2)} \tag{6.1}$$

where,
$$\Delta P_{f(1-2)} = \frac{\rho_2 v_2^2}{2}\left(\varphi_T + \varphi_O + \sum f \frac{L}{D_{vt}}\right) \tag{6.2}$$

and the Bernoulli equation for section 1 to 3 as

$$P_1 + \frac{\rho_1 v_1^2}{2} = P_3 + \frac{\rho_3 v_3^2}{2} + \Delta P_{f(1-3)} \tag{6.3}$$

where
$$\Delta P_{f(1-3)} = \frac{\rho_3 v_3^2}{2}\left(\varphi_T + \sum f \frac{L}{D_{vt}}\right) \tag{6.4}$$

Where P is the static pressure, ρ is the density of the fluid and v is the fluid velocity. In the figure 6.1 above, section 1, 2 and 3 are the compressed inlet, the cold exit and the hot exit condition, respectively. $\Delta P_{f(1-2)}$ is the frictional pressure drop between section 1 and section 2 while $\Delta P_{f(1-3)}$ is the frictional pressure drop between section 1 and section 3, φ_T is the local loss coefficient of the tee junction, φ_O is the local loss coefficient of the orifice plate, f is the friction factor of the pipe, D_{vt} is the diameter and L is the length of the RHVT. Equation 6.2 applied between port 1 and 2 of the RHVT contains both the orifice plate loss coefficients φ_O along with tee junction loss coefficient φ_T as the path from inlet 1 to cold outlet 2 contains both the tee junction and orifice plate. Whereas equation 6.4 applied between port 1 and 3 of the RHVT contains only the tee junction loss coefficient φ_T as the path from inlet 1 to cold outlet 3 contains only the tee junction. To determine the mass density of an ideal gas, the equation of state can be expressed as,

$$\rho_i = \frac{P_i}{RT_i}, where\ i = 1,2, \tag{6.5}$$

With the above basic equations the relationship between inlet and hot outlet temperature was given by Shannak [164] as

$$\frac{T_1}{T_{3,S}} = \frac{m_3}{m_1}\left[\frac{m_3}{m_2}\frac{1}{F_{(1-3)}} + 1\right] \tag{6.6}$$

while the relationship between hot and cold outlet temperature was given by

$$\frac{T_{2,S}}{T_{3,S}} = \frac{m_3^2}{m_2^2}\left[\frac{1}{F_{(2-3)}}\right] \tag{6.7}$$

where the model parameters $F_{(1-3)}$ and $F_{(2-3)}$ were determined based on experimental data and represented by empirical correlations in terms of the influencing parameters like cold air mass fraction θ_c, inlet pressure P_1 and inlet temperature T_1. Details of the expressions used for calculating $F_{(1-3)}$ and $F_{(2-3)}$ can be found in Shannak [164]. For further clarity these equations are reproduced here and used in the heat and mass transfer model.

$$\frac{1}{F_{(1-2)}} = \frac{T_1}{abT_1 + b^2cd} - \frac{1}{a} \tag{6.8}$$

$$\frac{1}{F_{(2-3)}} = \frac{T_1 - 2bc(\theta e + bg)}{a^2T_1 + a^2\theta c[\theta e + g(1-\theta^4)]} \tag{6.9}$$

where constant a, b, c and d are given as

$$a = \frac{1}{\theta} - 1 \tag{6.10}$$

$$b = 1 - \theta \tag{6.11}$$

$$c = 20.5\left(\frac{P_1}{P_{atm}}\right)^{0.6} \tag{6.12}$$

$$d = d_1 + d_2 + d_3 \tag{6.13}$$

$$d_1 = -47.531\theta^6 - 126.69\theta^5 - 135\theta^4 \tag{6.14}$$

$$d_2 = 72.18\theta^3 - 20.922\theta^2 \tag{6.15}$$

$$d_3 = 4.8847\theta + 0.0022 \tag{6.16}$$

$$e = Ln\left[\frac{1}{\theta}\right] \tag{6.17}$$

$$g = Ln\left[\frac{1}{1-\theta}\right] \tag{6.18}$$

Thus the cold outlet temperature $T_{2,S}$ and hot outlet temperature $T_{3,S}$ can be calculated from equation 6.6 and 6.7 respectively.

6.3 Validation and modification of heat transfer model

Shannak [164] had extensively compared cold and hot outlet temperature data computed from his thermal model with experimental data and also with data from published literature for different values of inlet pressure and temperature. In the present work outlet temperature values calculated from this model are also verified and the results are described in the following section

6.3.1 Validation of the heat transfer model

Subudhi and Sen [175] had published a collection of experimentally obtained thermal separation data in RHVT for a range of lengths, diameters, inlet pressures and cold mass fractions with air as working fluid. Some of these data have been used to verify the result from the thermal model adapted in present work.

Table 6.1: Comparison of experimental data (Subudhi and Sen [175]) with thermal model

Sr. No.	Reference	P_1 (kPa)	L (mm)	D_{vt} (mm)	d_i (mm)	$\theta_{c,opt}$	$\Delta T_{2,L}$ (K)	$\Delta T_{2,S}$ (K)	$\Delta T_{3,L}$ (K)	$\Delta T_{3,S}$ (K)
1	Hilsch [88]	709.27	230	4.6	1.1	0.23	45	42.36	13	7.61
2	Scheper [160]	202.65	914	38.1	6.35	0.26	11.7	13.07	3.9	3.63
3	Martynovskii & Alekseev [122]	607.95	450	9	2.3	0.3	38	39.19	16.3	11.02
4	Scheller & Brown [159]	618.08	1092	25.4	-	0.506	23	29.49	15.6	18.08
5	Bruun [31]	202.65	520	94	21.5	0.23	20	18.34	6	4.84
6	Stephan *et. al.* [174]	607.95	352	17.6	4.1	0.3	38	39.19	18	17.02
7	Promvonge & Eiamsa-ard [143]	455.96	720	16	2.0	0.38	18	19.33	8	13.83
8	Aljuwayhel *et. al.* [11]	303.97	100	19	1.0	0.1	11	8.83	1.2	0.75
9	Aydin & Baki [16]	607.95	750	18	6.0	0.2	50	45.32	15	15.3
10	Hamoudi *et. al.* [82]	506.62	100	2	0.8	0.57	18.5	19.53	11.8	9.89
11	Eiamsa-ard *et. al.* [62]	405.30	720	16	2.0	0.3	17	17.7	4	8.24
12	Valipour & Niazi [187]	405.30	400	19.05	-	0.24	21	21.56	5	5.45
13	Im & Yu [89]	202.65	280	20	8.1	0.5	17	19.12	12	12.6

The comparison is given in the table 6.1. In this table

$$\Delta T_{2,L} = T_1 - T_2 \qquad (6.19)$$

is the temperature drop in the cold outlet obtained from the experimental values reported by different researchers, and

$$\Delta T_{2,S} = T_1 - T_{2,S} \qquad (6.20)$$

is the temperature drop in the cold outlet calculated from Shannak [164] model respectively. Similarly in table 6.1,

$$\Delta T_{3,L} = T_3 - T_1 \qquad (6.21)$$

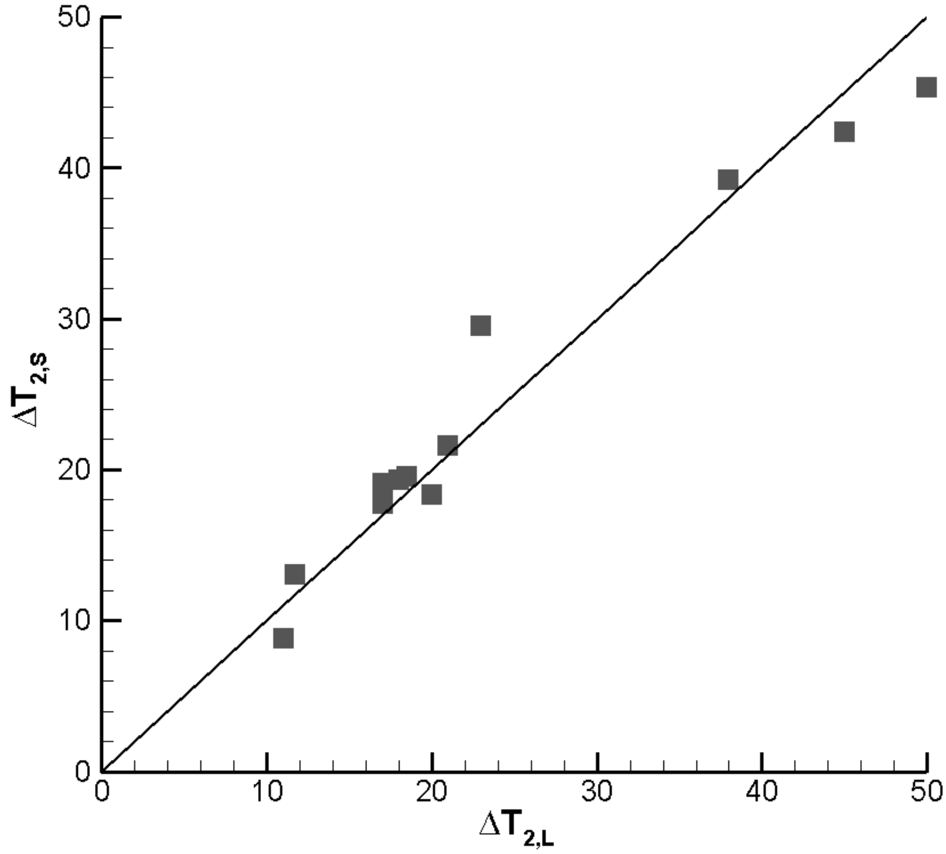

Fig. 6.2 Comparison of predicted temperature drop at the cold end of RHVT with experimental values reported in literature

is the temperature gain in the hot outlet obtained from the experimental values reported where as

$$\Delta T_{3,S} = T_{3,S} - T_1 \tag{6.22}$$

is the temperature gain at the hot outlet obtained from the Shannak [164] model respectively.

Now temperature drop at the cold end of RHVT predicted by the present code ($\Delta T_{2,S}$) is plotted with experimental values reported in literature ($\Delta T_{2,L}$) in figure 6.2. A 45º line is also plotted for comparison of the two sets of values. Similarly temperature rise at the hot end of RHVT predicted by the present code ($\Delta T_{3,S}$) is plotted with experimentally obtained values of temperature rise reported in literature ($\Delta T_{3,L}$) in figure 6.3. It can be seen from both the figures that the spread of the data points are uniform around the 45º

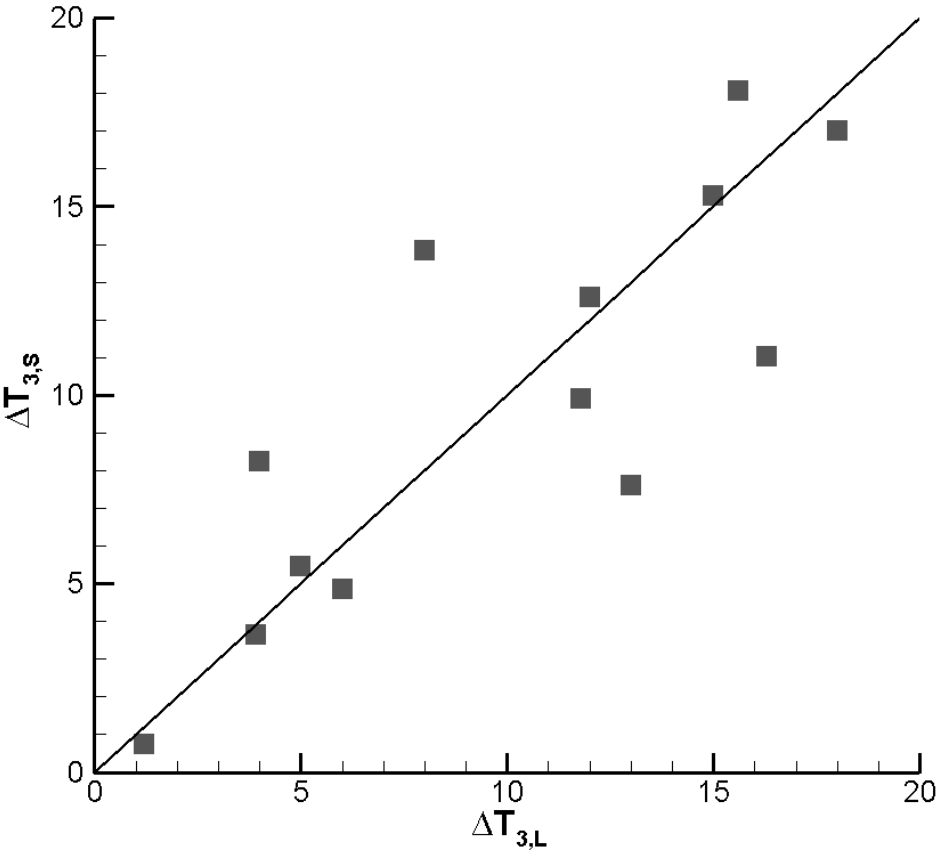

.

Fig. 6.3 Comparison of predicted temperature rise at the hot end of RHVT with experimental values reported in literature line. By comparing the temperature gain and loss data from plots 6.2 and 6.3 it could be concluded that the model could predict the thermal data published in the literature with acceptable accuracy for engineering purposes. The spread observed is more for hot end compared to the cold end of the RHVT.

6.3.2 Modification of heat transfer model

It was observed that Shannak [164] model did not consider the loss of heat from the hot end of the RHVT and gain of heat at the cold end of the RHVT because of their temperature difference from the surrounding. This correction of temperature had been incorporated in the present work. The average heat transfer coefficient had been calculated by the following equation given by Bejan and Krauss [25] where the dimensionless Rayleigh number and Prandtl number can be calculated from physical properties.

$$Nu = \frac{hD_{vt}}{k}\left\{0.6 + \frac{0.387Ra_D^{1/6}}{\left[1+(0.559/Pr)^{9/16}\right]^{8/27}}\right\}^2 \tag{6.23}$$

In equation 6.23 Rayleigh number can be calculated by the following equation

$$Ra_D = \frac{g\beta_f \Delta T D_{vt}^3}{\nu^2}.\frac{C_m \mu}{k} \tag{6.24}$$

The ΔT value used in the above equation for the cold end is given by $\Delta T_{2,S}$ (calculated from equation 6.20) and for the hot end is given by $\Delta T_{3,S}$ (calculated from equation 6.22). In both the equations inlet temperature T_1 can be replaced by ambient temperature T_{amb}.

The increase in temperature at the cold outlet of the RHVT due to heat gain from surrounding was calculated with the following heat balance equation

$$\Delta T_c = hA_c(T_{amb} - T_{2,S})/m_c C_m \tag{6.25}$$

Hence the corrected cold outlet temperature is calculated by

$$T_2 = T_{2,S} + \Delta T_c \tag{6.26}$$

Similarly the decrease in temperature at the hot outlet of the RHVT due to heat loss to surrounding is calculated using the heat balance equation

$$\Delta T_h = hA_h(T_{3,S} - T_{amb})/m_h C_m \tag{6.27}$$

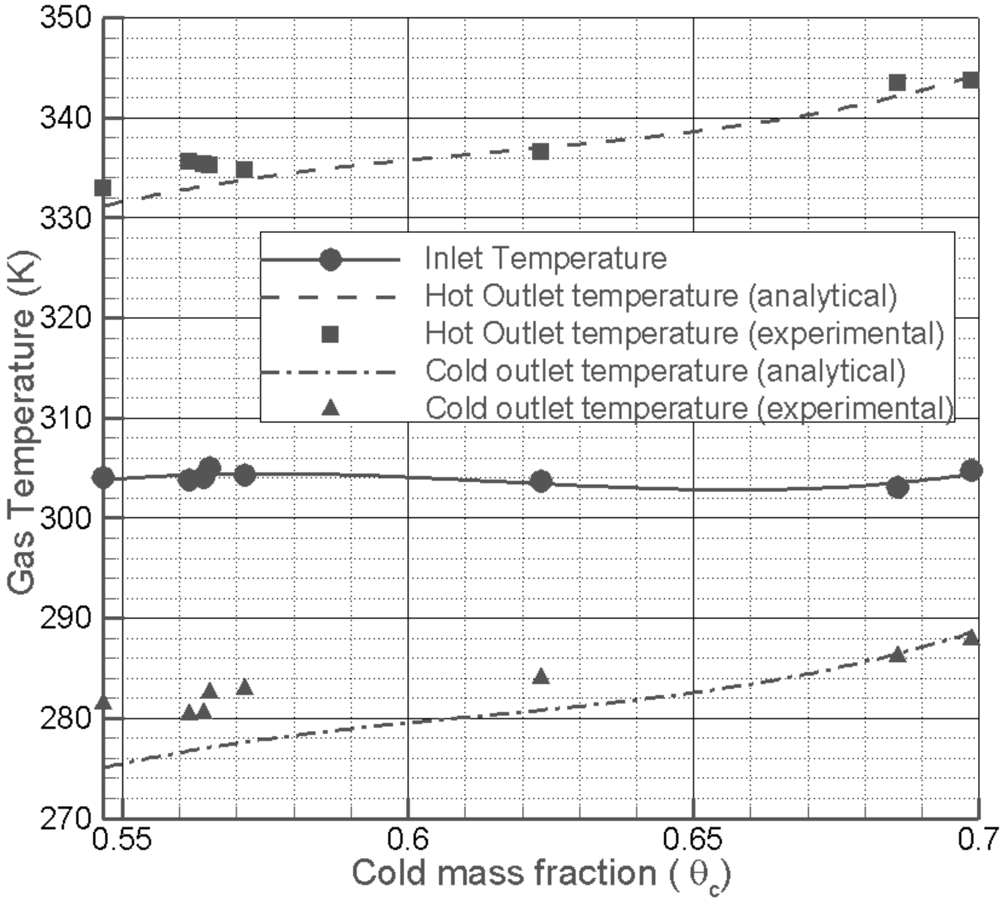

Fig. 6.4 Comparison of experimentally and analytically obtained outlet gas temperatures vs. cold air mass ratio for a given inlet air temperature and pressure

and the corrected hot outlet temperature is given by

$$T_3 = T_{3,S} - \Delta T_h \tag{6.28}$$

These corrections in cold and hot end temperatures have been incorporated in further calculations and the thermal model is called as modified Shannak [164] model.

In figure 6.4 a comparative study of outlet temperatures (at both cold and hot outlet of the RHVT) obtained from experiments conducted at our experimental facility and those obtained from the modified Shannak [164] model have been shown. For a range of cold mass fraction values obtained in the experiments with a 10H size vortex generator in a small size RHVT, the experimental values of inlet temperatures, cold outlet temperatures and hot outlet temperatures are plotted in the graph. For the same values of cold mass fraction and inlet temperature the outlet temperatures are calculated from the modified Shannak [164] model and plotted in the same graph. It can be observed from the graph that the modified Shannak [164] model for heat transfer could predict the hot and cold outlet air temperature within acceptable limits (±5%).

6.3.3 Numerical scheme for solving the governing equations for numerical model

With the introduction of modified Shannak [164] model the experimental temperature values at the cold and hot outlet can be substituted by numerically obtained values from the model. The numerical scheme used to solve the governing equation to calculate the concentration profile along the length of the RHVT is described in details in the previous chapter (section 5.3). After introducing the modified Shannak [164] model the scheme remains unchanged except in step 2 we invoke Shannak [164] model. In this step temperature at the hot outlet ($T_{3,S}$) is calculated using equation 6.6 and temperature at the cold outlet ($T_{2,S}$) is calculated using equation 6.7. The hot outlet temperature ($T_{3,S}$) calculated using Shannak [164] model is further corrected using equation 6.28 to get the final hot outlet temperature (T_3). Similarly the cold outlet temperature ($T_{2,S}$) calculated using Shannak [164] model is further corrected using equation 6.26 to get the final cold outlet temperature (T_2). These two outlet temperatures are used for further calculations as described in section 5.3 of this thesis.

6.4 Validation of the combined heat and mass transfer model

With the introduction of the modified heat transfer model as in the previous section, the requirement for conducting experiments for determining the cold and hot end temperature for a set of inlet condition became redundant. Further, the cap on highest value of inlet pressure achieved due to the limitation in capacity of compressor was removed. Hence with the help of the heat transfer model, cold and hot outlet temperature for any inlet pressure value can be calculated using the modified heat transfer model. As a result, requirement of conducting experiment to collect input data for the code could altogether be avoided. In the following sub-sections a validation study of the results from the combined heat and mass transfer model has been reported. The validation has been carried out with data obtained from the RHVT experimental setup described in chapter 4 as well as data available from literature.

6.4.1 Validation with in-house experimental results

In order to validate the results from the combined heat and mass transfer model developed in the present work, a set of experiments were conducted in a RHVT experimental facility. Details of the experimental setup, instruments and indicators used, their accuracy,

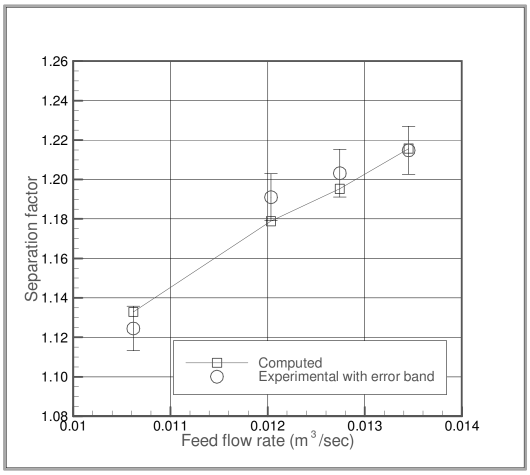

a. Hot end valve opening = 2.0 turns

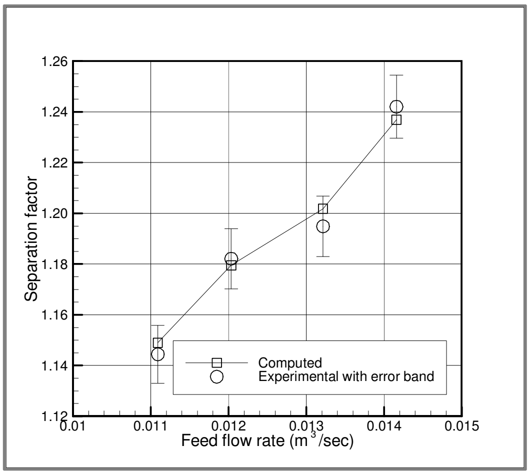

b. Hot end valve opening = 2.5 turns

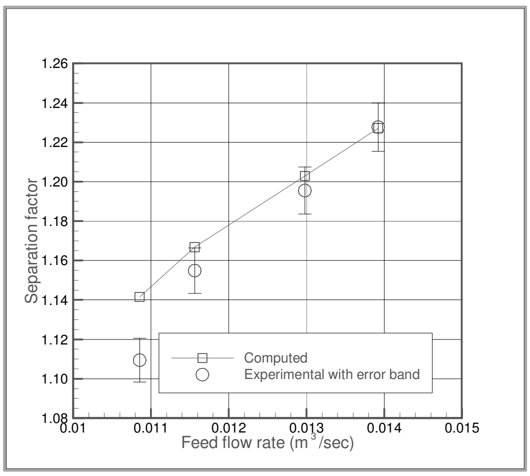

c. Hot end valve opening = 3.0 turns

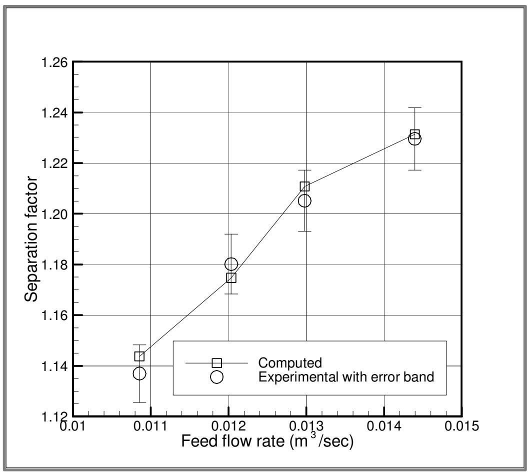

d. Hot end valve opening = 3.5 turns

Fig. 6.5 Feed flow rate vs. experimentally obtained and computed separation factor for different hot end valve opening for 10H vortex generator

geometrical dimensions of RHVT and specification of vortex generators were described in chapter 4 and are not repeated here. For experimental data reported in the present work three vortex generators (10H, 25H and 40H) were used and air as a binary mixture of nitrogen and oxygen has been considered as the working fluid.

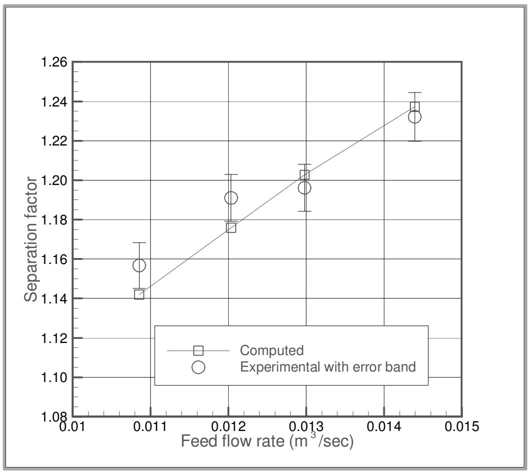

a. Hot end valve opening = 4.0 turns

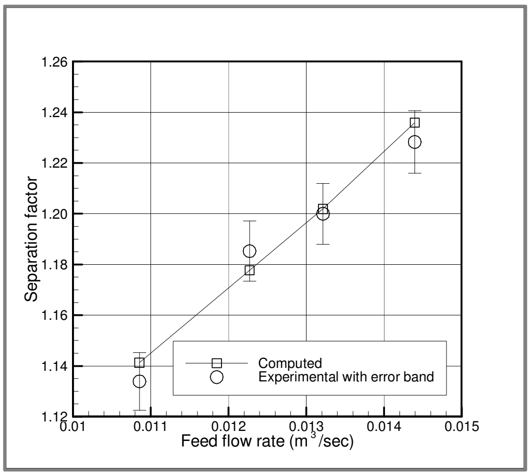

b. Hot end valve opening = 4.5 turns

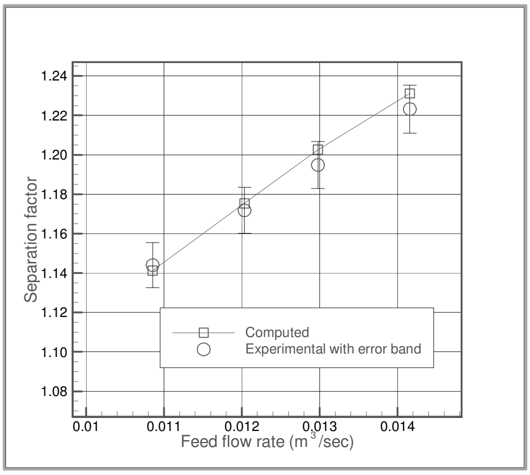

c. Hot end valve opening = 5.0 turns

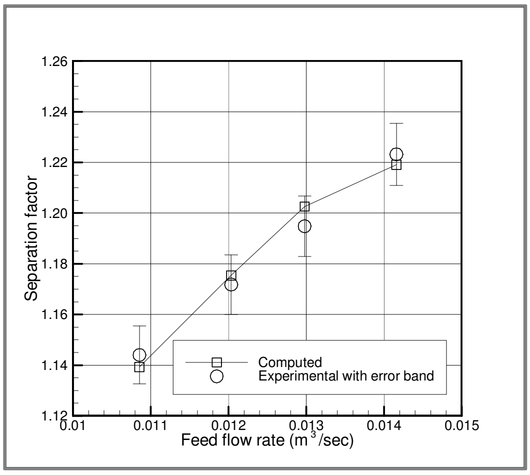

d. Hot end valve opening = 5.5 turns

Fig. 6.6 Feed flow rate vs. experimentally obtained and computed separation factor for different hot end valve opening for 10H vortex generator

A set of separation factor values were experimentally obtained by varying the inlet volumetric feed flow rates and fixed values of hot end valve openings (a measure of cold mass fraction). An uncertainty analysis of the separation factor calculated using experimental data from quadrupole mass spectrometer gives an error band of ±1%. These separation factor values with their error bands were compared in figure 6.5 (for hot end control valve opening values 2.0, 2.5, 3.0 and 3.5) and figure 6.6 (for hot end control valve opening values 4.0, 4.5, 5.0, 3.5 and 5.5) both for a 10H vortex generator with a set of theoretically calculated values of the separation factors from the combined heat and mass transfer model.

The separation factors were calculated with values of different variables like inlet pressure, temperature, flow rate and cold mass fraction same as that of the operating conditions of experiment. It can be seen from figure 6.5 and 6.6 (for a 10H generator) that among the eight values of hot end valve opening the difference between computed values and experimentally obtained values of separation factors are slightly higher for lower values of hot end valve openings like 2.0 and 3.0 (Opening 1.0 ≡ 360° open from fully closed condition, opening 2.0 ≡ 2.* 360° open from fully closed condition and so on). It can also be observed that for higher values of hot end control valve opening like 5.0 and 5.5, the agreement between experimental and theoretical values improves.

Figure 6.7 compares the separation factor values computed from the proposed simultaneous heat and mass transfer model with the experimental values obtained by varying the feed flow rates for a 25H vortex generator. For each set of separation factor vs. flow rate values the hot end valve opening value (which is an indication of cold mass fraction) is kept fixed. These values are 1.5, 2.0, 2.5, 3.0, 3.5 and 4.0 respectively. The experimentally obtained separation factors are plotted along with error bars for comparison. It can be seen from the figure that the computed values compare well with the experimental values.

Similar comparative studies have been carried out for a 40H vortex generator and results have been presented in figure 6.8. In these set of studies the hot end control valve opening values were kept at similar levels *i.e.* 1.5, 2.0, 2.5, 3.0, 3.5 and 4.0 respectively and for each value of hot end control valve opening, numerically (computed from the present code) and experimentally (from experiments carried out) obtained separation factor values are plotted against inlet feed flow rate to the RHVT unit. In this case also computed values compare well with the experimental values.

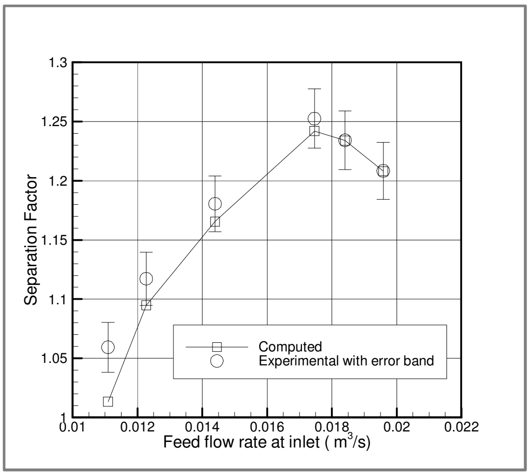

a. Hot end valve opening = 1.5 turns

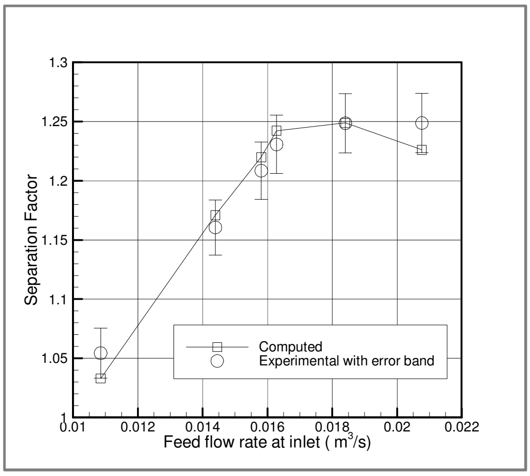

b. Hot end valve opening = 2.0 turns

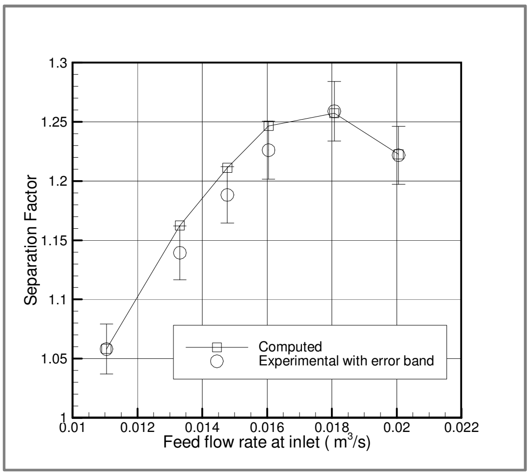

c. Hot end valve opening = 2.5 turns

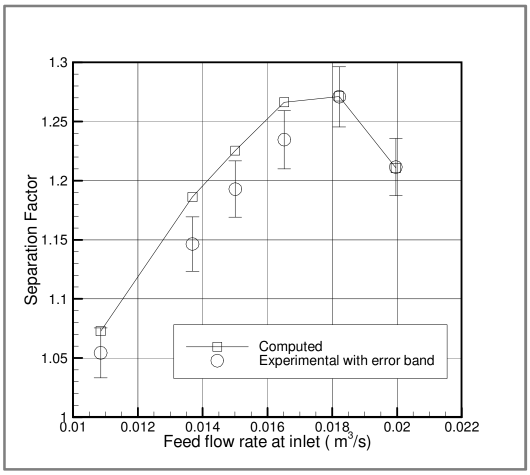

d. Hot end valve opening = 3.0 turns

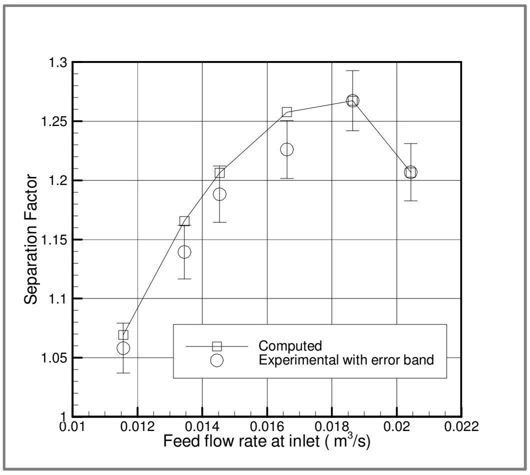

e. Hot end valve opening = 3.5 turns

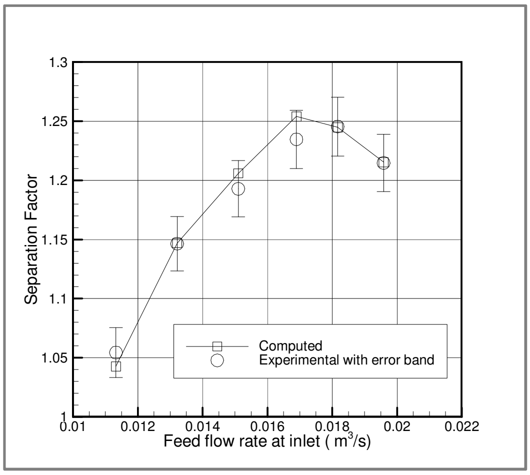

f. Hot end valve opening = 4.0 turns

Fig. 6.7 Feed flow rate vs. experimentally obtained and computed separation factor for different hot end valve opening for 25H vortex generator

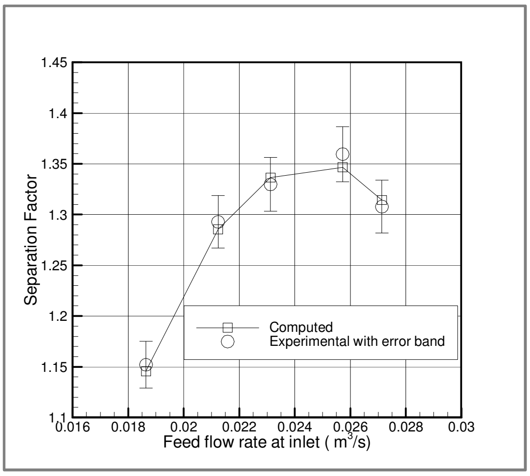

a. Hot end valve opening = 1.5 turns

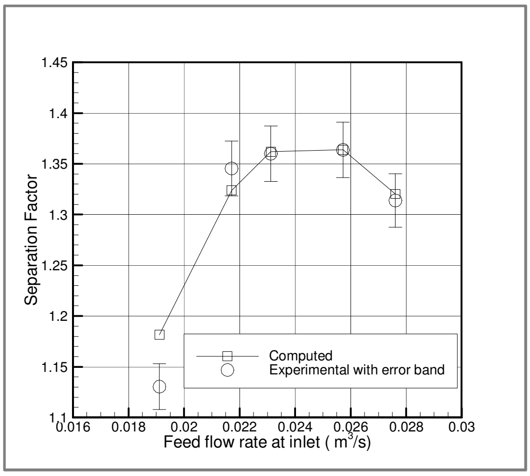

b. Hot end valve opening = 2.0 turns

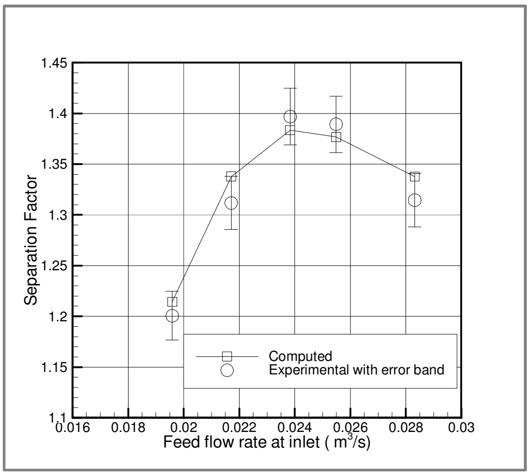

c. Hot end valve opening = 2.5 turns

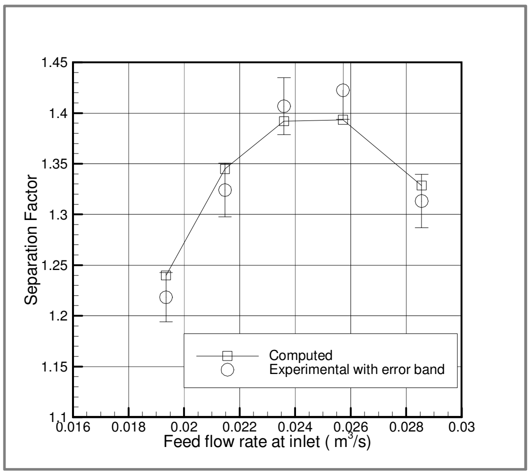

d. Hot end valve opening = 3.0 turns

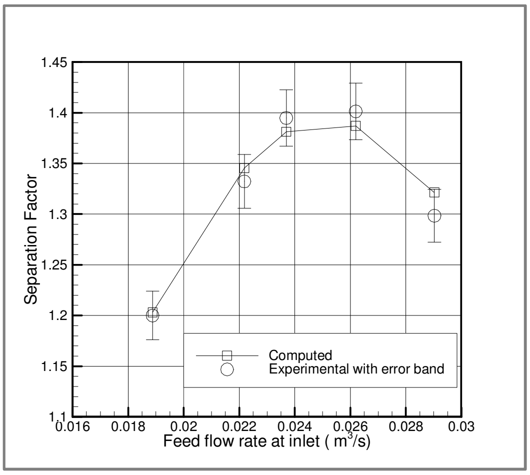

e. Hot end valve opening = 3.5 turns

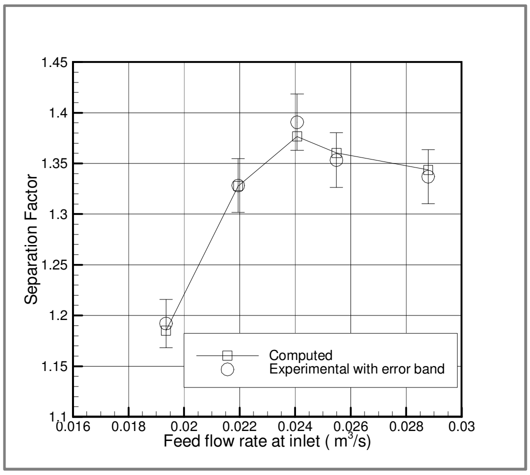

f. Hot end valve opening = 4.0 turns

Fig. 6.8 Feed flow rate vs. experimentally obtained and computed separation factor for different hot end valve opening for 40H vortex generator

6.4.2 Validation with results from literature

The data provided by Subudhi and Sen [175] and reported in table 6.1 can be used for calculating the separation factor of the RHVTs with given length, diameter and inlet diameter (except for the serial number 4 and 12) for air as working fluid. For a given inlet pressure, gas (air) properties and inlet jet diameter as the inlet diameter, Reynolds number at the inlet of the RHVT can be calculated by the following expression as given by Marshall [121].

$$Re = \frac{P_1 d_i}{\sqrt{T_1}} \cdot \frac{1}{\mu} \cdot \sqrt{\left[\frac{\gamma M_m}{R} \cdot \left(\frac{2}{1+\gamma}\right)^{(\gamma+1)/(\gamma-1)}\right]} \tag{6.29}$$

Hence the inlet mass flow rate can be calculated using the value of inlet Reynolds number obtained from equation (6.29) above.

$$m_1 = Re\frac{\mu A_i}{d_i} \tag{6.30}$$

Table 6.2: Separation factor, component and overall mass balance percentage error

Sr. No.	Calculated α	Percentage error in	
		component balance	overall mass balance
1	1.384858	3.48	-1.90
2	1.027798	-1.45	-0.34
3	1.351724	1.99	-2.05
5	1.007644	-1.05	-0.31
6	1.347319	2.08	-2.05
7	1.280517	0.75	-1.41
8	1.159103	0.83	-0.12
9	1.362066	3.17	-1.31
10	1.290862	1.50	-0.11
11	1.249952	1.00	-1.21
13	1.065369	-0.39	0.39

Now along with the inlet pressure, inlet gas temperature and temperatures at the two outlets (calculated from the modified Shannak [164] model), the inlet mass flow data are known. These set of data were used to calculate the concentration profile of the heavier species along the length of the RHVT using the one dimensional mass transfer model developed earlier. The concentration of heavier species (i.e. oxygen) in air, considered as a binary mixture of nitrogen and oxygen, can be calculated from this model at the cold and hot end of the RHVT. Hence we can calculate the separation factor of the lighter species for a binary separation as defined in equation (6.31)

$$\alpha = \frac{1-N_3}{N_3}\frac{N_2}{1-N_2} \tag{6.31}$$

Values of the separation factors and percentage error in component balance of the heavier species as well as the overall mass balance are tabulated in table 6.2. The serial numbers in the first column of table 6.2 correspond to that of table 6.1. It can be seen from table 6.2 that the percentage error in component and overall mass balance are within acceptable limit (±3.5%).

Further the calculated separation factors are plotted against the inlet pressure in figure 6.9 for the different RHVT configurations and operating conditions. A polynomial fit of the

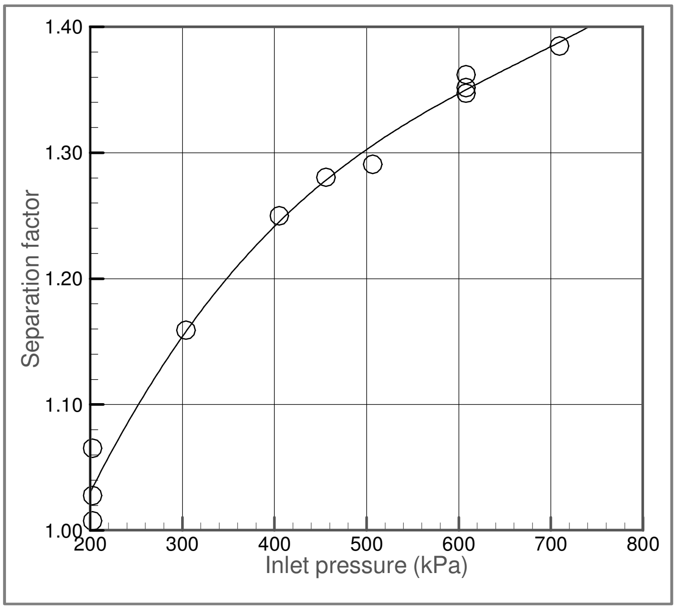

Fig. 6.9 Inlet pressure vs. separation factor for different RHVTs

separation factors vs. inlet pressure values from table 6.2 is drawn for a trend analysis of variation of separation factors with respect to inlet pressure. The fitted curve information is given below for a polynomial fit:

Goodness of Fit:

$$R^2 = 0.989278 \tag{6.32}$$

$$R^2 = 0.984682 \text{ (residual degrees of freedom adjusted)} \tag{6.33}$$

The fit is given by:

$$\text{Separation Factor} = A + B{*}P_1 + C{*}P_1^2 + D{*}\,P_1^3 \tag{6.34}$$

where,

A = 6.3488E-001

B = 2.5657E-003

C = -3.2730E-006

D = 1.6246E-009

It can be observed from figure 6.9 that for the different RHVTs at their optimum cold mass fraction, as the inlet pressure increases the value of separation factor initially increases at a higher rate. But at higher values of inlet pressure the slope of the curve becomes flatter. This behaviour of inlet pressure vs. separation factor curves will be discussed in detail in the next chapter. This polynomial fit can be used to estimate the separation factor of a RHVT for nitrogen-oxygen system based on inlet pressure.

6.5 Advantages and limitation of the model

The present work compares results obtained from experiments carried out and a one dimensional mathematical model for mass transfer in a medium sized RHVT using air as a binary mixture of nitrogen and oxygen. It was seen that using Chilton Colburn analogy we can calculate the mass transfer coefficient from the heat transfer coefficient for a device like RHVT where mass and heat transfer occurs simultaneously. The computed values of separation factors from the one dimensional mathematical model compare well with the experimental values of separation factors for the RHVT. The present mathematical model can compute mass transfer in a counter current RHVT based on inlet pressure, temperature, concentration, flow rate and outlet pressure, temperature and flow rate.

The theoretical prediction of the RHVT performance requires the aid of a Computational Fluid Dynamics (CFD) simulation. The modelling involves discretisation of flow domain and solution of high speed compressible flow field. Simulation of flow field and temperature distribution requires solution of three dimensional Navier Stokes equations along with the energy equation and ideal gas assumption. Generation of grid and running the solver requires large computation time. The computation time overhead increases considerably while employing advanced computational tools like Reynolds Average Navier Stokes (RANS), Large Eddy Simulation (LES) and Direct Numerical Simulation (DNS). In the present work a simple one dimensional mathematical model has been developed. This model can be used for rapid design and simulation of species separation in a RHVT. The mathematical model is tested for three different vortex generators (10H, 25H and 40H) over a wide range of hot end valve opening (1.5 turns to 5.0 turns) and inlet pressure (200 kPa to 800 kPa).

In the present model the mass transfer coefficient is calculated from heat transfer coefficient using the heat and mass transfer analogy. Therefore an error in the value of the heat transfer coefficient leads to error in the value of the mass transfer coefficient calculated. This is a limitation of the present model. Further the assumption of linear variation of temperature along the length of the RHVT from the inlet to the cold and hot outlet is rather simplistic. Another limitation of the present model is that because it is an one dimensional model, it cannot capture the onset as well as effects of turbulence which is three dimensional in nature. The major limitation of the present model i.e. the requirement of experimentally measured thermal profile to predict the concentration profile of a binary mixture of gas species along the length of the RHVT has been removed by introduction of a modified thermal model.

6.6 Summary

This chapter describes in detail the heat transfer model introduced in the mathematical model developed as part of the present research work to calculate simultaneous heat and mass transfer in the RHVT. Initially a semi-empirical model for mass transfer that makes use of the well known Chilton-Colburn analogy and requires experimental thermal data has been introduced. This model has been discussed in details in the previous chapter. A mathematical heat transfer model from literature have been adapted and suitably modified for the RHVT. This heat transfer model eliminates the need for experimental data required for the semi-empirical model. The outputs from the heat transfer model have been verified with data available in literature as well as from in house experiments carried out.

Next, the chapter focuses on validation of the present combined heat and mass transfer model. Validation studies have been carried out by comparing the output from the model with experimental data available from experiments carried out as a part of the present research work as well as with data available from literature. The chapter has been concluded by a section describing the advantages and limitations of the present mathematical model. The following conclusions can be drawn from the present discussion:

- The one dimensional heat and mass transfer model using Chilton-Colburn analogy described in the previous chapter is semi-empirical in nature and in the present chapter this model is modified by including a heat transfer model to make it fully theoretical.
- The computed values of separation factors from the one dimensional mathematical model compares well with the experimental values of separation factors for the RHVT.
- The mass transfer coefficient is calculated from heat transfer coefficient using the heat and mass transfer analogy. Therefore an error in the value of the heat transfer coefficient leads to error in the value of the mass transfer coefficient calculated. This is a limitation of the present model.
- Another limitation of the present model is that because it is a one dimensional model, it cannot capture the onset as well as effects of turbulence which is three dimensional in nature.

Chapter 7
Results and discussion

"The opposite of a correct statement is a false statement. But the opposite of a profound truth may well be another profound truth".
- Niels Bohr

7.1 Introduction

In chapter 5 and 6 we have discussed about the mathematical model proposed to explain the physical phenomenon of thermal as well as species separation inside a RHVT. An experimental set up to carry out thermal as well as species separation studies using the RHVT have been commissioned. Details of this setup have been discussed in chapter 4. Output from the mathematical model as well as results from the experimental setup are presented in this chapter.

Experiments in the test setup were carried out to generate process data involving independent parameters such as volumetric flow rates, temperatures and pressures of gas mixture at the inlet, opening of the hot end control valve and dependent parameters like flow rates, temperature and concentration of heavier components at the outlet of the RHVT. Air was used as working fluid. Composition and temperature of air at inlet, hot outlet and cold outlet were measured. The experimental set up has been extensively used to carry out validation studies of the result obtained from the mathematical model and validation test cases have been presented in chapter 5. Also it was found that thermal and species separations in RHVT were inter-related. Further experimental results from this setup as well as results from the mathematical model have been used to understand the effect of various parameters on the separation characteristics of the RHVT as well the sensitivity of the principal operating parameters on thermal and species separation. The results are presented along with discussions in the following sections of this chapter.

7.2 Results from mathematical model

The combined heat and mass transfer model described in chapter 5 has been used to calculate variation of oxygen concentration along the length of the RHVT from the inlet to the hot outlet in the two streams (peripheral and axial) of the flowing gas mixture. The axial oxygen concentration derived from the computer code for different values of inlet pressure have been plotted in the graphs shown in figure 7.1, 7.2 and 7.3 for vortex generators 10H, 25H and 40H respectively. Experiments are conducted to generate experimental thermal data which are used as input to the computer code based on the mathematical model. The plots are given for all the four cases of hot end control valve openings i.e. 2.5, 3.0, 3.5 and 4.0. The inlet pressures are varied in four levels and for each case inlet flow rates and cold mass fraction values are obtained experimentally. The inlet and outlet temperatures of gas (at both cold and hot outlet) are noted and used as input to the computer code. Air as a binary mixture of oxygen and nitrogen is used as the working fluid. Along with heat transfer, due to mass transfer between the peripheral and axial stream concentration of the peripheral and axial stream vary along the axis of the RHVT. The level of variations in inlet conditions is given in following table.

Table 7.1 Levels of variation in RHVT parameters

Parameters	Levels of variation
Vortex generators	10H, 25H, 40H
Hot end control valve opening	2.5, 3.0, 3.5,4.0 turns
Inlet pressure (kPa)	313.14, 392.60, 441.10, 490.20

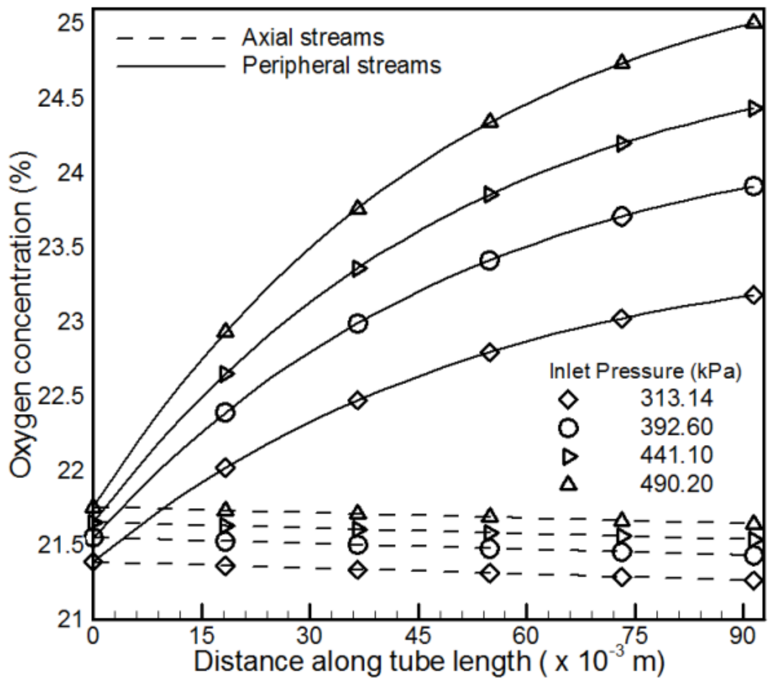

a. Hot end valve opening = 2.5 turns

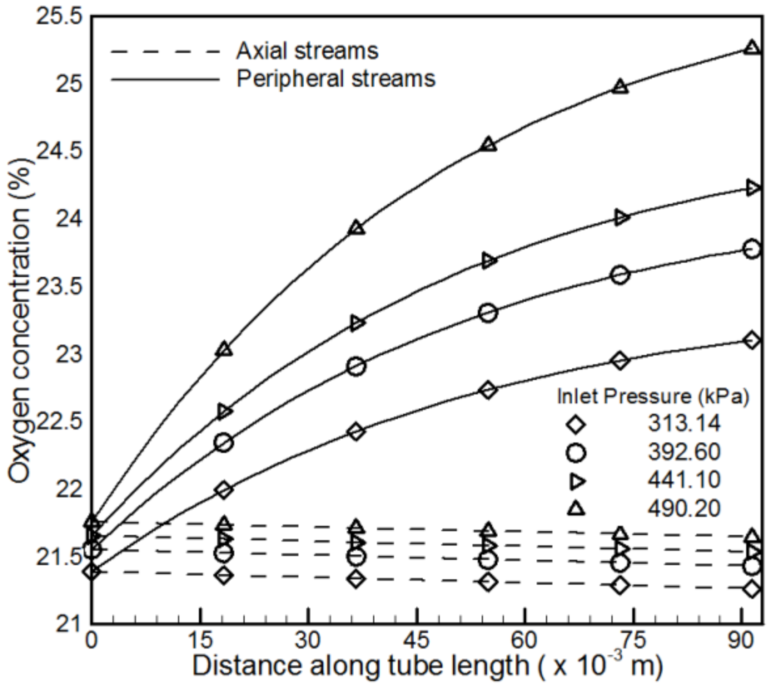

b. Hot end valve opening = 3.0 turns

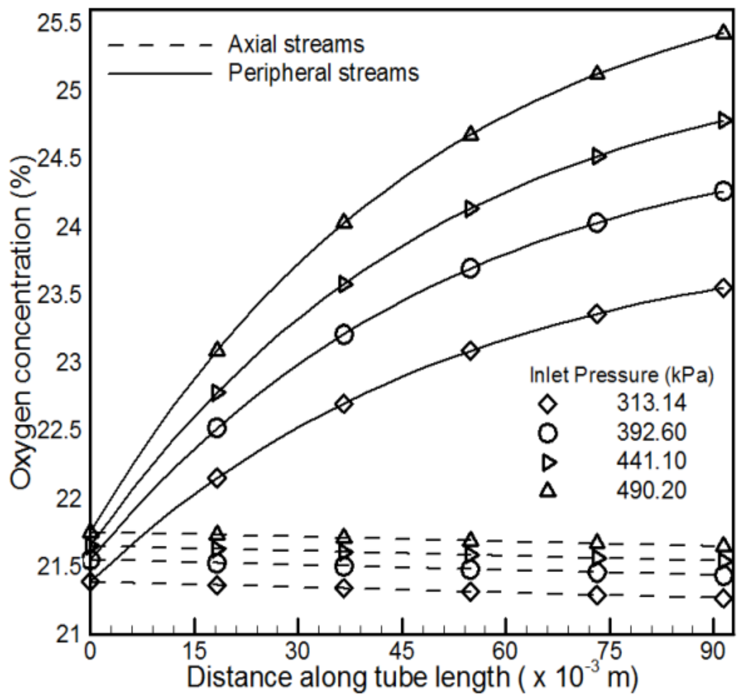

c. Hot end valve opening = 3.5 turns

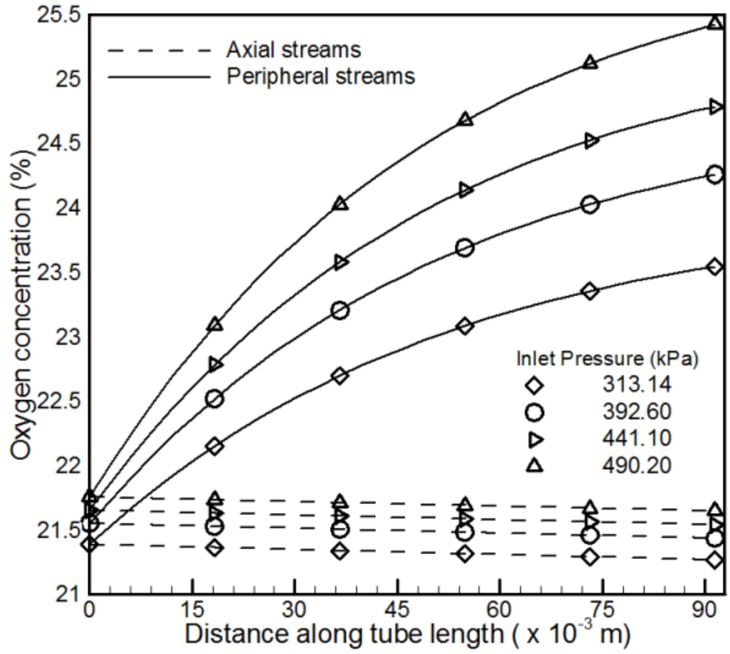

d. Hot end valve opening = 4.0 turns

Fig. 7.1 Distance vs. O_2 concentration (computed)in axial and peripheral streams for different hot end valve opening for a 10H generator

Now no experimental data for variation of oxygen concentration along the peripheral and axial stream are available for this configuration and can be obtained from a computational fluid dynamics simulation of flow field followed by solution of the species conservation equation.

It can be seen from the results, for 10H generator (figure 7.1) and for a fixed value of the hot end valve opening the concentration difference of heavier species in the gas mixture (i.e. oxygen) between the axial and peripheral streams increases continuously with increasing value of inlet pressure (which is directly proportional to inlet feed flow rate). This implies that the optimum separation factor for this generator is achievable at a still higher value of inlet pressure. Further it can be seen from the plots for 25H (figure 7.2) and 40H (figure 7.3) vortex generators, the maximum separation of oxygen concentration between the peripheral and axial streams occur at a value of inlet pressure which is less than the highest value of inlet pressure considered in this study. Hence it can be concluded that there is an optimum value of inlet pressure at which maximum species separation is observed for a given generator. The reason for this observation is discussed later in the parametric studies section of this chapter.

It can also be concluded from the graphs that this optimum value of inlet pressure changes with variation in hot end valve opening. This point can be illustrated by comparing the last two sets of graphs in figure 7.2 for hot end valve opening values of 3.5 and 4.0 respectively. We can see while the optimum value of inlet pressure is 313.14 kPa for the former case, this value is 294.12 kPa for the latter case. Hence we can conclude that species separation depends on the values of inlet pressure and hot end valve opening. Further it can be seen that while inlet pressure is an indicator of inlet flow rate, hot end valve opening is an indicator of the cold mass fraction of the unit (defined by equation (5.61)).

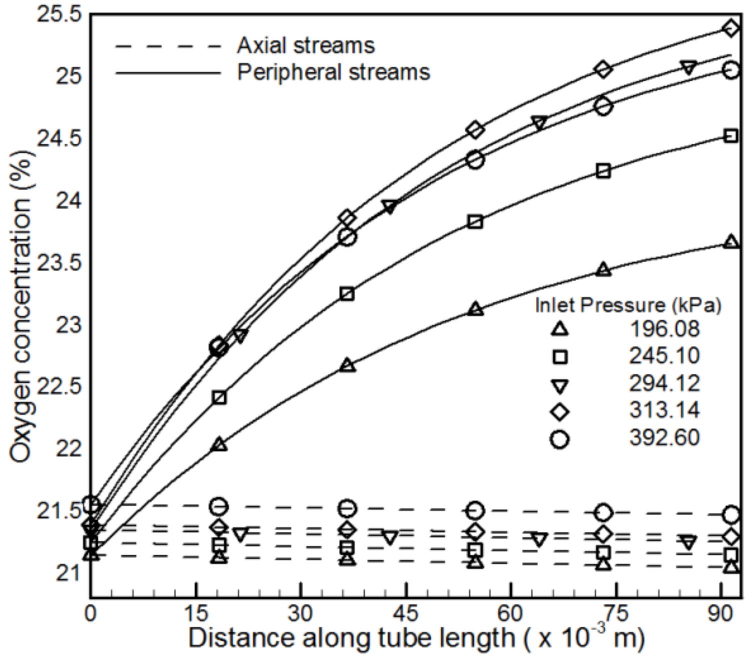

a. Hot end valve opening = 2.5 turns

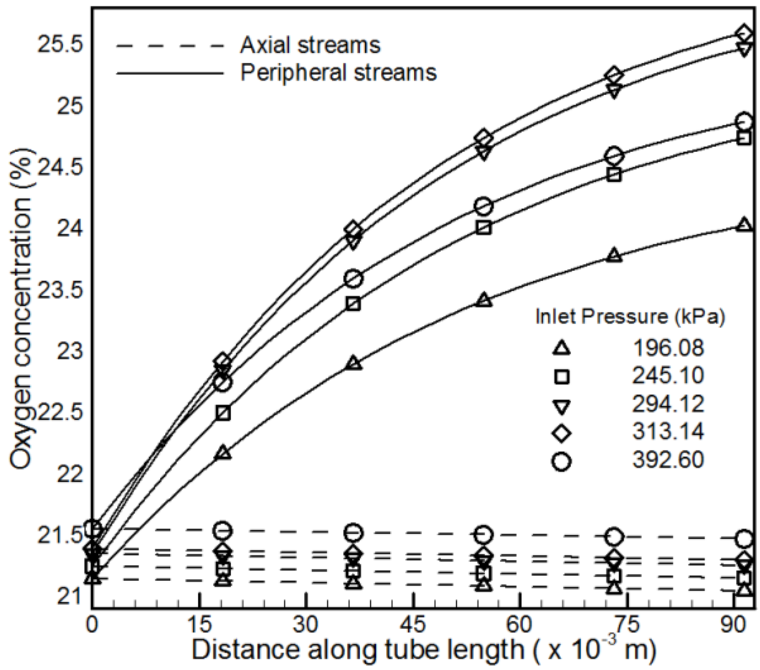

b. Hot end valve opening = 3.0 turns

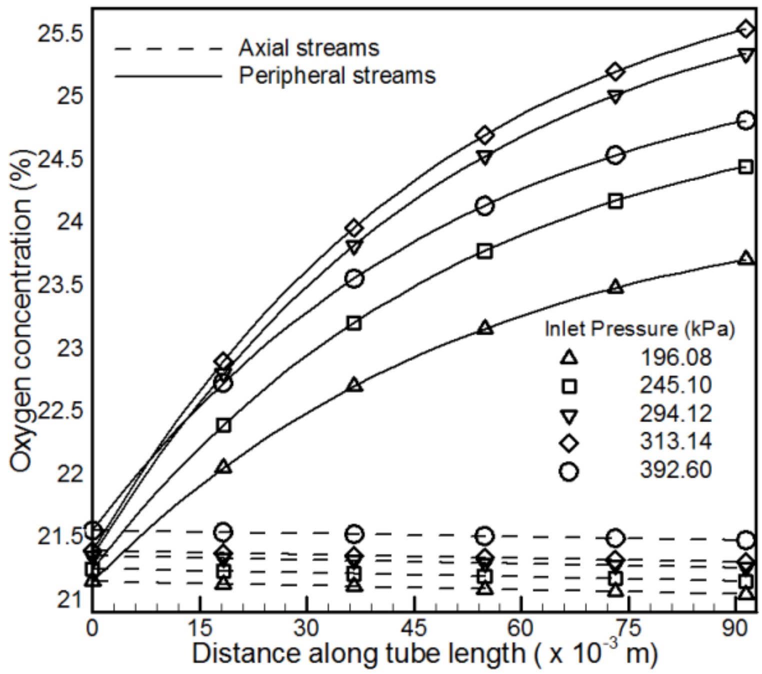

c. Hot end valve opening = 3.5 turns

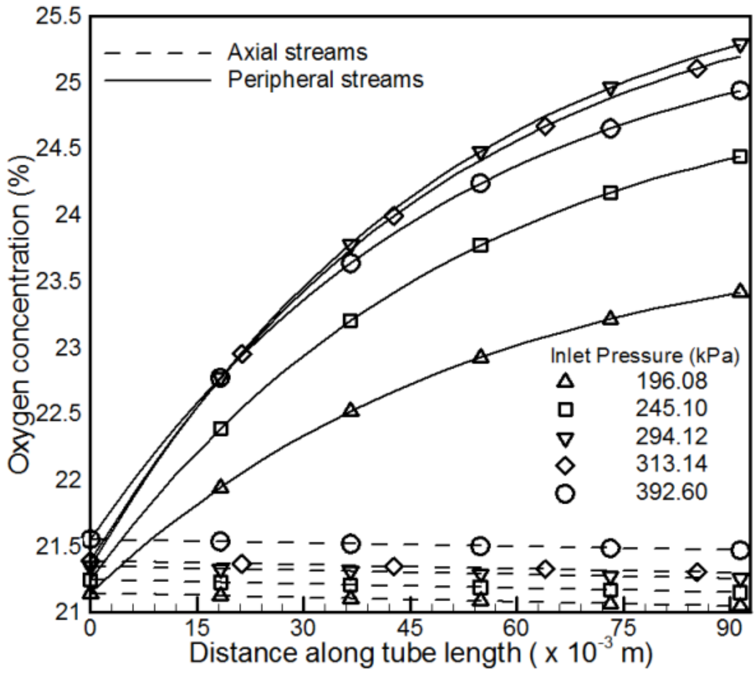

d. Hot end valve opening = 4.0 turns

Fig. 7.2 Distance vs. O_2 concentration (computed) in axial and peripheral streams for different hot end valve opening for a 25H generator

Along with the concentration build up of heavier species near the peripheral wall of the RHVT, the partial pressure of heavier species in gas stream at wall, P_w increases gradually. Hence the driving force for mass transfer, i.e. P- P_w, in equation (5.12), starts decreasing along the length of the RHVT near the hot end. As a result the concentration plots for the heavier species in the peripheral stream gradually flattens for all the hot end valve openings and inlet pressure values as shown in figure 7.1, 7.2 and 7.3.

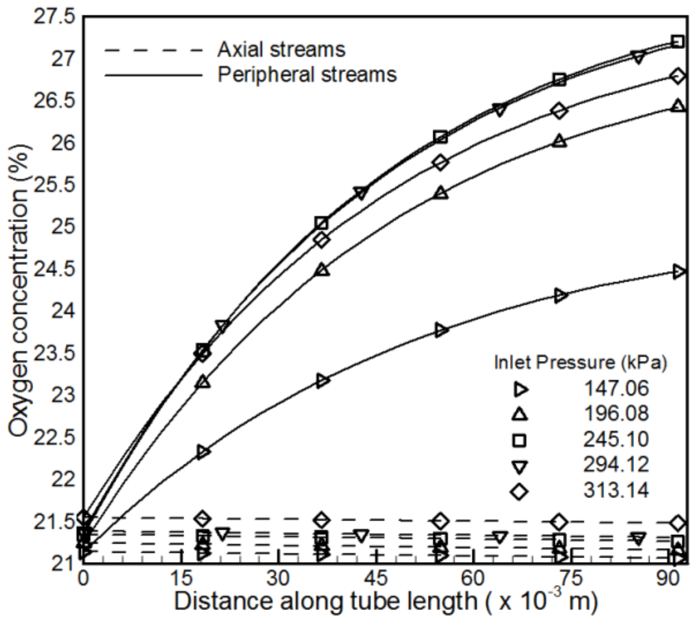

a. Hot end valve opening = 2.5 turns

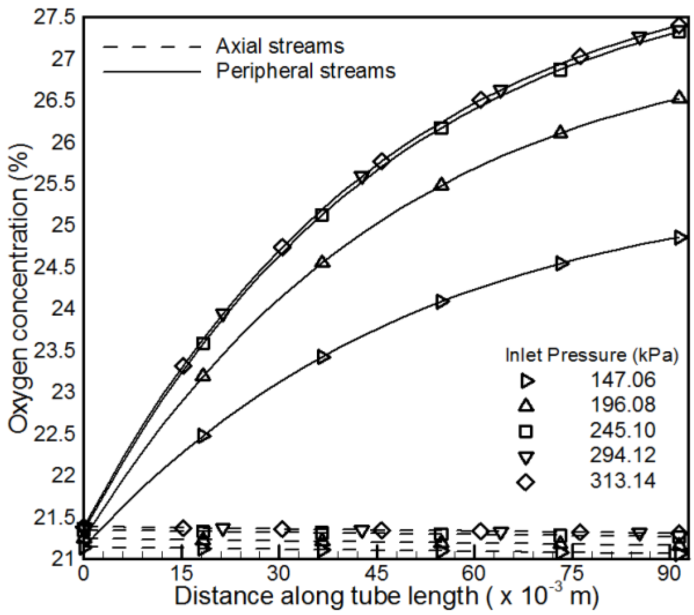

b. Hot end valve opening = 3.0 turns

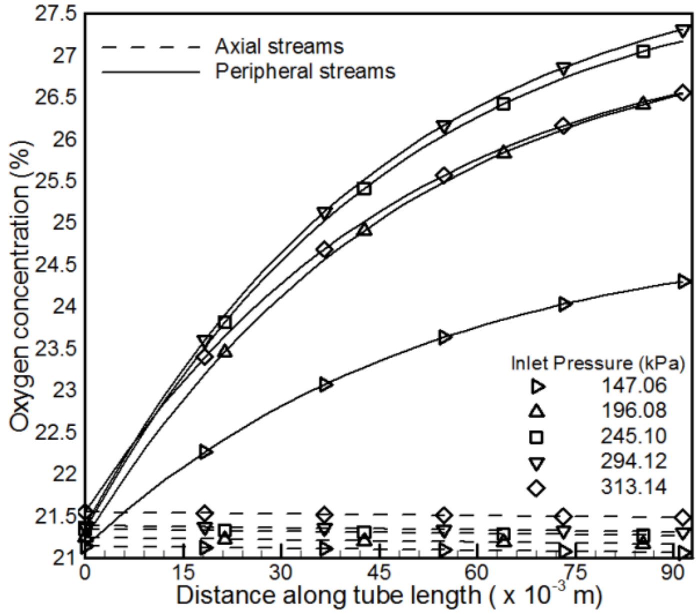

c. Hot end valve opening = 3.5 turns

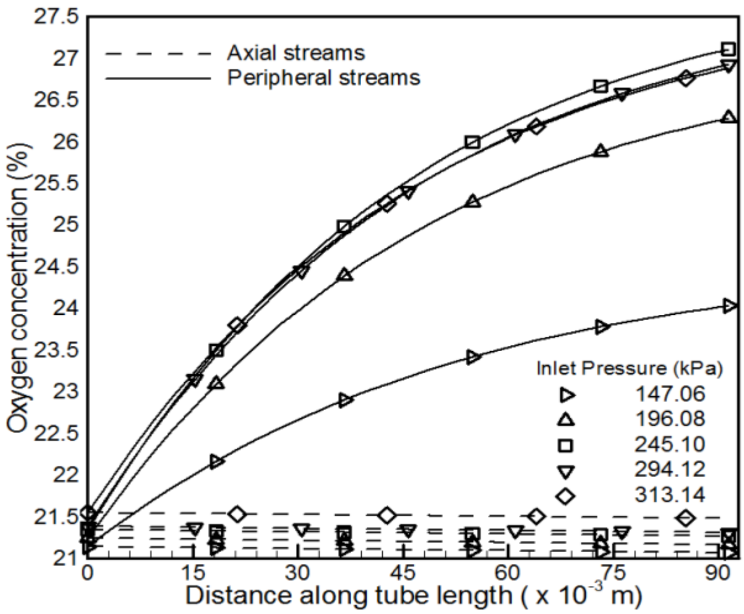

d. Hot end valve opening = 4.0 turns

Fig 7.3 Distance vs. O_2 concentration in axial and peripheral streams for different hot end valve opening for a 40H generator

7.3 Experiments carried out to study thermal separation

These set of experiments were carried out with a commercially available RHVT called as small RHVT with standard dimension. The dimensions of the small RHVT is given in chapter 4. Air is taken as the working fluid and a 10H vortex generator is used for thermal separation. The operating range of inlet flow rate for this type of RHVT is 2-8 scfm (standard cubic feet per minute) i.e. 9.438e-4 - 37.753e-4 m^3/s. The primary objective of the experimental investigation is to study the temperature separation phenomenon of the small RHVT. Compressed air has been provided from a rotary screw compressor. Air coming from the compressor line is introduced to the RHVT through the inlet nozzle. Working pressure at the inlet is varied from 0.5 kg/cm^2 to 4 kg/cm^2. The temperatures of the inlet flow (T_1), cold outlet flow (T_2) and hot outlet flow (T_3) and skin temperature of RHVT at three different locations are measured with class *B* Resistance Temperature Detectors (RTD) which have an accuracy of ± 0.42 °C at 25 °C temperature. Flow was controlled by the hot end control valve located at the end of the hot outlet side. This valve opening at the hot outlet is changed from a nearly closed position to its nearly open position in steps of 90°. Here a rotation of 360° (in anticlockwise direction) is regarded as one full turn and is a measure of the cold mass fraction defined by equation 5.61. The rotameter used for the volumetric flow measurement has a range of 0 to 50 scfm. The % error in rotameter reading is found as ± 1.4% in its range of operation. Similarly the error in pressure gauge reading is found as ± 2%. The locations of six different RTDs are shown in figure 7.4.

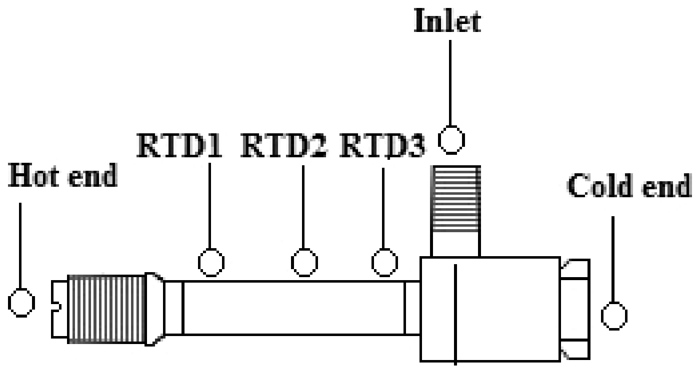

Fig. 7.4 Location of RTDs on the small RHVT

Figures 7.5a to 7.5f show the temperature recorded by these six RTDs vs. inlet pressure for different values of hot end control valve opening. It may be noted that the cold and hot end temperatures reported (T_2 and T_3 respectively) in the above graphs are mixing cup temperature at these two ends respectively. A close look into the results shows subzero temperature of air from cold outlet is obtained at certain values of hot end control valve opening and higher values of inlet air pressure. Maximum value of hot air temperature is

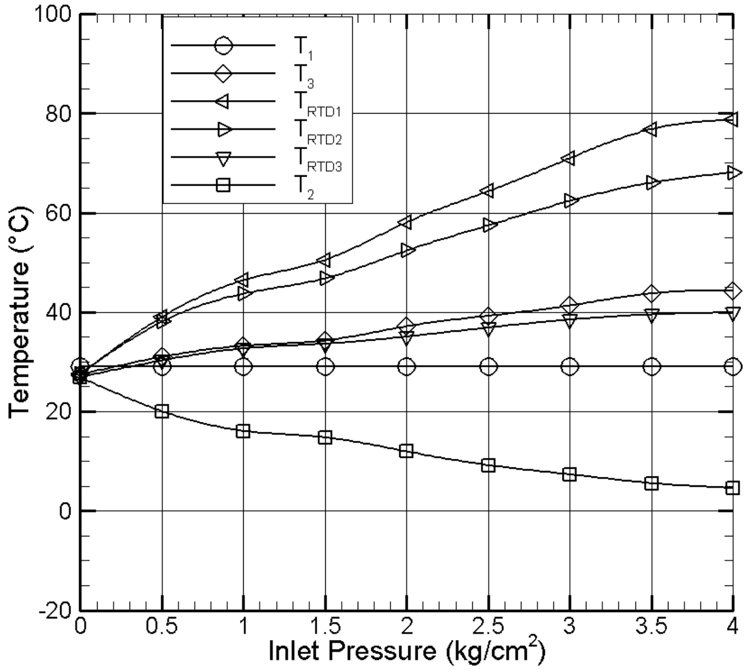

Fig 7.5a Inlet pressure vs. Temperature (experimental) for hot end control valve opening = 0.25

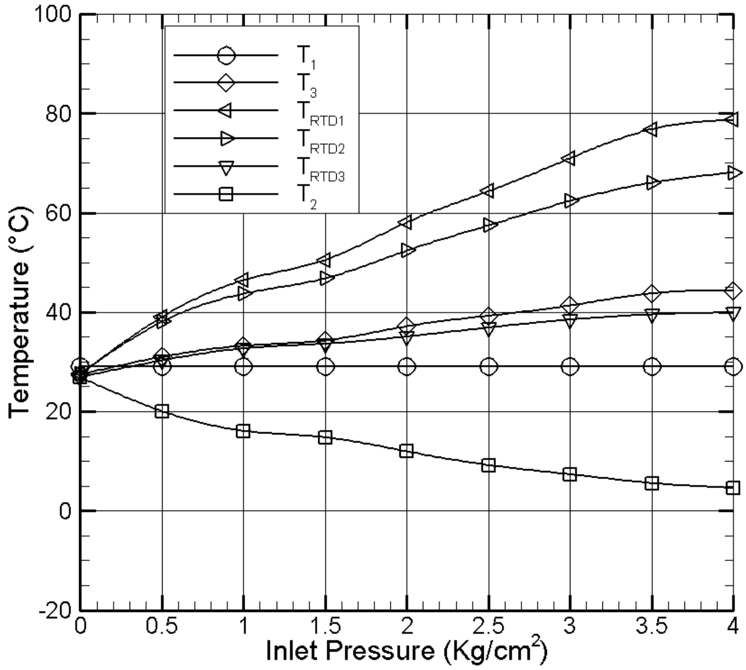

Fig 7.5b Inlet pressure vs. Temperature (experimental) for hot end control valve opening = 0.50

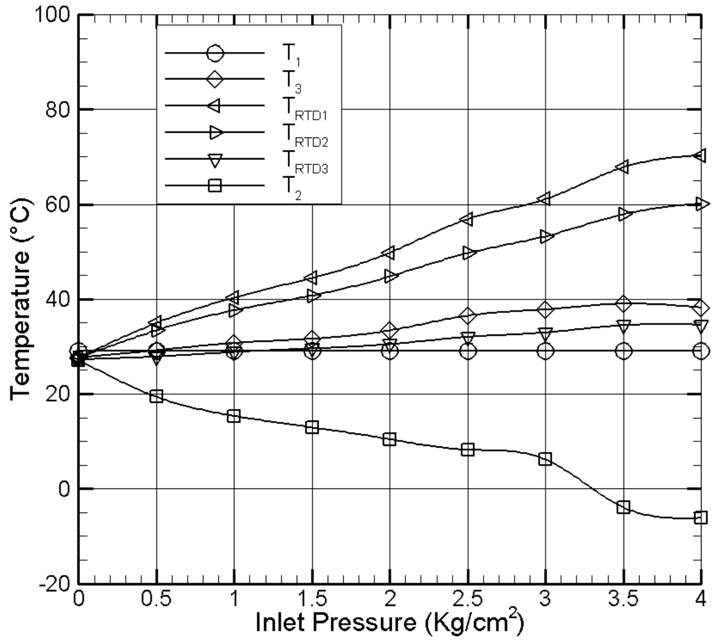

Fig 7.5c Inlet pressure vs. Temperature (experimental) for hot end control valve opening = 0.75

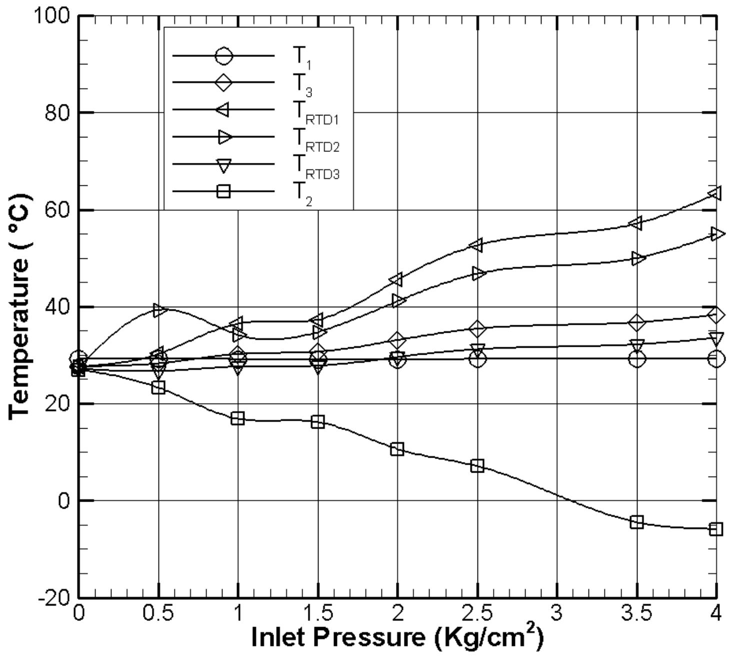

Fig 7.5d Inlet pressure vs. Temperature (experimental) for hot end control valve opening = 1.0

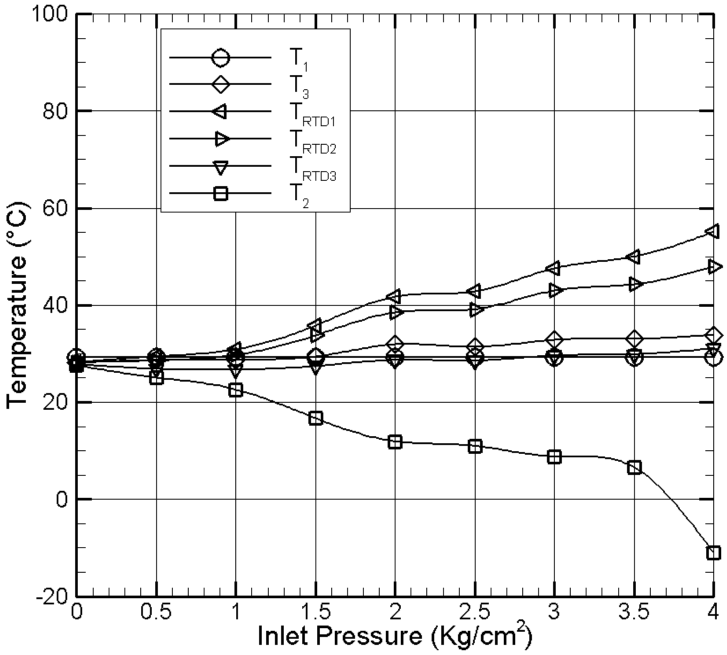

Fig 7.5e Inlet pressure vs. Temperature (experimental) for hot end control valve opening = 1.25

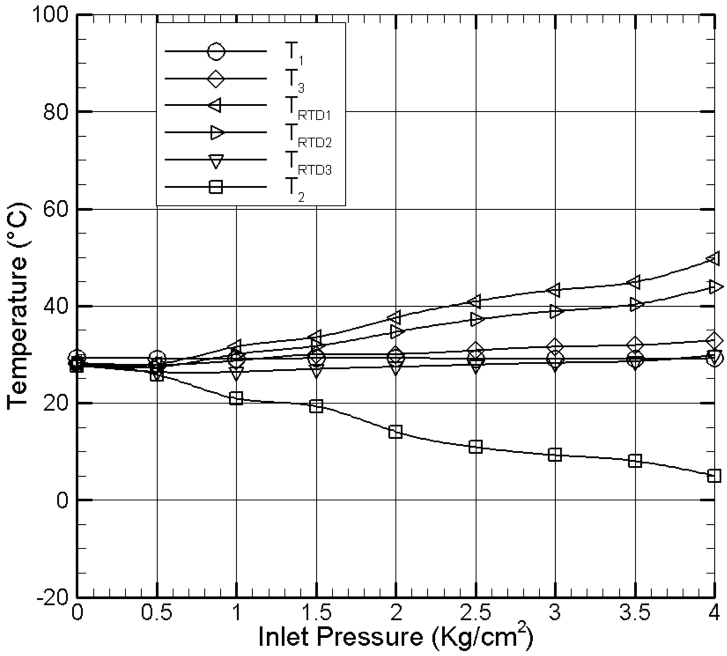

Fig 7.5f Inlet pressure vs. Temperature (experimental) for hot end control valve opening =1.50

obtained at minimum value of hot air control valve opening i.e. 0.25 as this condition corresponds to maximum compression of the air. As the hot end control valve opening value increases the maximum value of hot air temperature decreases. This phenomenon can be attributed to expansion of gas stream inside the RHVT and corresponding cooling effect. The maximum value of skin temperature is observed at RTD1 position. This is attributed to generation of a hotspot inside the RHVT. This value also decreases with increasing hot end control valve opening.

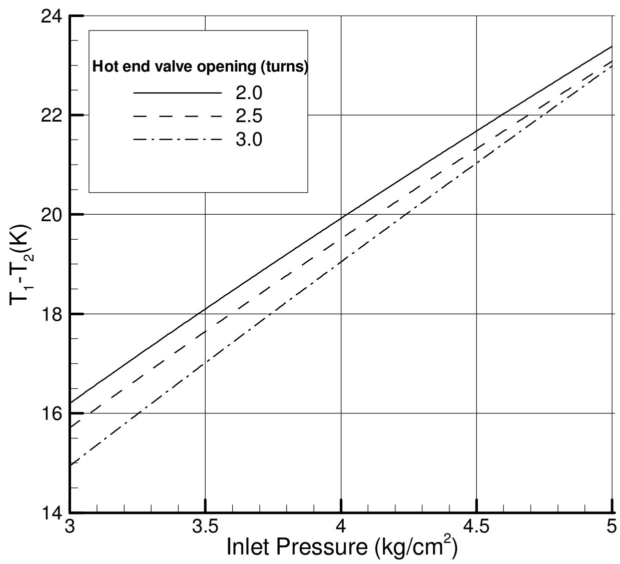

a. Hot end control valve opening: 2.0,2.5 and 3.0 turns

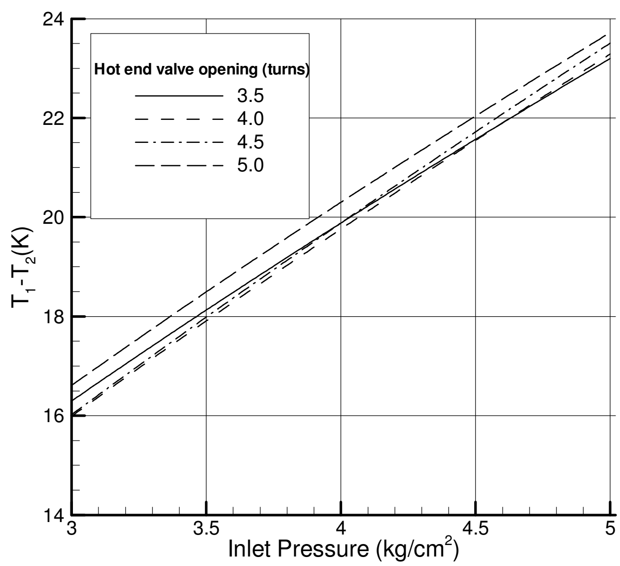

b. Hot end control valve opening: 3.5,4.0,4.5 and 5.0 turns

Fig 7.6 Difference between inlet and cold end temperatures vs. inlet pressure (experimental values) with different hot end valve openings for 10H generator

In figure 7.6 (a and b) the differences between inlet and cold end gas stream temperatures from the RHVT are plotted against varying inlet pressure and for various values of hot end screw opening as a parameter. These are experimentally obtained values and a 10H vortex generator has been used with air as the working fluid. This graph shows that maximum drop in cold end temperature separation values are obtained at highest value of inlet pressure.

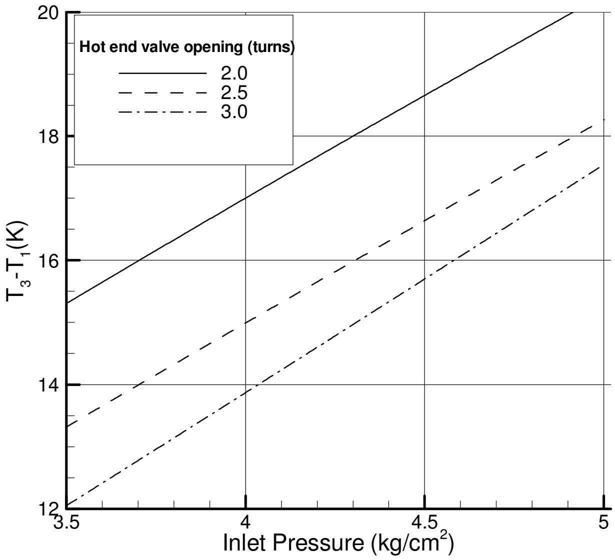

a. Hot end control valve opening: 2.0,2.5 and 3.0 turns

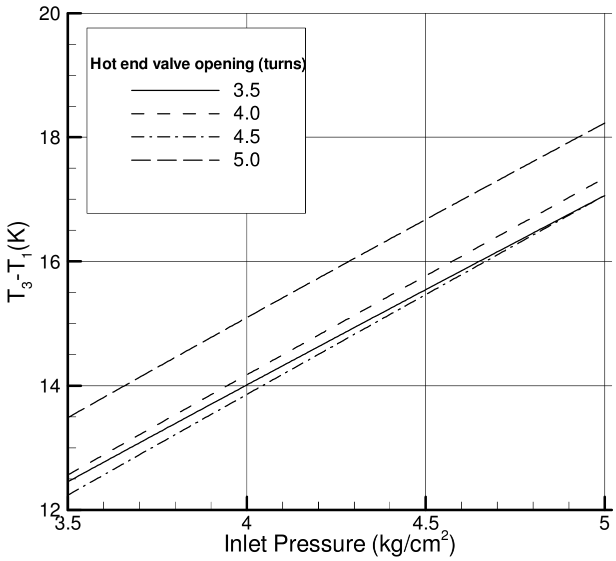

b. Hot end control valve opening: 3.5,4.0,4.5 and 5.0 turns

Fig 7.7 Difference between hot end and inlet temperatures vs. inlet pressure (experimental values) with different hot end valve openings for 10H generator

In figure 7.7 (a and b) the experimentally obtained temperature rise at hot outlet gas stream temperatures from the RHVT are plotted against varying inlet pressure and for various values of hot end screw opening as a parameter. Here also we can see as inlet pressure increases the rise in hot outlet temperature increases. Hence it is clearly observed that inlet pressure is an important parameter that can influence the thermal separation.

7.4 Experiments carried out to establish relation between heat and mass transfer

A set of experiments have been carried out in our experimental setup to understand the following two points

- Whether the mass and heat transfer in a RHVT are interrelated
- If they are interrelated then what is the nature of dependency between the heat and mass transfer

In order to carry out these experiments an ExAir^{TM} make mini RHVT has been used in the experimental setup described in chapter 4 of this thesis. The experimental procedure is also described in detail in the same chapter.

Two different vortex generators of H series, namely 10H and 40H have been used for experimentation with the ExAir^{TM} make RHVT. Further relation between thermal and species separation by the RHVT had been studied. The thermal separation in the RHVT has been defined by equation 3.6 in chapter 3 and repeated here for convenience as follows

$$Thermal\ separation = \frac{T_2/(T_1 - T_2)}{T_3/(T_3 - T_1)} \tag{7.1}$$

Also the head separation factor of the lighter species for a binary separation is defined by equation 3.5 in chapter 3 and repeated here for convenience as follows

$$Alpha = \frac{1-N_3}{N_3}\frac{N_1}{1-N_1} \tag{7.2}$$

The Reynolds number at the inlet of the RHVT can be calculated by the expression given by Marshall [121] and was given by equation 6.29.

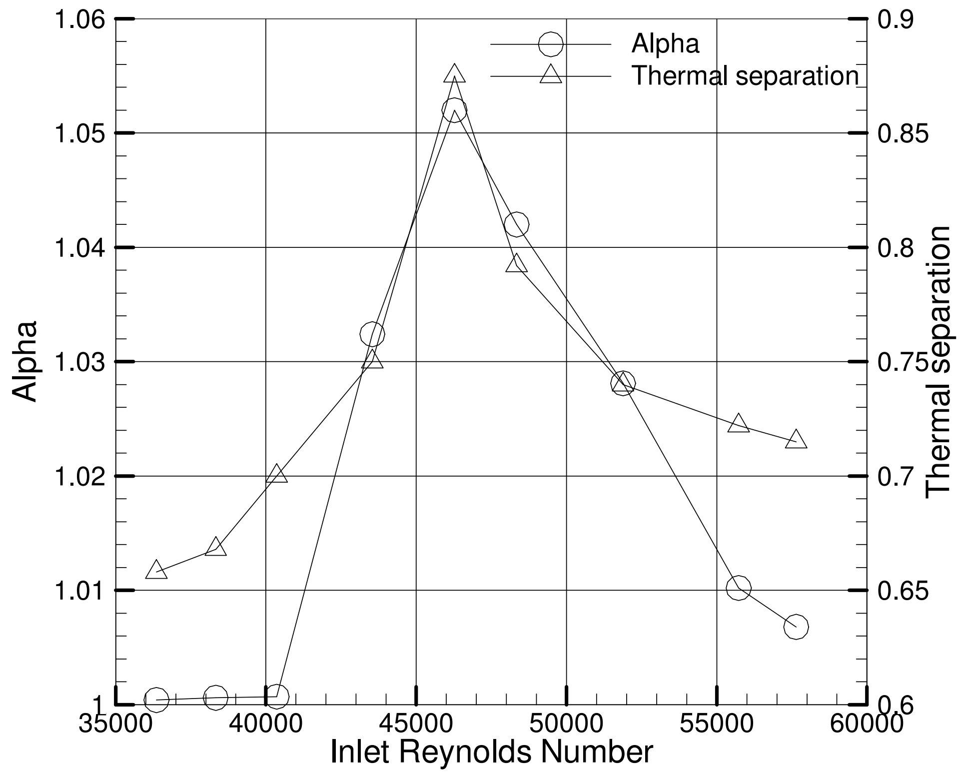
Alpha
Thermal separation
Alpha
Thermal separation
Inlet Reynolds Number
1.06
1.05
1.04
1.03
1.02
1.01
1
0.9
0.85
0.8
0.75
0.7
0.65
0.6
35000
40000
45000
50000
55000
60000

a.

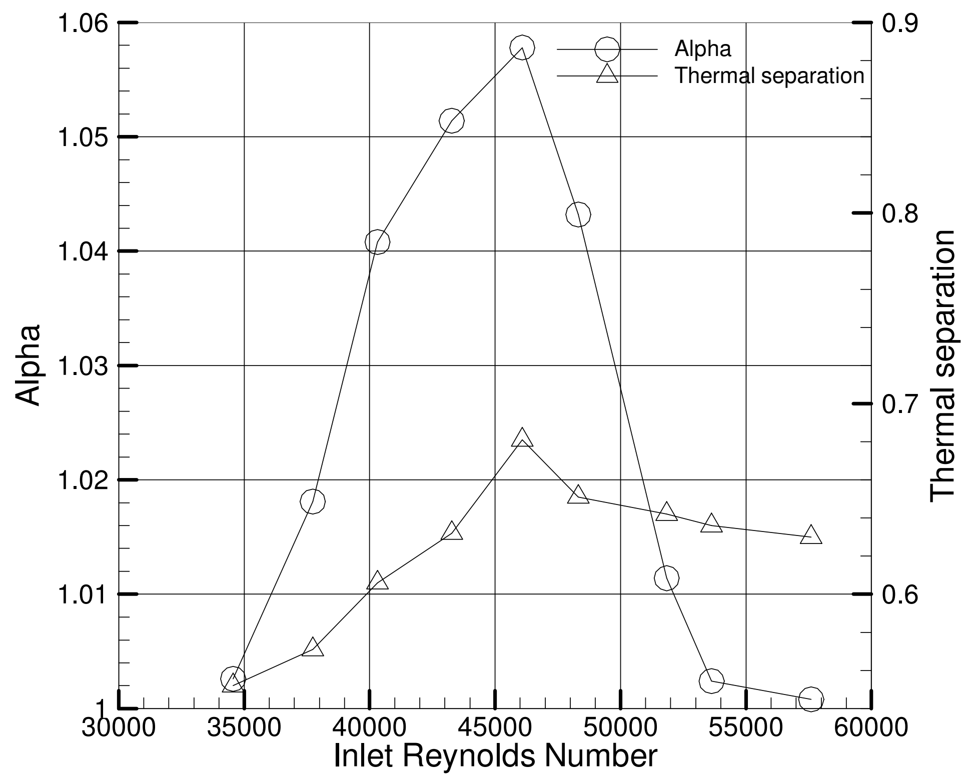
Alpha
Thermal separation
Alpha
Thermal separation
Inlet Reynolds Number
1.06
1.05
1.04
1.03
1.02
1.01
1
0.9
0.8
0.7
0.6
30000
35000
40000
45000
50000
55000
60000

b.

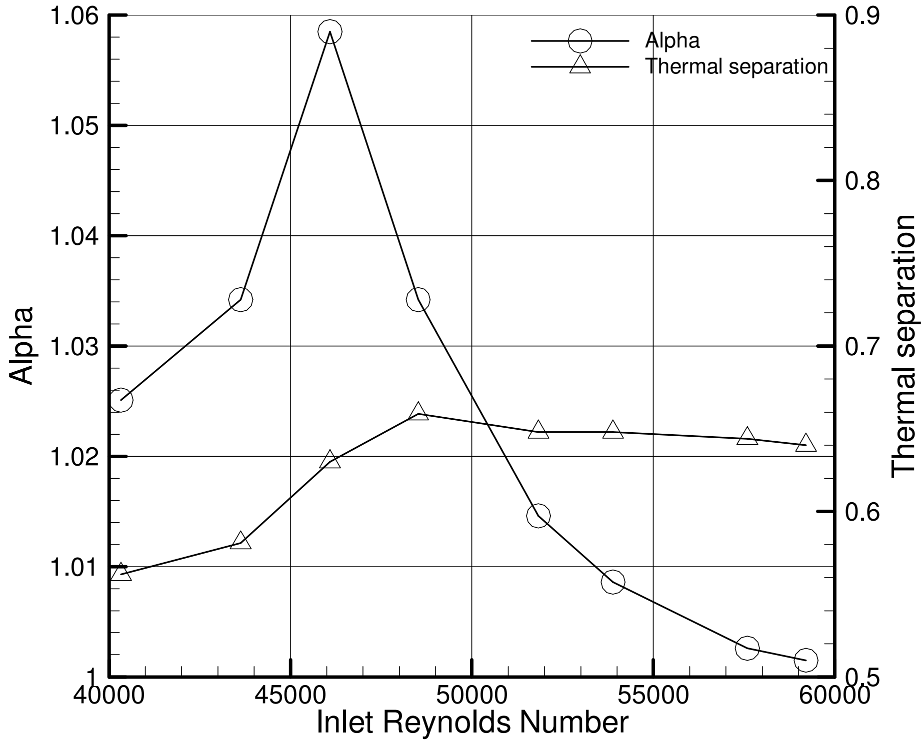
Alpha
Thermal separation
1.06
1.05
1.04
1.03
1.02
1.01
1
0.9
0.8
0.7
0.6
0.5
40000
45000
50000
55000
60000
Inlet Reynolds Number
Alpha
Thermal separation

c.

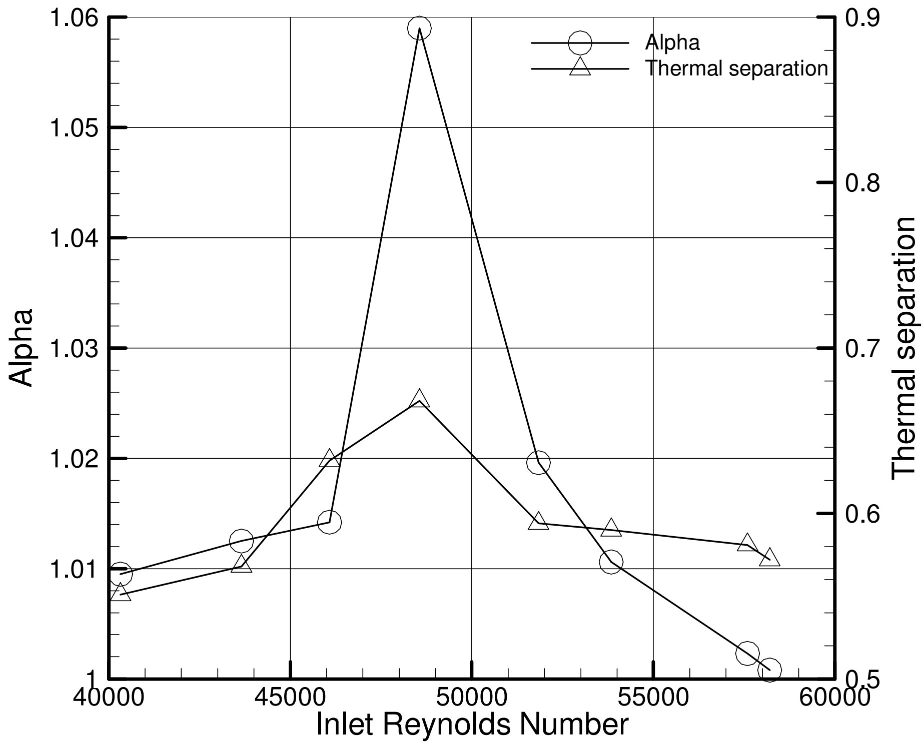
Alpha
Thermal separation
1.06
1.05
1.04
1.03
1.02
1.01
1
0.9
0.8
0.7
0.6
0.5
40000
45000
50000
55000
60000
Inlet Reynolds Number
Alpha
Thermal separation

d.

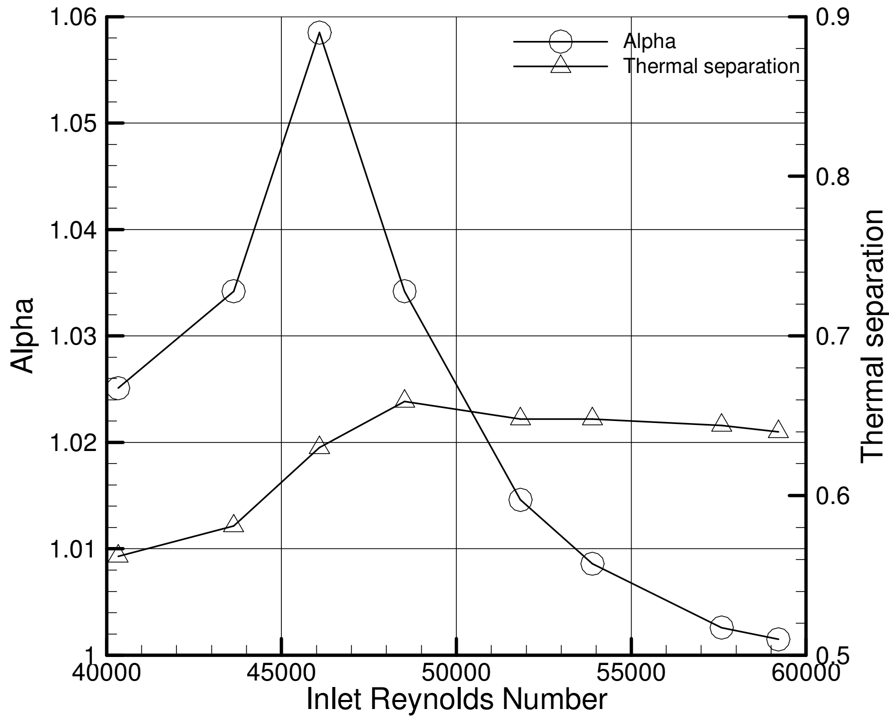

e.

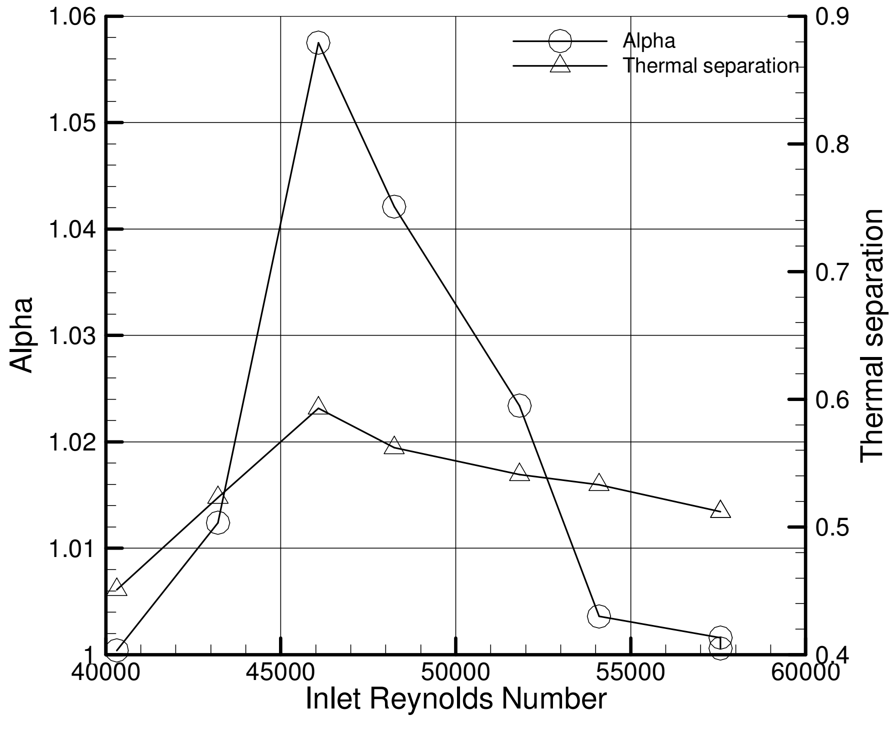

f.

Fig 7.8 Inlet Reynolds number vs. thermal separation and separation factor (Alpha) with 10 H generator for values of hot end screw openings a)2.0 b)2.5 c) 3.0 d)3.5 e)4.0 f)4.5

In figure 7.8 *a* to *f* thermal separation is calculated by using equation (7.1) and head separation factor *Alpha* is calculated by using equation (7.2). The inlet Reynolds number has been calculated using equation 5.34 and these two quantities were plotted against

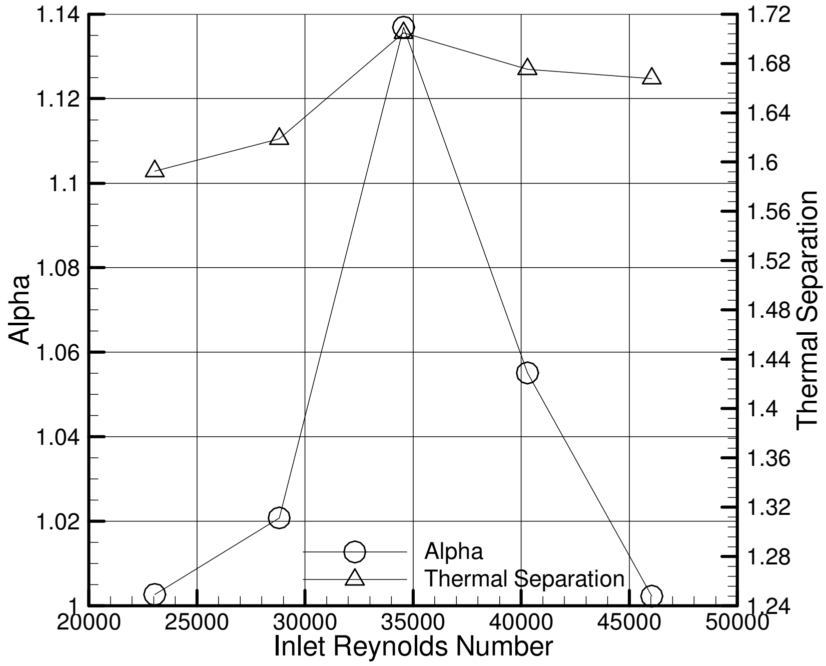

a

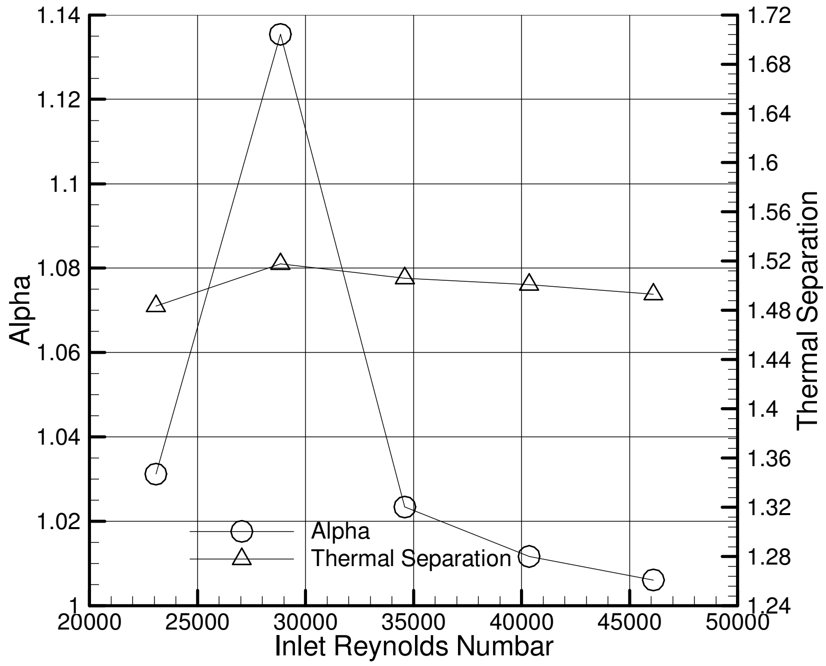

b.

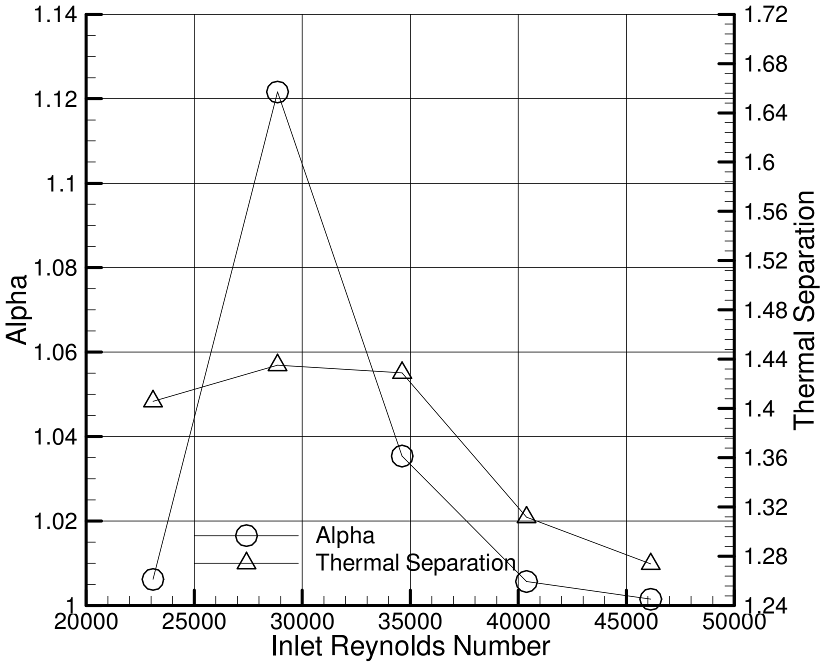

c

Fig 7.9 Inlet Reynolds number vs. thermal separation and separation factor (Alpha) with 40 H generator for values of hot end screw openings a)2.0 b)3.0 and c) 4.0

different inlet Reynolds number for the RHVT with 10H vortex generator. These values were plotted for six different hot end valve opening values of 2.0, 2.5, 3.0, 3.5, 4.0 and 4.5 respectively. Similar data had been plotted for RHVT with 40H vortex generator in figure 7.9 a, b and c for hot end screw opening values of 2.0, 3.0 and 4.0 respectively.

It was seen from the graphs that -

- Optimum values of thermal separation and species separation occurred at same inlet Reynolds number range for each values of hot end screw opening.
- It could also be seen that overall thermal separation decreased with increasing hot end screw opening.
- The overall values of both mass separation factor and thermal separation are higher for 40H vortex generator than the 10H vortex generator.
- It has been observed that the basis of heat and mass transfer was same (i.e. axial vortex flow inside the tube), and these two phenomenas were interrelated. Also they influence each other.

In the following section the different parameters that affect species separation in a RHVT has been discussed. A details survey of the information available in the literature on this topic is given in appendix D and E of this thesis.

7.5 Parametric studies using experimental and theoretical methods

In the following sections of the current chapter results of a number of parametric studies, carried out with different parameters of the RHVT in order to investigate their influence on thermal and species separation, have been discussed. Four such studies have been designed, in which the influence of the tube L_{vt}/D_{vt} ratio, size of the inlet nozzle, inlet pressure and cold mass fraction have been investigated. The experimental setup has been used for the first two parametric studies while the theoretical model has been used to study the combined effect of inlet pressure and cold mass fraction on thermal and species separation.

Table 7.2 Experimental / theoretical case studies with RHVT for various operating conditions

Case	L_{vt}(mm)	D_{vt} (mm)	L_{vt}/D_{vt}	Cold mass fraction (θ_c)	P_1 (bar)	N_{in}	Inlet nozzle area (sq. mm)	Parameter studied
1	a)108.0, b)150.5	a)13.8, b)12.7	a)7.82, b)11.85	0.0 -1.0	4.0	6	1.35 * 1.70	L_{vt}/D_{vt}
2	150.5	12.7	11.85	0.0 -1.0	4.0	6	a)1.35*1.70 b)0.826* 0.60	Inlet nozzle area
3 & 4	150.5	12.7	11.85	0.0 -1.0	2.0-10.0	6	1.35 X 1.70	Inlet pressure

In these studies hot end control valve opening is an important parameter which controls the cold mass fraction, θ_c. Another important parameter is inlet mass flow rate m_1 which is being controlled by the inlet pressure P_1. In the experimental setup the cold mass fraction is controlled by opening and closing the hot end control valve while the inlet pressure is controlled by flow control valve at the inlet. All these studies have been carried out with air as working fluid. The parameters used in these different case studies are listed in table 7.2.

It can be found from discussions in the previous section that pressure of the gas stream at the inlet and cold mass fraction are the two most influential operating parameters that controls the thermal as well as species separation in a RHVT. The combined case studies 3 and 4 shown in table 7.2 above, describes the effect of changing the inlet pressure and cold mass fraction of the RHVT on the thermal as well as species separation. For all cases (1-4) cold mass fraction is varied from 0.0 to 1.0. For experimental studies only stable values are reported. Results obtained from the mathematical model developed have been used for the parametric studies.

7.5.1 Influence of length to diameter ratio

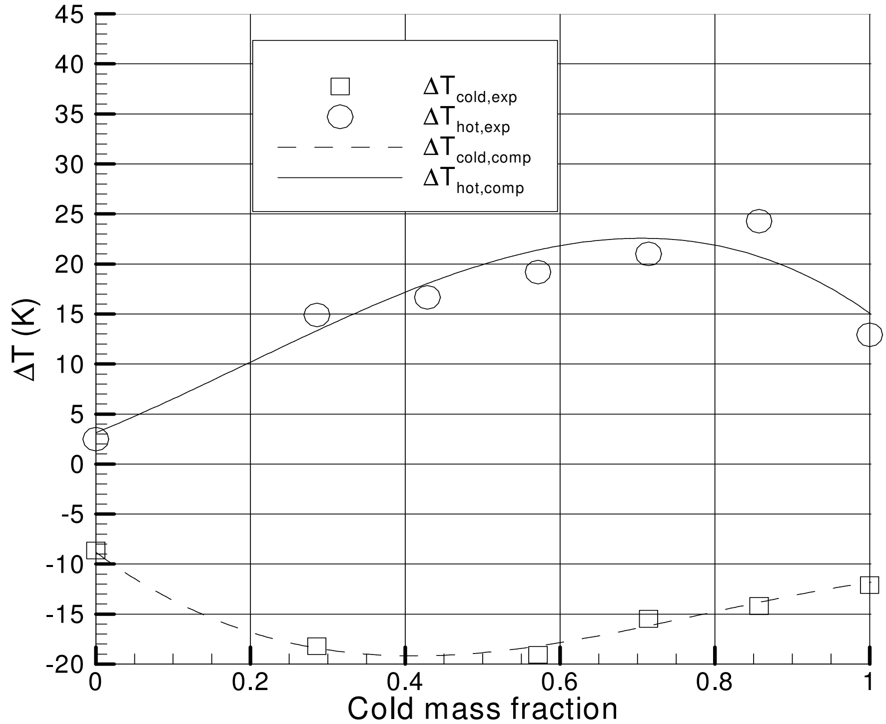

Fig. 7.10a Cold mass fraction vs. thermal separation (experimental and computed) for L/D ratio =7.82 at 4.0 bar inlet pressure

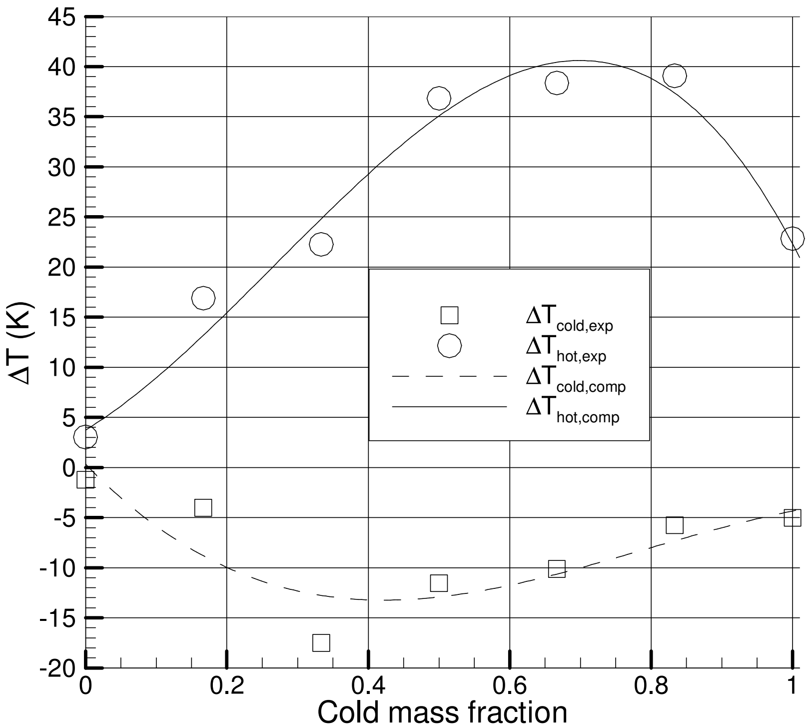

Fig. 7.10b Cold mass fraction vs. thermal separation (experimental and computed) for L/D ratio =11.85 at 4.0 bar inlet pressure

Two different values of tube length to diameter ratio (7.82 and 11.25) have been investigated in our experimental setup. The geometrical parameters of the RHVT used for this study have been listed under case 1 in table 7.2. The inlet and outlet temperatures are measured with PT100 RTDs. Results for the RHVT with L_{vt}/D_{vt} ratio 7.82, is shown in figure 7.10(a). Figure 7.10(b) shows the result for L_{vt}/D_{vt} ratio 11.85. In both the cases the two tubes operate under same operating conditions. In both figure 7.10(a) and 7.10(b) the temperature difference obtained at the hot end ($\Delta T_{hot} = T_3 - T_1$) and the cold end ($\Delta T_{cold} = T_2 - T_1$) are plotted against the cold mass fraction.

Influence of the length to diameter ratio of the RHVT on the thermal separation can be observed from figure 7.10. As the length to diameter ratio increases from 7.82 to 11.85, the maximum temperature difference between hot and cold end ($\Delta T = T_3 - T_2 = \Delta T_{hot} - \Delta T_{cold}$) increases. The maximum temperature differences ΔT, ΔT_{hot} and ΔT_{cold} are given in Table 7.3. From this table also we can see as the length to diameter ratio increases the thermal separation performance of RHVT increases. Gao [72] has shown in a similar study as the length to diameter ratio increases, the thermal separation performance of the RHVT also increases.

Table 7.3 Maximum thermal separation at fixed inlet pressure = 4 mbar and two different length to diameter ratios

P_1(bar)	L_{vt}/D_{vt}	ΔT_{max} (K)	$\Delta T_{hot,max}$ (K)	$\Delta T_{cold,max}$ (K)
4	7.82	38.26 at $\theta_c = 0.57$	24.08 at $\theta_c = 0.86$	-20.46 at $\theta_c = 0.43$
4	11.85	48.26 at $\theta_c = 0.45$	38.94 at $\theta_c = 0.84$	-17.24 at $\theta_c = 0.33$

Further, the influence of *L/D* ratio on the separation factor α of a RHVT having a 10H vortex generator at four different inlet pressure values (2.0, 4.0, 6.0 and 8.0 bar) have been studied numerically using the code developed. Results obtained are presented in figure 7.11 below. It can be seen in all the four cases initially α increase with increasing value of *L/D* ratio, reaches a maximum and then falls when the ratio is increased further. It can also be seen at lower value of inlet pressure α reaches its maximum value at L/*D* ratio of 14. At higher value of inlet pressure α reaches its maximum value at a lower L/D value of 12. Hence optimum value of L/D depends on inlet pressure.

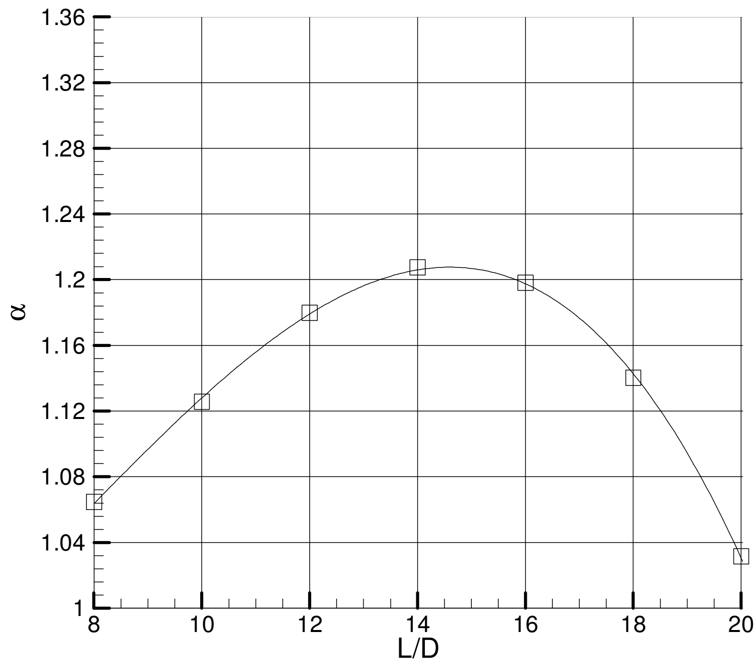

Fig. 7.11a L/D ratio vs. α (computed) for 10H generator at 2.0 bar inlet pressure and θ_c=0.3

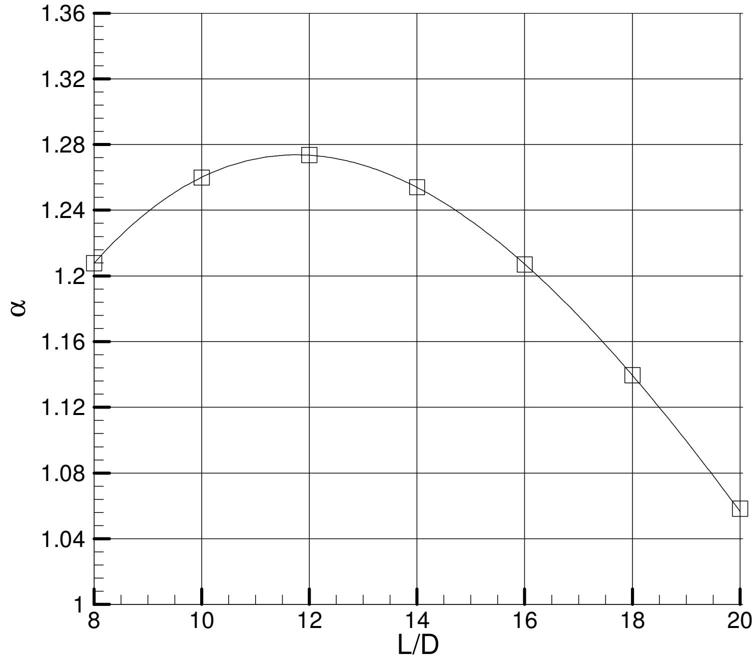

Fig. 7.11b L/D ratio vs. α (computed) for 10H generator at 4.0 bar inlet pressure and θ_c=0.3

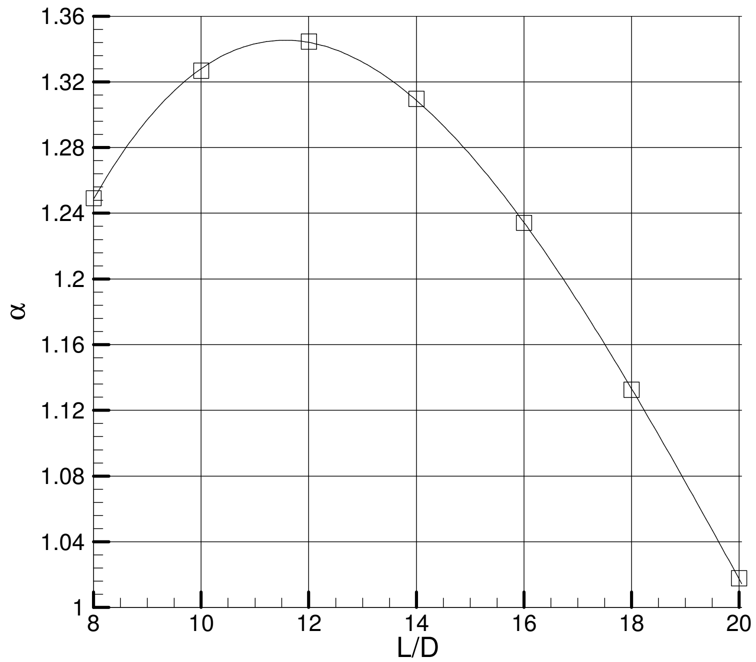

Fig. 7.11c L/D ratio vs. α (computed) for 10H generator at 6.0 bar inlet pressure and θ_c=0.3

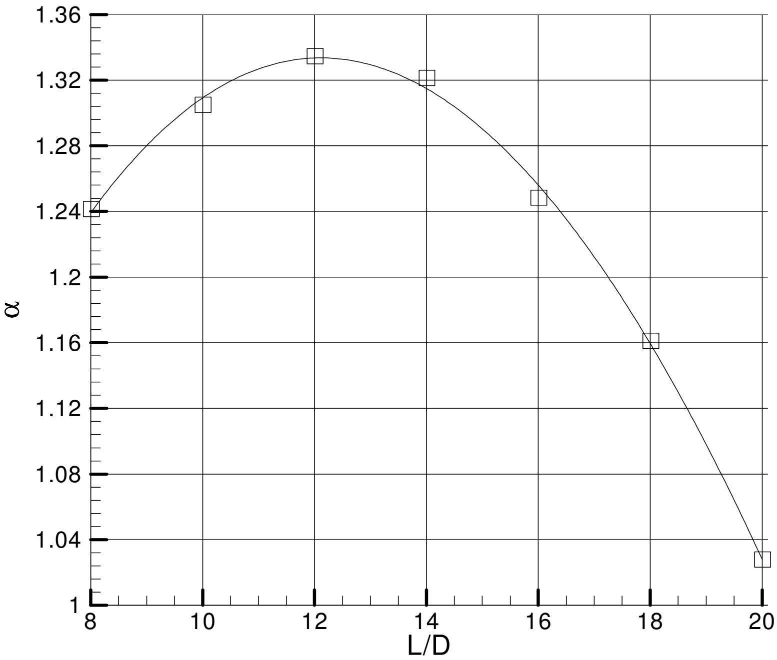

Fig. 7.11d L/D ratio vs. α (computed) for 10H generator at 8.0 bar inlet pressure and θ_c=0.3

7.5.2 Influence of inlet nozzle area

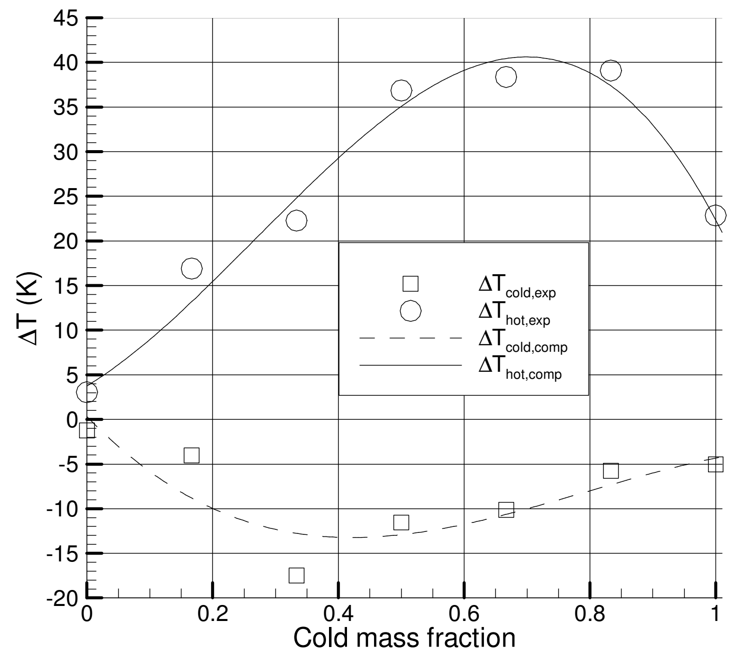

Fig 7.12a Cold mass fraction vs. thermal separation (experimental and computed) for nozzle opening area = 1.35*1.70 sq. mm at 4.0 bar inlet pressure and 0.3 hot end valve opening

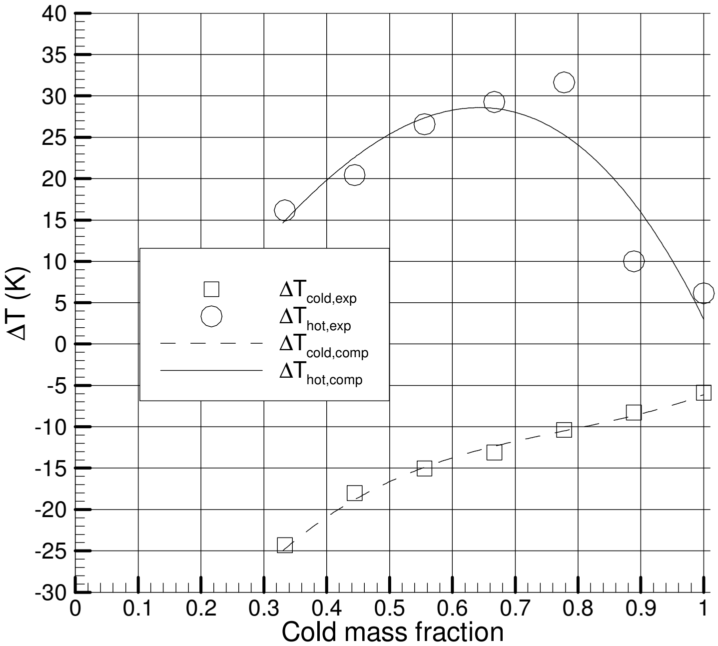

Fig. 7.12b Cold mass fraction vs. thermal separation (experimental and computed) for nozzle opening area =0.826 * 0.60 sq. mm at 4.0 bar inlet pressure and 0.3 hot end valve opening

Two sets of inlet nozzles having different inlet nozzle areas are used to study the influence of this parameter on separation performance of the RHVT. Both sets have six number of slot type nozzles but the inlet cross sections of the slots are different. The slots are symmetrically placed at the periphery of the vortex generator. The inlet cross section areas of these two sets of slots are 1.35 * 1.70 mm^2 and 0.826 * 0.60 mm^2 respectively. The total area of the inlet nozzle in two cases is 13.77 mm^2 and 2.97 mm^2 respectively. The inlet pressure is kept at 4.0 bar. All the other parameters are kept same. These conditions are described under case 2 in table 7.2.

Figure 7.12 shows the influence of nozzle inlet area on thermal separation. In figure 7.12a temperature difference at cold and hot end are plotted against cold mass fraction for individual nozzle opening area =1.35 * 1.70 mm^2 at 4.0 bar inlet pressure. Figure 7.12b depicts temperature difference at cold and hot end with respect to cold mass fraction for individual nozzle opening area = 0.826 * 0.60 mm^2 at 4.0 bar inlet pressure. There are six numbers of nozzles for both the cases. For the nozzle opening area = 0.826 * 0.60 mm^2, steady state temperature data were not available for cold mass fraction value below 0.33. It can be seen by comparing these two figures that as the total nozzle inlet area increases, for fixed inlet pressure and cold fraction, thermal separation increases. Table 7.4 gives the maximum temperature differences ΔT, ΔT_{hot} and ΔT_{cold} and the corresponding cold mass fraction value for two different nozzle inlet areas.

Table 7.4 Maximum thermal separation at fixed inlet pressure = 4 mbar and two different nozzle inlet areas

P_1(bar)	Nozzle inlet area (mm^2)	ΔT_{max} (K)	$\Delta T_{hot,max}$ (K)	$\Delta T_{cold,max}$ (K)
4	0.826 X 0.60	38.26 at $\theta_c = 0.57$	31.55 at $\theta_c = 0.78$	-23.91 at $\theta_c = 0.34$
4	1.35 X 1.70	48.26 at $\theta_c = 0.45$	38.94 at $\theta_c = 0.84$	-17.24 at $\theta_c = 0.33$

Further the species separation caused by the RHVT for two different nozzle inlet areas are shown in figure 7.13. In this figure variation of binary separation factor as a function of cold mass fraction has been plotted for two different nozzle sizes. It can be seen from figure 7.13 that as the total nozzle inlet area increases, the overall value of separation factor also increases. Further it can also be observed that as the size of the nozzle opening changes the value of cold mass fraction at which the maximum value of separation factor occurs, also changes.

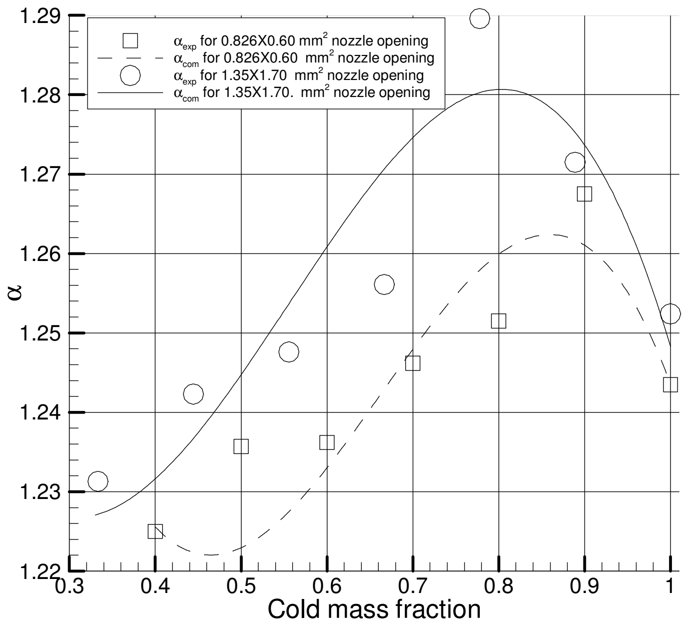

Fig. 7.13 Cold mass fraction vs. separation factor (computed and experimental) for two different nozzle opening areas at 4.0 bar inlet pressure

7.5.3 Effect of inlet pressure and cold mass fraction

In order to investigate the effect of variation in inlet pressure and cold mass fraction on thermal separation the mathematical model developed in chapter 5 has been used. Input parameters required for the computer code have been mentioned in section 5.2.5 of the same chapter. Out of these input parameters the values of inlet pressure and cold mass fraction are varied. Inlet pressure is varied in the range 200 to 1000 kPa and cold mass fraction is varied in the range 0.0 to 1.0. All other parameters including the geometrical dimensions (length and diameter of the tube) are kept fixed. The air temperatures from hot and cold outlets of the RHVT, calculated from the combined heat and mass transfer model as a function of cold mass fraction and inlet pressure as independent parameters are plotted in figure 7.14a and 7.14b respectively. The inlet air temperature for all the cases were considered as 300 K. Air is considered as the working fluid. It can be seen from the plots

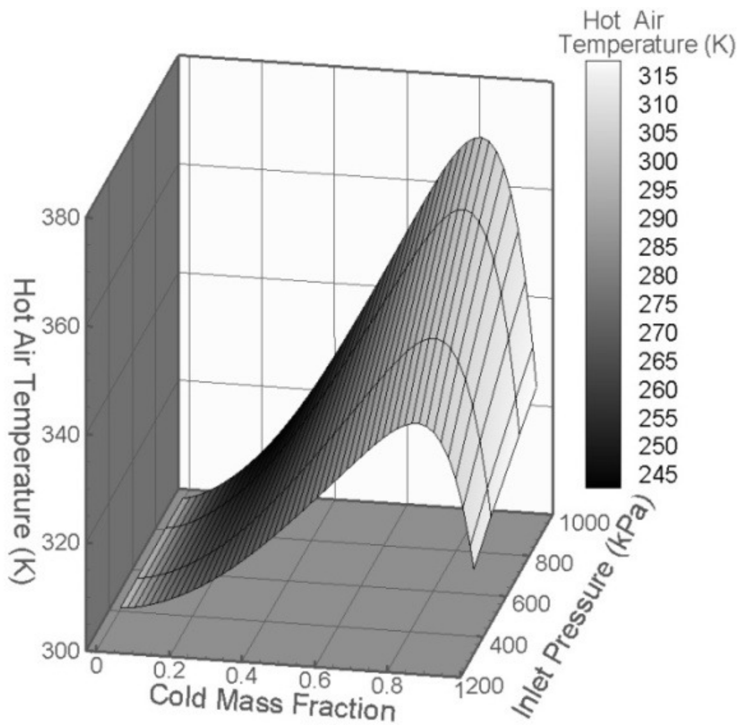

a.

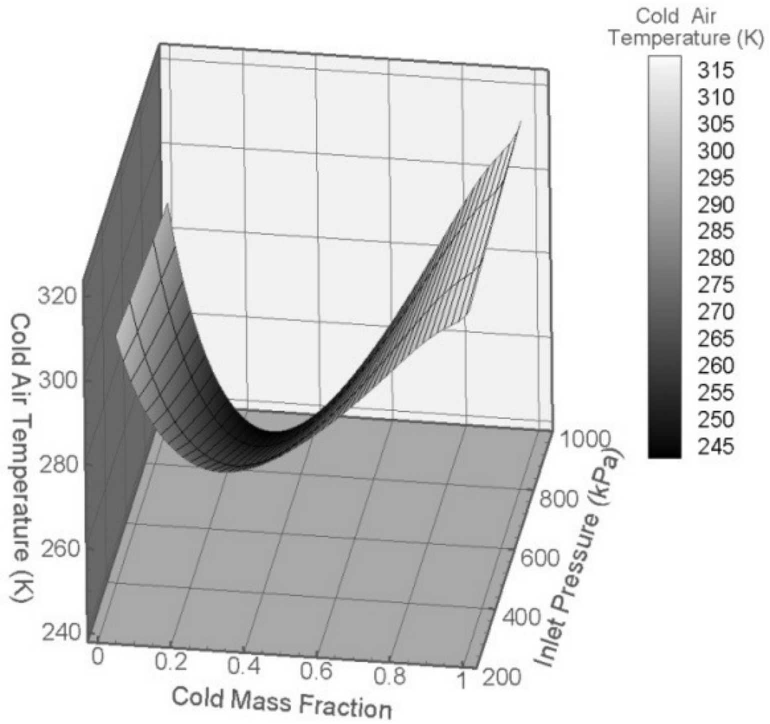

b.

Fig. 7.14 Cold mass fraction vs. computed air temperature under different inlet pressures at (a) hot and (b) cold outlet of RHVT

that for a fixed value of cold mass fraction the absolute change in hot and cold outlet temperature is a function of inlet pressure. Also it can be observed from figure 7.14a with increase in cold mass fraction the hot outlet temperature initially increases, goes through a maxima (at around $\theta_c = 0.85$) and then decreases. On the contrary it is observed from figure 7.14b that for a fixed value of inlet pressure as the cold mass fraction increases gradually the temperature of the cold outlet initially decreases, goes through a minima (at around θ_c=0.30) and then increases with increasing values of θ_c.

Further the separation factors computed from the present combined model have been plotted as a function of cold mass fraction and inlet pressure as independent parameters in figure 7.15. It can be seen from figure 7.15 that for a given value of cold mass fraction as the inlet pressure increases, the separation factor also increases but the increase in separation factor is not proportional to that of inlet pressure. As for example the ratio of four inlet pressures in figure 7.15 are 1:1.43:2.14:2.57,

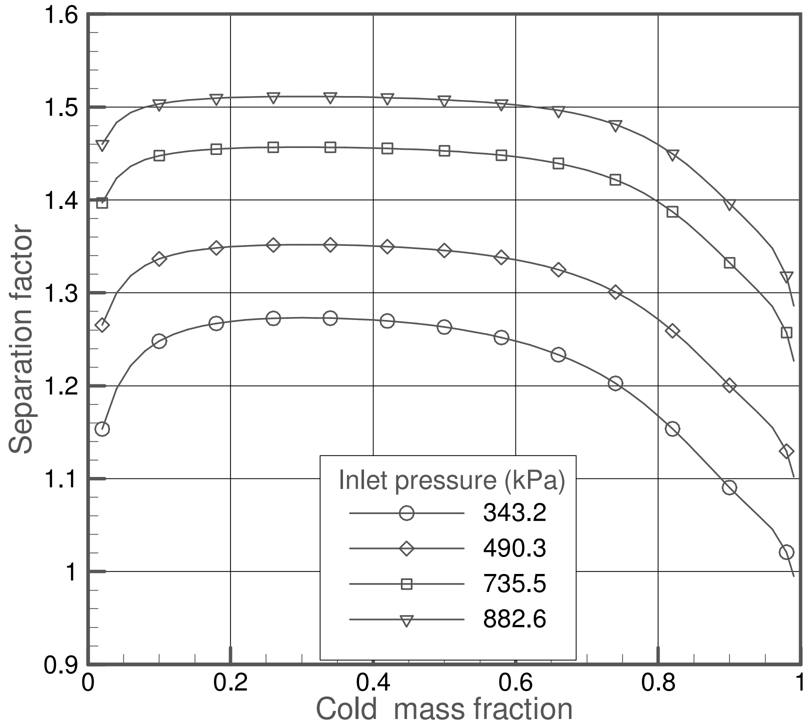

Fig. 7.15 Cold mass fraction vs. separation factor at different inlet pressures

whereas for a fixed cold mass fraction (*e.g.* 0.4), the ratio of separation factors are 1:1.06:1.14:1.18. Clearly as the inlet pressure increases the species separation factor saturates. Further for a fixed inlet pressure it can be seen that with increasing value of cold mass fraction initially the separation factors increases, then almost remains constant and finally decreases.

Hence in the above discussion the effects of important geometrical and thermo-physical parameters of the RHVT on separation performance have been studied and validated using the proposed mathematical model. A set of experimental data for three different vortex generators are provided in appendix C. In continuation to this endeavour an experimental setup (as described in chapter 4 of this thesis) is built to study flow pattern inside a RHVT system. Air is used as the working fluid in all the experiments.

7.6 Summary

Results obtained from the computer code developed and experiments conducted have been presented. The following observations can be made from the results obtained and subsequent discussion:

- The mathematical model is tested for three different vortex generators (10H, 25H and 40H) over a range of hot end valve opening values (2.5 opening to 4.0 opening) and inlet pressures (147 kPa to 314 kPa).
- The gradient of molar concentration of heavier species near the wall of RHVT initially increases along with distance from the inlet towards the hot outlet and then flattens gradually near the hot outlet. This phenomenon is observed due to reduction in driving force for mass transfer.
- There is an optimum value of inlet pressure at which maximum species separation is observed for a given generator. It can also be concluded that this optimum value of inlet pressure changes with variation in hot end valve opening.
- Experiments carried out to study thermal separation show that inlet pressure is the most important parameter that controls thermal separation. Another parameter that influences thermal separation is the cold mass fraction which is controlled by hot end control valve opening.
- Inlet pressure and cold mass fraction are the two operating parameters which influence species separation as well as thermal separation.
- The cause of thermal and mass separation is same (i.e. axial vortex flow inside the tube) and these two phenomena are interrelated and influence each other.
- Tube length, diameter, cold orifice diameter, size and number of inlet nozzles are important geometrical parameters that influence the thermal and species separation in a RHVT and each of these parameters has an optimum value at which the separation becomes maximum.

Chapter 8
Summary and suggestions for further work

"We live on an island surrounded by a sea of ignorance. As our island of knowledge grows, so does the shore of our ignorance".
- John Archibald Wheeler

8.1 Introduction

In this chapter a brief summary of the research work carried out and described in the thesis so far has been included. Subsequently the outcomes of the present research work have been listed along with the contributions to the field of thermal and species separation using RHVT as a separation device. Further a future course of studies required have also been included in this chapter.

8.2 Summary

Objective of the present research work is to investigate experimentally and numerically separation of gas species and energy under different operating conditions in a RHVT. The work was initiated by a simple set of experiments with a commercially available RHVT in which inter-dependence of mass and thermal separation in RHVT was studied. It was concluded from the experiment that mass and heat transfer are dependent on each other. Based on this finding a coupled thermal and mass separation model was built that uses the Chilton-Colburn analogy of simultaneous heat and mass transfer. A computer code based on this model can calculate the thermal and concentration profile along the axial length of the RHVT. Results from the computer code have been verified with data available in literature. Further a laboratory scale experimental setup was built in which both thermal and species separation could be studied using air as a binary mixture of oxygen and nitrogen. Experimental data obtained from this setup has been used to validate the code extensively. Next, a number of important geometric and operating parameters were identified. The computer code developed and the experimental setup were used to carry out parametric studies of the RHVT performance with respect to species separation. Also supporting data available in the literature has been used for parametric study.

8.3 Key findings of work

Following is a comprehensive list of key findings from the work carried out in the present research

- The cause of mass and thermal separation inside a RHVT is same (i.e. axial vortex flow inside the tube). These two phenomenas are interrelated and they influence each other. For a given value of hot end valve opening, it is observed that optimum thermal or species separation occurred at same range of Reynolds number. It could also be seen that overall thermal separation decreased with increasing hot end valve opening.

- Using Chilton Colburn analogy, we can calculate the mass transfer coefficient from the heat transfer coefficient for a device like RHVT in which mass and thermal separation occurs simultaneously.

- The computed values of separation factors from the one dimensional mathematical model compares well with the experimental values of separation factors for the RHVT.

- In the range of inlet pressure considered while separation factor increases continuously with feed flow rate for 10H vortex generator, its value goes through a maxima for 25H and 40H vortex generators.

- The optimum value of inlet flow rate for which separation factor becomes maximum is found to be a function of hot end valve opening which is related to cold mass fraction.

- The gradient of molar concentration of heavier species near the wall of RHVT initially increases along with the distance from the inlet towards the hot outlet and then flattens gradually near the hot outlet. This phenomenon is observed due to reduction in driving force for mass transfer.

- The present mathematical model can compute mass separation in a counter current RHVT based on inlet pressure, temperature, concentration, flow rate and outlet pressure, temperature and flow rate. This model can be used for rapid design and simulation of species separation in a RHVT.

- The mathematical model is tested for three different vortex generators (10H, 25H and 40H) over a range of hot end valve opening values (1.5 opening to 5.0 opening) and inlet pressures (147 kPa to 392 kPa). The agreement between experimental results and values predicted by the present mathematical model were within acceptable range.

- The mass transfer coefficient is calculated from heat transfer coefficient using the heat and mass transfer analogy. Therefore an error in the value of the heat transfer coefficient leads to error in the value of the mass transfer coefficient calculated. This is a limitation of the present model. Another limitation of the present model is that because it is a one dimensional model, it cannot capture the onset and effects of turbulence which is three dimensional in nature.

- The combined heat and mass separation model can calculate the thermal gradient along the length of the RHVT without using experimental thermal data.

- Results from the combined heat and mass separation model were compared with in-house experimental data as well as published data available in the literature. The deviations between measured and computed data were found within acceptable range.

- Inlet pressure and cold mass fraction are the two operating parameters which influence species separation as well as thermal separation.

- There is an optimum value of cold mass fraction at which maximum species separation is observed for a given inlet pressure and vortex generator. Cold mass fraction is controlled by hot end control valve opening.

- Tube length, diameter, cold orifice diameter, size and number of inlet nozzles are important geometrical parameters that influence the thermal and species separation in a RHVT and each of these parameters has an optimum value at which maximum separation is obtained.

8.4 Suggestions for future work

- A turbulence model can be introduced in the present heat and mass transfer model to capture the onset and effect of turbulence on the thermal as well as species separation.

- The model developed in this research work is one dimensional and hence development of a three dimensional model is recommended. This may help to predict the thermal as well as concentration gradient along the length of the RHVT more accurately.

- In the present experimental study inlet pressure of the RHVT is limited by available compressor line pressure. Hence a set of experiments at higher inlet pressure can be carried out.

- A simultaneous visualization of flow pattern inside the RHVT and parametric study is recommended to observe the effect of flow pattern on the thermal and species separation. This will help to develop a mechanistic model to quantitatively predict the influence of different geometric and operating parameters on the performance of the RHVT.

- The work should be extended to separation of mixture of species other than oxygen and nitrogen based on knowledge obtained in the present course of research. Particular emphasize should be given to isotopic separation.

Appendix A

Different methods of isotopic separation

A.1 Diffusion process

Commercial Uranium enrichment was first carried out by the diffusion process in the USA. It has since been used in Russia, UK, France, China and Argentina as well. It is a very energy-intensive process, requiring about 2400 kWh per SWU (Separative Work Unit - as discussed in section 1.3). The basic principle of this method is the equi-partition principle of statistical mechanics (Krass *et al.* [98]). By this principle in a gas consisting of several types of molecules each type will have the same average kinetic energy (KE)

$$KE = \frac{1}{2} M v^2 \tag{A.1}$$

Where M is the mass of the molecule per mole and v is the velocity of the molecule. Hence for two molecules of a gas with different mass e.g. M_1 = 349 (for $U^{235}F_6$) and M_2 = 352 (for $U^{238}F_6$) and velocity v_1 and v_2 but same kinetic energy

$$\langle KE_1 \rangle = \langle KE_2 \rangle \tag{A.2}$$

or,

$$\langle v_1 \rangle / \langle v_2 \rangle = \sqrt{M_2 / M_1} = \sqrt{352/349} = 1.0043 \tag{A.3}$$

The gaseous diffusion method exploits this slight difference in average velocities of the isotopes by forcing the gas mixture to diffuse through a porous barrier under a pressure difference. The barrier is a thin wall of porous material containing numerous very small holes (Fig. A.1). The faster molecules of lighter isotopes ($U^{235}F_6$) will encounter the holes more often than the slower ones of heavier isotope ($U^{238}F_6$) and will therefore be slightly more likely to pass through the barrier.

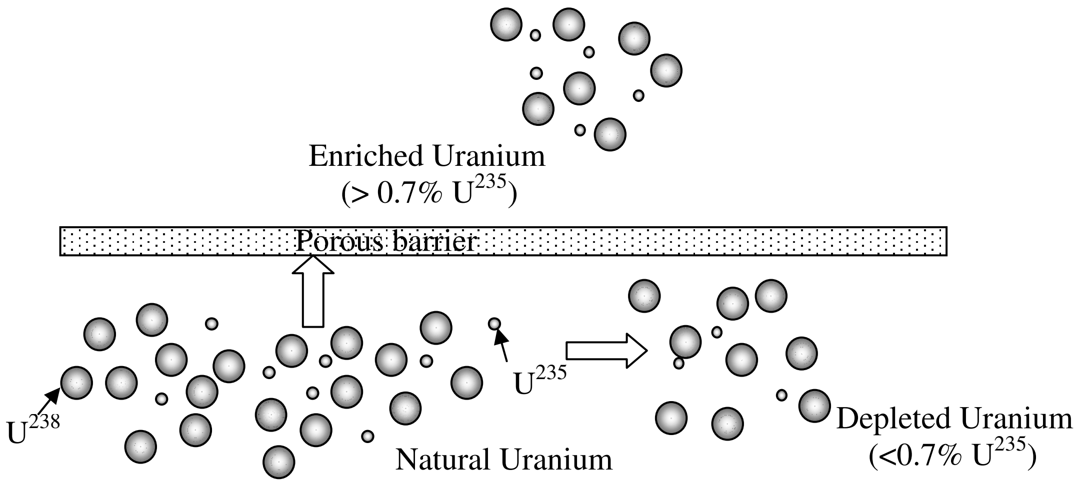

Fig. A.1 Gaseous diffusion isotopic enrichment process

The gas which emerges on the other side of the barrier is enriched in the U^{235} isotope, since the concentration of the desired isotope on the feed side gradually decreases as the enriched material diffuse through the barrier. The average diameter of holes (pores) must be much less than the mean free path of a molecule. The average diameter of UF_6 molecule is 0.7 nm. At 500 mbar pressure and 80 °C average separation of molecules = 5nm, while the mean free path is 85 nm. Therefore average pore size of the barrier should be around 20-40 nm and thickness of few microns. The material of construction of the barrier is sintered nickel powder, ceramic, aluminium, teflon etc. The barrier must be thin so as to have adequate permeability at reasonable pressure and resistant to corrosion. This process is repeated many times in a series of diffusion stages or a cascade. Each stage consists of a compressor, a diffuser and a heat exchanger to remove the heat of compression. The enriched product is withdrawn from one end of the cascade and the depleted waste is removed at the other end. The gas must be processed through some 1400 stages to obtain a product with a concentration of 3% to 4% of lighter isotope. Diffusion plants typically have a small amount of separation through a single stage (hence the requirement of large number of stages arises) but are capable of handling large volumes of gas.

A.2 Gas centrifugation

The gas centrifugation process utilizes a unique design that allows gas to constantly flow in and out of the centrifuge. Unlike most centrifuges the gas centrifuge utilizes continuous processing, allowing cascading, in which multiple identical processes occur in succession.

In a gas centrifuge, the gas molecules are subjected to a strongly rotating centrifugal field (Benedict and Pigford, [27]). The heavier $U^{238}F_6$ molecules are thrown to the peripheral region while the lighter $U^{235}F_6$ molecules are concentrated near the centre. The elementary radial separation factor is given by

$$q_{radial} = e^{\frac{\Delta M v_a{}^2}{2RT}} \tag{A.4}$$

where,

$\Delta M = M_2 - M_1$

v_a = Peripheral speed of the rotor

R = Universal gas constant

T = Absolute temperature

The elementary separation effect obtained above may be multiplied many fold in axial direction by inducing a counter-current flow inside the centrifuge. The enhanced axial separation factor that includes the effect of counter-current flow is much higher than the elementary radial separation factor. For a total reflux condition, the maximum axial separation between the product and waste stream is

$$q_{axial,max} = \{q_{radial}\}^{\frac{L}{\sqrt{2}a}} \tag{A.5}$$

The cylindrical rotor with feeding arrangement spins at high speed around its axis, in a vacuum casing as shown in figure A.2 below, creating the centripetal force on the gaseous components as they enter the cylindrical rotor. The heavier isotopes are concentrated preferentially near the rotor wall while the lighter isotopes are concentrated preferentially near the axis of the rotor. There are two output lines, one located at the top of the centrifuge and the other located at the bottom. By introducing a counter current flow the heavier molecules shall preferentially collected to the bottom of the centrifuge (depleted end) while the lighter molecules shall preferentially collected to the top of the centrifuge (enriched end).

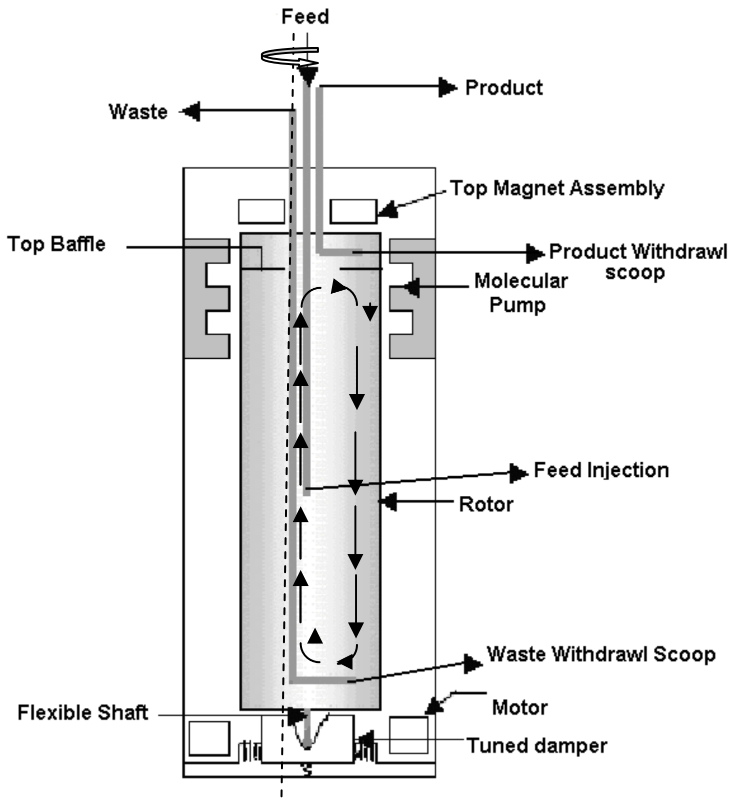

Fig. A.2 Schematic of gas centrifuge

The output lines take these enriched and depleted streams to other centrifuges to continue to the centrifugation process in a series of parallel arrangements called cascade. The centrifuge process consumes less than 10% of the energy consumed by gaseous diffusion plant. This process has been commercially used by Russian enrichment plants and Europian consortium called URENCO. A number of plants are in operation world over.

A.3 Laser isotopic separation

Laser enrichment processes have been the focus of interest for some time. They are a possible third-generation technology promising lower energy inputs, lower capital costs and lower tails assays, hence significant economic advantages. One of these processes is almost ready for commercial use. Laser processes are in two categories: atomic and molecular. Atomic vapour laser isotopic separation (AVLIS) processes work on the principle of photo-ionisation, whereby a powerful laser is used to ionise particular atoms present in a vapour of isotopic metal. An electron can be ejected from an atom by light of a certain frequency. The laser techniques for isotope use frequencies which are tuned to ionise a selective lighter atom but not the heavier atom. The positively-charged light isotope ions are then attracted towards a negatively-charged plate and get collected. Figure A.3 gives schematic diagram of AVLIS process.

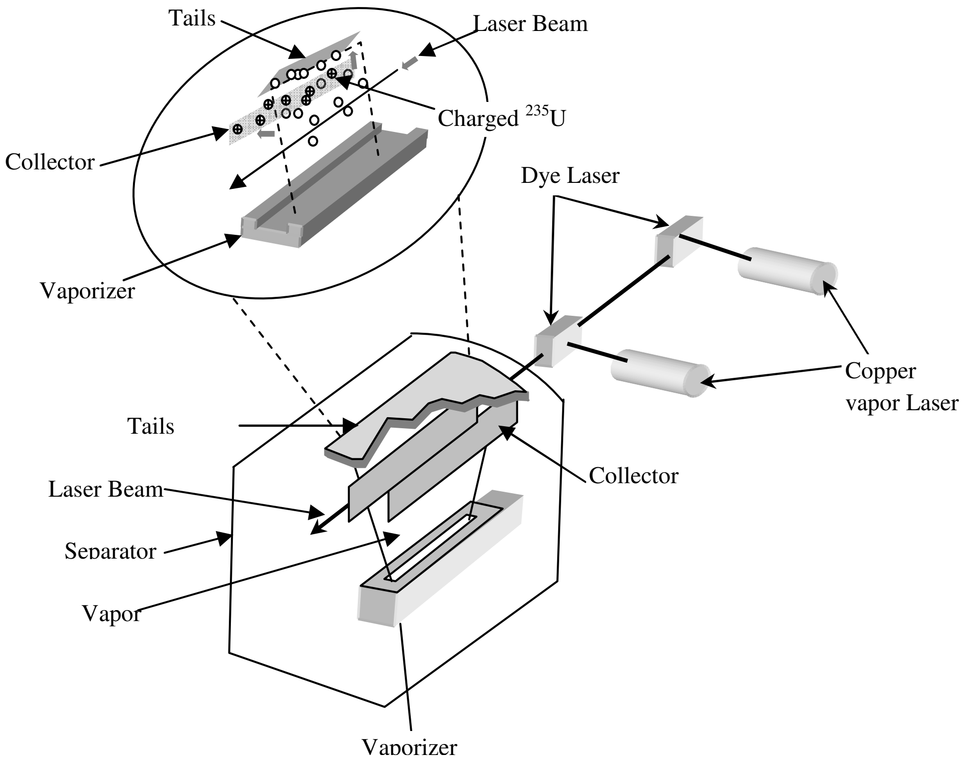

Fig. A.3 Schematic of an AVLIS module

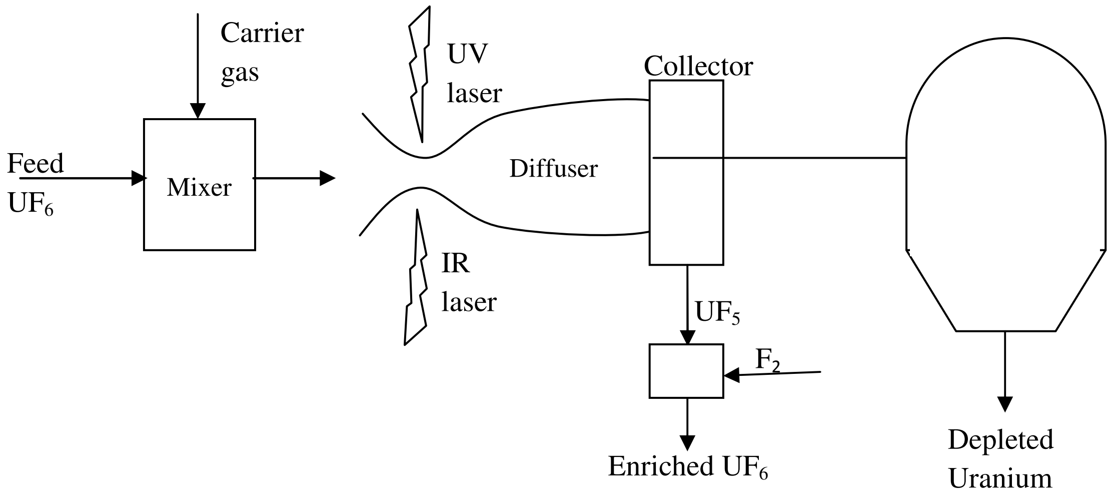

Fig. A.4 Schematic of an MLIS module

The molecular laser isotopic separation (MLIS) process works on the principle of photo-dissociation of process gas into a solid form, using tuned laser radiation as discussed above to break the molecular bond. This then enables the ionized solid to be separated from the unaffected gaseous molecules containing heavier atoms, hence achieving a separation of isotopes. Figure A.4 gives schematic diagram of MLIS process.

A.4 Electromagnetic process

A very early endeavour for isotopic separation was the electromagnetic isotope separation (EMIS) process using Calutrons. A Calutron is a mass spectrometer used for separating the isotopes of Uranium (Krass, *et al.* [98]). Ions of heavier and lighter isotopes are separated because they describe arcs of different radii when they move through a magnetic field. The process is very energy-intensive - about ten times that of diffusion. It was developed by Ernest O. Lawrence [1901-1958] during the Manhattan Project. In a mass spectrometer, a vaporized sample is bombarded with high energy electrons, which cause the sample components to become positively charged ions. They are then accelerated by an electric field and subsequently deflected by magnetic fields, ultimately colliding with a plate and producing a measurable electric current. Since the ions of the different isotopes have the same electric charge but different masses, the heavier isotopes are bent less by the magnetic field, causing the beam of particles to separate out into several beams by the

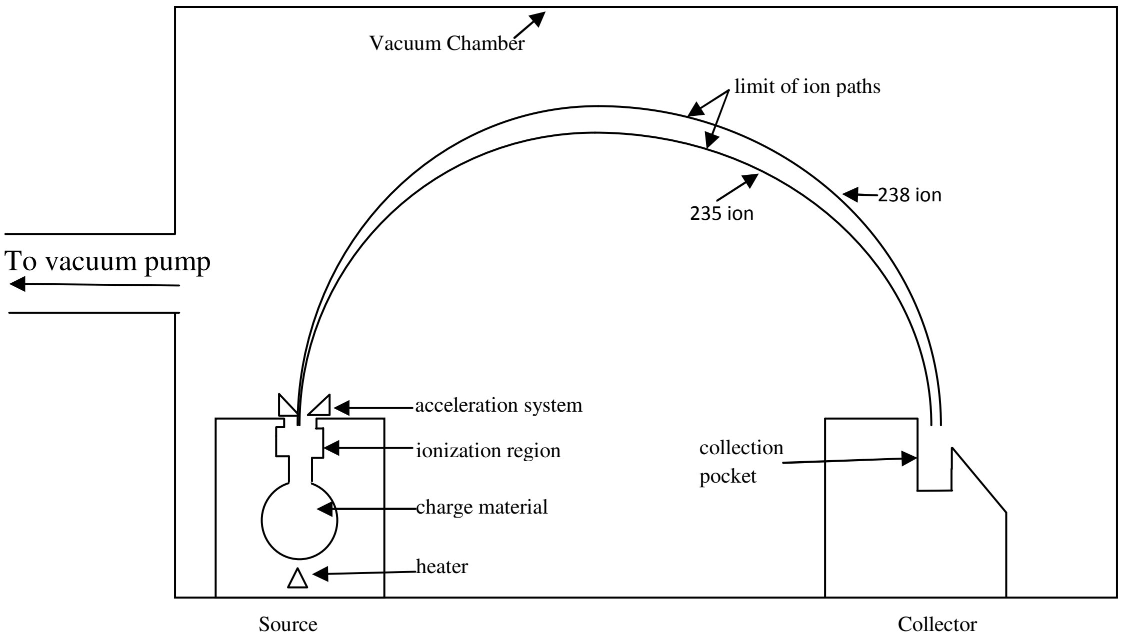

Fig A.5 Calutron method

mass ratio and therefore, striking the collector plate at different locations. Figure A.5 gives schematic diagram of EMIS process.

Appendix B

Quadrupole Mass Spectrometer

B.1 Principle and operation of quadrupole mass spectrometer

A mass spectrometer is an instrument that can detect different electrically charged particle inside a magnetic field based on their difference in charge to mass ratio. It is regularly used for measuring the masses of particles like atoms, molecules and isotopes by ionizing them and subjecting them to an electro-magnetic field where particles of different masses follow different trajectories. This instrument is widely used to identify substances by sorting out its components, measure relative abundances of different isotopes in an isotopic mixture, to analyse degree of separation of different components in a separation process.

The main mass spectrometer operations are

- Ionisation of vaporised samples
- Acceleration of ion stream
- Deflection of ion stream
- Detection of ion streams

The entire process occurs under high vacuum of 10^{-6} to 10^{-8}torr, since the acceleration of ions inside the mass spectrometer device is not possible at atmospheric pressure due to collision with air molecules.

In the year 1900 J. J. Thomson and F. W. Aston had showed that a continuous stream of charged particles travelling in vacuum deflects when it passes through a magnetic or electric fields. The extent of bending depends on the masses of the particles and also on the electrical charges they carry. In a mass spectrometer the charged particles (ions) pass through a deflecting field. This deflecting field is produced by carefully designed electrodes and/or magnetic poles of given strength. The beam of ions is initially made to pass through a series of electric and magnetic field combinations those separate out all particles with a given velocity and rest of the particles are eliminated from the system. Next the beam of ions with similar velocity enters a chamber under high degree of vacuum where it follows a semi-circular path under the influence of a magnetic field. The mass of the particles in the beam solely determine the radius of this path, as all the remaining factors that can affect the radius of the path i.e. velocity and charge of the particles are identical. Thus if the beam of particles contain atoms of different mass number, they follow a different radius of curvature. Hence the particles with different mass number can be distinctly distinguished.

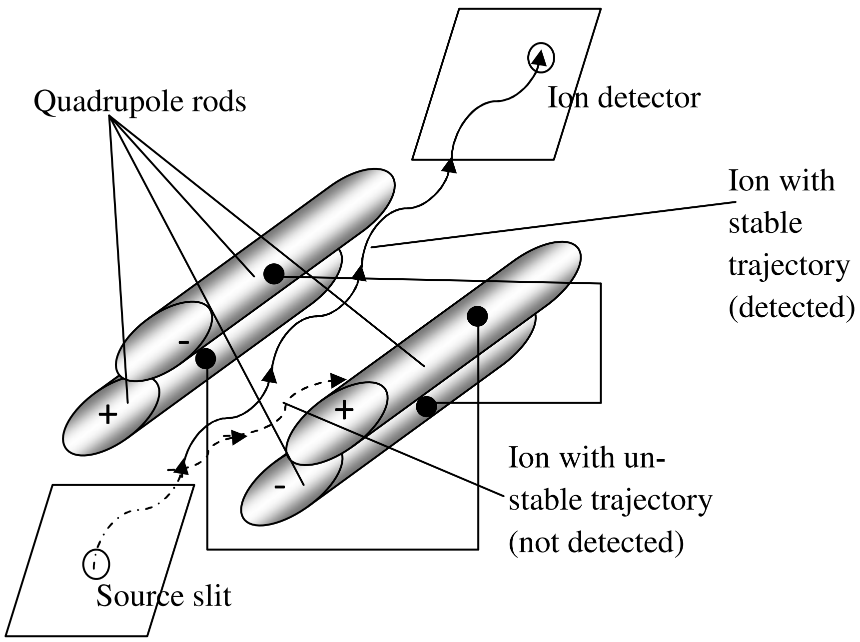

Fig. B.1 Schematic of a quadrupole mass spectrometer

Downard [54] have described the working principle of a quadrupole mass spectrometer or residual gas analyzer. The mass analyzer section of quadrupole mass spectrometer consists of four rods arranged in parallel where those opposite of one another are electrically connected (figure B.1). The quadrupole has a number of advantages over magnetic sector mass analyzers including the low cost of construction, their compact size, and fast scanning capability (Oehme [136]). A voltage of opposite polarity *(+/- ve*) is applied to adjacent rods consisting of a direct current (DC) component (denoted U) and a radio frequency (*RF*) component (denoted $V_{RF}cos(\omega' t)$) where ω' is the angular frequency of the *RF* field. Ions are accelerated out of the ion source along the z-axis between the rods. They experience forces in the x and y direction that cause them to oscillate toward and away from the rods. In practice, the voltages U and V_{RF} are held at a fixed ratio to maximize the mass resolution that can be achieved. A complete mass spectrum is obtained by scanning the voltages U and V_{RF} where this fixed ratio is maintained. Ideally the voltages U and V_{RF} should be held constant throughout the passage of ions of a particular mass to charge ratio m_i/z_e through the analyzer. Thus by varying the U and V_{RF} ratio we can allow for the majority of ions of a particular m_i/z_e to reach the detector and rest of the ions strike the rods and do not reach the detector.

Ions in the stream detected by the ion detector collide with the wall of the metal box inside the detector section. Individual ion acquires an electron from the pool of free electrons in the metal and becomes neutral. This creates a void in the metal and another electron jumps into the void to fill it which is also picked by the next ion arriving at the collision point with the metallic wall. This shuffling of the electrons eventually gives rise to a steady electric current which is fed to an amplifier and the amplified signal is recorded. Higher is the rate of ion stream arriving in the detector higher is the strength of the signal. A computer software processes this signal and plots the abundance of the species present in the sample.

Figure B.2*a* and B.2*b* show typical outputs from a quadrupole mass spectrometer for sample obtained from the hot and cold end of the RHVT respectively. In these figures relative abundance of the isotopes is plotted in the y- axis against the mass to charge ratio m_i/z_e of the isotopes in the x-axis. The vertical axis reads relative abundance or alternatively relative intensity and corresponds to the current received by the recorder which is directly proportional to the number of ions arriving at the detector. Higher is the current corresponding to a particular ion, higher is the abundance of that isotope.

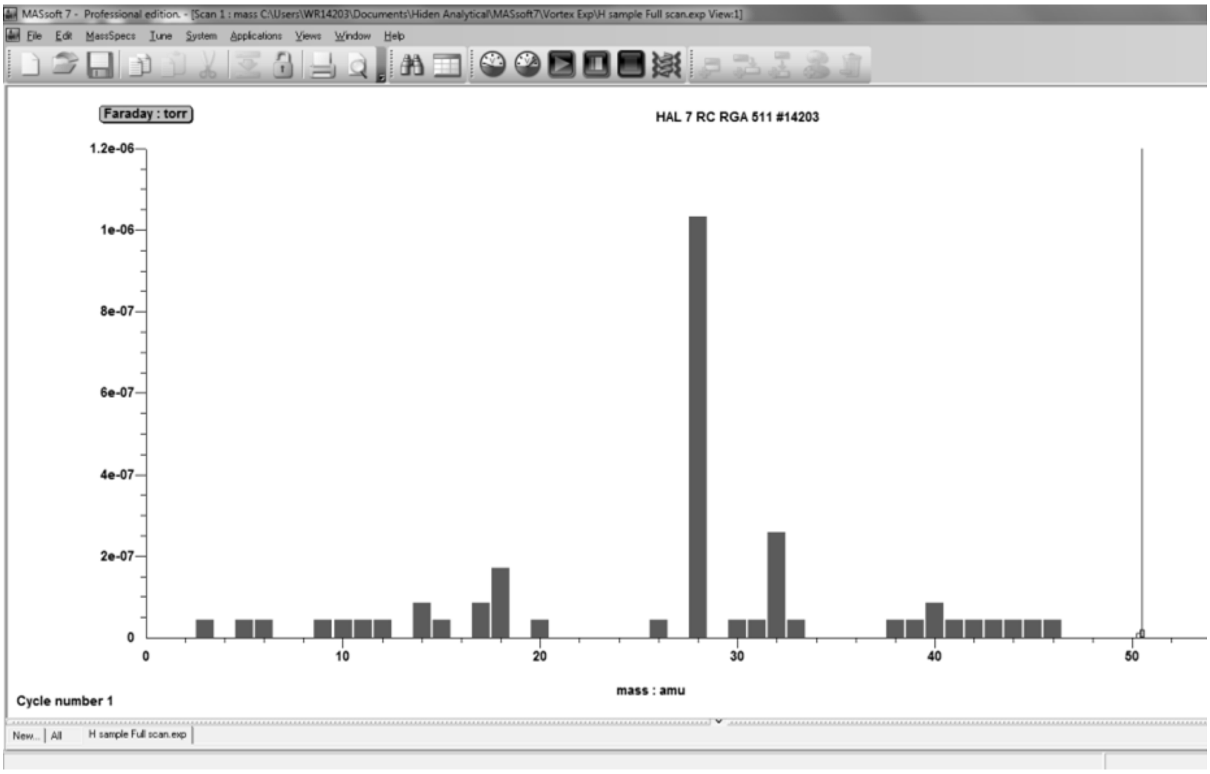

Fig. B.2a QMS reading for air sample analysis from hot end section of the RHVT

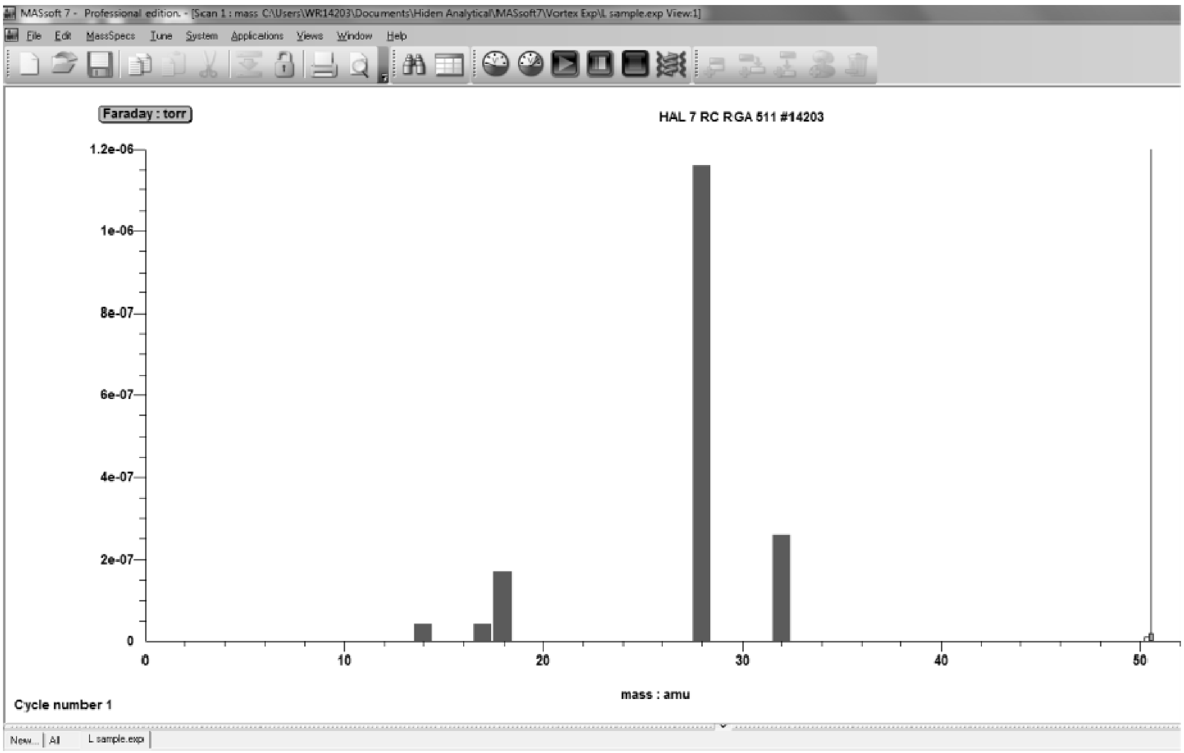

Fig. B.2b QMS reading for air sample analysis from cold end section of the RHVT

Appendix C

RHVT experimental data

C.1 Notations used in the experimental data tables

Table C.1 Meaning of notations used

Notation	Meaning	Unit
Open	Hot end control valve opening	turn
In_pr	Inlet pressure	bar
C_out_pr	Cold outlet pressure	bar
C_N2	Concentration of nitrogen at cold outlet	%
C_O2	Concentration of oxygen at cold outlet	%
H_N2	Concentration of nitrogen at cold outlet	%
H_O2	Concentration of oxygen at cold outlet	%
In_t	Inlet temperature	ºC
C_out_t	Cold outlet temperature	ºC
H_out_t	Hot outlet temperature	ºC
C_Out_Fl	Cold outlet flow	LPM
H_Out_Fl	Hot outlet flow	LPM

C.2 Data for 10H vortex generator

open (turn)	In_pr (bar)	C_out_pr (bar)	C_N2 (%)	C_O2 (%)	H_N2 (%)	H_O2 (%)	In_t (deg C)	C_out_t (deg C)	H_out_t (deg C)	C_out_Fl (LPM)	H_out_Fl (LPM)
2.0	3.5	0.04	82.41	17.58	83.56	16.43	27.48	09.08	41.83	10.5	12.0
2.0	4.0	0.04	84.93	15.06	84.27	15.72	25.57	06.37	44.64	12.0	13.5
2.0	4.5	0.04	84.39	15.60	84.30	15.69	27.59	05.43	45.79	13.0	14.0
2.0	5.0	0.05	83.79	16.20	83.41	16.58	27.60	04.26	47.36	13.5	15.0
2.5	3.0	0.02	84.79	15.20	85.09	14.90	27.69	12.50	38.92	09.0	12.0
2.5	3.5	0.03	82.85	17.14	83.00	16.99	27.70	09.47	41.41	10.5	13.0
2.5	4.0	0.03	83.02	16.97	82.66	17.33	27.70	07.70	43.18	11.5	14.0
2.5	4.5	0.04	82.25	17.74	82.03	17.96	27.79	06.45	44.42	13.0	15.0
2.5	5.0	0.05	81.90	18.09	81.79	18.20	27.82	05.30	45.61	14.0	16.0
3.0	3.0	0.01	77.63	22.36	76.37	23.62	28.01	13.09	38.23	09.0	12.0
3.0	3.5	0.01	75.34	24.65	74.12	25.87	28.09	11.14	40.06	10.0	13.0
3.0	4.0	0.02	73.27	26.72	73.22	26.77	27.98	08.70	42.18	10.5	14.0
3.0	4.5	0.03	74.98	25.01	75.52	24.47	28.04	07.12	43.51	12.5	15.0
3.0	5.0	0.04	76.14	23.85	76.49	23.50	28.06	05.11	45.61	13.5	16.0
3.5	3.5	0.04	74.36	25.63	74.18	25.81	28.01	09.92	40.41	10.0	13.0
3.5	4.0	0.04	77.61	22.38	77.39	22.66	28.04	08.11	42.14	11.5	14.0
3.5	4.5	0.05	77.35	22.64	77.27	22.72	28.11	06.49	43.67	12.5	15.0
3.5	5.0	0.07	77.54	22.45	77.73	22.26	28.15	05.01	45.16	14.0	16.5
4.0	3.5	0.02	77.27	22.72	76.40	23.59	27.93	10.06	40.48	10.0	13.0
4.0	4.0	0.03	77.31	22.68	80.25	19.74	27.98	08.25	42.08	11.5	14.0
4.0	4.5	0.03	80.20	19.79	79.56	20.43	28.16	06.37	44.16	12.5	15.0
4.0	5.0	0.04	78.76	21.23	79.56	20.43	28.21	05.09	45.41	14.0	16.5
4.5	3.5	0.02	82.31	17.68	82.36	17.63	28.15	10.10	40.48	10.0	13.0
4.5	4.0	0.02	81.14	18.85	80.12	19.87	28.16	08.40	41.80	12.0	14.0
4.5	4.5	0.03	80.01	19.98	80.12	19.87	28.25	06.50	43.84	13.0	15.0
4.5	5.0	0.04	79.67	20.32	79.66	20.33	28.43	04.89	45.50	14.0	16.5
5.0	3.5	0.03	83.43	16.56	82.27	17.22	28.16	09.53	41.76	10.0	13.0
5.0	4.0	0.04	84.34	15.65	83.77	16.22	28.18	08.07	43.05	11.5	14.0
5.0	4.5	0.05	83.32	16.67	82.41	17.58	28.24	06.30	44.97	12.5	15.0
5.0	5.0	0.06	81.94	18.05	81.57	18.42	28.38	04.50	46.67	14.0	16.0

C.3 Data for 25H vortex generator

open (turn)	In_pr	C_out_pr (bar)	C_N2 (%)	C_O2 (%)	H_N2 (%)	H_O2 (%)	In_t (deg C)	C_out_t (deg C)	H_out_t (deg C)	C_out_Fl (LPM)	H_out_Fl (LPM)
1.5	1.5	0.03	80.73	19.27	80.81	19.19	30.13	15.46	51.19	14.0	09.5
1.5	2.0	0.045	80.89	19.11	80.67	19.33	30.13	13.46	55.84	15.5	10.5
1.5	2.5	0.08	80.74	19.26	80.66	19.34	30.25	11.34	60.53	18.5	12.0
1.5	3.0	0.14	79.09	20.91	78.73	21.27	30.35	09.56	64.87	22.5	14.5
1.5	3.5	0.17	78.55	21.45	77.91	22.09	30.39	09.04	66.69	24.0	15.0
1.5	4.0	0.20	78.47	21.53	78.19	21.81	30.45	08.36	66.88	26.0	15.5
2.0	1.5	0.00	79.11	20.89	78.87	21.13	30.40	16.47	48.95	13.0	10.0
2.0	2.0	0.05	79.94	20.06	79.20	20.80	30.51	12.23	55.21	18.0	12.5
2.0	2.5	0.07	79.49	20.51	79.34	20.66	30.58	10.67	58.54	19.5	14.0
2.0	3.0	0.08	78.67	21.33	78.92	21.08	30.61	09.27	61.49	20.0	14.5
2.0	3.5	0.13	78.26	21.74	78.60	21.40	30.69	07.99	63.99	23.0	16.0
2.0	4.0	0.19	77.66	22.34	78.80	21.20	30.89	06.65	67.25	27.0	17.0
2.5	1.5	0.01	78.86	21.14	78.27	21.73	30.64	15.17	50.53	13.2	10.2
2.5	2.0	0.03	77.84	22.16	78.62	21.38	30.76	11.80	55.92	16.0	12.2
2.5	2.5	0.04	78.10	21.90	78.32	21.68	30.75	10.42	58.18	18.0	13.3
2.5	3.0	0.075	78.04	21.96	78.27	21.73	30.84	08.76	61.38	19.5	14.5
2.5	3.5	0.12	78.32	21.67	77.21	22.28	30.91	07.11	64.63	22.0	16.3
2.5	4.0	0.14	78.14	21.85	77.71	22.28	31.01	06.46	65.87	24.7	17.5
3.0	1.5	0.01	79.14	20.86	80.36	19.64	30.50	14.24	51.36	12.8	10.2
3.0	2.0	0.03	80.00	20.00	79.74	20.26	30.58	11.12	56.17	16.2	12.8
3.0	2.5	0.05	77.67	22.33	79.32	20.68	30.67	09.67	58.81	18.0	13.8
3.0	3.0	0.07	79.59	20.41	78.48	21.52	30.70	08.20	60.94	20.0	15.0
3.0	3.5	0.12	78.59	21.41	78.56	21.44	30.88	06.78	63.67	21.9	16.7
3.0	4.0	0.14	79.40	20.60	79.24	20.76	30.85	06.02	64.96	24.5	17.8
3.5	1.5	0.01	77.63	22.37	79.42	25.81	30.22	13.54	51.29	13.5	11.0
3.5	2.0	0.03	77.20	22.80	77.81	22.19	30.32	11.10	55.12	16.0	12.5
3.5	2.5	0.04	78.59	21.41	77.67	22.33	30.38	10.06	57.07	17.5	13.3
3.5	3.0	0.08	77.04	22.96	78.11	21.89	30.55	08.02	60.44	20.2	15.0
3.5	3.5	0.12	78.38	21.62	77.05	22.95	30.58	06.58	62.98	22.5	17.0
3.5	4.0	0.165	78.10	21.90	77.12	22.82	30.75	05.59	64.99	25.2	18.1
3.5	4.5	0.19	77.42	22.58	77.29	22.71	31.02	04.60	67.50	26.8	19.5
4.0	1.5	0.01	79.68	20.32	79.20	20.80	30.50	14.30	50.14	13.2	10.8
4.0	2.0	0.02	79.39	20.61	78.97	21.03	30.53	11.45	54.07	15.5	12.5
4.0	2.5	0.05	79.08	20.92	78.71	21.29	30.59	09.33	57.95	18.0	14.0
4.0	3.0	0.08	79.44	20.56	79.18	20.82	30.84	07.85	60.61	20.3	15.5
4.0	3.5	0.11	78.88	21.12	78.41	21.59	30.85	07.02	62.09	22.0	16.8
4.0	4.0	0.14	79.32	20.68	78.44	21.23	30.87	06.01	63.64	24.0	17.5
4.0	4.5	0.19	78.96	21.04	78.49	21.51	31.17	04.90	65.98	26.5	19.2

C.4 Data for 40H vortex generator

open (turn)	In_pr	C_out_pr (bar)	C_N2 (%)	C_O2 (%)	H_N2 (%)	H_O2 (%)	In_t (deg C)	C_out_t (deg C)	H_out_t (deg C)	C_out_Fl (LPM)	H_out_Fl (LPM)
1.5	2.0	0.26	83.92	16.07	82.93	17.06	28.30	16.50	50.50	27.0	12.5
1.5	2.5	0.34	82.31	17.68	81.95	18.04	28.30	15.59	52.89	31.0	14.0
1.5	3.0	0.43	81.77	18.22	81.69	18.30	28.37	14.86	56.04	34.0	15.0
1.5	3.5	0.53	84.96	15.03	83.23	16.76	28.48	14.53	58.00	37.5	17.0
1.5	4.0	0.64	83.53	16.46	82.83	17.16	28.48	14.17	60.11	40.0	17.5
2.0	2.0	0.26	82.88	17.11	84.43	15.56	27.98	15.60	50.05	26.5	14.0
2.0	2.5	0.34	84.65	15.34	84.15	15.48	28.04	14.71	52.45	30.0	16.0
2.0	3.0	0.40	84.11	15.88	83.62	16.37	28.15	14.18	55.38	32.0	17.0
2.0	3.5	0.48	83.38	16.61	83.31	16.68	28.56	13.90	56.79	36.0	18.5
2.0	4.0	0.58	83.31	16.68	83.14	16.85	28.58	13.58	57.85	38.5	20.0
2.5	2.0	0.25	83.59	16.40	84.06	15.93	27.59	15.20	47.60	26.0	15.0
2.5	2.5	0.32	84.71	15.28	84.39	15.60	27.77	14.26	50.69	29.0	17.0
2.5	3.0	0.40	83.42	16.57	83.06	16.93	27.82	13.65	52.13	32.5	18.0
2.5	3.5	0.48	82.82	17.17	82.54	17.45	27.86	13.18	53.42	35.0	19.0
2.5	4.0	0.56	82.49	17.50	82.38	17.61	27.93	12.90	54.51	38.0	22.0
3.0	2.0	0.26	82.86	17.13	82.42	17.57	27.34	14.90	47.91	26.0	15.0
3.0	2.5	0.32	82.96	17.03	81.09	18.90	27.39	13.99	50.30	29.0	16.5
3.0	3.0	0.40	82.30	17.69	81.96	18.03	27.49	13.44	51.46	32.0	18.0
3.0	3.5	0.47	84.81	15.18	84.66	15.33	27.74	12.97	53.26	35.0	19.5
3.0	4.0	0.59	81.99	18.00	81.90	18.09	27.84	12.73	54.27	38.0	22.5
3.5	2.0	0.23	83.83	16.16	85.25	14.74	27.81	15.06	46.64	25.0	15.0
3.5	2.5	0.30	83.16	16.83	83.10	16.89	27.86	14.18	50.48	30.0	17.0
3.5	3.0	0.39	82.50	17.49	82.55	17.44	28.01	13.60	52.40	32.0	18.0
3.5	3.5	0.46	84.96	15.03	84.94	15.05	28.12	13.18	53.79	35.0	20.5
3.5	4.0	0.56	84.37	15.62	83.23	16.76	28.39	13.01	54.55	38.5	23.0
4.0	2.0	0.26	80.19	19.80	80.41	19.58	26.90	14.35	46.52	26.0	15.0
4.0	2.5	0.34	84.15	15.84	82.56	17.43	26.96	13.67	48.34	29.5	17.0
4.0	3.0	0.42	84.14	15.85	83.67	16.32	27.01	12.90	50.02	33.0	18.0
4.0	3.5	0.49	83.13	16.86	83.05	16.94	27.21	12.44	52.24	35.0	19.0
4.0	4.0	0.59	83.72	16.27	83.70	16.29	27.40	12.13	53.41	38.5	22.5
4.5	2.0	0.23	83.00	16.99	82.55	17.44	27.82	15.34	46.98	25.5	15.0
4.5	2.5	0.30	83.68	16.31	83.37	16.62	28.02	14.11	49.66	29.0	17.0
4.5	3.0	0.39	83.96	16.03	83.16	16.83	28.02	14.11	49.66	29.0	17.0
4.5	3.5	0.46	84.50	15.49	84.40	15.59	28.09	13.02	52.91	35.0	20.0
4.5	4.0	0.56	83.81	16.18	84.46	15.53	28.55	12.68	54.69	39.0	23.0

Appendix D

Effect of geometric parameters on thermal and species separation

In this section analyses of two important sets of parameters that influence the thermal as well as species separation performance of a RHVT have been presented. The first set consists of the geometrical characteristics of the RHVT i.e. diameter and length of the hot and cold tubes, the cold orifice diameter and number of inlet nozzles. These are basically design parameters of the RHVTs and are fixed during their design. The results of the analyses are presented in this section. In the second set, effect of important operating parameters like inlet gas pressure, inlet gas flow rate and cold mass fraction have been analyzed. The results of the analyses are presented in the next section of this chapter. For each parameter, the thermal and species separation mechanism and the flow-fields inside the RHVT are explored by investigating the pressure, velocity, and temperature fields. The principal geometric parameters are RHVT length, diameter, cold orifice diameter, number of intake nozzles and their opening areas. There effect on species separation is discussed below in details.

D.1 Effect of tube length

Thermal separation in a RHVT depends on the length of the tube. It has been reported by various researchers that as the length of RHVT increases, the thermal separation (T_3 - T_2) increases. Earlier researches carried out by Parulekar [139], Otten [138], Raiskii and Tunkel [149] have employed divergent tubes in a RHVT. The aim of these works was twofold i.e. to reduce the length of the unit and to improve energy separation performance by maximizing the hot outlet temperature or minimizing the cold outlet temperatures. Later Takahama and Yokosawa [179] have tried to shorten the length of RHVT by using shorter divergent tubes. They have compared their results with those from the straight RHVTs and found that the use of a divergent tube with a small angle of divergence led to an improvement in temperature separation and enable shortening the length of the unit. Gao [72] have experimentally shown that with increasing length of the RHVT the maximum temperature difference obtained increased. Raiskee and Tunkel [149] have shown that most efficient thermal separation happens in RHVT with length to diameter ratio (L_{vt}/D_{vt}) ≥ 20. As the absolute length of the RHVT decreases ($L_{vt}/D_{vt} \leq 20$), its thermal separation performance decreases sharply. Most of the RHVT researches were done with $L_{vt}/D_{vt} \geq 24$. Takahama [177] have conducted experiments with a RHVT of length $150D_{VT}$. As the flow inside the RHVT gets separated into two streams, one of the streams moves towards the hot end along the peripheral region while the other stream moves in the opposite direction towards the cold end along the axial core region. The peripheral stream that is discharged from the hot end attains higher temperature than the inlet temperature. On the other hand the axial stream is discharged at a lower temperature than the inlet temperature. Camiré [33] have observed that if the hot stream is required to be separated at an appreciably high temperature, the tube need to be longer than the back flow core to avoid mixing of hot and cold gas at the two outlets of the RHVT.

Linderstrom-Lang [113] had described the reason behind species separation in a RHVT was pressure diffusion in centrifugal force field. As described by Linderstrom-Lang [113] "the vortex tube acts essentially as a centrifuge, i.e. that pressure diffusion is responsible for at least the major part of the separation" and "axial flows play an important role in establishing the net gas-separation effect". Hence it followed that this radial separation could be multiplied in axial direction by formation of a pair of parallel counter current streams eventually enriching one stream and depleting the other at two ends of the RHVT. The rates of diffusional separation or separative exchange in radial direction per unit tube length was given by

$$u = 2\pi\, \rho D_f \frac{\Delta M}{RT} v_\theta^2 N(1-N) \tag{D.1}$$

As per the above equation (D.1) species separation should increase along with the length of the RHVT. But Linderstrom-Lang [113] had shown that shorter length of RHVT produced a higher species separation compared to longer RHVTs. This phenomenon could be explained by alteration in flow pattern and onset of turbulent mixing at longer RHVTs. The increase in turbulent kinetic energy at the dividing region between core and periphery would decrease species separation. This had been shown both by Computational Fluid Dynamics (CFD) model and experimental measurements by researchers like Raiskee and Tunkel [149], Skye *et. al*. [168], Bramo and Pourmohamoud [30] among others.

D.2 Effect of tube diameter

A set of experiments have been carried out by Negm *et al.* [130] with different tube diameters to compare their thermal separation characteristics. They have reported that up to an optimum value of the inside (wetted) diameter of the RHVT the thermal separation performance increases with increasing value of tube diameter. This optimum value was reported as 16 mm. Beyond this value of diameter, thermal separation starts decreasing. They have explained this observation to Reynolds number *Re*, which is a ratio of inertial to viscous forces. At smaller value of diameter, *Re* value is small, the inertial forces that drive the azimuthal motion are weak and the vortex effect detoriates resulting into smaller thermal separation. As diameter increases, the value of Reynolds number increases and inertial forces starts dominating over the viscous forces (friction forces) which are presumably responsible for thermal separation process and hence performance detoriates. Therefore an optimal value of tube diameter can be obtained which gives highest thermal separation. Agarwal *et. al.* [3] have found that the RHVT of L_{vt}/D_{vt} ratio 17.5 performs optimally. Saidi *et. al.* [158] have experimentally found that the optimum value for L_{vt}/D_{vt}.

Promvonge *et. al.* [143] had observed when diameter of the RHVT was varied, keeping both feed inlet pressure condition and RHVT length fixed, back pressure at the inlet of the RHVT varied inversely with the diameter. When the diameter of the RHVT was higher, the back pressure remained low and hence specific volume was high. This in turn would reduce the azimuthal component of velocity in both the axial and peripheral layers of gas and a flat pressure profile would be obtained. Hence it could be concluded that the rate of pressure diffusion in the radial direction was reduced which in turn reduced the species separation in the binary gas mixture. On the other hand a smaller diameter RHVT would produce high back pressure and hence the specific volume of air would reduce. Therefore azimuthal velocities between the peripheral and the axial regions would not differ substantially due to the lower specific volume. This would reduce the centrifugal pressure difference between the two streams in the peripheral and the axial regions and thus the rate of mass transfer between those streams would remain low. Hence we would get an optimum value of the RHVT diameter which would produce a maximum separation. Similar results had been reported by Marshall [121]. Tapering the RHVT contributes to separation process in RHVT used for gas separation.

D.3 Effect of cold orifice diameter

Westley [196] have experimentally optimized the geometry of the RHVT and found cold end orifice area ≡ $0.167A_{vt}$ produces maximum thermal separation. Soni [172] have proposed an optimum value of cold end orifice area up to ≡ $0.145A_{vt}$. Promvonge and Eiamsa-ard [147] have experimentally investigated the effect of cold orifice diameter on temperature separation phenomenon in a counter-flow type RHVT. They have reported the temperature reduction and isentropic efficiency of the RHVT with variable size of the cold orifice diameter from $0.4D_{vt}$ to $0.9D_{vt}$. They have found lower thermal separation with small cold orifice diameter ($0.4D_{vt}$) while a cold orifice diameter beyond $0.7D_{vt}$ also shows reduction in thermal separation in the tube. Saidi and Valipour [158] have shown that for cold orifice diameter < $0.5D_{vt}$, increasing cold orifice diameter causes the cold outlet temperature difference to increase. They have also found that for cold orifice diameter > $0.5D_{vt}$ increasing cold orifice diameter causes the cold outlet temperature difference to decrease.

In another work Eiamsa-ard and Promvonge [62] had discussed in details the effect of cold orifice diameter on the flow field inside a RHVT. According to them higher back pressure in the RHVT would be generated when the cold orifice diameter was small, resulting, as discussed in the previous section, in lower species separation. On the contrary, when the cold orifice was large it would draw air directly from the inlet and thus azimuthal velocities in the axial as well as peripheral layers would be dampened. This would result into lower species separation. Nimbalkar and Muller [135] had pointed that a swirling secondary loop was formed when the cold orifice diameter was smaller than the diameter of the axial backflow core, and a return flow was generated at the cold end, inside the RHVT. This return flow could force a mixing of axial gas stream depleted with heavier component of the mixture with the peripheral gas stream enriched with heavier component. Hence species separation was reduced at lower cold orifice diameter. When the cold orifice diameter was equal to the diameter of the axial backflow core, this return flow was not generated. At this value of cold orifice diameter optimum species separation was possible. Again when cold orifice diameter was made bigger than the axial backflow core diameter the enriched peripheral stream entered the axial zone and mixed with the axial depleted stream. Thus species separation was reduced at higher value of cold end orifice diameter.

D.4 Effect of intake nozzle number and area

Saidi and Valipour [158] have shown the effect of intake nozzle number on thermal separation. As the number of intake nozzle increases, cold and hot streams are mixed in the main tube due to onset of turbulence and efficiency of thermal separation is reduced. Gao [72] have shown for a fixed inlet condition of mass flow rate and pressure, the exhaust temperature (i.e. thermal separation) is same for different number of intake nozzles with scaled geometry. Behera *et. al.* [23] have investigated the effect of nozzle shape and size on thermal separation using a computer code and turbulence model. Eiamsa-ard and Promvonge [61] have observed that an inlet nozzle with very small opening area would cause considerable pressure drop in the nozzle. This would result into lower azimuthal velocities and hence lower thermal separation. On the other hand if the nozzle opening area is made very large then structure of vortices shall get disturbed resulting into low diffusion of kinetic energy and hence lower thermal separation. They have also observed that if the nozzles are located away from the orifice then it would lead to low tangential velocities near the orifice and hence low temperature separation. Hence the inlet nozzle location should be as close as possible to the orifice to yield high tangential velocities near the orifice which results into higher thermal separation.

It has been observed for a given geometry of RHVT and fixed inlet condition, as the numbers of intake nozzles were increased, the intensity of turbulence and pressure loss at the entrance of the vortex chamber were also gradually increased. Hence it could be concluded that with increasing number of nozzles the turbulent mixing of two partially separated streams of heavier and lighter components of the inlet gas mixture had increased. Also with increase in pressure loss the azimuthal velocity head was decreased which had resulted into lower centrifugal diffusion. Hence with increasing number of intake nozzles the overall separation effect in a RHVT had decreased. Similar results had been obtained by Mohammadi and Farhadi [126] for the separation of Liquefied Petroleum Gas (LPG) from a mixture of LPG and nitrogen. Im and Yu [89] had suggested that nozzle exit velocity would decrease as their opening areas were increased. This would result into generation of lower intensity vortex inside the vortex chamber. As the vortex generation was reduced this would result into fall in species separation, due to reduction in centrifugal field.

D.6 Effect of other geometrical parameters

The hot-end control valve is not a critical component in the RHVT. Aydin and Baki [16] have given the optimum value for the angle of the cone-shaped control valve as approximately 50°. Rounding off the tube entrance improves the performance of the RHVT (Gao [72]). With a muffler at the cold end thermal separation performance of the system is better than that without muffler (Kuroda [103]). Saidi and Yazdi [157] have shown that smooth finishing of inner surfaces of the tube results in better temperature separation and performance of RHVT.

Appendix E

Effect of operating and other parameters on thermal and species separation

The principal operating parameters are inlet flow rate, inlet pressure and cold mass fraction. Their effects on thermal and species separation are discussed below in details. A large number of literatures are available on the effect of these parameters on thermal separation and the effects are well known. But not many studies have been reported on parametric studies for species separation with the operating parameters of a RHVT.

E.1 Effect of inlet flow rate and inlet pressure

The inlet pressure is the necessary driving force for the thermal separation. Aydin and Baki [16] have experimentally shown that the higher the inlet pressure, the greater is the temperature difference of the outlet streams. Martynovskii and Alekseev [123] reported that increasing the inlet pressure resulted in large temperature difference between hot and cold gas temperatures. Saidi and Valipour [158] have shown that the fall in gas temperature coming out from the cold outlet (T_1-T_2) can be increased by increasing the inlet pressure, while the thermal efficiency of the system goes through an optimum at specific inlet pressure. Shannak [164] found that a 40% change of the inlet pressure may lead to 2% change of the hot and cold temperature. According to Martynovskii and Alekseev [123] and Gulyaev [76], inlet temperature does not significantly affect the thermal separation in a RHVT. Hence it can be concluded that inlet pressure has a strong influence on thermal separation although the inlet temperature has negligible effect on temperature separation.

Saidi and Valipour [158] had shown that by increasing the inlet pressure of the RHVT the flow velocity at the outlet of the entrance nozzle could be increased up to the point where choking of the flow took place. Ahlborn *et. al.* [4] had shown that the inlet flow rate was a function of normalized pressure drop between the inlet and the cold end of the RHVT

$$X = \frac{(P_1 - P_2)}{P_o} \tag{E.1}$$

Hence it could be concluded that for a fixed value of outlet pressure the inlet flow rate was directly proportional to the inlet pressure. It had been observed that practically in many cases, though the compressor connected to the RHVT could generate the required inlet pressure but the supply flow rate fell short due to lack in compressor capacity. Hence it is required to be ensured that both the inlet pressure and flow rate can be generated by the compressor. The inlet or overall mass flow rate of the working gas supplied into the RHVT is an important factor influencing the performance. Chatterjee *et. al.* [34] had experimentally shown that there was an optimum value of inlet pressure or inlet flow rate at which maximum species separation was observed for a given generator and fixed value of the hot end valve opening. At lower inlet pressure as the pressure was gradually increased the swirling velocity of gas streams also increased. This would give rise to higher centrifugal pressure diffusion and species separation would gradually increase. As inlet pressure was further raised to a higher value, heavier species would get collected at the peripheral streams and this would cause a reduction of difference in partial pressure of the heavier species between peripheral and axial regions. Hence at higher inlet pressure species separation would reduce considerably and the separation factor would go through a maxima.

E.2 Effect of cold mass fraction

The cold mass fraction of a RHVT is defined by

$$\theta_c = \frac{m_2}{m_2 + m_3} \tag{E.2}$$

All the researchers (like Aydın and Baki [16], Saidi and Yazdi [157], Singh *et al.* [167]) have found, both experimentally and theoretically, that cold mass fraction, θ_c has a significant influence on thermal separation. θ_c can be varied from 0.0 to 1.0. Now at lower values of θ_c , gas velocity at cold orifice is low and the frictional loss at the orifice plate is minimum. Hence with increase of pressure downstream of the orifice plate, gas temperature decreases. As θ_c increases beyond certain value gas velocity at the cold orifice starts increasing which leads to higher friction and eddy formation. Both of these phenomenon cause increase in cold outlet gas temperature. On the other hand temperature of the gas from hot exit increases as we decrease the value of θ_c gradually from 1.0 and reaches a maximum at a θ_c value at around 0.85. As θ_c is further decreased from 0.85 to 0.0, gas temperature from hot exit keeps decreasing from the highest value to inlet gas temperature. At higher value of θ_c, hot mass flow rate is small and hence the acceleration in the inner pipe is not large enough to overcome the viscous resistance. In this condition higher friction among the gas molecules and tube inner wall leads to increase in gas temperature. As θ_c decreases the hot gas flow rate increases and able to achieve acceleration high enough to overcome viscous force. As viscous force decreases friction among the molecules and tube wall decreases. This leads to decrease in hot end gas temperature (Shannak [164]).

The effect of cold mass fraction on the gas separation had been investigated by Mohammadi and Farhadi [126] both experimentally and computationally for a mixture of gases and it had been reported that the molar recovery percent of the heavier species at hot end increased slightly with increase in cold mass fraction. In this experiment, geometry of the RHVT and inlet flow conditions were kept unchanged. An explanation of this phenomenon can be found from the expression of elementary separation factor for an aerodynamic process of species separation like RHVT that Becker [21] had provided. For a multicomponent mixture the expression was

$$\epsilon_A = \frac{\theta_l - \theta_h}{\theta_h(1-\theta_l)} \tag{E.3}$$

where θ_l is the partial cut of the lighter component and θ_h is the partial cut of the heavier component in a multi component isotopic mixture. Now it is evident from the above equation (7.6), that with increasing cold mass fraction θ_l had been continuously increased while

θ_h had been continuously decreased. This had increased the numerator and decreased the denominator of equation (7.6) and hence the value of elementary separation factor was increased. Physically this can be explained by the fact that the value of cold mass fraction is increased by closing the hot end control valve which activates momentum transfer that result into improved species separation (Im and Yu, [89]). But, the gradient of molar concentration of heavier species near the wall of RHVT initially increases along with the increasing value of cold mass fraction. As more and more mass transfer occurs this gradient gradually flattens due to reduction in driving force for mass transfer at higher values of cold mass fraction. At the limiting values of cold mass fraction separation factor starts reducing.

E.4 Effect of other operating parameters

Temperature of the inlet gas does not affect significantly the thermal separation performance of RHVT. Gulayev [76] found that for a given inlet pressure and cold mass fraction the cold outlet gas temperature is approximately proportional to the inlet temperature. Further, gas properties have some effect on thermal separation. Maximum temperature drop at the cold outlet is proportional to Prandtl number. Specific heat ratio (γ) is the inlet gas characteristic that affects the amount of energy separation in the RHVT. Saidi and Valipour [158] have observed that cold outlet gas temperature drop increases with increasing thermal conductivity. Martynovskii and Alekseev [123] have reported cold outlet gas temperature drop and thermal efficiency are minimized while increasing the moisture content of gas. Many studies have found that using the RHVT with insulation to reduce energy loss to surroundings shows higher thermal separation in the tube than that having no insulation. Aydın and Baki [16] have reported that gas with lesser molecular weight attain higher thermal separation. Experimental studies by Balmer [19] showed the temperature separation existed when high pressure water was used as working media in the tube.

Appendix F

The concept of value function

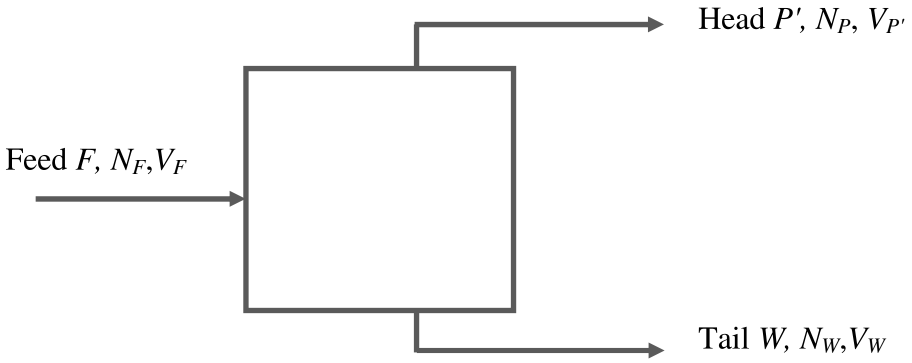

Fig F.1 Value function of a binary mixture in a three-stream separating element

For a three-stream species separating element, like the RHVT unit, we have the feed, product and waste flows. The magnitudes of these flows (in moles per unit time) are designated by F, P', and W respectively; the mole fraction of the desired isotope in any stream is designated as N with the appropriate subscript. In figure 1.4 F, P' and W are flow rate of feed, head fraction (product) and tail fraction (waste) respectively while N_F, N_P and N_W are the fraction of one of the isotopes in the mixture. Further a function $V(N)$ called value function has been associated with each stream of the separating element which is defined as [Benedict et. al. (1981)]

$$V(N) = (2N - 1)ln\frac{N}{1-N} \tag{F.1}$$

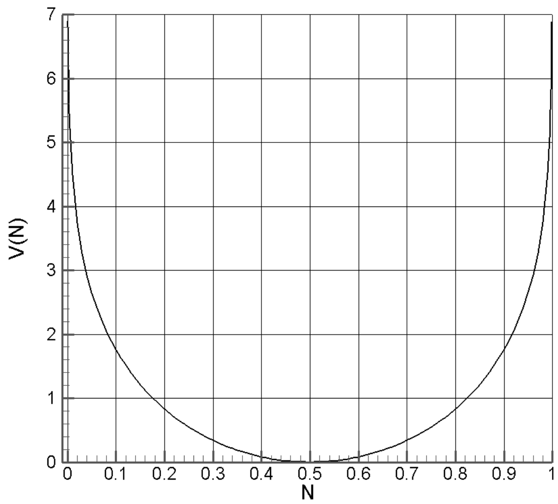

Fig F.1 Value function vs. species concentration

It is a function only of composition and is dimensionless. It is plotted in Fig F.2. It is symmetrical about ***N = 0.5.*** At this value of N, V(N) vanishes. It is positive for all other *N* and increases without limit as *N* approaches zero or unity. This expresses the fact that a plant of infinite size is required to produce a pure isotope.

References

1. "Visualization of inner flow in a counter-flow type vortex tube", Abe, J., Nakano, F. Journal of the flow visualization society of Japan, (1987).Volume 7 Issue 26, pp.227-230.
2. "Flow visualization in a vortex tube by using a tuft method", Abe, J., Yoshinaga , A. & Nishio T. Journal of the flow visualization society of Japan, (1989).Volume 9 Issue Supplement, pp.103-106.
3. "Experimental investigation of vortex tube using natural substances", Agarwal, N., Naik, S. S. & Gawale, Y. P. International communication in heat and mass transfer, (2014).Volume 52, pp. 51-55.
4. "The vortex tube as a classic thermodynamic refrigeration cycle", Ahlborn, B. K., Gordon, J. M. J Appl Phys, (2000). Volume 88(6): pp. 3645–3653. https://doi.org/10.1063/1.1289524.
5. "Secondary flow in a vortex tube". Ahlborn, B. K., Groves, S. Fluid Dynamics Research (1997). Volume 21: pp.73–86. https://doi.org/10.1016/S0169-5983(97)00003-8.
6. "The heat pump in a vortex tube", Ahlborn, B., Keller, J.U. & Rebhan, E. J. Non-Equilib. Thermodyn, (1998), Volume 23 (2): pp. 159–165.
7. "Low-pressure vortex tubes". Ahlborn, B., Camire, J., Keller, J. U.. J Phys D: Appl Phys; (1996).Volume 29: pp. 1469–1472.
8. "Limits of temperature separation in a vortex tube". Ahlborn, B., Keller, J. U., Staudt, R., Treitz, G., Rebhan, EJ Phys D: Appl Phys ; (1994). Volume 27: pp.480–488.
9. "Some interesting developments relating to gas dynamics in the application of UCOR process for isotope separation". Alant, T. G., Schumann, W. A. Twelfth International symposium on rarefied gas dynamics, (1980). University of Virginia, July 7-11.
10. "Flow friction and heat and mass transfer in a swirled flow". Alimov, R. Z. Journal of Engineering Physics and thermo physics, (1966). Volume 10(4): pp.251–257. https://doi.org/10.1007/BF00837815.
11. "Parametric and internal study of the vortex tube using a CFD model". Aljuwayhel, N. F, Nellis, G. F. & Klein, S. A. International Journal of Refrigeration, (2005). Volume 28:442-450. https://doi.org/ 10.1016/j.ijrefrig. 2004.04.004.
12. "A study on temperature separation in a large vortex tube". Amitani, T., Adachi, T. & Kato, T. Japan Soc Mech Eng (1983).Volume 49: pp.877–884.

13. "Vortex tube applications", Applegate, M. Proceedings of the conference on cooling of airborne electronic equipment, Ohio State University Engineering Series, (1952). vol. XXI, No. 2, pp. 207-209.
14. "Observation of large-scale hydrodynamic structures in a vortex tube and the Ranque effect", Arbuzov, V.A., Dubnishchev, Y.N., Lebedev, A.V., Pravdina, M.Kh., Yavorskii, N.I. Tech. Phys. Lett. (1997). Volume 23 (12); pp. 938–940.
15. "Vortex Tube Applications in Micro-Power Generation", Arslan, S., Mitrovic, B. & Muller, M. R. International Joint Power Generation Conference Scottsdale, (2002). Arizona, USA.
16. "An experimental study on the design parameters of a counter flow vortex tube", Aydın, O. & Baki, M. Energy J; (2006). Volume 31(14): pp.2763–2772.
17. "Investigations on the Ranque Hilsch (Vortex) Tube", Baker, P. S. & Rathkamp, W. R. ORNL-1659, ORNL, (1954). Tennesse.
18. "Progress in air separation with the vortex tube", Balepin, V. & Rosholt, D. In Proceedings of the 34th Joint Propulsion Conference and Exhibit, (1998). Volume AIAA-98-3776, Cleveland, Ohio, USA. https://doi.org/10.2514/6.1998-3776.
19. "Pressure -driven Ranque -Hilsch temperature separation in liquids", Balmer, R.T. Trans. ASME, J. Fluids Engineering , (1988). 110: pp 161 – 164.
20. "Energy transfer in a vortex". Barnes, W. P. Jr., Master of Science thesis, (1948). Dept. of Mechanical Engg. Massachusetts Institute of Technology.
21. "Separation Nozzle", Becker, E. W. Book chapter 5, Uranium Enrichment, (1979). Ed. Villani, S., Springer-Verlag, New York.
22. "Numerical investigations on flow behaviour and energy separation in Ranque–Hilsch vortex tube", Behera, U., Paul, P.J., Dinesh, K. & Jacob, S. Int. J. Heat Mass Transfer, (2008). Volume 51: pp. 6077–6089.
23. "CFD analysis and experimental investigations towards optimizing the parameters of Ranque–Hilsch vortex tube", Behera, U., Paul, P.J., Kasthurirengan, S., Karunanithi, R., Ram, S.N., Dinesh, K., Jacob, S. Int. J. Heat Mass Transfer, (2005). Volume 48: pp.1961–1973.
24. "Numerical analysis on the heat and work transfer due to shear in a hot cascade Ranque–Hilsch vortex tube", Bej, N., Sinhamahapatra, K. P. Int. J of Refrigeration, (2016). Volume 68: pp. 161-176.
25. "Heat transfer handbook", Bejan, A. & Krauss, A. D. (2003). Published by John Wiley & Sons, Inc., Hoboken, New Jersey.

26. "Temperature separation and friction losses in vortex tube", Benbella, A.S. Heat Mass Transfer. (2004). Volume 40; pp. 779–785.
27. "Nuclear chemical engineering", Benedict, M., Pigford, T. H., & Levi, H. W. Second Edition, (1981). McGraw-Hill Book Company, New York.
28. "Study of the effects of stationary member in the rotating flow field of High Speed Rotor Unit", Bera, T. K. (2013). PhD Thesis, HBNI.
29. "Convective heat transfer and its action on the Ranque effect in the vortex tube", Borissov, A. A., Kuibin, P. A., Okulov. V. L. ASME Fluids Eng Div: Exp Numer Flow Visualiz; (1993). Volume 172: pp.195–200.
30. "Computational fluid dynamics simulation of length to diameter ratio effects on the energy separation in a vortex tube", Bramo, A. R. & Pourmahmoud, N. Thermal Science, (2011). Volume 15, No. 3, pp. 833-848. https://doi.org/10.2298/TSCI10100 4008B.
31. "Experimental investigation of the energy separation in vortex tubes", Bruun, H. H. J Mech Eng Sci; (1969).Volume 11(6): pp. 567–582.
32. "Theoretischer Beitrag Zur Arbeit Von R. Hilsch Uber das Wirebelrohr", Burkhadt, G. Zeitschrift Fur Naturforschung, (1948).Vol. 3a, No. 1, pp. 46-51.
33. "Experimental investigation of vortex tube concept", Camiré, J. Master Thesis, (1995). University of British Columbia, Canada.
34. "Experimental study of heat and mass transfer in Ranque Hilsch Vortex tube", Chatterjee, M., Mukhopadhyay, S. & Vijayan,P. K. International Journal of Advance Research, (2016). Volume 4 (7), pp 666-674.(ISSN 2320-5407).
35. "1-D Model for Mass Transfer Calculation in Vortex Tube using Heat and Mass Transfer Analogy", Chatterjee, M., Mukhopadhyay, S. & Vijayan, P. K. American Journal of Heat and Mass Transfer, (2017). Volume 4 No. 1 pp. 1-24. https://doi.org/10.7726/ajhmt.2017.1001.
36. "Species separation in Ranque-Hilsch vortex tube using air as working fluid", Chatterjee, M., Mukhopadhyay S & Vijayan, P. K. (2018). Heat and Mass Transfer, Volume May 2018, No. 1: pp. 1-14. https://doi.org/10.1007/s00231-018-2386-3.
37. "Laser cutting of GFRM using assisted cooling-air generated by vortex tube", Chen, M.F., Hsiao, W.T., Ho, Y.S., Huang, W.L., Chen, Y.P. Proceedings of the 8th Asia-Pacific Conference on Materials Processing, (2008). Guilin-Guangzhou.
38. "Heat (mass) transfer between an impinging jet and a rotating disk", Chen, Y.M., Lee, W.T. & Wu, S.J. Heat Mass Transfer, (1998). Volume 34 (2-3), pp 195-201.

39. "Mass transfer (absorption) coefficients prediction from data on heat transfer and fluid friction", Chilton, T.H. & Colburn, A.P. Industrial and Engineering Chemistry (1934). Volume 26, 11, pp 1183-1187, ISSN: 0888-5885.
40. "Local Heat/Mass Transfer Measurement on the effusion plate in impingement/effusion cooling systems", Cho, H.H. & Rhee, D.H. Journal of Turbo machinery (2001). Volume 123, pp. 601-608.
41. "Local heat transfer characteristics in a single rotating disk and co-rotating disks", Cho, H.H., Won, C.H., Ryu, G.Y. & Rhee, D.H. (2003). Micro system Technologies, 9, (6-7), pp. 399-408.
42. "Acoustic streaming as a mechanism of the Ranque-Hilsch effect", Chu, J. G. (1982). PhD dissertation, University of Tennessee, Knoxville.
43. Cobb, E. C. & Saunders, A., (1956). "Heat Transfer from a Rotating Disk", Proceeding of the Royal Society A., 236, pp 343.
44. "Thermodynamics and Fluid Mechanics of a Ranque–Hilsch Vortex tube", Cockerill, T. Masters thesis, (1998). University of Cambridge, England.
45. "A method of correlating forced convection heat transfer data and a comparison of fluid friction", Colburn, A. P., Trans. Am. Inst. Chem Eng., (1933). Volume 29, pp.174.
46. "Coherent transport of angular momentum – the Ranque–Hilsch tube a paradigm", Colgate, S.A., Buchler, J.R. Ann. New York Acad. Sci. (2000). Volume 898; pp. 105.
47. "Experimental study of two-phase propane expanded through the Ranque–Hilsch tube". Collins, R. L., Lovelace, R. B. Trans ASME J Heat Transfer; (1979). Volume 101: pp.300–305.
48. "The vortex tube", Corr, J.E. Data Folder No. 45289, (1948). General Electric Co., Research Division, Schenectady, New York.
49. "Experimental results of a vortex tube air separator for advanced space transportation", Crocker, A. M., White, S. M. & Bremer, F. Jr. In Proceedings of the 39th Joint Propulsion Conference and Exhibit, (2003). AIAA-2003-4451, Huntsville, Ala, USA. https://doi.org/10.2514/6.2003-4451.
50. "Diffusion: Mass Transfer in Fluid Systems (2nd ed.)". Cussler, E. L. (1997). New York: Cambridge University Press.
51. "An Analysis of the Energy Separation in Laminar and Turbulent Compressible Vortex Flows", Deissler, R. G., Perlmutter, M. Heat Transfer and Fluid Mechanics Institute, (1958). Stanford University Press.

52. "Analysis of the flow and energy separation in a turbulent vortex", Deissler, R.G. & Perlmutter, M. International Journal of Heat and Mass Transfer, (1960).Volume 1, Issues 2–3, pp. 173-191.
53. "Theoretical and experiment study of vortex tubes", Dornbrand, H. A. F. Tech. Report 6123, Republic Aviation Corporation, Contract No. AF 33(038) 5770, E.O. (1950). No. 664-776.
54. "Mass spectrometry; A preparative course", Downard, K. , (2004). The Royal Society of Chemistry.
55. "Design of batch desublimer", Dunthorn, D. I. No. KL-6220. (1968). Oak Ridge Gaseous Diffusion Plant, Tennese.
56. "Comparison of different turbulence models in predicting the temperature separation in a Ranque–Hilsch vortex tube", Dutta, T., Sinhamahapatra, K.P., Bandyopdhyay, S. S. International journal of refrigeration (2010). Volume 33; pp. 783 – 792.
57. "Numerical investigation of gas species and energy separation in the Ranque-Hilsch vortex tube using real gas model", Dutta, T., Sinhamahapatra, K. P. & Bandyopadhyay, S. S. International Journal of Refrigeration, (2011). Volume 34, no. 8, pp. 2118–2128. https://doi.org/10.1016/j.ijrefrig.2011.06.004.
58. "CFD Analysis of Energy Separation in Ranque-Hilsch Vortex Tube at Cryogenic Temperature", Dutta, T., Sinhamahapatra, K. P. & Bandyopadhyay, S. S. Journal of Fluids, (2013).vol. 2013, Article ID 562027, pp. 1–14.
59. Eiamsa-ard, S., Promvonge, P. (2006). "Numerical prediction of vortex flow and thermal separation in a subsonic vortex tube", J Zhejiang Univ SCI Int Appl Phys Eng J ;7(8):1406–1415.
60. "Numerical investigation of the thermal separation in a Ranque–Hilsch vortex tube". Eiamsa-ard, S., Promvonge, P. Int J Heat Mass Transfer; (2007). 50(5–6): pp. 821–832.
61. "Experimental investigation on energy separation in a counter-flow Ranque–Hilsch vortex tube: effect of cooling a hot tube", Eiamsa-ard, S., & Promvonge, P. Renewable and Sustainable Energy Reviews (2008). Volume 12: pp. 1822–1842.
62. "Experimental investigation on energy separation in a counter-flow Ranque–Hilsch vortex tube: effect of cooling a hot tube", Eiamsa-ard, S., Wongcharee, K., Promvonge, P. Int. Commun. Heat Mass Transf.; (2010). Volume 37:156–162. https://doi.org/10.1016/j.icheatmasstransfer.2010.02.007.

63. "Parameters which determine the vortex effect", V. M., Kalashnikov, V. N. & Raiskii, Yu. D. Izv. AN SSSR, Mekhanika Zhidkosti i Gaza, Entov, (1966).Vol. 2, No. 3, pp. 32-38.
64. "Large eddy simulations of the flow field and temperature separation in the Ranque–Hilsch vortex tube", Farouk, T. & Farouk, B. International Journal of Heat and Mass Transfer, (2007). Volume 50 : pp. 4724–4735.
65. "Simulation of gas species and temperature separation in the counter-flow Ranque-Hilsch vortex tube using the large eddy simulation technique", Farouk, T., Farouk, B. & Gutsol, A. International Journal Heat Mass Transfer (2009). Volume 52, pp. 3320-3333. https://doi.org/10.1016/j.ijheatmasstransfer.2009.01.016.
66. "Vortex tube separator may solve weight/space limitations", Fekete, L. A. World Oil, (1986). July, pp. 40-44.
67. "Numerical investigations of the compressible flow and the energy separation in the Ranque–Hilsch vortex tube", Frohlingsdorf, W. & Unger, H. Int. J. Heat Mass Transfer, (1999). Volume 42 : pp.415–422.
68. Frohlingsdorf, W. (1997). "Unters chungenzur kompressiblen Stro¨mung und Energietrennungim Wirbelrohrnach Ranque und Hilsch", PhD dissertation, Ruhr-Universitat-Bochum, In German.
69. "Energy migration in the vortex refrigerator", Fulton, C. D. Report on term project, No.31, (1948a). Dept. of Mechanical Engg., Massachusetts Institute of Technology.
70. "Thermodynamics of the vortex refrigerator", Fulton, C. D. Report on term project, No. 1, (1948b). Dept. of Mechanical Engg., Massachusetts Institute of Technology.
71. "Ranque's tube", Fulton, C.D. J. ASRE Refrig. Eng. (1950). Volume 58: pp. 473–479.
72. "Experimental Study on the Ranque-Hilsch Vortex Tube", Gao, C. PhD Thesis, (2005). Eindhoven University of Technology, the Netherlands.
73. "Experimental study on a simple Ranque–Hilsch vortex tube", Gao, C. M., Bosschaart, K. J., Zeegers, J. C. H., Waele, A.T. A. M. Cryogenics; (2005). Volume 45(3): pp.173–183.
74. "Performance assessment of vortex tube and vertical ground heat exchanger in reducing fuel consumption of conventional pressure drop stations", Ghezelbash, R., Farzaneh-Gord, M., Sadi, M. Applied Thermal Engineering (2016). Volume 102: pp. 213–226.

75. "Demonstrating the achievement of the lower temperatures with two-stage vortex tubes", Guillaume, D. W., Jolly, J. L. Rev Sci Instrum ; (2001). Volume 72(8): pp. 3446–3448.
76. "Ranque effect at low temperatures", Gulyaev, A. I. J Eng Phys (1965). Volume 9(3): pp. 242–244.
77. "A New Approach to Waste Heat and Pressure Energy Systems", Gupta, U. S., Mishra, S. K., Bohra, M. IJRMET (2013). Volume 4, Issue 1.
78. "The Ranque effect", Gutsol, A. Physics-Uspekhi (1997). Volume 40(6): pp.639–658. https://doi.org/10.1070/PU1997v040n06ABEH000248.
79. "On the working principle of the Hilsch Gadget", Haar, D. T., & Wergeland, H, Det Kongelige Norske Videnskabers Selskab, Forhandlinger, B. D. (1948). Volume XX, NR. 15, pp. 55-58.
80. "Experimental investigation of centrifugal refrigeration", Haddox, R. Jr., Hunter, J. W. & Plunkett, W. H. Bachelor of Science thesis, (1947). Dept. of Mechanical Engg. Massachusetts Institute of Technology.
81. "A investigation of micro-scale Ranque-Hilsch vortex tube", Hamoudi, A. F., Master's thesis, (2006). University of Windsor.
82. "Performance characteristics of a microscale Ranque–Hilsch vortex", Hamoudi, A. F., Fartaj, A., Rankin, G.W. J. Fluids Eng. (2008). Volume 130 (10); pp. 1012061–1012068.
83. "Review of fluid flow and convective heat transfer within rotating disk cavities with impinging jet", Harmand, S., Pelle, J., Poncet, S. & Shevchuk I.V. International Journal of Thermal Science, (2013). Volume 67: pp. 1-30.
84. "Experimental Study of the Velocity and Temperature Distribution in a High-velocity Vortex-type Flow", Hartnett, J. P., Eckert, E.R.G. Heat Transfer and Fluid Mechanics Institute, (1956).Stanford University Press. pp. 135–150.
85. "Experimental study of the velocity and temperature distribution in a high velocity vortex-type flows", Harnett, J. & Eckert, E. Trans. ASME, (1957). Volume 79: pp.751-758.
86. "Convection heat and mass transfer from a disk", He, Y., Ma, L. & Huang, S. Heat Mass Transfer (2005). Volume 41 (8), pp. 766-772.
87. "Gas liquefaction using a Ranque-Hilsch Vortex Tube: Design criteria and bibliography", Hellyar, K. G. PhD Thesis, (1979). MIT.

88. "The use of the expansion of gases in a centrifugal field as cooling process", Hilsch, R. Review of Scientific Instruments. (1947). Volume 18 (2): pp. 108–113. doi:10.1063/1.1740893. Translated from the original German article: Rudolf Hilsch (1946) "Die Expansion von Gasen im Zentrifugalfeld als Kälteprozeß" (The expansion of gases in a centrifugal field as a cooling process), Zeitschrift für Naturforschung, 1 : 208–214. Available on-line at: Zeitschrift für Naturforschung.
89. "Effects of geometric parameters on the separated air flow temperature of a vortex tube for design optimization", Im, S. Y. & Yu, S. S. Energy (2012). Volume 37 pp. 154-160. https://doi.org/10.1016/j.energy.2011.09.008.
90. "Effects of geometric parameters on the separated air flow temperature of a vortex tube for design optimization", Im, S. Y. & Yu, S. S. Energy (2012). Volume 37 pp. 154-160. https://doi.org/10.1016/j.energy.2011.09.008.
91. "Principles of Heat and mass transfer", Incropera, F. P., Dewitt, D. P., Bergman, T. L. & Lavine A. S. Seventh edition, (2017). John Willey and Sons, Singapore.
92. "Quantitative study of the Hilsch heat separator", Johnson, A. F. Canadian Journal of Research, (1947). Volume 25, Section F, No. 5, pp. 299-302.
93. "Friction Laws and energy transfer in circular flow", Kassner, R. & Knoernschild, E. Technical report No.F-TR-2198-ND, (1947). GS-USAF Wright Patterson Air Force Base No. 78.
94. "Numerical simulation of swirling flows in vortex tubes", Kazantseva, O.V. Piralishvili, Sh. A., Fuzeeva, A. A. High Temp. (2005). 43 (4): pp. 608–613.
95. "A Vortex Contactor for Carbon Dioxide Separations", Kevin, T. R., Michael, M., Anna, P., Douglas, S. & Terry, T. (2001). Idaho National Engineering and Environmental Laboratory.
96. "The vortex tube—a universal device for heating, cooling, cleaning, and drying gases and separating gas mixtures", Khodorkov, L., Poshernev, N.V., Zhidkov, N.V. Chemical and Petroleum Engineering (2003). Volume 39, 7-8, pp. 409–415.
97. "Application of Hilsch tube to aircraft and missiles", Knoernschild, E. M. & Morgenson, O. Jr. Army Air Forces, Air Material Command, Engineering Division, Equipment Laboratory, (1948). No.-MCREXE-664-510A, GS-USAF Wright Patterson Air Force Base No. 128.
98. "Uranium Enrichment and Nuclear Weapon proliferation", Krass, A. S., Boskma, P., Elzen, B. & Smit, W. A. (1983).Sipri, London and New York; Taylor and Francis Ltd.

99. "Heat transfer and friction in turbulent vortex flow", Kreith, F. & Margolis, D. Applied Science Research, Sec A, (1959). Volume 8.
100. "Local heat-transfer coefficients on the rotating disk in still air", Kreith, F., Taylor, H. & Chong, J. P. International Journal of Heat and mass Transfer, (1959). Volume 81, pp 95.
101. "Results of vortex tube usage in diesel exhaust gas recirculation system", Kukis, V.S., Omelchenko E.A. & Raznoshinskaia A.V. Procedia Engineering (2015). Volume 129, pp. 151 – 155. https://doi.org/10.1016/j.proeng.2015.12.024.
102. "Enrichment of methane concentration via separation of gases using vortex tubes" Kulkarni, M., Sardesai, C. J Energy Eng; (2002). Volume 128(1): pp. 1–12.
103. "An experimental study of temperature separation in swirling flow". Kuroda, H. PhD dissertation, (1983). University of Tennessee, Knoxville.
104. "Acoustic streaming in swirl flow and the Ranque–Hlisch (vortex tube) effect", Kurosaka, M. J Fluid Mech (1982). Volume 124: pp.139–172. https:// doi.org/ 10.1017/S0022112082002444.
105. "Ranque Hilsch effect revisited: temperature separation effect traced to orderly spinning waves or vortex whistle". Kurosaka, M., Chu, J. Q., Goodmann, J. R., In: AIAA 82-0952, (1982). AIAA/ASME third joint thermo-physics of fluids plasma and heat transfer conference, USA.
106. "Detailed heat/mass transfer distributions in a rotating smooth channel with bleed flow", Kyung, M. K., Sang, I. K., Yun, H. J., Dong, H. L. & Hyung, H. C. Transactions of the ASME, (2007). Volume 129, pp. 1538.
107. "An experimental and analytical study of vortex flow temperature separation by superposition of spiral and axial flows: Part I", Lay, J. E Trans ASME J Heat Transfer ; (1959a). Volume 81(4): pp. 202–212.
108. "An experimental and analytical study of vortex flow temperature separation by superposition of spiral and axial flows: Part II." Lay, J. E Trans ASME J Heat Transfer ; (1959b). Volume 81(4): pp. 213–222.
109. "Gas-Dynamic Methods of Temperature Stratification", Leont'ev, A. I. (2002). Fluid Dynamics, Volume 37(4).: pp.512–529 Translated from Izvestiya Rossiiskoi Academii Nauk, Mekhanika Zhidkosti i Gaza 6–26.
110. "Vortex tube optimization theory", Lewins, J., Bejan, A. Energy J; (1999). Volume 24: pp.931–943.

111. "Droplet behaviour in a Ranque-Hilsch vortex tube", Liew, R., Michalek, W. R., Zeegers, J. C. H., Kuerten., J. G. M. Journal of Physics: Conference Series 318, (2011). 13th European Turbulence Conference (ETC13). https:// doi.org/10.1088/1742-6596/318/5/052013.
112. "A heat transfer relation for swirl flow in a vortex tube", Lin, S., Chen, J. R., Vatistas, G. H. Can J Chem Eng J ; (1990). Volume 68(6): pp. 944–947.
113. "Gas separation in the Ranque-Hilsch vortex tube", Linderstrom-Lang, C.U. Journal Heat Mass Transfer (1964). Volume 7, pp. 1195-1206.
114. "A model of the gas separation in a Ranque-Hilsch vortex tube", Linderstrom-Lang, C.U. Acta Polytechnica Scandnavica Physics including nucleonics series(1967a). no. 45.
115. "On gas separation in a Ranque Hilsch Vortex Tube", Linderstrom-Lang, C.U. Z. Naturforschg, (1967b). Volume 22(a); pp. 835-837.
116. "Gas separation in the Ranque-Hilsch vortex tube model calculations based on flow data", Linderstrom-Lang, C.U. (1971). Riso report, Denmark.
117. "A theoretical investigation of the Hilsch tube", Lustick, L. Master of Science thesis, (1950).Dept. of Mechanical Engg. Syracuse University, USA.
118. "The vortex tube", MacGee, R. Jr. Master of Arts thesis, (1950). Boston University Graduate School, USA.
119. "Unit Operations of Chemical Engineering (5th Edition)", McCabe, W.L., J.C. Smith, and P. Harriott, (1993). McGraw-Hill, pp. 348-52.
120. "Computational analysis of energy separation in a counter-flow vortex tube based on inlet shape and aspect ratio", Manimaran, R. Energy, (2016). Volume 107: pp. 17-28.
121. "Effect of Operating Conditions, Physical Size, and Fluid Characteristics on the Gas Separation Performance of a Linderstrom-Lang Vortex Tube", Marshall, J. International Journal Heat Mass Transfer, (1977). Volume 20, pp. 227-231. https://doi.org/10.1016/0017-9310 (77); pp. 90209-15.
122. "Investigation of the parameters of a vortex flow inside a Ranque_Hilsch tube", Martynov, A. V. & Brodyanski, V. M. Journal of Engineering Physics, (1967). Volume 12, No. 5, pp. 639-644.
123. "Investigation of the vortex thermal separation effect for gases and vapors", Martynovskii, V. S., Alekseev, V. P. Sov Phys-Tech Phys (1957). Volume 26(2): pp. 2233–2243.

124. Flow Visualization. Merzkirch, W. Author, Edition, revised. (1987). Publisher, Academic Press,. ISBN, 0124913512, 9780124913516.
125. "Maxwellian demon at work", Milton, R. M. Industrial and engineering chemistry, (1946). Volume 38(5), pp 5.
126. "Experimental and numerical study of the gas–gas separation efficiency in a Ranque–Hilsch vortex tube", Mohammadi, S. & Farhadi, F. Separation and Purification Technology, (2014). Volume 138, pp. 177-185. https:// doi.org/ 10.1016/ j.seppur.2014.10.022.
127. "Vortex heat exchanger cooling for infrared detectors", Nash, J. M. USA: Annual Meeting of the Optical Society of America; (1974).
128. "Design of the vortex cooler", Nash, J. M. American Society of Mechanical Engineers, Annual design engineering conference, New York, USA. (1975).
129. "Vortex expansion devices for high temperature cryogenics. In: Proceedings of the intersociety energy conversion engineering conference", Nash, J. M. (1991). IECEC'91, USA,. p. 521–525.
130. "Generalized correlations for the process of energy separation in vortex tubes", Negm, M. I. M, Serag, S. Z. & Abdel S. M. Modelling, Simulation and control, B, ASME Press, (1988). Volume 14, 4, pp. 47-64.
131. "Performance characteristics of energy separation in double stage vortex tubes", Negm, M. I. M., Serag, A. Z., Abdel Ghany, S. M. Model Simulate Control B: Mech. Therm. Eng. Mater. Resour. Chem ;14: (1988a). pp.21–32.
132. Nexflow product catalogue, (2013). http://www.nex-flow.com/vortex_tube.htm.
133. Nexflow™ Air product Corp. (2009). FRIGID-X Vortex tubes, Nexflow™ product brochure, Richmond Hill, ON, Canada.
134. "Vortex flow of compressible fluid", Nickerson, J. R. Master of Science thesis, (1949). Dept. of Aeronautical Engg. Massachusetts Institute of Technology.
135. "An experimental investigation of the optimum geometry for the cold end orifice of a vortex tube", Nimbalkar, S. U. & Muller, M.R. Applied Thermal Engineering, (2009). Volume 29; pp. 509–514. https://doi.org/10.1016/j.applthermaleng.2008.03.032
136. "Practical Introduction to GC-MS Analysis with Quadrupoles", Oehme, M. John Wiley & Sons. (1999).
137. "Vortex flow". CRC Press. Ogawa, A. (1992).
138. "Production of cold air", Otten, E. H. London: Engineering. . (1958). pp. 154.

139. "The short vortex tube". Parulekar, B. B. The Journal of Refrigeration (1961). Volume 4: pp.74–80.

140. "Flow in viscous vortex", Pengelly, C. D. J Appl Phys (1957). 28: pp.86–92.https://doi.org/10.1063/1.1722578.

141. Piralishvili, S. A., Polyaev, V. M. (1996). "Flow and thermodynamic characteristics of energy separation in a double circuit vortex tube—an experimental investigation". Int J Exp Therm Fluid Sci ;12(4): pp. 399–410.

142. Poshernev, N.V. & Khodorkov, I.L. (2004). "Natural-gas tests on a conical vortex tube (CVT) with external cooling", Chemical and Petroleum Engineering 40, 3-4, pp. 212–217.

143. Promvonge, P. & Eiamsa-ard, S. (2005). "Investigation on the Vortex Thermal Separation in a Vortex Tube Refrigerator", ScienceAsia31 pp. 215-223.

144. Promvonge, P. (1997). "A numerical study of vortex tubes with an algebraic Reynolds stress model", PhD thesis. University of London.

145. Promvonge, P. (1999). "Numerical simulation of turbulent compressible vortex-tubes flow", the third ASME/JSME Joint Fluid Engineering, Sanfrancisco, USA.

146. Promvonge, P., Eiamsa-ard, S. (2004). "Experimental investigation of temperature separation in a vortex tube refrigerator with snail entrance". ASEAN J Sci Technol Dev; 21(4): pp. 297–308.

147. Promvonge, P., Eiamsa-ard, S. (2005). "Investigation on the vortex thermal separation in a vortex tube refrigerator", ScienceAsia J; 31(3): pp. 215–223.

148. Rafiee, S. E. & Sadeghiazad, M. M. (2014). "Three-dimensional and experimental investigation on the effect of cone length of throttle valve on thermal performance of a vortex tube using k-ε turbulence model", Applied Thermal Engineering 66, pp. 65-74. https://doi.org/10.1016/j.applthermaleng.2014.01.073.

149. Raiskii, Yu. D. & Tunkel, L. E. (1974). "Influence of vortex tube configuration and length on the process of energetic gas separation", Journal of Engineering Physics 27: 1578. https://doi.org/10.1007/BF00863014.

150. Ranque, G. J., (1933). "Experiences sur la détente giratoire avec production simultanes d'un echappement d'air chaud et d'un echappement d'air froid (Experiments on vorticial expansion with the simultaneous production of an outflow of hot air and an outflow of cold air)", Journal de Physique et le Radium, Supplement, 7th series, 4 : 112S-114S.

151. Ranque, G. J., (1934). "Method and apparatus for obtaining from a fluid under pressure two currents of fluids at different temperatures", U.S. Patent no. 1,952,281 (filed: December 6, 1932; issued: March 27, 1934).
152. Reed, G. A. (1947). "Vortex tube refrigeration", Master of Science thesis, Dept. of Aeronautical Engg. Massachusetts Institute of Technology.
153. Reynolds, A.J. (1961). "Studies of Rotating Fluids: I. Plane Axisymmetric Flow. II. The Ranque–Hilsch Vortex Tube", PhD Thesis, University of London.
154. Reynolds, A. J. (1961a). "On the dynamics of turbulent vortical flow", Z Angew Math Phys 12: pp.149–158. https://doi.org/10.1007/BF01601014.
155. Reynolds, A. J. (1961b). "Energy flow in a vortex tube", Z Angew Math Phys 12: pp:343–356. https://doi.org/10.1007/BF01591284.
156. Riu, K., Kim, J. & Choi, I. (2004). "Experimental Investigation on Dust Separation Characteristics of a Vortex Tube", JSME International Journal, B, Vol. 47, No. I, pp. 29-36.
157. Saidi, M. H, Yazdi, M. R. (1999). "Exergy model of a vortex tube system with experimental results", Energy 24: pp. 625–632.
158. Saidi, M. H. & Valipour, M. S. (2003). "Experimental modelling of vortex tube refrigerator", Appl Therm Eng; 23: pp.1971–1980.
159. Scheller, W. A. & Brown, G. M. (1957). "The Ranque-Hilsch vortex tube", Ind. Eng Chem. 49(6): pp. 1013-1016. https://doi.org/10.1021/ie50570a035.
160. Scheper, G. W. Jr. (1949). "Flow patterns and a heat transfer theory for the vortex heating and refrigerating tube", Master's Thesis, Union College, Schenectody, NewYork.
161. Scheper, G.W. (1951). "The vortex tube–internal flow data and a heat transfer theory". J. ASRE Refrigerating Eng, 59: pp. 985–989.
162. Schlenz, D. (1982). "Kompressible strahlgetriebene drallstromung in rotationssymmetrischen Kanalen", PhD thesis. Technische Fakultat Universitat, Erlangen-Nurnberg.
163. Shamsoddini, R., Nezhad, A. H. (2010). "Numerical analysis of the effects of nozzles number on the flow and power of cooling of a vortex tube", International journal of refrigeration 33: pp. 774 – 782. https://doi.org/10.1016/j.ijrefrig.2009.12.0 29.
164. Shannak, B. A. (2004). "Temperature separation and friction losses in vortex tube", Heat and Mass Transfer, 40, pp.779–785. https://doi.org/10.1007/s00231-003-0485-1.

165. Sibulkin, M. (1962). "Unsteady, viscous, circular flow Part 3. Application to the Ranque-Hilsch vortex tube", Journal of Fluid Mechanics, Volume 12, Issue 2,pp. 269-293.

166. Simo˜es-Moreira, J. R. (2010). "An air-standard cycle and a thermodynamic perspective on operational limits of Ranque–Hilsh or vortex tubes", international journal of refrigeration 33; pp. 765–773.

167. Singh, P. K, Tathgir, R. G, Gangacharyulu, D, Grewal, G. S. (2004). "An experimental performance evaluation of vortex tube", IE(I) J-MC 84: pp. 149–153.

168. Skye, H. M., Nellis, G. F. & Klein, S. A.,(2006). "Comparison of CFD Analysis to Empirical Data in a Commercial Vortex Tube", Int. J. Refrig., 29, 1, pp. 71-80. https://doi.org/10.1016/j.ijrefrig.2005.05.004.

169. Smith, J.L. Jr. (1962a). "An analysis of the vortex flow in the cyclone separator", Trans. ASME, J. B. Engg 84: pp. 609‑618.

170. Smith, J.L. Jr. (1962b). "An experimental study of the vortex in the cyclone separator", Trans. ASME, J. B. Engg. 84: pp. 602‑608.

171. Soni, Y. & Thomson W.J. (1975). "Optimal design of Ranque - Hilsch tube", Transactions of ASME: Journal Of Heat Transfer, 94(2), pp. 316-317.

172. Soni, Y. (1973). "A parametric study of the Ranque-Hilsch tube", PhD dissertation, University of Idaho Graduate School, U.S.A..

173. Sprenger, H. (1952). "Uber thermische Effekte bei resonanzrohren", Reerat gehalten anlässlich der Jahresveresammlung der Schweizerishen Physikaliken Gesellschaft in Bern.

174. Stephan, K., Lin, S., Durst, M., Huang, F. & Seher, D. (1983). "An investigation of energy separation in a vortex tube", Int. J. Heat Mass Transfer., 26, pp.341–348. https://doi.org/10.1016/0017-9310 (83)90038-8.

175. Subudhi, S., Sen, M. (2015). "Review of Ranque–Hilsch vortex tube experiments using air, Renewable and Sustainable Energy Reviews", 52, pp. 172–178. https://doi.org/10.1016/j.rser.2015.07.103.

176. Takahama, H. & Yokosawa, H. (1981). "Energy separation in vortex tubes with a divergent chamber", Trans ASME Journal Heat Transfer ,103:pp196–203.

177. Takahama, H. (1965). "Studies on vortex tubes (1) Experiments on efficiency of energy separation (2) On profiles of velocity and temperature", Bulletin of JSME, 8 (1965), 31, pp. 433-440.

178. Takahama, H., Kawamura, M., Kato, B., Yokosawa, H. (1979). "Performance characteristics of energy separation in a steam operated vortex tube", Int J Eng Sci;17: pp.735–744.

179. Takahama, H., Yokosawa, H. (1981). "Energy separation in vortex tubes with a divergent chamber", Trans ASME J Heat Transfer;103: pp. 196–203.

180. Thakare, H. R. & Parekh, A. D. (2015 a). "Computational analysis of energy separation in counter - flow vortex tube", Energy 85: pp. 62-77

181. Thakare, H. R., Monde, A., Patil, B. S., Parekh, A. D. (2015 b). "Numerical Investigation of Flow Characteristics in Counter Flow Vortex Tube", Procedia Engineering 127: pp. 170 – 176.

182. Thakare, H. R., Monde, A., Parekh, A. D. (2015 c). "Experimental, computational and optimization studies of temperature separation and flow physics of vortex tube: A review", Renewable and Sustainable Energy Reviews 52: pp.1043–1071.

183. Tien, C. L., & Campbell, D. T. (1963). "Heat and mass transfer from rotating cone", Journal of Fluid Mechanics, 17(01), pp. 105-112.

184. Thomas H. Pigford, Hans Wolfgang Levi.,(1980). "Nuclear chemical engineering", Manson Benedict, - 2d ed., New York: McGraw-Hill, - McGraw-Hill series in nuclear engineering, 1008 pages.

185. Trofimov, V. M. (2000). "Physical effect in Ranque vortex tubes", JETP Lett. 72 (5): pp. 249–252.

186. Valipour, M. & Saidi, M. H. (2003). "Experimental modelling of vortex tube refrigerator", Applied Thermal Engineering, 23, pp. 1971-1980.

187. Valipour, M. S. & Niazi, N. (2011). "Experimental modelling of a curved Ranque-Hilsch vortex tube refrigerator, International Journal of Refrigeration", 34,: pp.1109-1116. https://doi.org/10.1016/j.ijrefrig.2011.02.013

188. Van Deemter, J. J. (1952). "On the theory of the Ranque Hilsch cooling effect", Appl Sci Res A :174–196. https://doi.org/10.1007/BF03184927.

189. Venkatesan, R. & Fogler, H. S. (2004). "Comments on Analogies for Correlated Heat and Mass Transfer in Turbulent Flow", AIChE Journal, Vol. 50, No. 7, pp. 1623-1626.

190. Vennos, S. L. N. (1968). "An experimental investigation of the gaseous vortex", PhD thesis. Rensselaer Polytechnic Institute.

191. Vonnegut, B. (1949). "Vortex thermometer for measuring true air temperature and true air speeds in flight", Report No. PB 99102, Project Cirrus.

192. Webster, D. S. (1950). "An analysis of the Hilsch vortex tube", Refrigeration Engineering, 58, Feb.vol 2, pp. 153-171.

193. Westley, R. (1953). "A note on the application of the vortex tube to ventilated suits", College of Aeronautics, Tech. Note Aero.

194. Westley, R. (1954a). "Optimum design of a vortex tube for achieving large temperature drop ratios", The College of Aeronautics, Cranefield, UK.

195. Westley, R. (1954b). "A bibliography and survey of the vortex tube", College of Aeronautics. Cranfield note, UK.

196. Westley, R. (1955). "Optimum design of a Vortex Tube for achieving larger temperature drop ratios", Cranfield College Note 30, College of Aeronautics.

197. Whitaker, J. M. (2005). "Uranium enrichment plant characteristics - A training Manual for the IAEA", ORNL/TM-2005/43, ISPO/310-R1.

198. Wilk, J. (2011). "Application of Mass/Heat Transfer Analogy in the Investigation of Convective Heat Transfer in Stationary and Rotating Minichannels", Book Chapter, Heat Transfer - Theoretical Analysis, Experimental Investigations and Industrial Systems, Ed. Belmiloudi, A., InTech. Chap. 14, pp. 379-396.

199. Williamson, U. A. F. & Tompkins J. A. (1951). "Practical notes on the design of a vortex tube", R.A.E. Technical note, No. Mech. Eng. 67.

200. Xue, Y., Arjomandi M. & Kelso R. (2011). "Visualization of flow structure in a vortex tube", Experimental Thermal and Fluid Science, Vol. 35(8), pp. 1514-1521. https://doi.org/10.1016/j.expthermflusci.2011.07.001.

201. Xue, Y., Arjomandi, M. & Kelso, R. (2012). "Experimental study of the flow structure in a counter flow Ranque–Hilsch vortex tube", International Journal of Heat and Mass Transfer 55: pp. 5853–5860. https://doi.org /10.1016/j.ijheatmasstransfer. 2012.05.081.

202. Yang, J.B. (1991). "Mathematical Model of Vortex Tube and Experimental Study of Optimizing Performance Parameters in Vortex Tube", Master Thesis, Xi’an Jiaotong University, Xi’an, China.

203. Yilmaz, M., Kaya, M., Karagoz, S., Erdogan, S., (2009). "A review of design criteria for vortex tubes", Heat and Mass Transfer, Vol. 45, pp. 613-632. https://doi.org/10.1007/s00231-008-0447-8.

204. Zaslavskii, B.I., Yur’ev, B.V. (1998). "Flow structure in a flat vortex chamber", J. Appl. Mech. Tech. Phys. 39 (1).

205. Zepeda, D. P., Arjonilla, C. E., Elizabeth, C., Forgach, S. and Koo, M. L. (2012). "Visualization of Flow Inside a Ranque-Hilsch Tube", J. Klapp et al. (eds.), Fluid Dynamics in Physics, Engineering and Environmental Applications, Environmental Science and Engineering.

206. Zhang, Y.B. (1993). "The Theoretical and Experimental Study on Vortex Tube", Master Thesis, Xi'an Jiaotong University, Xi'an, China.

LIST OF ABBREVIATIONS

ACES	Air Collection and Enrichment System
ASM	Algebraic Slip Model
AVLIS	Atomic Vapour Laser Isotopic Separation
CFD	Computational Fluid Dynamics
DC	Direct Current
DNS	Direct Numerical Simulation
EMIS	Electro- Magnetic Isotope Separation
EVOP	Evolutionary Operation
FPS	Frames Per Second
GFRP	Glass Fibre Reinforced Plastic
HAZ	Heat Affected Zone
KE	Kinetic Energy
LDV	Laser-Doppler Velocimetry
LES	Large Eddy Simulation
MIT	Massachusetts Institute of Technology
MLIS	Molecular Laser Isotopic Separation
ORNL	Oak Ridge National Laboratory
QMS	Quadrupole Mass Spectrometer
QUICK	Quadratic Upstream Interpolation for Convective Kinematics
RANS	Reynolds Average Navier Stokes
RF	Radio Frequency
RGA	Residual Gas Analyzer
RHVT	Ranque Hilsch Vortex Tube
RNG	Re-Normalization Group
RTD	Resistance Temperature Detectors
SOU	Second Order Upwind
SST	Shear Stress Transport
STP	Standard Temperature and Pressure
SWU	Separative Work Unit
UCOR	Uranium Enrichment Corporation of South Africa
URENCO	Uranium Enrichment Consortium

LIST OF SYMBOLS

A	Cross section area of tube portion of RHVT (m^2)
A_c	Exposed cold surface area (m^2)
A_h	Exposed hot surface area (m^2)
A_i	Inlet cross section area (m^2)
$Alpha$	Head Separation Factor
A_{vg}-K_{vg}	Alphabetic code for dimension of different parts of vortex generator (mm)
A_{vt}	Cross sectional area of vortex tube (m^2)
C_f	Friction coefficient
C_m	Mean specific heat of gas in stream (J/kg K)
c_p	Specific heat of the fluid (J/kg K)
d_i	Vortex tube inlet diameter (m)
D	Wetted diameter of vortex tube (m)
D_f	Coefficient of diffusion (m^2/s)
D_{vg}	Diameter of vortex generator (mm)
D_{vt}	Inner diameter of vortex tube section (mm)
E_{in}	Rate of heat energy entering a control volume (Joule/s m^3)
E_{out}	Rate of heat energy leaving a control volume (Joule/s m^3)
E_w	Rate of heat energy transferred to the wall of a control volume (Joule/s m^3)
f	Friction factor of pipe
F	Feed flow rate to a separating element, mole/s
$F_{(1\text{-}3)}$	Model parameter between inlet and hot outlet
$F_{(2\text{-}3)}$	Model parameter between cold and hot outlet
g	Gravitational acceleration (=9.81 m/s^2)
G	Rate of mass flux of gas mixture (kg/m^2 s)
Gr_D	Grashof Number $\left(=\frac{g\beta_f \Delta T D_{vt}^3}{\nu^2}\right)$
h	Convection heat transfer coefficient (W/m^2 K)
h_m	Mass flux (kg/s m^2)
H_{wall}	Total moles of heavier species reaching wall of the control volume (kg mole)
j_h	Colburn j factor for heat transfer
j_m	Colburn j factor for mass transfer
K	Mass transfer coefficient (kg mole/s m^2 Pa)

k	Thermal conductivity of fluid (W/m K)
K_1	Mass transfer coefficient (m/s)
L	Length of vortex tube (m)
L_{vt}	Length of vortex tube (m)
m	Mass of heavier species reaching unit area of RHVT wall (kg /m^2)
M	Mass of the molecule per mole (kg/kg mole)
M_1	Molar weight of heavier species (kg /kg mole)
m_1	Inlet mass flow rate (kg/s)
m_2	Cold outlet mass flow rate (kg/s)
m_3	Hot outlet mass flow rate (kg/s)
m_i	Mass of a charged particle (kg)
M_m	Mean molecular weight of gas (kg/kg mole)
m_{tot}	Total inlet flow rate (kg/s)
N'	$(\mathrm{Pr}/\mathrm{Sc})^{2/3}$
N	Concentration in mole fraction of the lighter component
n	Total number of moles
N_1	Mole fraction of heavier species at inlet
N_2	Mole fraction of heavier species at hot outlet
N_3	Mole fraction of heavier species at cold outlet
n_a	Mole of component *a* present in the mixture
N_F	Mole fraction of required species in feed
N_{in}	Number of inlet nozzle
N_P	Mole fraction of required species in product
Nu	Nusselt Number $\left(\frac{hD}{k}\right)$
N_W	Mole fraction of required species in waste
P	Partial pressure of heavier species in gas stream at core (Pa)
P'	Product flow rate from a separating element (mole/s)
p	Total pressure of a gas mixture (Pa)
P_1	Inlet pressure (Pa)
P_2	Cold outlet pressure (Pa)
P_3	Hot outlet pressure (Pa)
p_a	Partial pressure of component *a* (Pa)
P_c	Exhaust pressure (Pa)
P_e	Perimeter of flow channel (m)

P_{gf}	Logarithmic mean partial pressure of lighter species (Pa)
P_i	Partial pressure of lighter species in axial gas stream (Pa)
P_{iw}	Partial pressure of lighter species at wall (Pa)
P_{min}	Experimentally measured minimum value of the pressure (kg/m^2)
P_o	Average pressure between inlet and cold outlet (Pa)
P_O	Total pressure at the outer radius of the vortex tube (Pa)
Pr	Prandtl number $\left(\frac{C_p\mu}{k}\right)$
P_T	Total pressure (Pa)
P_w	Partial pressure of heavier species in gas stream at wall (Pa)
Q	Flow rate of heavier species (kg mole/s)
q_{radial}	Radial separation factor of a gas centrifuge
$\dot{r}$	Separative exchange in radial direction per unit tube length (kg/m-s)
r_{cr}	Critical radius (m)
R	Universal gas constant (8.314 J / mol K)
R_{ab}	Abundance ratio
Ra_D	Rayleigh number ($Gr_D Pr$)
Re	Reynolds number $\left(\frac{\mathrm{D}v\rho}{\mu}\right)$
Sc	Schmidt number $\left(\frac{\mu}{\rho Ð}\right)$
St	Stanton number $\left(\frac{h}{\rho v c_p}\right)$
St_m	Mass transfer Stanton number $\left(\frac{h_m}{\rho v}\right)$
t	Time (s)
T	Average gas temperature (K)
T_1	Inlet temperature (K)
T_2	Cold outlet temperature (K)
T_3	Hot outlet temperature (K)
T_{amb}	Ambient temperature (K)
$T_{2,S}$	Cold outlet temperature calculated from Shannak model (K)
$T_{3,S}$	Hot outlet temperature calculated from Shannak model (K)
T_{min}	Experimentally measured minimum value of temperature (K)
$T_{RTDX,\ X=1,2,3}$	RHVT skin temperature at different locations (K)
U	Direct current (DC) component of voltage (Volt)
u	Diffusional separation rate in radial direction per unit tube length (kg/m s)

V	Flow rate of lighter species (kg mole/s)
V_1	Inlet volumetric flow rate (m^3/s)
v	Velocity of bulk gas stream (m/s)
v_1	Inlet gas velocity (m/s)
v_2	Cold outlet gas velocity (m/s)
v_θ	Azimuthal / tangential component of gas velocity (m/s)
v_z	Axial component of gas velocity (m/s)
V	Velocity of fluid (m/s)
v	Molecular velocity (m/s)
v_0	Nozzle exit velocity (m/s)
$V(N)$	Value function of stream having concentration N
V_{RF}	Radio Frequency (RF) component of voltage (Volt)
W	Waste flow rate from a separating element (mole/s)
X	Normalized pressure ratio
x	Bulk average concentration of heavier species in gas stream (kg mole/m^3)
x_z	Bulk average mole fraction of heavier species at axial location z
z_e	Charge of a particle (Coulomb)
z	Distance along length of RHVT (m)

Greek symbols

α	Separation factor
β	Tail separation factor
β_f	Coefficient of thermal expansion of fluid (K^{-1})
γ	Ratio of specific heats
$\partial P_{\text{reading}}$	Error in pressure transducer reading (kg/m^2)
∂P_{tran}	Accuracy in pressure transducer (kg/m^2)
ΔM	Difference in molecular weight of two species (kg/kg mole)
$\Delta P_{f(1-2)}$	Frictional pressure drop between inlet and cold outlet (Pa)
$\Delta P_{f(1-3)}$	Frictional pressure drop between inlet and hot outlet (Pa)
∂T_{RTD}	Maximum possible error in temperature measurement (K)
$\partial T_{\text{scanner}}$	Accuracy in RTD scanner (^oK)
ΔT	Maximum temperature difference between hot and cold end, T_3 - T_2 (K)
$\Delta T_{2,L}$	Drop in cold outlet temperature, experimental value from literature (K)
$\Delta T_{2,S}$	Drop in cold outlet temperature, from Shannak model (K)

$\Delta T_{3,L}$	Rise in hot outlet temperature, experimental value from literature (K)
$\Delta T_{3,S}$	Rise in hot outlet temperature, from Shannak model (K)
ΔT_h	Temperature fall due to heat loss to ambient at hot outlet (K)
ΔT_c	Temperature rise due to heat addition from ambient at cold outlet (K)
ΔT_{cold}	Temperature drop obtained at the cold end, T_2-T_1 (K)
ΔT_{hot}	Temperature rise obtained at the hot end, T_3-T_1 (K)
Δz	Thickness of control volume (m)
Đ	Diffusivity (m^2/s)
ε	Dissipation rate of turbulent kinetic energy (J/kg s)
$\in_A$	Elementary separation factor for a multicomponent gas mixture
θ	Cut, ratio of product to feed flow rate
θ_c	Cold mass fraction
θ_h	Partial cut of the heavier component
$\theta_{c,opt}$	Optimum value of cold mass fraction
θ_l	Partial cut of the lighter component
κ	P_w/P
μ	Viscosity of gas at core (Pa s)
μ_s	Viscosity of gas at wall surface (Pa s)
ν	Kinematic viscosity (m^2/s)
ρ	Density of mixture (kg/m^3)
ρ_1	Density of the gas at the inlet (kg/m^3)
ρ_2	Density of the gas at cold outlet (kg/m^3)
ρ_3	Density of the gas at hot outlet (kg/m^3)
ρ_a	Density of component a (kg/m^3)
φ_O	Loss coefficient of the orifice plate
φ_T	Loss coefficient of the tee junction
ω	Specific rate of dissipation (1/s)
ω_v	Vorticity (rotation/s)

ω'	Angular frequency of the *RF* field (radians/s)
Γ	Vortex circulation (m^2/s)

Thesis Highlight

Name of the Student: Mihir Chatterjee

Name of the CI/OCC: BARC **Enrolment No.:** ENGG01201304034

Thesis Title: Investigation of gas Species and Thermal Separation in Ranque-Hilsch Vortex Tube

Discipline: Engineering Sciences **Sub-Area of Discipline:** Chemical Engineering

Date of viva voce: 04 September 2020

Objective of the present research work is to investigate experimentally and numerically separation of gas species and energy under different operating conditions in a RHVT. The work was initiated by a simple set of experiments with a commercially available RHVT in which inter-dependence of mass and thermal separation in RHVT was studied. It was concluded from the experiment that mass and heat transfer are dependent on each other. Based on this finding a coupled thermal and mass separation model was built that uses the Chilton-Colburn analogy of simultaneous heat and mass transfer. A computer code based on this model can calculate the thermal and concentration profile along the axial length of the RHVT. Results from the computer code have been verified with data available in literature. Further a laboratory scale experimental setup was built in which both thermal and species

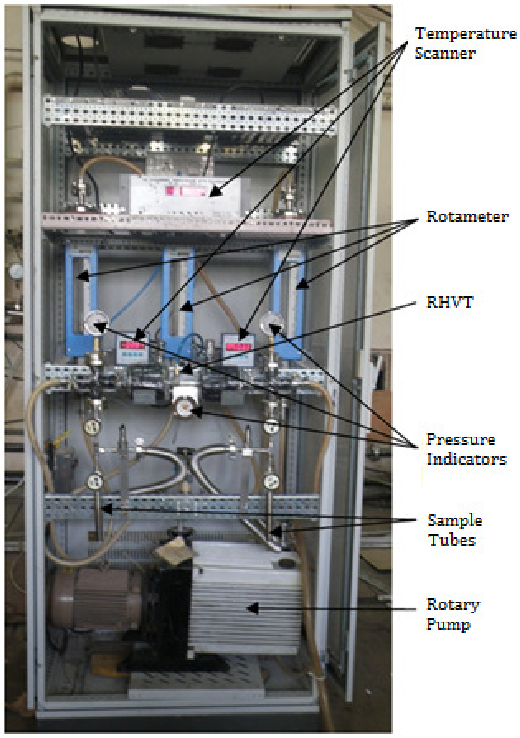

Fig 1 RHVT experimental setup

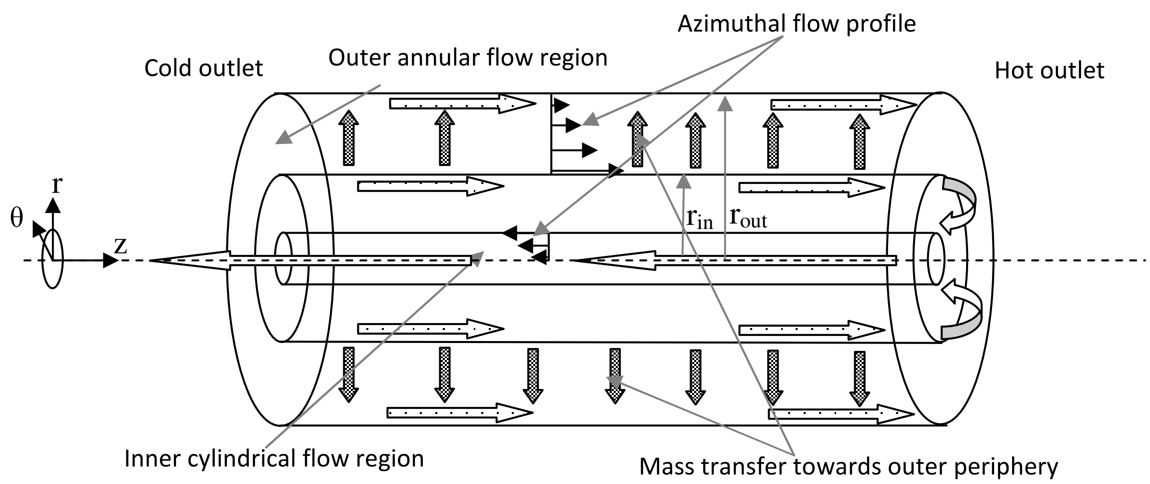

Fig 2 Proposed model of species separation inside RHVT

separation could be studied using air as a binary mixture of oxygen and nitrogen. Experimental data obtained from this setup has been used to validate the code extensively. Next, a number of important geometric and operating parameters were identified. The computer code developed and the experimental setup were used to carry out parametric studies of the RHVT performance with respect to species separation. Also supporting data available in the literature has been used for parametric study.